Cationic Oligomeric Surfactants: Novel Synthesis and Characterization

Kathryn A. Topp

A thesis submitted for the degree of
Doctor of Philosophy

School of Chemistry,
The University of Sydney,
Sydney, Australia.

April 2006

"Our education should... help us to distinguish between things that are worthy and things that are worthless, between realities and shams."

Winifred West

Statement of originality

This thesis describes work carried out in the School of Chemistry at the University of Sydney between March 2002 and April 2006. Except where otherwise acknowledged, the work presented is my own, and has not been submitted for a higher degree at any other university or institution.

More specifically, some of the results reported here are due to the work of collaborators. All the atomic force microscopy was performed by Dr. Robert Chan and Regina Schwering. Dr. Chan also aided in the determination of several of the critical micelle concentrations. The mass spectrometric characterization of the surfactant oligomers in Chapter 5 was overseen by Dr. Kelvin Picker. Jeanette McAlpine performed the SAXS measurement in Chapter 6. My supervisor Greg Warr guided me in the running of small-angle neutron scattering experiments. Alternative unimers for the LELA reaction, which are listed in the conclusion of Chapter 5, were suggested by Professor David Black. Theoretical calculations relating to the pyridinium charge-transfer complexes in Chapter 7 were performed by Dr. Jeff Reimers.

In almost all cases, the polymerizable surfactants were synthesized by the Organic Synthesis Centre within the School of Chemistry. The PhCOBF chain-transfer catalyst described in Chapter 3 was synthesized and provided to me by John Biasutti from the University of New South Wales.

The remainder of the research presented in Chapters 3–8 is my own work, which has been guided by advice and suggestions from my supervisor and associate supervisor, Professor Greg Warr and Associate Professor Christopher Barner-Kowollik.

Kathryn A. Topp
Sydney, Australia
April, 2006

Acknowledgements

There are many people I would like to thank for their contributions over the last four years.

On a suggestion from Bob Prud'homme, Greg Warr and his black sense of humour dreamt up this project and then gave me the space to complete it. He is responsible for my fascination with surfactant chemistry and for introducing me to the great technique of small-angle neutron scattering. He was also supportive of the teaching I did on the side, for which I am grateful.

Partway through the project, Chris Barner-Kowollik became my associate supervisor, and not only provided advice on polymer chemistry but was also generous with equipment and chemicals. Andrew Ah Toy and the CAMD group gave me practical help in grappling with finicky chain-transfer polymerizations.

Many people gave me advice and assisted me with experimental techniques, in particular Liz Carter, Chris Fellows, Chris Ferguson, Kate Jolliffe, Ian Luck, Kelvin Picker and Pat Stamford. David Black made some important corrections to my mechanistic interpretation of the LELA reaction as well as suggestions for further work. Robert Chan and Regina Schwering performed AFM measurements for me and Nirmesh Jain gave me a hand in setting up some of my SANS experiments. Sev Sternhell was always ready for a discussion on anything from mountaineering to NMR.

Although snowed under with his own work, Jeff Reimers generously performed the charge-transfer calculations in Chapter 7 for me, and helped in their interpretation.

Past and present members of the Warr group, particularly Jeannette McAlpine, Annabelle Blom, Paul Fitzgerald, Lela de Campo and Regina Schwering, may have been disturbed by my increasingly animated opinions on the subject of polymer chemistry, but they hid it admirably and provided a good deal of friendship, support and help.

The great faith shown in me by Deirdre Macpherson, John McMath and my two classes at St. Andrews Cathedral School kept me enthusiastic about science when the

postgraduate reality was so grim.

I must also offer thanks to Asaph Widmer-Cooper, with whom I got into this in the first place; Pat Giltrap, Laura Giltrap, Ross McKerracher and Laina Hall, who were great housemates; Boris Kuhlmey, whose attitude to experimentation, whether on crocodile meat or photonic crystals, was an inspiration in itself; and my running mates – physical exertion is good for the soul.

Thanks also to Mum, Dad, Steph and Fin, who got me to the starting line, and who were interested, sympathetic and enthusiastic at just the right moments.

And last of all, best of all, to Tom – for everything.

Contents

List of Figures

List of Tables

Abstract

Oligomeric surfactants, sometimes referred to as gemini surfactants, consist of two or more amphiphilic 'monomer' units linked together by spacer groups. The chemical identity of the spacer group is unconstrained, and it joins the individual units at or near the hydrophilic headgroups.

Oligomeric surfactants display a range of interesting properties, including very low critical micelle concentrations, high surface activity and unusual rheology and self-assembly. Consequently they have many potential applications, both scientific and industrial. Until now, their use has been limited by the cost of their synthesis, which in some cases involve long and difficult procedures. This project developed from the idea that a synthesis based on polymerization could prove a useful and versatile method for producing these surfactants.

The chemical starting point for this project was a series of polymerizable surfactants ('surfmers'), upon which polymerization was performed. Two families of surfmers were investigated, both cationic and based on methacrylate and vinylpyridinium moieties respectively. The physical behaviour of these surfactants – a number of which are new – was investigated using standard techniques; these included the determination of the critical micelle concentration, characterization of phase behaviour, neutron scattering and surface adsorption.

In producing oligomers, the initial focus was on free-radical polymerization, with control of molecular weight to be achieved by chain-transfer techniques. Due largely to analysis problems, this work proved unsuccessful. In its place a new reaction, not based on conventional polymerization methods, has been developed.

The vinylpyridinium surfmers mentioned above readily undergo addition across the double bond to produce alkyl ring substituents. Under basic conditions, these alkylpyridiniums undergo an elimination/addition reaction in which they link together to form oligomers. This reaction can be started or stopped by raising or lowering the pH of the

reaction solution, and has been performed in both organic and aqueous solutions. It is referred to in this thesis as LELA(Linkage by ELimination/Addition).

The LELA reaction was used to produce mixtures of oligomers, the phase behaviour and surface adsorption of which were examined. Small-angle neutron scattering was used to monitor the reaction in real time and identify changes in self-assembly as the average oligomer length increased. Progress was also made towards a chromatographic protocol that would allow mixtures to be separated into their components and the pure oligomers to be studied.

Finally, some of the compounds studied display interesting pH-dependent chromophoric properties which were also found to occur with other simple alkylpyridinium species. They are tentatively ascribed to inter- and intramolecular charge-transfer complexes, and evidence towards this conclusion was collected and is presented along with relevant calculations.

Chapter 1

Introduction

"Soap and education are not as sudden as a massacre, but they are more deadly in the long run."

Mark Twain, A Curious Dream

The primary aims of this work were to develop a polymerization-based synthesis for oligomeric surfactants, and to then study series of oligomeric surfactants made by that method. In chasing this goal, my research spanned a broad range of fields, and this introduction provides a brief review of the literature in those areas. Section 1.1 deals with the basics of surfactant science and introduces the two families of surfactants with which this work is concerned – oligomeric surfactants and polymerizable surfactants. Section 1.2 deals with polymer chemistry, and looks specifically at a few methods of controlling the molecular weight of polymers: clearly the most important barrier to overcome in producing oligomeric molecules. While this thesis contains a conspicuous lack of results achieved with these techniques, they are nonetheless important and should not be discounted in future work on surfactant oligomers. Section 1.3 on the chemistry of vinylpyridine compounds seems, perhaps, the most incongruous. Yet while it represents the greatest departure from the course as it was originally plotted, in the end it was the map that showed where X marks the spot.

1.1 Surfactant chemistry

1.1.1 The physical behaviour of surfactants

Soap has been around for a long time. Two to three thousand years ago, the ancient Babylonians and Egyptians knew that combining animal or plant fats with caustic ashes produced a substance which foamed nicely and made washing easier. Pliny the Elder wrote of a substance that the Gauls and Germans produced from ashes and tallow and which they used in their hair as a kind of pomade [1]. The Romans developed the process for themselves at a later stage, as did the Arabs, and over the last millennium the production and use of soap has grown steadily all over the world.

These original soaps were the salts of fatty acids: products of the base-catalyzed hydrolysis of the glycerides and other esters that comprise many naturally occurring fats and oils. The hydrophilic carboxylate functionality ($-CO_2^-$) that was the result of the hydrolysis reaction gave the long-chain hydrocarbon 'tail' to which it was attached a useful property – the ability to cause oil to dissolve in water. The science behind this and a multitude of other elegant, intriguing and useful properties is the science of surface-active agents or 'surfactants'.

The most common taxonomy of modern surfactants divides them according to the nature of the hydrophilic 'head' of the molecule. One kingdom is composed of ionic surfactants. These are salts: the headgroup carries a charge and is associated with a counterion. Ionic surfactants may further be divided, according to the sign of the charge they bear, into families of anionic surfactants (like the original carboxylate soaps), cationic surfactants and zwitterionic surfactants (which carry both a positive and a negative charge on the headgroup, and have no counterion). The other kingdom comprises nonionic surfactants, which carry no charge. Their surfactant properties arise from the presence of a water-soluble organic group, commonly based on alcohol groups or the ethylene oxide ($-CH_2CH_2O-$) unit.

The properties of surfactants arise from the different solubilities of the head and tail of the surfactant. Part polar, part apolar, surfactants perform extraordinary feats of self-assembly in order to preserve a delicate thermodynamic balance and thereby remain solvated. While they are generally used and studied in aqueous systems, some are also known to self-assemble in organic solvents and ionic liquids [2].

The following sections briefly describe the empirical observations and thermodynamic deductions upon which the field of surfactant self-assembly is based.

Micellization

Above a certain temperature (the Krafft temperature) and concentration (the critical micelle concentration or CMC), surfactants in aqueous solution spontaneously aggregate into clusters known as micelles. While the exact nature of a micelle was for many years the subject of controversy, it is now accepted that the basic micelle formed by most surfactants in dilute aqueous solution is globular in shape, and consists of a core of alkyl chains surrounded by a 'shell' of solvated headgroups.

The hydrocarbon core is considered to be liquid-like. However, because of the restriction placed on their movement by the surfactant head, surfactant tails have slightly lower entropy than molecules in a droplet of pure hydrocarbon. For this reason also, the outer regions of the core tend to be more ordered than the inner parts [3, 4].

The solvated shell surrounding the core is known as the palisade layer. This comprises the surfactant headgroups and water of hydration. If the surfactant is ionic, it also contains a certain fraction of the surfactant counterions, and is known as the Stern layer. The exact number of these determines the ionization degree of the micelle as a whole, and is dependent on the binding strength of the counterion. This is related to the Hofmeister series and is believed to be a function of the ion's polarizability [5–7]. Counterions not bound to headgroups form the Gouy-Chapman, or diffuse layer. Further out from this is a continuum of free water.

The micelle is a dynamic structure, and two equilibria can be identified. The first describes the process of single surfactant molecules entering and leaving existing micelles, and thus the 'residence time' of a surfactant molecule in a micelle. The second describes the continual formation and dissolution of whole micelles, and thus the micelle lifetime. Both of these processes are dependent on a suite of variables, not least of which is the structure of the surfactant itself. In general however, micelle lifetimes are two or three orders of magnitude longer than the residence time of individual molecules [8].

Thermodynamics and the packing parameter

The contributions to the free energy of an aqueous surfactant system include:

- interfacial tension and entropic effects due to contact between the alkyl chains or micelle cores and surrounding water (the 'hydrophobic effect');
- repulsion between surfactant headgroups, which can be of steric, solvation or electrostatic origin (the latter in the case of ionic surfactants);

- the packing of surfactant tails within aggregates; and
- geometric constraints arising from the surfactant structure.

For each surfactant molecule at the surface of a micelle, there are three planes in which forces occur that affect its free energy (see Figure 1.1). In the plane of the surfactant headgroups (x), a repulsive force exists, which tends toward increasing the area a_o occupied by each headgroup. At the boundary between the hydrophobic micelle core and the palisade layer (y), interfacial tension is an attractive contribution, tending to minimize the size of this interface. Within the core of the micelle (z) there are attractive van der Waals forces, but also repulsive entropic contributions, which tend to increase the volume occupied by each alkyl chain. In practice the forces at z are rarely considered, and the micelle core is treated as an incompressible liquid with the same density as the corresponding bulk hydrocarbon.

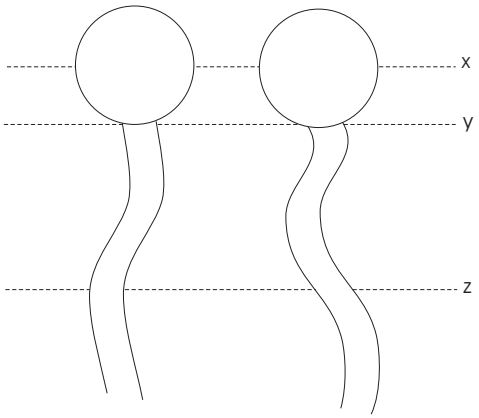

Figure 1.1: Planes in which forces act at the surface of a micelle. Plane x represents headgroup repulsion, plane y the surface tension between the hydrocarbon core and aqueous continuum, and plane z the alkyl chain packing. (after Mitchell et al. [9]).

These contributions to the free energy of a surfactant molecule in a micelle, μ_N^o, have been summarized as [9]:

$$\mu_N^o = \gamma a + \frac{c(r)}{a} + g \tag{1.1}$$

where γ is the surface tension, a is the headgroup area, $c(r)$ is a function of the radius r that describes the headgroup repulsion, and g includes all other contributions, including the hydrophobicity of the the alkyl tail in water. For the case of ionic surfactants, $c(r)$

can be approximated by a simple capacitance model, assuming that the electrostatic repulsion between headgroups outweighs any steric or solvation effects [10, 11].

However, this relation neglects an important geometric contribution. This arises from the constraints placed on any self-assembled structure by the dimensions of the surfactant molecule forming it. For instance, consider a surfactant molecule with all-trans alkyl chain length l, headgroup area a and volume v. A spherical micelle formed from N molecules (i.e. with aggregation number N) must then have radius $r \leq l$, surface area $A = Na$ and volume $V = Nv$.

With this in mind, and using the geometric expressions describing the volume and surface area of spheres, cylinders and bilayers, Israelachvili, Mitchell and Ninham derived a dimensionless parameter to describe the geometric profile of a surfactant. This is known as the packing parameter [11]:

$$P \equiv \frac{v}{al} \tag{1.2}$$

For $P \leq 1/3$ (e.g. a surfactant with a large headgroup and moderate tail), spherical micelles will form. For $1/3 < P \leq 1/2$, (e.g. moderate headgroup and moderate tail) a less highly curved structure is preferred, and cylinders will form. For $1/2 < P \leq 1$ (e.g. surfactants with two alkyl chains), the conditions favour low-curvature or flat structures such as bilayers. This qualitative expression therefore leads to a method for rationalizing – and to some extent predicting – the self-assembly behaviour of any surfactant.

Phase behaviour

As described above, a surfactant generally forms micelles at low concentrations in water. However, as its concentration is increased, the surfactant is observed to self-assemble into a variety of geometrically distinct structures, or phases. It is important to note that not all surfactants form all possible phases; indeed, most form only a subset, and some form nothing but micelles. The phases formed by any given surfactant are dependent on the forces and constraints discussed above, but are most easily rationalized in terms of preferred surface curvature or, more formally, the packing parameter P.

In general, all self-assembled structures are based on one of the three primitive geometries considered in the derivation of P: spheres, cylinders and bilayers. Which of these is favoured depends both on P and the surfactant volume fraction (see Figure 1.2).

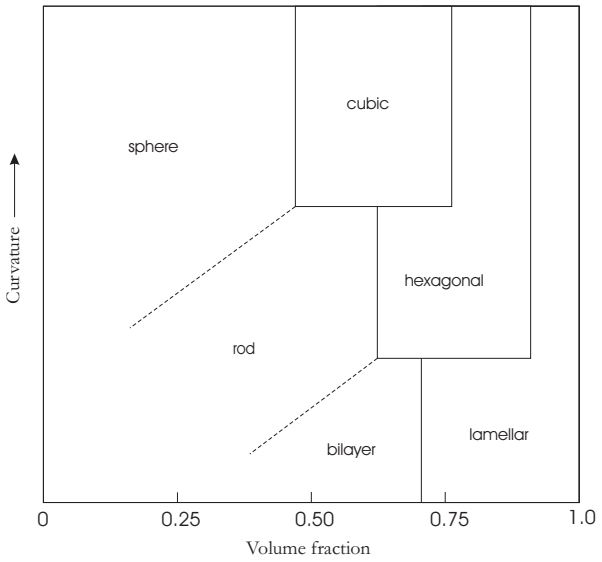

Figure 1.2: General relationship between surfactant volume fraction, preferred interfacial curvature and phase geometry (after Mitchell et al. [9]).

For instance, a surfactant with high P may still form spherical micelles at low concentrations, but these will tend towards less curved structures – rod-like and/or bilayer-type (disc-like) micelles – as the surfactant concentration increases.

At higher concentrations, lyotropic liquid crystals form. Like micelles, these mesophases occur in a structural progression from high to low curvature with increasing surfactant concentration. They are commonly identified with polarizing microscopy by their relative viscosities and varying optical textures.

For surfactants with low P, as concentration increases the spherical micelles eventually become so populous that intermicellar repulsion forces them into an ordered state (simple, body-centred or face-centred cubic). This is the discrete or micellar cubic phase (I_1), and takes the form of an isotropic and highly viscous gel.

An increasing volume fraction of surfactant and decreasing volume fraction of water causes a decrease in a_o (and therefore an increase in P) for such a surfactant. In this case, and for intermediate-P surfactants that naturally form rod-like micelles, the hexagonal phase (H_1) occurs. This consists of long cylindrical micelles in a hexagonal close-packed arrangement, and is birefringent and generally somewhat less viscous than the cubic phase.

At higher concentrations again, structures of very low curvature form. The lamellar

phase (L_α) is the most common of these, comprising large bilayer sheets (lamellae) that lie parallel to one another. This is also birefringent and of variable viscosity. Other bilayer-based structures are also known. For instance, a phase known as the normal bicontinuous cubic phase (V_1) often forms at concentrations between the hexagonal and lamellar phases. This has the macroscopic characteristics of the discrete cubic phase, but consists of one of several three-dimensional, highly symmetrical, branched micelle structures with zero net curvature. Perforated bilayers known as mesh phases and randomly oriented branching bilayers known as sponges have also been observed.

At $P > 1$, surfactants form 'reversed' phases, in which the continuous medium is hydrocarbon, and micelle or mesophase cores are composed of the hydrated headgroups. In most, though not all cases, these phases form in ternary systems, with the addition of a hydrocarbon or other apolar species. The reversed structures are known as V_2 (reversed bicontinuous cubic), H_2 (reversed hexagonal), I_2 (reversed discrete cubic) and reversed micelles.

Discrete fragments of the bulk mesophases are also known to exist under certain circumstances. Easily the most common of these are vesicles or liposomes, which are spherical structures consisting of a lamellar (bilayer) wall enclosing an aqueous interior. In the last decade however, successful attempts have been made to stabilize submicron-sized fragments of other mesophases – in particular the reverse cubic and reverse hexagonal phases. Such particles are referred to as hexosomes or cubosomes, are generally produced by microfluidization or sonication of the bulk phase in water, and may be coated with diblock copolymers to prevent their reaggregation [12, 13]. A significant amount of research is directed at loading these tiny, porous particles with drugs or other molecules and using them as carriers or slow-release agents [14].

Adsorbed layer structures

In addition to their bulk phase behaviour, surfactants are known to adsorb to surfaces in a manner consistent with their packing parameter. For instance, atomic force microscopy has been used to show that surfactants with low P will adsorb to a hydrophilic, charged mica surface as distorted spheres (globules), whereas surfactants preferring low-curvature structures will adsorb as cylinders or bilayers [15]. Hemimicelles or monolayers are found to form on hydrophobic substrates such as graphite [16]. Overall, the adsorbed morphology is dependent on the nature of the surfactant, the surface (in particular its hydrophilicity and charge density) and the presence of additives such as

salt [17, 18].

1.1.2 Gemini surfactants

One of the primary variables determining the physical properties of surfactants is a_o, the headgroup area. It is therefore natural to wonder how these properties might change if for a given headgroup, a_o could be altered. With ionic surfactants, this is easily managed by the addition of salt. However, an arguably more elegant and certainly more permanent way of achieving such an effect is through the use of oligomeric surfactants.

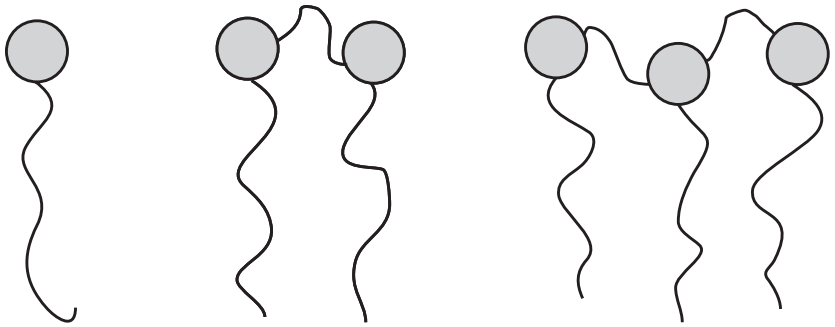

Figure 1.3: (left) Conventional surfactant; (middle) dimeric surfactant; (right) trimeric surfactant.

An oligomeric surfactant consists of two or more amphiphilic 'monomer' units, linked together by spacer groups (Figure 1.3) [19]. As illustrated in Figure 1.4, the spacer group can be located anywhere along the length of the surfactant. However, surfactants linked at or near the tail end are known as bolaform surfactants, and have different properties to their headgroup-linked cousins. They will not be dealt with here.

Restricting the location of the spacer to at or near the headgroup, however, still covers an extensive suite of variations. In 1991, Menger coined the term 'gemini' [20] to refer to dimeric molecules of this type, although the general class of compounds includes larger oligomers such as trimers and tetramers [21–23].

The chemical nature of gemini surfactants is essentially unconstrained, save by the synthetic methods used to make them. Geminis have been produced with headgroups that are cationic, anionic and nonionic [22]; carbohydrates [24–26] and amino acids [27, 28] have also been incorporated. Tails of all lengths, including some with unsaturated groups or fluorinated carbons [29] have been studied. In addition, geminis need not be symmetric. 'Heterogeminis' have been synthesized with tails of different lengths [30,31],

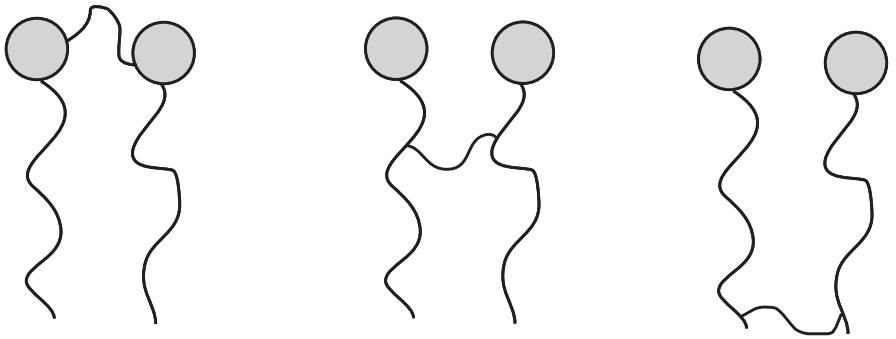

Figure 1.4: (left and middle) Gemini surfactants are linked at or near the headgroup; (right) bolaform surfactant.

with different headgroups [32], and with both, such as the asymmetric zwitterionic geminis made by Menger et al. [33, 34].

There are also few limits placed on the nature of the spacer group. Rigid spacer groups are formed from aromatic [35] or unsaturated groups [36], while long methylene chains serve as flexible linkers [37]. They may be hydrophobic (e.g. alkyl- or aryl-based), or rendered hydrophilic by the inclusion of ethylene oxide units [38]. The length of the spacer is also of great interest, since varying it affords control over the distance between the headgroups [39].

The final structural variable is the number of monomer units linked together; that is, the progression from monomer to dimer to trimer and so forth. However, because of the difficulty of synthesizing larger geminis, only a few studies involving these compounds exist [40, 41].

Synthesis

In producing such a variety of gemini structures, a similar variety of synthetic methods has been used [19]. These range from simple one-step organic reactions to the enzymatic and chemo-enzymatic processes used to produce certain amino acid geminis [28, 42]. It is unnecessary to review all of these techniques here; however, because this thesis deals with new methods for producing cationic oligomeric surfactants, it is worth briefly mentioning the most common methods used in synthesizing these compounds.

Bis-quaternary ammonium geminis with simple carbon-chain spacers are the easiest of the oligomeric surfactants to synthesize, and were therefore the first to be widely studied. The most common route typically involves reacting either a di-tertiary amine

and a haloalkane, or a dihalide and a tertiary amine under reflux in ethanol or propanol (Figure 1.5). While the reaction can sometimes take days to complete due to the low reactivity of the halide, the quaternary ammonium gemini product is generally obtained in high yield [43, 44].

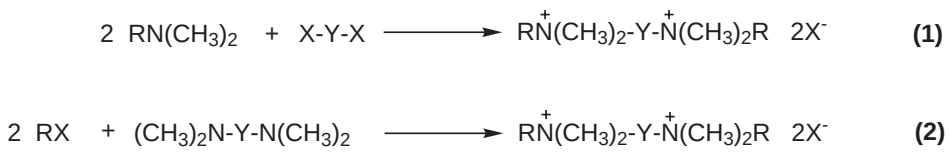

Figure 1.5: Common synthetic routes to cationic gemini surfactants; the R-group becomes the surfactant tails, the Y-group the spacer and X – a halide – the counterion.

This method and variations on it have been used to produce cationic geminis with a variety of sizes and functionalities [19, 45]. In some routes, epichlorohydrin is employed in place of the dihalide, which produces oligomers with hydroxy-functionalized spacers [46]. However, the purification of cationic oligomers becomes increasingly difficult for the longer species, given they have a relatively low tendency to crystallize. Column chromatography is also problematic, although some progress has been made in this regard [47].

An alternative synthesis exists that partially addresses these problems. It involves the reaction of acid chloride with amine to form a di- or tri-amide. The carbonyl groups are reduced with $LiAlH_4$, and the resulting amines are then quaternized with an appropriate reagent (e.g. methyl halide). In this route, the intermediates are readily purified by column chromatography and a purer product can be obtained [19].

Properties and applications

Gemini and oligomeric surfactants have received increasing scientific and commercial attention in the last decade. Much of this interest has been generated by the fact that they show great enhancements in many of the properties typically shown by surfactants.

Because of the greater amount of hydrocarbon per molecule, the critical micelle concentrations (CMCs) of geminis are typically one order of magnitude lower than those of the corresponding monomeric surfactant.* The CMC is strongly affected by chain length and counterion, as in monomeric surfactants, but surprisingly little by

*Note that there exists some inconsistency in the literature regarding the definition of an analogous monomeric surfactant.

the length or nature of the spacer. This means that the potential exists to chemically or biologically functionalize the spacers of geminis without adversely affecting their surfactant properties [19]. In the few existing studies of homologous series of oligomers, the largest decrease in CMC has been found between the monomer and dimer. To obtain a further decrease of similar magnitude, the surfactant size must be doubled again, i.e. from dimer to tetramer [41].

Micelles of geminis have been shown to have slow dynamics relative to monomeric surfactants. Equilibrium takes longer to achieve, with both micelle lifetimes and surfactant residence times in micelles being significantly greater [48]. Aggregation numbers are typically larger than those of monomeric surfactants as a result of the decreased curvature supported by the molecules [40, 41]. In addition, premicellar aggregation is often observed, and is attributed to the greater hydrophobic surface area of each molecule. This becomes increasingly significant for geminis with larger spacer groups and for longer oligomers [37, 49].

In terms of the packing parameter, the effect of linking surfactants together into oligomers is to decrease a_o and increase v (the tail volume), thereby increasing P (the packing parameter). Oligomeric surfactants therefore tend to form lower-curvature (or reversed) structures. Geminis with short spacers have been observed to show unusually high viscosity and even viscoelastic behaviour in dilute aqueous solutions [50, 51]. This behaviour was investigated in detail for the diquaternary ammonium bromide called 12-2-12, which has two dodecyl chains and a -CH_2CH_2- spacer. Cryo-TEM images of the surfactant at concentrations between 0.26 wt% and 1.5 wt% show that it forms spherical micelles which, as the concentration increases, are accompanied and then replaced by extremely long thread- or worm-like micelles [52]. Such structures are believed to account for the surfactant's unusual rheological properties.

Certain geminis are also known to form unusual self-assembled structures. Twisted ribbons, fibres and helices have been produced from chiral geminis, including a conventional cationic gemini, 16-2-6, paired with L- or D-tartrate [53, 54]. Asymmetric zwitterionic geminis have been prepared that form coacervates – a fluid isotropic phase that is immiscible with its own solvent. These are believed to have a sponge-like structure [33, 55].

Geminis show good adsorption to air-liquid, liquid-liquid and liquid-solid interfaces, and are particularly efficient at reducing the surface tension of water [23]. They have excellent solubilizing and foaming properties [51, 56], and depending on the nature of

the spacer, may have very low Krafft temperatures [57].

As a consequence of these properties, many potential applications are anticipated for oligomeric surfactants. These include cleaning agents and detergents, cosmetics, textile dyeing, emulsion polymerization and dispersion stabilization, pharmaceutical and biological applications and preparative and analytic chemistry. However, their use in industry is currently limited by the cost of their production and the need for a greater understanding of their structure-function relationships [19].

1.1.3 Polymerizable surfactants

In the last two decades, a significant number of studies have been undertaken on polymerizable surfactants, or 'surfmers' [58, 59]. These molecules combine the chemical reactivity of conventional monomers with the physical behaviour of surfactants, and therefore represent a useful bridge between the fields of polymer and surfactant science.

A wide variety of surfmers appear in the literature, differing both in the functional groups they employ and in the location of the polymerizable moiety. Figure 1.6 illustrates the variety that exists among the surfmer family.

There are a number of areas in which surfmers find application. One is in emulsion polymerization, where their ready incorporation into growing polymer chains means that the common problem of residual free surfactant in the latex product is circumvented [60–62].

They have also been widely employed in attempts to make micro- or nanostructured materials. Some researchers have approached this goal via copolymerization with conventional monomers. Such methods have produced potentially useful materials that may be, but are not necessarily related to the self-assembled structures naturally formed by the unreacted monomer. These include microporous materials (showing no long-range order) [63, 64], organized hydrogels and nanolatex particles [58, 65, 66].

Other areas of research have developed from the desire to make permanent the self-assembled structures of surfactants. In such work, the preservation of the original phase geometry is of great interest. Early studies utilized surfmers having the polymerizable group at the end of the tail (e.g. sodium 10-undecanoate) [67]. These reactions produced soluble 'polymeric micelles' but, because polymerization severely constrains the movement of the surfactant tails, the micelle cores are not liquid-like [68]. The polymerization of lamellar phases was similarly investigated, but phase separation was

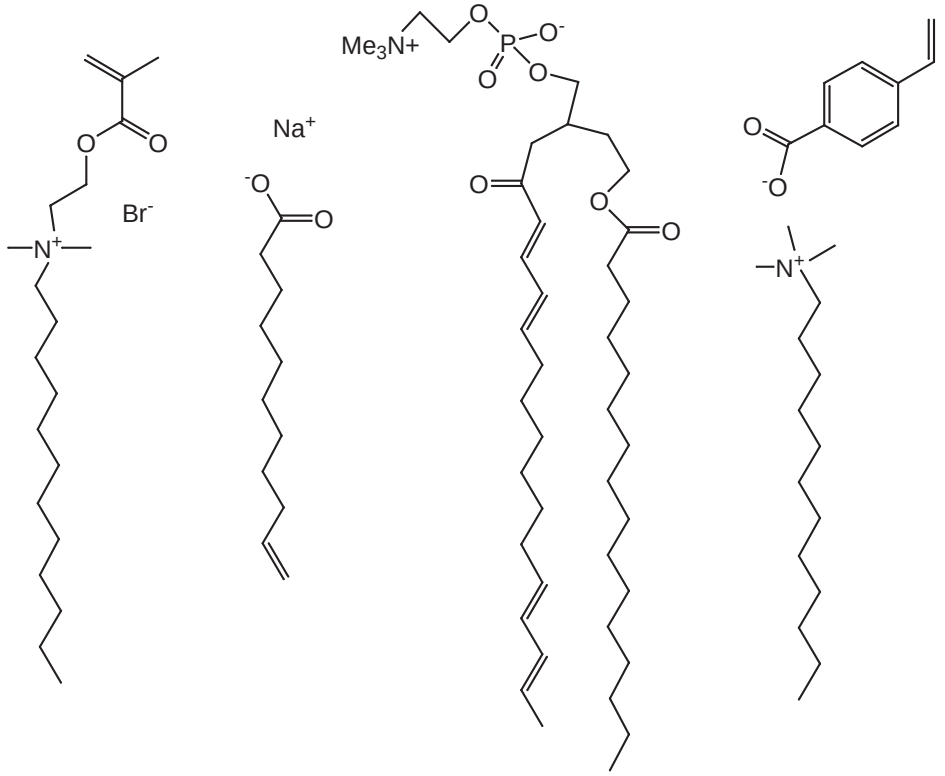

Figure 1.6: The polymerizable group that defines a surfmer can be located anywhere within the molecule.

common [58]. Recently, worm-like micelles were produced by the addition of sodium tosylate to methacryloyloxyundecyltrimethylammonium bromide (a quaternary ammonium surfactant with a methacrylate group at the end of the tail). Polymerization yielded structures that retained the radius of the original micelles but were significantly longer [69].

Similar attempts have been made to polymerize structures formed by surfmers having the polymerizable moiety near the headgroup [58]. These often give insoluble polymer products whose structure – if any – bears no resemblence to the original surfactant structures [70]. The most successful examples of structure preservation use systems where the thermodynamics of the final polymer most closely mimic those of the surfmer; that is, the preserved structure is both thermodynamically and kinetically stable. This has been achieved by O'Brien et al. using phospholipid-based surfmers. In these molecules, the polymerizable group is located just below the headgroup, which is believed to be the least mobile part of the molecule when self-assembled. Polymerization then

caused minimal restriction to the movement of the molecules, and hence minimal perturbation to the overall system [71, 72].

The effect of the position of the polymerizable group in the surfmer has a significant effect on the kinetics of polymerization [73]. In reactions of tail-functionalized monomers, the polymerizable group has a high local concentration as a result of being sequestered inside the micelle: this aids fast propagation. In addition, it is shielded from polymerizable groups in other micelles, so topological polymerization is more likely. If the surfactant is head-functionalized, the local concentration of vinyl bonds is somewhat decreased, and propagation is slower. It has been suggested that in this case, propagating chains are more likely to come in contact with reactive groups in neighbouring micelles, producing longer, less soluble polymers [58]. A similar rationalization has been used to explain the results of copolymerization of tail-functionalized and head-functionalized methacrylate surfmers with conventional monomers [65].

Given that the speed of monomer exchange between micelles has been shown to be significantly faster than the expected rate of propagation in such a system [74], it is likely that polymerization is not confined by the micellar structure. In these systems, the growing chains are not topologically confined by the micellar structure [8, 75].

In recent years, researchers have also begun to investigate the polymerization of adsorbed structures on surfaces, in the hope of achieving nanopatterning and low-friction applications.

1.2 Polymerization

1.2.1 Mechanisms

The process of forming a polymer from its constitutent monomer units is known as polymerization and can take place by a number of different mechanisms. These can be classified into two main groups on the basis of the mechanism – step (sometimes called condensation) polymerization and chain polymerization. Within the class of chain polymerizations, a further distinction can be made on the basis of the chemical nature of the growing polymer chain, between free-radical polymerization and ionic polymerization [76]. The latter two mechanisms are most relevant to this work.

Free-radical polymerization

Free-radical polymerization is one of the most widely used synthetic techniques now in existence. In comparison to ionic mechanisms, it is relatively robust in the face of impurities, and with the techniques developed over the last few decades, can now be used to make a vast range of products with finely tuned properties [77, 78].

The distinguishing feature of this form of polymerization is that the propagating species is a free radical. The basic mechanism consists of three steps, represented in Figure 1.7.

Initiation is accomplished using a species which dissociates thermally or photolytically, or which reacts with another compound (as in a redox couple), to produce radicals. These react with the less-substituted end of the vinyl bond in the monomer to produce a propagating chain.

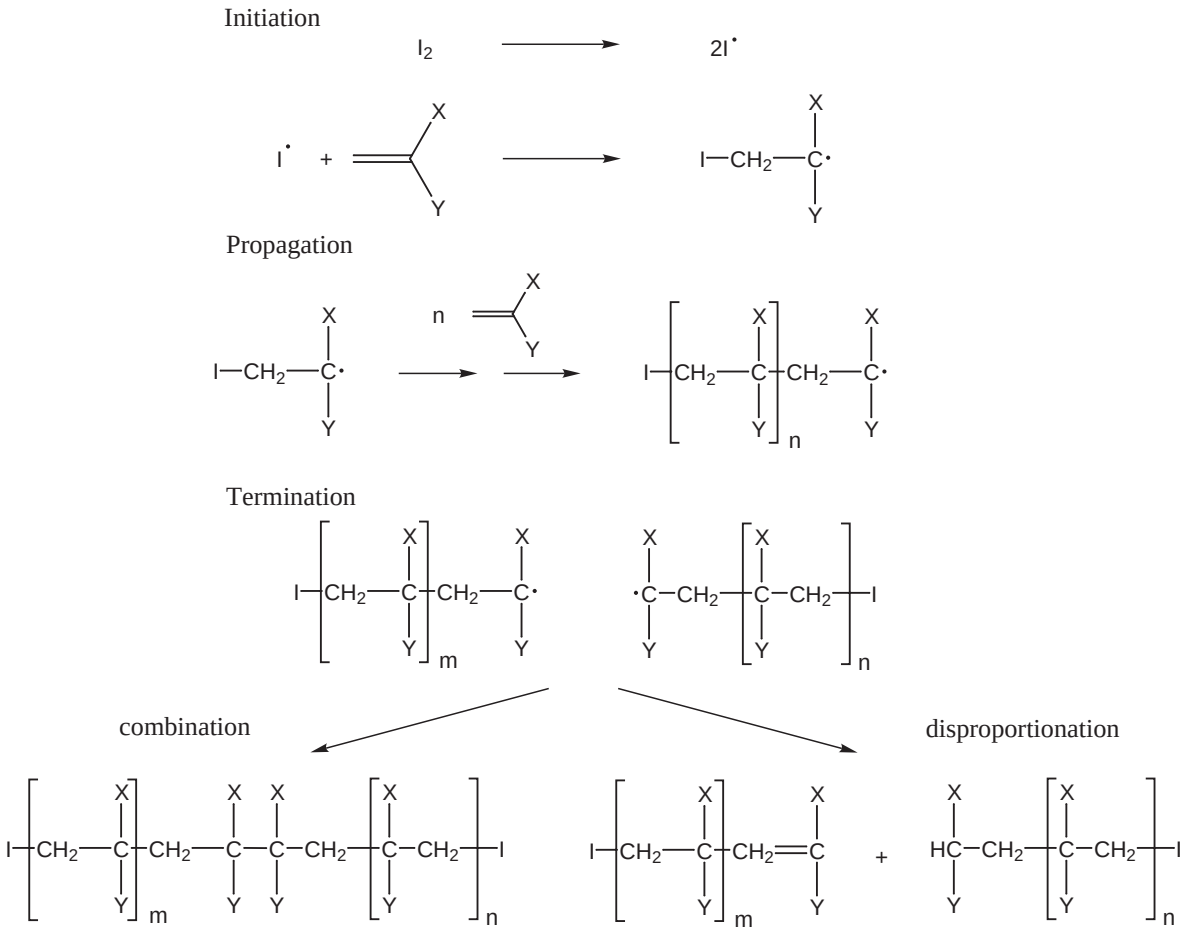

Figure 1.7: The general mechanism of free-radical polymerization [77].

The mechanistic features of the reaction and certain characteristics of the final polymer are heavily influenced by the reactivity of the monomer, expressed as its rate of propagation, or k_p. Each monomer has a unique k_p, which is primarily determined by its chemical structure; specifically, its ability to form a stable radical. Chain growth ends when termination occurs, either by combination between two unpaired free radicals, or by disproportionation, in which one radical abstracts a hydrogen from the other, thereby terminating both.

Ionic polymerization

Ionic polymerization, like free-radical polymerization, proceeds by a chain reaction, but is distinguished primarily by the ionic nature of the initiator and propagating chains. Rates tend to be faster than free-radical reactions, and the results are extremely sensitive to the presence of impurities [76]. Because the propagating species is ionic, termination can never occur by combination as in free-radical polymerization, but it can occur if the ionic centre is deactivated or destroyed by reacting with the counterion, solvent or impurities in the system.

In a sufficiently well-designed system, however, it is possible to prevent termination, giving rise to a 'living' polymerization. In such a reaction, the charged propagating centre of each polymer chain remains active once all the monomer is consumed, and can continue growing if more monomer is made available. This is particularly useful for the production of block copolymers, and polymers of well-defined molecular weights [76].

1.2.2 Controlling molecular weight

Because it has such a significant impact on the final properties of the material, control over the molecular weight and molecular-weight distribution of a polymer is a crucial issue, particularly in free-radical polymerization. A number of methods have been developed in pursuit of this goal [76, 79, 80]. These include living polymerizations, conventional chain transfer (using compounds such as alkylthiols), atom-transfer radical polymerization (ATRP) and nitroxide-mediated polymerization (NMP). Two of the most common, and those that were directly relevant to this project are catalytic chain transfer (CCT), and reversible addition-fragmentation chain transfer (RAFT), both of which are chain-transfer techniques.

One of the problems with conventional radical polymerization is the uncontrolled

nature of termination [77, 78]. There are a number of mechanisms by which this may occur. One is recombination, in which two propagating radicals irreversibly join to form a longer, dead, polymer chain. Another is disproportionation, in which one radical abstracts a hydrogen from the other to produce one saturated and one olefinic chain. With high initiator concentrations the likelihood of primary radical termination (termination by the combination of propagating chain and initiator radical) increases. To some extent the 'chain transfer to monomer' reaction may also occur, in which a propagating chain abstracts a hydrogen from a monomer, yielding a dead polymer chain and a monomeric radical [77]. These processes affect the polydispersity of the product and also make the synthesis of low molecular-weight polymers problematic. In addition, they prevent living polymerization and the production of block copolymers.

Initial attempts at reducing molecular weight in a controlled manner used chain transfer agents such as halocarbons and alkyl thiols [77,81]. These species (S) terminate propagating chains by the transfer of an atom (halogen or hydrogen respectively in the above examples), and become radicals themselves:

$$\mathrm{P}_n^{\cdot} + \mathrm{S} \xrightarrow{k_{\mathrm{tr,S}}} \mathrm{P}_n + \mathrm{S}^{\cdot} \tag{1.3}$$

In some cases, the new radical goes on to initiate a new polymer. A chain-transfer agent S is characterized by its chain-transfer constant (C_{tr}), which is defined as the ratio of the rate constant of transfer to that substance to the propagation rate constant ($k_{\mathrm{tr,S}}/k_{\mathrm{p}}$) [76]. This is an expression of how long a propagating radical will continue to grow before it undergoes a chain-transfer event.

The effect of chain transfer is to reduce the average molecular weight of the final material. The primary disadvantage is that for most conventional chain-transfer agents, large amounts must be added if a significant reduction in molecular weight is desired [77]. In syntheses of very low molecular weight species, this is not only inefficient but means the chain-transfer agent is present in the final product. This leads to issues of toxicity and the escape of volatile material.

The two techniques mentioned above address the termination-related problems of free-radical polymerization using two different approaches. Catalytic chain transfer (CCT) catalyses the chain transfer to monomer reaction; it requires only very small amounts of chain-transfer agent and leaves no substituent attached to the polymer molecules [80]. Reversible addition-fragmentation chain-transfer polymerization (RAFT) is a relatively recent discovery. Not being catalytic, this method requires the addition of

larger amounts of chain-transfer agent than CCT, and relies on the reversible capping of propagating chains. However the chemistry of RAFT agents is extremely versatile, and they provide a high degree of control over the production of both high and low molecular-weight species [82].

1.2.3 Catalytic chain transfer

In the early 1980s, Enikolopyan et al. discovered that certain cobalt complexes were able to catalyse the chain transfer to monomer reaction in methacrylate polymerizations [83, 84]. Their method produced a significant decrease in the molecular weight of the product with little effect on the yield, and required only ppm quantities of the complexes. Developments in the use of these catalysts have led to a technique that is now widely used for the production of low molecular-weight polymers and macromonomers [80].

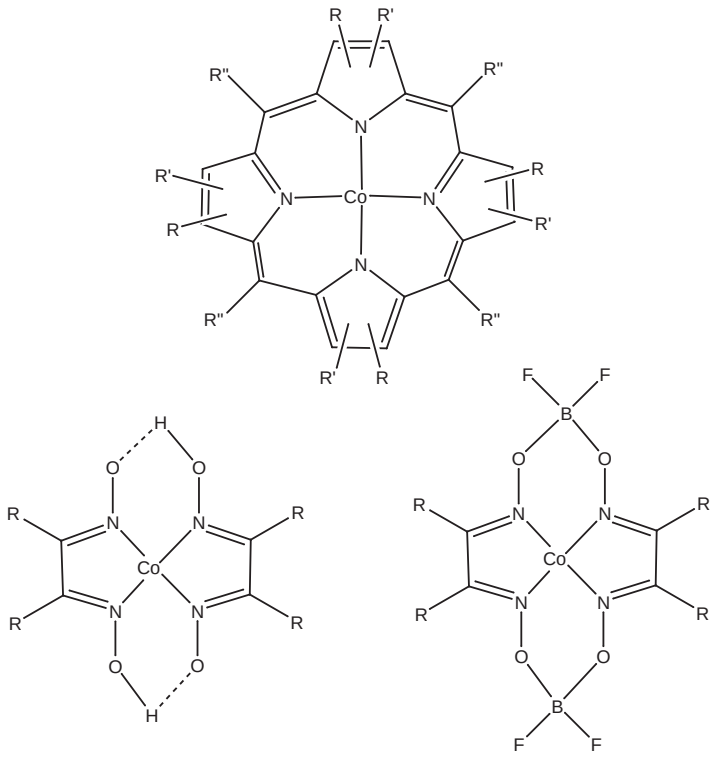

Figure 1.8: (above) cobalt porphyrins; (below) cobaloximes.

The complexes that show catalytic chain transfer activity are primarily cobaloximes and porphyrins (see Figure 1.8). Other compounds (e.g. molybdenum and chromium complexes) have also been studied, but cobalt-based species have remained the most

popular and effective. The mechanism was for some time a matter of conjecture, but is now generally assumed to involve the cobalt hydride [80, 85]:

$$\mathrm{P}_n^{\cdot} + \mathrm{LCo^{II}} \xrightarrow{k_{\mathrm{tr}}} \mathrm{P}_n^{=} + \mathrm{LCo^{III}H} \tag{1.4}$$

$$\mathrm{LCo^{III}H} + \mathrm{M} \xrightarrow{k_{\mathrm{r}}} \mathrm{M}^{\cdot} + \mathrm{LCo^{II}} \tag{1.5}$$

The reaction commences in the usual manner by the addition of an initiating species, which produces propagating radicals ($\mathrm{P}_n^{\cdot}$). Chain transfer (with rate constant k_{tr}) occurs when one of these radicals encounters the catalyst ($\mathrm{LCo^{II}}$). The catalyst abstracts a hydrogen atom from $\mathrm{P}_n^{\cdot}$, producing a dead polymer with an unsaturated terminal bond ($\mathrm{P}_n^{=}$), and the cobalt hydride ($\mathrm{LCo^{III}H}$). The reinitiation/regeneration step (1.5) occurs when the hydrogen atom is transferred to a monomer (with rate constant k_{r}), thereby regenerating the catalyst and forming a new propagating species.

Hydrides of cobalt complexes are well known in the inorganic chemistry literature. However in the presence of radicals, the lifetime of the $\mathrm{LCo^{III}H}$ species is so short as to make it impossible to observe experimentally [80].

The formation of $\mathrm{LCo^{III}H}$ is also extremely fast. Forster et al. compared chain-transfer reactions of *n*-dodecanethiol and a cobaloxime (bis[(difluoroboryl)diphenylglyoximato] cobalt(II)) with methacrylate monomers of varying viscosity. While the C_{tr} of the thiol remained similar in all cases, that of the cobaloxime decreased dramatically for the more viscous monomers. This provides strong evidence that whereas chemical control predominates in thiol chain transfer, the hydrogen abstraction by $\mathrm{LCo^{II}}$ is so fast that diffusion becomes rate-limiting [86].

The activity of chain-transfer catalysts is sensitive to a wide variety of factors, making kinetic measurements and reproducible results difficult [80]. Many of the complexes are very sensitive to the presence of oxygen, so that in addition to rigorous degassing of reaction solutions being necessary, peroxide initiators cannot generally be used. Solvent and pH are also factors, and depending on the combination of monomer and catalyst, a suite of side reactions may be possible. Despite these sensitivities, CCT is nevertheless a fairly versatile technique, and has even been shown to work in aqueous systems, although it requires a feed rather than a batch process to overcome decomposition of the catalyst [87].

Prediction of molecular weights in chain-transfer reactions generally make use of the Mayo equation [76, 88]:

$$\frac{1}{\overline{\mathrm{DP}}_n} = \frac{1}{\overline{\mathrm{DP}}_{n0}} + \frac{C_{\mathrm{tr}}\,[\mathrm{LCo^{II}}]}{[\mathrm{M}]} \tag{1.6}$$

where $\overline{\mathrm{DP}}_n$ and $\overline{\mathrm{DP}}_{n0}$ are the number-average degree of polymerization with and without the addition of chain-transfer agent.

In reactions utilizing high concentrations of a very active catalyst however (i.e. for large C_{tr} and $[\mathrm{LCo^{II}}]$), this equation can predict a $\overline{\mathrm{DP}}_n$ of less than 1. Using the assumption that the smallest unit produced in such a reaction would be a dimer, Gridnev modified this equation for cases in which species of low molecular weight (i.e. $\overline{\mathrm{DP}}_n < \sim 15$) are produced [80, 89]:

$$\overline{\mathrm{DP}}_n = 2 + \frac{[\mathrm{M}]}{C_{\mathrm{tr}}\,[\mathrm{LCo^{II}}]} \tag{1.7}$$

This relationship assumes that C_{tr} is independent of $\overline{\mathrm{DP}}_n$, which is known to be incorrect for low molecular weights. Nonetheless, it is a useful approximation, and avoids the need to determine the rate constants for all the radical species [80].

Because of the size and complexity of chain-transfer catalysts, theoretical studies of structure-function relationship are scarce. Empirical observations have revealed some common traits, however. For instance, a core of four nitrogen atoms in the ligand appears necessary; replacing some of the nitrogens with oxygen or sulfur atoms removes the catalytic nature of the complex. The shape of the complex appears to have an effect, with catalytic properties more common when the four nitrogens are coordinated in the equatorial plane and are surrounded by a planar conjugated macrocycle. Bulky substituents on the macrocyclic ligand that cause it to twist can reduce catalytic activity. The presence of an extended network of π-bonds and/or hydrogen bonds to delocalize the electron density in the complex appears to be necessary. Redox potentials have also been implicated [80].

One of the largest areas of application for catalytic chain transfer is in the production of macromonomers. The terminal double bond in CCT products makes them particularly useful for applications (e.g. paints and other coatings) requiring low-viscosity materials that can be further reacted or cross-linked for strength [85, 90]. End-group functionality can be introduced to the macromonomers, either by isomerizational CCT or by reaction of the terminal double bond [80, 85, 91]. Functionalization may also be produced by performing the CCT reaction with a mixture of monomers with very different reactivities. For instance, given a mixture of monomer A (with high k_{p} for both homo- and heteropolymerization, and low k_{tr}), and monomer B (with low k_{p} and high k_{tr}), CCT oligomers can be produced which are homopolymers of A but with a single terminal unit of B [90].

Macromonomers are also used in reversible addition-fragmentation chain transfer (RAFT; see following section), since short methacrylate oligomers and α-methylstyrene dimers are known to have RAFT functionality [80, 92].

1.2.4 Reversible addition-fragmentation chain transfer (RAFT)

The chemistry underlying reversible addition-fragmentation chain transfer was first discovered in the late 1980s by Zard et al. [93], and was later named and elaborated upon by the CSIRO Division of Molecular Science [79, 94, 95]. The number of publications relating to it has been increasing exponentially ever since, and several reviews have recently been published [82, 96–98]. The beauty of this technique lies in its versatility. It allows precise control over DP_n, produces polymers with a narrow molecular-weight distribution, and can be adapted to bulk, organic and aqueous solution reactions. In addition, it produces living polymers, making block, star and other complex polymer architectures possible. The reaction conditions it requires are generally the same as those used for conventional free-radical polymerization.

Although there are some exceptions, the vast majority of RAFT agents in current use are based on the dithioester group, to which a leaving group (R) and non-leaving or activating group (Z) are attached (Figure 1.9). The key to the chain-transfer functionality lies in a series of linked equilibria, by which the propagation of the growing polymer radical is controlled [99].

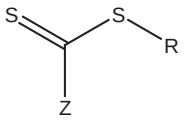

Figure 1.9: Basic structure of a RAFT agent.

Figure 1.10 shows a schematic of the mechanism of a RAFT polymerization [82, 100, 101]. The reaction begins like a conventional polymerization, with an initiator species producing radicals that react with monomer (M) to produce growing polymer chains ($P_n^{\cdot}$). At some point, these chains encounter a molecule of RAFT agent, and react with the carbon-sulfur double bond to produce a macroRAFT radical. The C=S bond then reforms, expelling either the polymer chain or R, in which case a new radical ($R^{\cdot}$) is formed. $R^{\cdot}$ can then go on to initiate the growth of a new polymer chain.

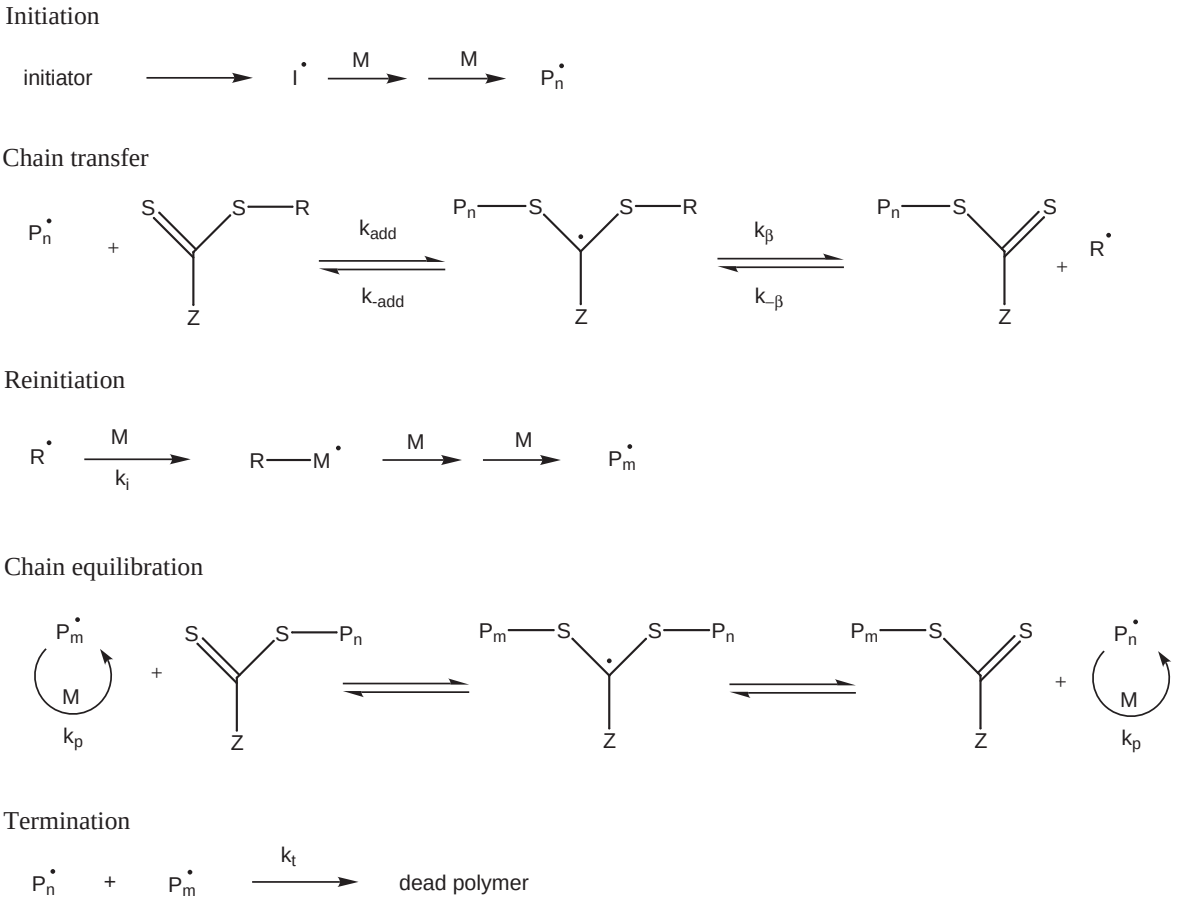

Figure 1.10: Mechanism of chain transfer with a RAFT agent [82].

Subsequently, another radical ($P_m^{\cdot}$) may react with the reformed C=S bond, expelling P_n, which then recommences propagation. After a time equilibrium is attained, with polymer chains undergoing a rapid rate of exchange between a 'dormant' state in which they are attached to a RAFT agent, and a reactive, free-radical state. Alongside these equilibria various side reactions take place, such as reversible coupling or termination due to the reaction of two radical intermediates [102, 103].

This continues until the supply of monomer is exhausted, or physical effects prevent further reaction. The product is then a polymer of low polydispersity, each molecule of which is capped by a RAFT unit. Where necessary, this can generally be removed; the most common methods are aminolysis, thermal elimination and radical-induced reduction [82].

The end result is control over the degree of polymerization and polydispersity of the

end product. In general, the molecular weight of the end product is easily predicted. In a reaction with monomer M of molecular weight m_M, RAFT agent of molecular weight m_{RAFT}, and initiator I which decomposes with efficiency f into d fragments, the theoretical number-average molecular weight ($\bar{M}_\mathrm{n}$) of the product can be described by the following expression [82, 99]:

$$\bar{M}_\mathrm{n}(calc) = \frac{[\mathrm{M}]_0 - [\mathrm{M}]_\mathrm{f}}{[\mathrm{RAFT}]_0 + df([\mathrm{I}]_0 - [\mathrm{I}]_\mathrm{f})} m_\mathrm{M} + m_\mathrm{RAFT} \tag{1.8}$$

In most cases, I is used in sufficiently small amounts that initiator-related terms can be ignored.

Before the RAFT mechanism was named, reversible chain-transfer polymerizations were reported [93, 104, 105], but problems were experienced with the polydispersity of the products. In 1998, the technique was given the name by which it is now known and the first dithioester RAFT agents were described [79]. Since then, a wide variety of RAFT agents has been synthesized [82], including functionalized dithiobenzoates, dithiocarbamates, xanthates and trithiocarbonates (see Figure 1.11). In all of these, it is the reactive C=S bond and the weak S-R bond that are responsible for the RAFT character of the molecule.

As with conventional chain-transfer agents, the chain-transfer constant (C_tr) for

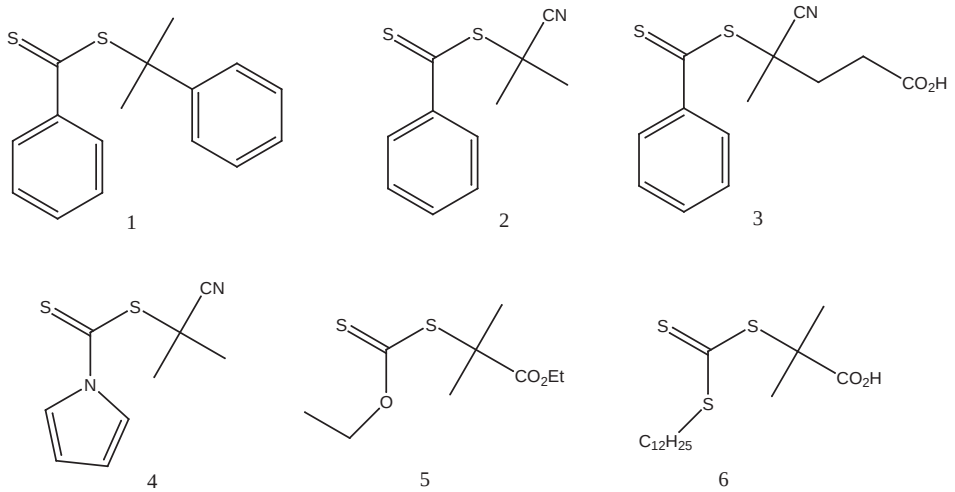

Figure 1.11: Examples of RAFT agents; cumyl dithiobenzoate (1) is one of the most versatile and widely used RAFT agents; tertiary cyanoalkyls make good leaving groups (2); the leaving group can be functionalized if desired (3); 4, 5 and 6 are examples of a dithiocarbamate, xanthate and trithiocarbonate respectively.

RAFT agents is equal to $k_{\mathrm{tr}}/k_{\mathrm{p}}$. However in this case, k_{tr} is dependent on the addition and fragmentation rate constants (see Figure 1.10, chain-transfer step) [100]:

$$k_{\mathrm{tr}} = k_{\mathrm{add}} \frac{k_\beta}{k_{-\mathrm{add}} + k_\beta} \tag{1.9}$$

Essentially, this relationship expresses the efficiency with which a molecule of RAFT agent caps a propagating radical and initiates a new one. C_{tr} is affected by a complex combination of chemical and physical conditions, and varies over five orders of magnitude for dithioester compounds [100]. These conditions include the nature of the R and Z groups, the relative reactivity of the monomer, and reaction conditions such as solvent and temperature.

For instance (see the chain-transfer step in Figure 1.10), k_{add} and k_β depend on how good a leaving group R is in comparison to monomer M (or chain P_n). If R is worse, or only slightly better, then little or no chain transfer occurs (i.e. k_{tr} is low). This difference in leaving-group ability between R and P_n also implies a different value of C_{tr} for the RAFT agent once it has capped a polymer chain. This affects the overall reaction rate and the polydispersity of the product [99]. Efficient chain transfer also relies on $\mathrm{R}^{\cdot}$ being an effective (re-)initiator [82]. Once the reaction is well under way however, the relevant leaving groups will be polymer radicals, with their own k_β and k_{add}, so that the character of the reaction changes with time.

The activating group (Z) plays a part by influencing the reactivity of the C=S bond. Aryl Z-groups tend to boost C_{tr}, with RAFT agents carrying alkyl, pyrrole, alkoxy and dialkylamino Z-groups having respectively smaller activities. Xanthates and dithiocarbamates (Figure 1.11) also have generally low transfer constants [100]. This is explained in terms of the contiguous oxygen or nitrogen atoms allowing resonance with a zwitterionic form, thereby reducing the double-bond character of the thiocarbonyl group and reducing k_{add} [94].

While many RAFT agents act as ideal chain-transfer agents, certain systems have shown inhibition (a delay in the apparent onset of reaction that corresponds to the time taken to consume the initial RAFT agent) or retardation (a decrease in the rate of polymerization) [82]. This tends to occur with RAFT agents carrying Z-groups that stabilize the intermediate macroRAFT radical [102]. The phenyl Z-group of cumyl dithiobenzoate (CDB) strongly stabilizes the macroRAFT radical, and polymerizations of CDB and styrene show significant retardation. Replacing the phenyl group with a

benzyl group removes this behaviour. Non-stabilizing Z-groups also lower the temperature at which the RAFT agent is effective [106].

A particular advantage of the RAFT technique is its living character. The polymer produced in a RAFT reaction has the functional RAFT agent as its terminal unit. Therefore, if further (perhaps different) monomer is added, the chain-transfer equilibria are re-established and the polymer chains will propagate further. In this way, block, dendritic and other complex polymers can be produced [82, 107].

The RAFT mechanism is also easily adaptable to aqueous systems, meaning it has applications in emulsion polymerization [97, 101]. It has also been adapted to the production of amphiphilic di- and triblock copolymers [108] that display self-assembly behaviour; in some cases this is pH-dependent [109, 110]. RAFT has been used to control the polymerization of cationic monomers [111, 112], and recent reports describe reactions being performed at room temperature, allowing the use of monomers sensitive to hydrolysis [113].

1.3 Aspects of the chemistry of vinylpyridines

1.3.1 General chemistry

Pyridine and pyridinium compounds have been known in the literature since the 19th century. They were found to form important components in a number of enzymes or enzyme substrates, including NADH [114], and this drove a significant body of research into their chemistry during the 20th century [115, 116].

Like other amines, the pyridine ring is basic, and in acidic solution exists in equilibrium with its protonated pyridinium form. In addition, it can react with an alkyl halide to produce an *N*-alkylpyridinium halide. This is a special case of quaternization and is sometimes referred to as the Menshutkin reaction [117–119].

2- and 4-substituted vinylpyridine compounds are extremely reactive under certain conditions, being particularly susceptible to acid-catalysed attack by nucleophiles. This is less the case for the 3-substituted isomer. The reactivity of the *ortho* and *para* isomers can be explained to a large extent by the charge delocalization made possible by resonance with a pyridone methide structure [117, 118, 120, 121]. As Figure 1.12 illustrates, the nitrogen atom in the unquaternized form must bear a negative charge. In contrast, the charged nitrogen in the quaternized form significantly increases

the electron-withdrawing power of the pyridyl ring, thereby contributing to the electrophilicity of the vinyl bond. Compounds existing in this pyridone methide structure tend to be very unstable, however, and only a few have ever been isolated [122, 123].

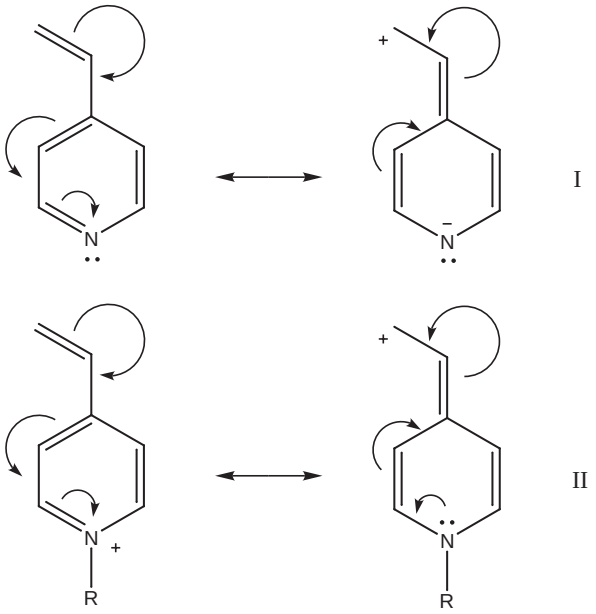

Figure 1.12: Resonance structures possible for vinylpyridine (I) and vinylpyridinium (II; R = H or alkyl).

Substantial experimental evidence has been amassed to support this idea, including studies on the reaction of quaternized vinylpyridines with cyanide and sulfite [120], sulfide [124], thiourea [125] and a wide variety of amines [126, 127]. In all cases, quaternization (either with a proton or an alkyl group) improved the rate of reaction. In some examples it was necessary for the reaction to proceed at all. Doering, for example, mentions that while hydrogen cyanide reacts readily with 2-vinylpyridine, sodium cyanide does not [120].

It has also been shown that α-methyl and methylene groups on alkylpyridinium rings (particularly in the *para* position) can undergo proton exchange with deuterium under mildly basic conditions [117, 122, 127]. The zwitterionic compound that results is stabilized by the same type of resonance (Figure 1.13). More recently, the 9-methyl group of 9,10-dimethylacridinium chloride (Figure 1.14) was shown to have a pK_{a} close to that of acetic acid (p$K_{\mathrm{a}} = 4.74$) [128]. Work on elimination reactions of (2-haloethyl)pyridines and (2-haloethyl)-*N*-methylpyridinium iodides has also demonstrated the importance of the quinonoid resonance structure in the reactivity of these species [129, 130].

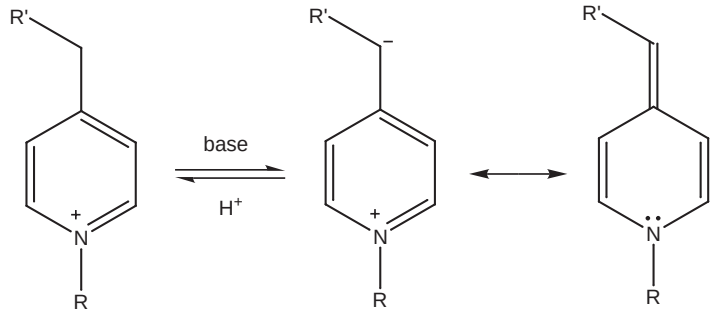

Figure 1.13: The zwitterion formed when alkylpyridiniums lose an α-proton is stabilized by resonance with the pyridone methide structure.

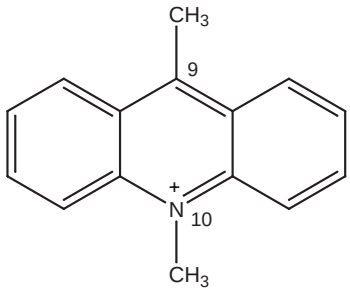

Figure 1.14: The 9,10-dimethylacridinium cation.

Vinylpyridines also possess the obvious property of being polymerizable, and have consequently enjoyed significant attention from polymer chemists (polymerization reactions of this class of compounds are dealt with in Section 1.3.2). The polymers formed from them can be extensively modified by virtue of their ability to be quaternized. Neutral polyvinylpyridine can be made a polyelectrolyte simply through the addition of acid; alternatively, it may be rendered permanently charged via the Menshutkin reaction. Thus, the polymer from a single type of monomer is not only subject to the conventional variables of molecular weight and solvent environment, but can also be changed from a neutral species, to a polyelectrolyte (fully or partially charged, permanent or pH-sensitive), or a polysoap (with varying lengths of hydrophobic chain) [131–138].

For these reasons, the quaternization of both simple pyridines [136, 139, 140] and polyvinylpyridines [141–143] has been extensively studied. Research into the kinetics of the latter reaction has shown that it proceeds at a slower rate than would be predicted on the basis of simple second-order kinetics, with solvent effects and steric and electrostatic repulsion being implicated in the retardation [137]. Work has also been done on

the viscosity, solubilization and other properties of poly-4-vinylpyridine quaternized to varying degrees with ratios of ethyl and dodecyl chains [131–134].

1.3.2 Polymerization

Some of the most extensive investigations into the chemistry of vinylpyridines and -pyridiniums have centred on the variety of ways in which they can undergo polymerization. (Note that the work described here relates only to 2- and 4-vinylpyridine.) Following initial observations that vinylpyridines exhibited 'spontaneous' polymerization under a variety of conditions [144–146], a steady stream of publications appeared on the mechanism of initiation in this reaction. The groups of Salamone, Kabanov and Ringsdorf were particularly active in this field, and their combined efforts, though not always in agreement, showed that few sets of conditions can be contrived under which this class of compounds is unable to undergo polymerization [145–163].

While a number of questions remain unanswered, the principal possible mechanisms of polymerization have been elucidated (Figure 1.16).

1. Vinylpyridine and vinyl-*N*-alkylpyridinium monomers are readily polymerized by conventional radical and ionic methods (see Section 1.2 for details of these methods) [156].

2. When small amounts of acid are added to vinylpyridine, an ionene polymer results (Figure 1.15). Initiation involves nucleophilic attack of unquaternized vinylpyridine on the activated vinyl bond of a quaternized molecule. The rate of this reaction was shown to be maximal at the pK_a of vinylpyridine; this is in accordance with a propagation step that involves an unquaternized terminal group attacking the vinyl bond of a quaternized monomer [144, 149, 151, 152, 162].

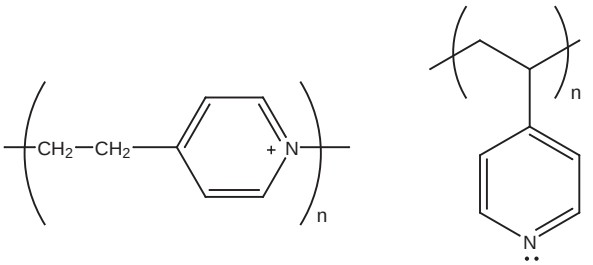

Figure 1.15: (left) Ionene and (right) conventional polymer formed from 4-vinylpyridine.

3. Vinylpyridine mixed with an excess of acid can lead to conventional polyvinylpyridine. Initiation is due to residual unquaternized vinylpyridine, meaning polymerization can be caused or prevented to a large extent by certain methods of mixing. The greater concentration of acid means that propagation cannot occur to any significant extent via the nucleophilic nitrogen. It therefore proceeds ionically via the vinyl bonds, with the zwitterionic terminal group stabilized by pyridone methide resonance [151, 152].

4. In a similar fashion, polymerization occurs during the quaternization reaction of vinylpyridine with alkyl halide [145, 146]. Permanent alkylation takes the place of the acid-base equilibrium.

5. Other nucleophilic species (e.g. sodium cyanide, various amines) can also initiate polymerization. As above, acid catalysis is necessary to activate the double bond of vinylpyridine monomers, but vinylalkylpyridiniums do not require this. Common counterions such as halides or sulfate are insufficiently reactive to initiate polymerization [151–153].

6. Polymerizable cation/anion pairs can be made by mixing vinylpyridine with acidic monomers such as vinylsulfonic acid [155]. 4-vinylpyridinium styrenesulfonate was found to be particularly susceptible to spontaneous copolymerization. This was originally thought to be due to the two species forming a charge-transfer complex which facilitated the reaction [157]. More recently, however, it has been suggested that a simple Coulombic attraction underlies the reaction [164].

7. Vinylpyridine spontaneously polymerizes when mixed with concentrated sulfuric acid. The exact mechanism has not been deciphered, but was suggested to be cationic in nature [154].

1.3.3 Charge-transfer complexes

Nitrogen heterocycles are notable in that they are commonly found in inter- and intramolecular complexes. One such class of complexes is based on charge-transfer interactions. These are defined as being strong intermolecular interactions that cannot be described using dispersion, dipole-dipole, dipole-induced-dipole or similar forces. They tend to involve simple integral ratios of the components (although exceptions exist),

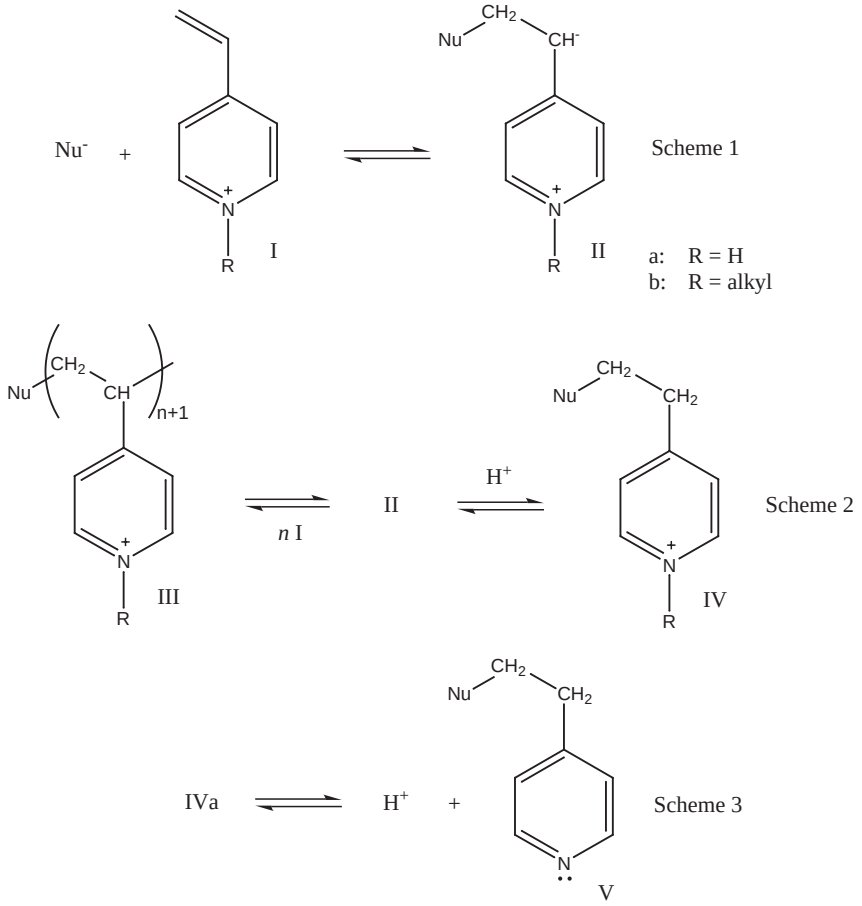

Figure 1.16: General reaction schemes for the spontaneous or nucleophile-initiated polymerization of vinylpyridines and vinylpyridiniums (after [152]). Scheme 1: Initiation takes place by nucleophilic attack on a quaternized vinylpyridine (I) producing a zwitterion (II). This species is stabilized by resonance (see Figure 1.13). Scheme 2: II can go on to react with further I, producing polymer (III). Alternatively, it may become protonated (IV). In the case of IVb, this prevents further polymerization. Scheme 3: IVa may become unquaternized and therefore nucleophilic (V), enabling further propagation to produce the ionene polymer.

and they often have very fast rates of formation and decomposition, making their development seem almost instantaneous [114].

Charge-transfer interactions take place between complementary species: electron acceptors and electron donors (see Figure 1.17), both of which can be further divided into increvalent and sacrificial types.

Donors are often aromatic molecules with electron-donating substituents or lone pairs. Increvalent donors have lone pairs (n-donors), while sacrificial donors (σ- or π-

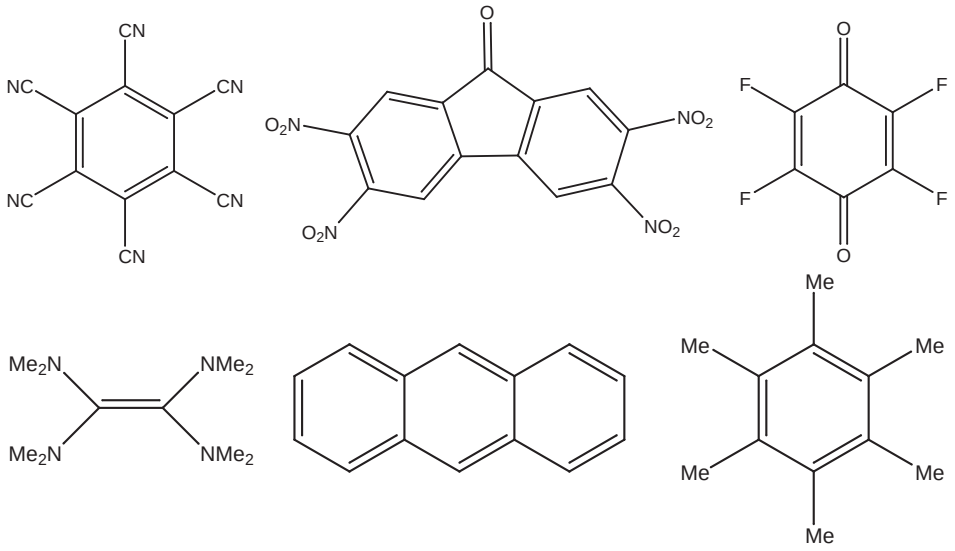

Figure 1.17: (top row) Electron acceptors - hexacyanobenzene, 2,4,5,7-tetranitrofluorenone and fluoranil; (bottom row) electron donors - tetrakis(dimethylamino)ethylene, anthracene and hexamethylbenzene.

donors) donate an electron from a bonding orbital. Some aza-aromatics and aromatic amines are able to act as both n- and π-donors.

Increvalent electron acceptors have a vacant orbital, and some (e.g. boron halides, aluminium halides and tin (IV) chloride) form such strong complexes with n-donors that covalent bonding occurs. Sacrificial acceptors can also be of σ or π type. The relatively weak σ-acceptors include hydrogen halides, halo-substituted paraffins and halogens. More common are π-acceptors, which include aromatic and other unsaturated systems (e.g. quinones, acid anhydrides, and aromatic rings substituted with electron-withdrawing groups) [114].

Charge-transfer complexes are often identified by their electronic absorption spectra, since they generally show peaks that are not present in the spectra of any of the components. These are the result of electronic transitions from the ground state to an excited state of the complex. They often appear at considerably longer wavelengths than the absorptions of the component molecules [114].

Both pyridines and pyridiniums are known to take part in charge-transfer complexes. Pyridine compounds act as electron donors; for instance, they show n-donor behaviour when mixed with iodine and IBr [114]. N-alkylpyridiniums have been shown to form complexes with halides, particularly the iodide anion [115, 165–168]. The absorption

wavelength of the complex formed by these species shows a sensitivity to the solvent environment, particularly when the pyridinium is substituted with electron-withdrawing groups. This is thought to be due to the different dipole orientations of the complex in the ground and excited states; the relative stability of these (and therefore the excitation energy of the complex) is dependent on their interaction with the solvent dipole [166].

This sensitivity has found application in the measurement of solvent polarities and ionizing power [169]. It has also been employed in the characterization of pyridinium-based surfactants. Ray and Mukerjee used shifts in the charge-transfer band shown by dodecylpyridinium halides to study critical micelle concentration, counterion binding and the polarity of the Stern layer [170–172].

Charge-transfer interactions in large molecules and polymers have also been studied. Slough made a series of studies of large aromatic molecules such as the benzoquinolines, and concluded that they could act as both donors and acceptors under different conditions [173, 174]. He also studied a variety of pyridine-based polymers – including poly-2-vinylpyridine, a copolymer of 2-vinylpyridine and styrene, and poly-2-vinyl-*N*-methylpyridinium iodide – finding that they formed charge-transfer complexes with iodide, bromide and chloride ions [175]. Mixtures of electron-donor polymers with electron-acceptor polymers have also been examined, and the properties of the resulting materials show significant differences to those of the component polymers [176].

In addition to complexes formed in mixtures, charge-transfer complexes exist which are intramolecular in nature. The prerequisite for such a complex is a molecule that contains both electron-acceptor and electron-donor groups, unconnected by a conjugated pathway. If a molecular orientation is possible such that there is sufficient overlap between the highest occupied molecular orbital (HOMO) of the donor moiety and the lowest unoccupied molecular orbital (LUMO) of the acceptor, then a charge-transfer interaction between them may occur [114]. A significant number of these compounds contain pyridine or pyridinium moieties (Figure 1.18).

A number of groups have made use of such interactions to aid in the self-assembly of large molecules [179–182]. For instance, Ghosh and Ramakrishnan synthesized a flexible polymer which they called a ‘foldamer’ [180]. It incorporates electron-donor and electron-acceptor units separated by polyoxyethylene sections. Under the correct conditions, this polymer takes on a well-defined secondary folded structure. This rearrangement is driven by the formation of charge-transfer complexes between the donor and acceptor units, and reinforced by crown-ether-type complexation of metal ions by

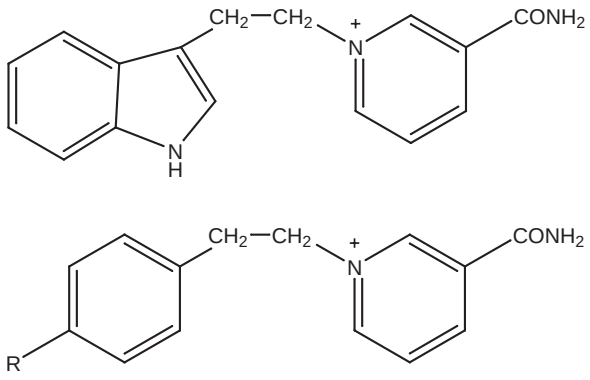

Figure 1.18: Simple chloride salts of these organic cations have been shown to undergo intramolecular charge transfer (R = H, NH_2, OCH_3, OH, CH_3, Cl) [177, 178].

the polyoxyethylene sections.

At various times, charge-transfer complexes have also been implicated in the initiation and propagation of polymerization reactions [157, 183–185]. Some reports note that while the reaction mixture is coloured, the final polymer is not [183]. In such situations, while a charge-transfer complex may well be forming among species in solution, it is unclear whether the complex plays a pivotal role in the propagation of the polymer [164]. In other situations, electron-deficient monomers that will not homopolymerize are found to spontaneously copolymerize with electron-rich monomers (e.g. trinitrostyrene with 4-vinylpyridine [184]). However, more recent work on combinations of electron-rich and -poor monomers which are unable to undergo charge-transfer complexation suggests that even this effect can be explained without resorting to charge transfer ([164] and references therein). The lack of evidence for charge-transfer complexes playing a role in polymerization reactions does not, however, preclude the existence of intramolecular charge-transfer interactions between complementary neighbouring units in an existing polymer [179–182, 184].

1.4 Aims of the project

Though the three preceding sections are somewhat diverse, they came together in this project for the purpose of developing a synthesis for oligomeric surfactants that relies on polymerization rather than conventional organic synthetic methods.

Part of the initial impetus was provided by the thesis of Kathryn McGrath [186].

McGrath was attempting to stabilize surfactant mesophase structures formed from polymerizable surfactants by initiating polymerization in situ. However in a number of systems, despite utilizing high concentrations of initiator, very low conversion was reported. This project began with the thought that in such a reaction the degree of polymerization was likely to be fairly low, and that the reaction conditions might be manipulated in order to produce a yield of oligomeric (rather than high molecular weight) species.

Such a method could be extremely useful for a number of reasons, both scientific and economic. So far, oligomeric surfactants have been synthesized from scratch, and some require long and difficult procedures. While methods are improving and production is becoming more efficient, the application of oligomeric surfactants in industry is limited by their cost, and their use in academic research tends to rely on access to a good organic synthetic laboratory. A method based on polymerization would ideally require an uncomplicated set of conditions that could easily be adjusted in order to change the molecular weight of the end product. Such a method would greatly simplify the production of oligomeric surfactants, making them more easily available for research and practical applications.

Obviously a method based on polymerization is unsuitable for producing every kind of oligomeric surfactant. The range of possible spacer groups is limited for instance, and to make asymmetric geminis a specially designed copolymerization system would have to be designed. Yet these are neither serious deficiencies nor, in the case of the latter, necessarily insurmountable. For the production of homologous series of oligomeric surfactants (i.e. the dimer, trimer, tetramer etc. of a given surfmer), such a method would be extremely useful. Homologous series have repeatedly proven to be powerful scientific tools and, using variables such as chain length, counterion and head-group size, have already been used to great effect in surfactant science [187–189].

Because of the nature of polymerization, it is unlikely that the method could be made sufficiently specific as to produce a 100% yield of a specific oligomer. Rather, by adjusting the reaction conditions the product would be tuned to contain a distribution of oligomers, centred on the desired length. If necessary, such a mixture could be purified, but it is arguable that having the power to produce a continuously variable distribution of oligomer lengths is as useful as being in possession of pure samples of each length. This has already proven to be the case with commercial polyoxyethylene surfactants, also produced by polymerization, which are not pure products but consist

of distributions of molecular weights.

In addition to considerations of economics and availability, there are other reasons for pursuing such a method. The literature contains many attempts to preserve surfactant mesophases by polymerization, a number of which have failed because the thermodynamics of the polymeric product prevented it from retaining the complex geometry and high surface area of the original mesophase. If the polymerization reaction could be controlled both in terms of rate and in the length of the molecules produced, it could serve as a tool for observing in real time the alterations in micellar or mesophase geometry due to the changing oligomer length. For this reason, it is desirable to develop a method that can be performed in aqueous solution, and which has – or can be modified to have – relatively slow kinetics.

The structure of the remainder of the thesis is as follows. Chapter 2 details the experimental methods used in the course of this work, covering organic synthesis, polymerization techniques, chemical analysis methods and the physical techniques used to characterize surfactant behaviour. Methacrylate-based surfactants were the first surfactants employed in this work, and the physical characterization of the monomers and attempts at oligomerization using free-radical methods are presented in Chapter 3. Later, vinylpyridinium-based surfactants were substituted for the methacrylates, and Chapter 4 contains the physical characterization of these compounds. Chapter 5 covers the successful oligomerization of the vinylpyridinium surfactants using a novel linkage process based on an elimination/addition reaction, while Chapter 6 shows the physical characterization of the oligomers produced. Chapter 7 looks at the unexpected pH-sensitive chromophoric properties of the pyridinium-based oligomers and possible reasons for them. Finally, Chapter 8 presents an overall discussion of the work in this thesis and its conclusions.

Chapter 2

Methods

"God bless the lost, the confused, the unsure, the bewildered, the puzzled, the mystified, the baffled, and the perplexed."

Michael Leunig

2.1 Introduction

This chapter is divided into four sections. Section 2.2 deals with the synthetic procedures and ion exchange methods used to produce the compounds in this work, and also lists the acronyms used to refer to the polymerizable surfactants. Section 2.3 details the experimental procedures used in making and attempting to make surfactant oligomers via polymerization. Section 2.4 describes the chemical analytical techniques employed for reaction monitoring and product characterization. Finally, Section 2.5 details the techniques used to physically characterize the surfactants. Unless otherwise specified, all experimental procedures were performed by the author.

2.2 Synthetic procedures

2.2.1 Naming conventions

Most of the compounds used in this work have rather cumbersome names, and are therefore referred to by acronyms. Tables 2.1, 2.2 and 2.3 give a sample structure for

each of the surfactant families mentioned in later chapters, along with the acronym for each variation within the family.

Acronym	Full name
MEODAB	*N*-(2-methacryloyloxyethyl)-*N*-octyl-*N*, *N*-dimethylammonium bromide
MEDDAB	*N*-(2-methacryloyloxyethyl)-*N*-dodecyl-*N*, *N*-dimethylammonium bromide
MEDDAC	*N*-(2-methacryloyloxyethyl)-*N*-dodecyl-*N*, *N*-dimethylammonium chloride
MEDDAA	*N*-(2-methacryloyloxyethyl)-*N*-dodecyl-*N*, *N*-dimethylammonium acetate
MEHDAB	*N*-(2-methacryloyloxyethyl)-*N*-hexadecyl-*N*, *N*-dimethylammonium bromide
MEHDAC	*N*-(2-methacryloyloxyethyl)-*N*-hexadecyl-*N*, *N*-dimethylammonium chloride
MEHDAA	*N*-(2-methacryloyloxyethyl)-*N*-hexadecyl-*N*, *N*-dimethylammonium acetate

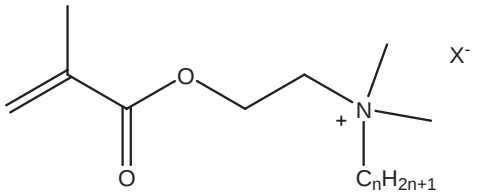

Table 2.1: The methacrylate family of surfmers. Monomer functionality is provided by the methacryloyl moiety, and in this work, the surfactant structure variables are chain length and counterion.

2.2.2 Polymerizable surfactants

MEODAB, MEDDAB, MEHDAB, 2VDPT and 4VDPT were synthesized by the Organic Synthesis Centre (OSC) at the University of Sydney, and used as received, with no impurities evident by proton NMR. Methanol of 99.5+% purity from Sigma-Aldrich was used as received. All water was deionized.

To produce the other surfactants used in this work, anion exchange was performed on the bromide and trifluoromethanesulfonate salts provided by the OSC. A typical exchange from MEDDAB to MEDDAC ran as follows. The appropriate amount of Amberlite IRA-400(OH) exchange resin was loaded into a column and rinsed with at least six column volumes of 1 M HCl (or NaCl) in 1:1 water/methanol. Excess acid or salt was then rinsed from the column using at least six column volumes of 1:1 water/methanol, or until the pH of the mobile phase returned to 7. A 0.1 M solution of

Acronym	Full name
2VDPT	2-vinyl-*N*-dodecylpyridinium trifluoromethanesulfonate
2VDPB	2-vinyl-*N*-dodecylpyridinium bromide
2VDPC	2-vinyl-*N*-dodecylpyridinium chloride
2VDPA	2-vinyl-*N*-dodecylpyridinium acetate
4VDPT	4-vinyl-*N*-dodecylpyridinium trifluoromethanesulfonate
4VDPB	4-vinyl-*N*-dodecylpyridinium bromide
4VDPC	4-vinyl-*N*-dodecylpyridinium chloride
4VDPA	4-vinyl-*N*-dodecylpyridinium acetate

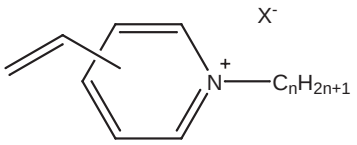

Table 2.2: The vinyldodecylpyridinium family of surfmers. Monomer functionality is provided by the vinyl moiety, and in this work, the surfactant structure variables are the ring substitution position and the counterion.

Acronym	Full name
2MDPC	2-(2-methoxyethyl)-*N*-dodecylpyridinium chloride
4MDPC	2-(2-methoxyethyl)-*N*-dodecylpyridinium chloride
4MDPB	4-(2-methoxyethyl)-*N*-dodecylpyridinium bromide

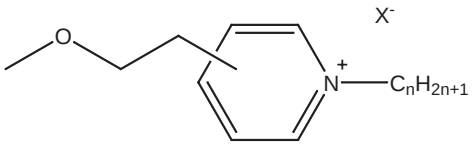

Table 2.3: The alkyldodecylpyridinium family of surfactants. These compounds are produced from the vinyldodecylpyridinium surfactants and form oligomers by an elimination/addition mechanism. In this work, the surfactant structure variables are the ring substitution position and the degree of oligomerization.

MEDDAB in 1:1 water/methanol was prepared and run through the column at a rate of about 5 mL min^{-1}. An extra 10–20 mL of mobile phase was used to flush adsorbed surfactant from the column. Methanol was then removed from the resulting solution under vacuum without heating, and the solution freeze-dried to obtain MEDDAC. In order to minimize spontaneous polymerization, care was taken to avoid exposing the

surfactant to heat or light.

Positive-ion electrospray mass spectrometry was used to ensure that no bromide remained. In this technique, in addition to the primary peak from the cation, quaternary ammonium surfactants show ion cluster peaks corresponding to two surfactant cations and one counterion [190]. This allows the presence of the more strongly binding bromide or trifluoromethanesulfonate to be detected. The exchange of the trifluoromethanesulfonate ion could also be checked with ^{19}F NMR.

2.2.3 2-phenylprop-2-yl dithiobenzoate (RAFT agent)

2-phenylprop-2-yl dithiobenzoate, also known as cumyl dithiobenzoate (see Figure 1.11), is widely used as a chain-transfer agent for reversible-addition fragmentation chain-transfer polymerization. Being unavailable commercially, it was therefore synthesized via a well-established procedure used at the Centre for Advanced Macromolecular Design (CAMD) at UNSW.

Benzyl chloride (12.6 g, 0.1 mol) was added dropwise over one hour to a round-bottomed flask containing elemental sulfur (6.4 g, 0.2 mol), 25% sodium methoxide solution in methanol (43 g) and methanol (30 mL). The resulting brown solution was then heated and allowed to reflux under dry conditions at 80°C overnight. After cooling to room temperature, the mixture was filtered to remove precipitated sodium chloride and the methanol removed under vacuum. The resulting brown solid was then redissolved in distilled water (100 mL), and washed with diethyl ether (3×50 mL). A final layer of ether was added to the solution and the two phase mixture was then acidified with 32% aqueous hydrochloric acid until the aqueous layer lost its characteristic brown colour and the top layer was deep purple. The organic layer was then dried over calcium chloride and the residual ether removed under vacuum to afford dithiobenzoic acid as a deep purple oil (11 g, 70% yield).

Dithiobenzoic acid (11 g) and α-methylstyrene (20% excess) were dissolved in n-hexane (10 mL) and allowed to reflux at 80°C overnight in the presence of a small amount of paratoluenesulfonic acid as catalyst (1%). The resulting solution was purified by washing with dilute sodium hydroxide (3×5 mL) and distilled water (3×5 mL), followed by fractional column chromatography on silica gel with hexane eluent. Hexane was removed from the final product under vacuum.

^{1}H NMR: δ 2.03 (s, 6H, CH_3), 7.20–7.86 (m, 10H, CH).

2.2.4 4-alkyl-*N*-methylpyridinium iodides

In investigating the pH-related chromophoric properties of the vinylpyridinium oligomers (see Chapter 7), it was necessary to synthesize some small, non-polymerizable analogues. These were 4-methyl-, 4-ethyl- and 4-*tert*-butyl-*N*-methylpyridinium iodide, produced by the well-known quaternization reaction of alkylpyridines with methyl iodide [119]. A typical synthesis was as follows.

4-methylpyridine (0.46 g, 5 mmol) and methyl iodide (0.95 g, 5.5 mmol) were dissolved in acetone (5 mL) and stirred overnight at room temperature. The solvent was removed under vacuum, and the residue dissolved in distilled water (5 mL) and washed with ether (3 × 2 mL). The aqueous solution was freeze-dried to give 4-methyl-*N*-methylpyridinium iodide (0.96 g, 82% yield). No impurities were detectable by proton NMR, and the product was used without further purification.

4-methyl-*N*-methylpyridinium iodide

^{1}H NMR (MeOD): δ 2.68 (s, 3H, CH_3), 4.36 (s, 3H, NCH_3), 7.92 (d, 2H, CH), 8.74 (d, 2H, N*CH*).

4-ethyl-*N*-methylpyridinium iodide

^{1}H NMR (MeOD): δ 1.36 (t, 3H, CH_3), 2.99 (s, 2H, CH_2), 4.36 (s, 3H, NCH_3), 7.95 (d, 2H, CH), 8.76 (d, 2H, N*CH*).

4-*tert*-butyl-*N*-methylpyridinium iodide

^{1}H NMR (MeOD): δ 1.46 (t, 9H, CH_3), 4.37 (s, 3H, NCH_3), 7.95 (d, 2H, CH), 8.76 (d, 2H, N*CH*).

2.3 Polymerization techniques

2.3.1 Self-initiation

Solutions of surfmer were made to a concentration of 0.1 M. For reaction in a non-self-assembled state, the surfmer was dissolved in chloroform or toluene and for micellar solutions, the surfmer was dissolved in water. Samples (1–3 mL) were prepared in glass ampoules and deoxygenated either by bubbling with nitrogen or by the freeze–pump–

thaw method. They were sealed under nitrogen and placed in a thermostatted water bath to react.

2.3.2 Excess initiator

Solutions for polymerization were prepared with initiator concentrations of 10, 20, 40, 60 or 80 mol% relative to the surfmer concentration of 0.1 M. For reaction in a non-self-assembled state, the surfmer was dissolved in chloroform, toluene or dimethylsulfoxide (DMSO), and the reaction was initiated with 2,2'-azobisisobutyronitrile (AIBN) or benzoyl peroxide. For micellar solutions, the surfmer was dissolved in water and 2,2'-azobis(2-amidinopropane) hydrochloride (V50) was used as the initiator.

Samples (1–3 mL) were prepared in glass ampoules, and deoxygenated either by bubbling with nitrogen the freeze–pump–thaw method and sealed under nitrogen. They were then placed in a temperature-controlled water bath (without stirring) at between 50°C and 80°C for around 24 hours.

Polymerizations using this technique were also performed while being monitored by small-angle neutron scattering. Samples consisted of 0.5 M surfactant in D_2O with 10 mol% V50, and were deoxygenated by bubbling with nitrogen. Sample cells (2 mm path length) were flushed with nitrogen gas, filled with reaction solution and capped. The samples were placed in the thermostatted sample holder and heated to 80°C. Spectra were acquired every 10 minutes for up to 2 hours.

2.3.3 Reversible addition-fragmentation chain transfer

Polymerizations using the reversible addition-fragmentation chain transfer (RAFT) technique were carried out in dimethylsulfoxide with 0.1–0.5 M surfmer, 1–5 mol% AIBN or V88 as initiator and the appropriate mole percent of cumyl dithiobenzoate (Section 2.2.3). Samples (5–10 mL) were prepared in small round-bottomed flasks, sealed with rubber septa and deoxygenated by bubbling with nitrogen for a time appropriate to the reaction volume. They were then placed in a 60°C water bath with magnetic stirring for between 22 and 24 hours.

Where a RAFT reaction was to be monitored by infrared spectroscopy (see Section 2.4.3), the sample was mixed and transferred to a 10 mm pathlength Infrasil cell (Starna Optical). This was sealed with a rubber septum and the solution carefully bubbled with nitrogen. The cuvette was then placed in the heated sample holder in the

spectrometer, and brought up to the required temperature to initiate the reaction.

2.3.4 Catalytic chain transfer

The catalyst used in these polymerizations was bis[(difluoroboryl)diphenyl-glyoximato] cobalt(II) (PhCOBF). This was a gift from John Biasutti and Christopher Barner-Kowollik at CAMD, who estimated the chain-transfer constant to methyl methacrylate ($C_{s(MMA)}$) to be between 5000–10000. It was used as received.

Methyl methacrylate and dimethylaminomethacrylate

Bulk polymerizations of the 'model' monomers, methyl methacrylate (MMA) and dimethylaminomethacrylate (DMAEMA), were carried out with PhCOBF as chain-transfer catalyst and AIBN as initiator. Dilute polymerizations were performed on monomer solutions of approximately 2 M in ethyl methyl ketone (EMK) using the same catalyst and initiator. A typical procedure follows.

Monomer or monomer solution (10 mL) was deoxygenated by bubbling with nitrogen for approximately 30 minutes. Using a vacuum-tight syringe to exclude oxygen, it was then added to a sealed Schlenk flask containing 1 mol% AIBN and sufficient PhCOBF to give a theoretical degree of polymerization of 2. Both the syringe and the Schlenk flask had previously been evacuated and flooded with nitrogen four times. The sealed flask was then placed in a thermostatted water bath at 60°C for 4-5 hours. The reaction was stopped by cooling the flask, and the polymer was then isolated by evaporating off solvent and/or residual monomer, first in a fume cupboard, and then in a vacuum oven at 30°C.

Methacrylate surfactants

Polymerizations of MEDDAB and other methacrylate surfactants were performed on 1 N solutions of the monomer in EMK, with PhCOBF as catalyst and AIBN as initiator. A typical procedure follows.

EMK (12 mL) was deoxygenated by bubbling with nitrogen for approximately 40 minutes. PhCOBF (1×10^{-3} g) and AIBN (5×10^{-3} g) were weighed into one Schlenk flask, and MEDDAB (1.65g) was weighed into another. Both of these were evacuated and flushed with nitrogen four times. Using a vacuum-tight, deoxygenated syringe, 7 mL of EMK were transferred to the catalyst/initiator Schlenk flask, and 1 mL of the

resulting mixture was then transferred to the MEDDAB flask. A further 3 mL of pure solvent was then added to the MEDDAB flask, giving a total solvent volume of 4 mL. The sealed MEDDAB flask was then placed in a thermostatted water bath at 60°C for 4-5 hours. The reaction was stopped by cooling the flask, and the solvent was removed from the polymer by evaporation in a fume cupboard.

2.3.5 Alkylpyridinium unimers and oligomers

2- and 4-(2-methoxyethyl)-*N*-dodecylpyridinium unimers

The vinylpyridinium surfactants were converted into methoxyethyl-substituted compounds by nucleophilic addition of methoxide. The method was identical for both isomers. A typical procedure follows.

4-vinyl-*N*-dodecylpyridinium chloride (0.7 mmol) was dissolved in methanol (50 mL), and sodium hydroxide (0.35 mmol) in methanol (50 mL) was added to it quickly and with vigorous stirring. The colourless solution immediately became yellow, and then rapidly green. Approximately sixty seconds after adding the hydroxide solution, the reaction was quenched by the addition of concentrated hydrochloric acid (0.1 mL or as much as was required to turn completely remove the green colour). The methanol was removed by evaporation under vacuum, and the product dissolved in acetone and filtered to remove salt and oligomeric species. The acetone was removed by evaporation under vacuum to give a viscous liquid.

This was purified using a variation of the chromatographic method described by Bluhm and Li [47, 191]. A column of silica gel was passified with 12 wt% NaBr in methanol, rinsed with pure methanol, and the surfactant was then eluted with 85:15 v/v chloroform/methanol. The fractions were collected and analysed on TLC plates that had been soaked in 6 wt% NaBr in methanol and then dried. The eluent was evaporated from the combined fractions under vacuum.

Excess sodium bromide from this process was removed from the surfactant by dissolving it in water and then extracting it into chloroform. The chloroform was removed under vacuum to give 4MDPB as a waxy solid. The chloride salt could be obtained by ion exchange using the method described in Section 2.2.2.

It should be noted that the purified unimer showed a very high tendency to spontaneously oligomerize, particularly upon removal of chloroform. For this reason, a small amount of acetic acid was generally added to the chloroform solution before evapora-

tion. This prevents the LELA reaction and – at least in the case of dilute aqueous solutions – does not have a significant impact on the surfactant's physical behaviour.

2-(2-methoxyethyl)-*N*-dodecylpyridinium chloride

^{1}H NMR (MeOD): δ 0.90 (t, 3H, CH_3), 1.3–1.4 (broad s, 18H, $(CH_2)_9CH_3$)), 1.97 (m, 2H, NCH_2CH_2), 3.34 (s, 3H, OCH_3), 3.44 (t, 2H, $CHCH_2CH_2O$), 3.86 (t, 2H, $CHCH_2CH_2O$), 4.67 (t, 2H, NCH_2), 7.94 (t, 1H, $NCHCH$), 8.10 (d, 1H, $CCHCH$), 8.48 (t, 1H, $CCHCH$), 8.91 (d, 1H, $NCHCH$).

^{13}C NMR (MeOD): δ 14.4 (CH_3), 23.7, 27.4, 30.2, 30.4, 30.5, 30.6, 30.7, 31.9, 33.0 (carbon chain), 33.8 (CH_2CH_2O), 59.2 (OCH_3), 59.5 (NCH_2), 71.1 (CH_2CH_2O), 127.1 ($NCHCH$), 130.8 ($CCHCH$), 146.3 ($CCHCH$), 146.7 ($NCHCH$), 158.4 (C).

4-(2-methoxyethyl)-*N*-dodecylpyridinium chloride

^{1}H NMR (MeOD): δ 0.90 (t, 3H, CH_3), 1.3–1.4 (broad s, 18H, $(CH_2)_9CH_3$)), 1.99 (m, 2H, NCH_2CH_2), 3.19 (t, 2H, $CHCH_2CH_2O$), 3.34 (s, 3H, OCH_3), 3.77 (t, 2H, $CHCH_2CH_2O$), 4.57 (t, 2H, NCH_2), 7.99 (d, 2H, $NCHCH$), 8.85 (d, 2H, $NCHCH$).

^{13}C NMR (MeOD): δ 14.4 (CH_3), 23.7, 27.2, 30.1, 30.4, 30.5, 30.6, 30.7, 32.4, 33.0 (carbon chain), 36.7 (CH_2CH_2O), 59.0 (OCH_3), 62.3 (NCH_2), 71.6 (CH_2CH_2O), 129.7 ($NCHCH$), 144.9 ($NCHCH$), 162.4 (C).

2- and 4-(2-methoxyethyl)-*N*-dodecylpyridinium oligomers: the LELA reaction

Oligomers of the vinylpyridinium surfactants were produced by a similar method to the unimer. Monomer was dissolved in methanol to a concentration of approximately 15-20 mM. A similar volume of sodium hydroxide in methanol (of varying concentration) was added to the monomer solution quickly and with vigorous stirring. The reaction was quenched when desired by the addition of concentrated hydrochloric acid, and the methanol removed by evaporation. The product was dissolved in chloroform, filtered to remove salt, and the solvent removed under vacuum. The residue was then dissolved in water and filtered to remove any longer insoluble polymer, and finally freeze-dried to give the oligomeric mixture as a viscous isotropic liquid.

Oligomers could also be produced by directly from the MDP unimers. In this case, the pH of a solution of 2- or 4MDPC unimer was raised and oligomerization proceeded

spontaneously. The reaction was quenched when desired by the addition of hydrochloric or acetic acid. Work-up then proceeded as described above.

Oligomers of 2-(2-methoxyethyl)-*N*-dodecylpyridinium chloride

^{1}H NMR (MeOD): δ 0.90 (t, 3H, CH_3), 1.3–1.4 (broad s, 18H, $(CH_2)_9CH_3$)), 1.98 (m, 2H, NCH_2CH_2), 2.36 (m, 2H, backbone), 3.34 (s, 3H (dependent on oligomer length), OCH_3), 3.54 (m, 1H, backbone), 4.68 (t, 2H, NCH_2), 8.00 (t, 1H, NCH*CH*), 8.36 (d, 1H, C*CH*CH), 8.60 (t, 1H, CCH*CH*), 8.99 (d, 1H, N*CH*CH).

Oligomers of 4-(2-methoxyethyl)-*N*-dodecylpyridinium chloride

^{1}H NMR (MeOD): δ 0.90 (t, 3H, CH_3), 1.3–1.4 (broad s, 18H, $(CH_2)_9CH_3$)), 2.01 (m, 2H, NCH_2CH_2), 2.25 (m, 2H, backbone), 3.34 (s, 3H (dependent on oligomer length), OCH_3), 3.54 (m, 1H, backbone), 4.60 (t, 2H, NCH_2), 8.22(d, 2H, NCH*CH*), 8.93 (d, 2H, N*CH*CH).

2.4 Chemical analysis techniques

2.4.1 Size exclusion chromatography

Initial SEC measurements were performed by Dr. Chris Ferguson in the Key Centre for Polymer Colloids at the University of Sydney. Samples were dissolved in an appropriate solvent (generally THF or methanol) at a concentration of approximately 10 mg mL^{-1}.

Later measurements were performed at CAMD using a Shimadzu modular LC system comprising a solvent degasser, pump, autoinjector, column oven, and refractive index detector. The system was equipped with a Polymer Laboratories 5.0 μm bead-size guard column (50 × 7.5 mm), followed by four linear PL/Phenomenex columns (105, 104, 103 and 100 Å). The eluent was THF at 40°C with a flow rate of 1 mL min^{-1}. Calibration curves were generated using both poly(methyl methacrylate) and polystyrene standards in molecular weight ranges between 580 and 1.95×10^6 g mol^{-1}. The injection volume was 50 μL (3 to 5 mg mL^{-1}). SEC traces were evaluated using the Cirrus 2.0 software package (PL).

2.4.2 High-performance liquid chromatography

HPLC was performed using a Waters system comprising a manual pump, autosampler, guard column, reverse-phase C18 Symmetry 5.1 μm column, conductivity detector and ultraviolet-visible absorbance detector. The UV-VIS detector was used principally for the pyridinium surfactants. Analytes were first scanned in a conventional UV-VIS spectrophotometer to determine the wavelength of maximum absorbance, and this was then entered into the Waters detector. For 2- and 4-substituted compounds, these maxima were 269 nm and 257 nm respectively.

For the analysis of conventional surfactants and the polymerizable surfactants, the mobile phase consisted of a solution of 0.2 M sodium chloride in methanol/water (generally 10 or 20 vol% water) pumped at 0.7 mL min^{-1}. For the more hydrophobic mixtures of oligomers, the mobile phase was 0.2 M sodium chloride in 80 vol% methanol, 10 vol% water and 10 vol% dichloromethane. The organic solvents were chromatographic grade, the water was deionized and the sodium chloride was reagent grade. The mixed mobile phases were filtered under vacuum and degassed by sonication.

In order to unambiguously identify the vinylpyridinium oligomers produced by the anionic reaction (Section 2.3.5), HPLC coupled with mass spectrometric detection was used. This was done with the help of Dr. Kelvin Picker in the School of Chemistry's in-house separations laboratory. Data were obtained on a TSP system consisting of a vacuum membrane degasser, pump, autosampler, Phenomenex Luna C18 (2) column (150 $\times$ 2.0 mm ID, 5 μm particle size), photodiode array detector and a ThermoQuest Finnigan LCQ Deca mass spectrometer with electrospray inlet. Samples were eluted at a rate of 0.2 mL min^{-1} on a solvent gradient running from 0.2 M sodium acetate in 80 vol% methanol, 10 vol% water and 10 vol% dichloromethane to 0.2 M sodium acetate in 90 vol% methanol and 10 vol% dichloromethane.

2.4.3 Near-infrared spectroscopy

High initiator and RAFT-controlled polymerizations of MEDDAB (see Section 3.3) were monitored with on-line Fourier transform near-infrared (FT-NIR) spectroscopy. Monomer conversions were determined by following the decrease in intensity of the first overtone of the stretching vibration of the α-C-H on the double bond (6170 cm^{-1}). Measurements were taken using a Bruker IFS66\S Fourier transform spectrometer equipped with a tungsten halogen lamp, a CaF_2 beam splitter, thermostatted cuvette holder and

a liquid-nitrogen-cooled InSb detector. Samples were prepared as described in Section 2.3.3. Each spectrum was collected over the range $8000 - 4000\,\mathrm{cm}^{-1}$, and was calculated from the added interferograms of twelve scans with a resolution of $4\,\mathrm{cm}^{-1}$. For conversion determination, a linear baseline was selected between 6240 and $6120\,\mathrm{cm}^{-1}$. The integrated absorbance between these two points was subsequently used to calculate the monomer to polymer conversion via Beer-Lambert's law.

2.4.4 Mass spectrometry

Much of the mass spectrometric identification in this work (electrospray and MALDI) was peformed by Dr. Keith Fisher in the School of Chemistry's internal mass spectrometry unit. With the assistance of Andrew Ah Toy at CAMD, attempts were made to identify MEDDAB oligomers using the Centre's Thermo Finnigan LCQ Deca ion-trap electrospray mass spectrometer. This instrument was coupled with a Thermo Finnigan HPLC system comprising a solvent-mixing unit, pump, auto-sampler, two low molecular-weight, high-resolution size exclusion chromatography columns (Phenomenex Phenogel 50 and 100 Å, bead size $5\,\mu$m, column temperature 25°C) and a UV/VIS detector set to the absorption maximum of the dithiobenzoate end groups in the polymeric material at 500 nm.

As described in Section 2.4.2, the identification of vinylpyridinium oligomers was performed by Kelvin Picker in the School of Chemistry's separations unit using an LC-MS system.

2.4.5 Nuclear magnetic resonance

NMR experiments in this work were conducted on the School of Chemistry's Bruker Avance 300MHz machine at 300K. Deuterated chloroform, methanol and water were used as solvents and the solvent residual peak was used as a reference.

2.4.6 Ultraviolet-visible spectroscopy

All ultraviolet-visible absorption measurements were taken using a Cary 5E spectrophotometer, using a 10 mm pathlength quartz cell with a ground glass stopper. For the alkylpyridinium charge-transfer experiments in Chapter 7, methanol solutions of known alkylpyridinium concentration were prepared and an initial spectrum collected. The

cuvette was then removed from the spectrophotometer and the relevant amount of triethylamine pipetted into it. The lid was replaced and carefully inverted several times to ensure mixing. Spectra were then collected every fifteen minutes for the duration of the experiment.

2.5 Physical characterization of surfactants

2.5.1 Critical micelle concentration: conductimetry

The critical micelle concentration (CMC) of surfactants can be detected by a variety of methods, all of which rely on a change in the physical characteristics of the solution when micellization occcurs. One of the most common methods for ionic surfactants is conductimetry, because of its simplicity and its insensitivity to impurities [192].

CMCs are determined by measuring the conductivity of a surfactant solution as a function of the surfactant concentration. A plot is obtained with two linear regions that intersect at the critical micelle concentration (see Figure 2.1). The reduced slope of the region above the CMC reflects the fact that all of the surfactant ions added after the CMC are incorporated into micelles, therefore contributing less to an increase in the conductivity of the solution. That in general there is still a positive slope after the CMC is due to the contribution of the micelles and of free surfactant counterions.

The degree of micelle ionization (α) is the charge carried by each micelle normalized to the aggregation number N, and is calculated as $\alpha = 1 - Q/N$, where Q is the number of counterions bound to the surface of the micelle. This is estimated by taking the ratio of the slopes of the two regions in the conductivity plot [193].

The CMCs in this work were all determined using this method. A solution of the surfactant was prepared with a concentration of around twenty times the estimated CMC. This was titrated into 20 mL of deionized water in a jacketed beaker, thermostatted at 25°C. Conductivity measurements were taken with an Oakton CON500 conductimeter, and plotted against surfactant concentration to determine the CMC.

2.5.2 Solution behaviour: small-angle neutron scattering

Scattering techniques are a common tool in surfactant chemistry, and are used for characterizing both micellar and ordered mesophase structures [194]. Small-angle neutron scattering is particularly useful for micellar systems, because the significant difference

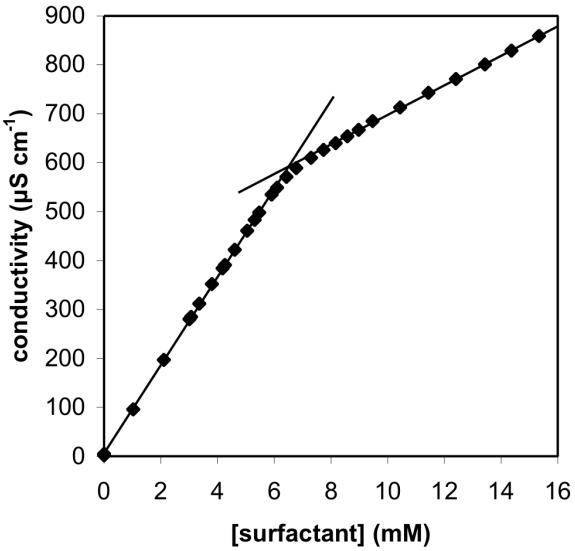

Figure 2.1: Sample conductivity plot; the CMC is taken as the concentration at the intersection of the two linear regions.

in scattering length density between hydrogen and deuterium means that excellent contrast can be obtained between, for example, micelles of a hydrogenous surfactant and a continuum of heavy water.

Small-angle neutron scattering experiements were performed at the National Center for Neutron Research (NCNR) at the National Institute for Standards and Technology (NIST) in Gaithersburg, Maryland, USA. Samples of surfactant were made up at the required concentration in D_2O (99.8 atom% D, Sigma-Aldrich) and loaded into either the NCNR's locally machined titanium demountable cells with quartz windows, or quartz 'banjo' cells (Hellma), both having a 1 mm pathlength.

Measurements on most of the methacrylate and vinylpyridinium surfactants were performed in December 2004 using the NG-1 8 m (source-to-detector distance) instrument. Cells were placed in a water-jacketed automatic sample-changer; 'room temperature' was set at 23°C. For most samples, spectra were collected at sample-to-detector distances of 2.3 and 3.8 m, with the collection time generally 10–15 minutes. The momentum transfer range was $0.03 < q < 0.30\,\text{Å}^{-1}$.

All other measurements, including the kinetic oligomerization runs, were performed in April 2006 on the 30 m (source-to-detector) instruments NG-3 and NG-7. Cells were placed in a water-jacketed automatic sample-changer; 'room temperature' was set at 25°C. Most spectra were collected at sample-to-detector distances of 1.2, 5 and 13.5 m.

The momentum transfer range was $0.003 < q < 0.50\,\text{Å}^{-1}$.

Samples for the kinetic runs were mixed immediately before being loaded into the cell and placed in the beam; spectra were collected at 1.8 m at a maximum frequency of one per minute in order to capture as much relevant information as possible.

Scattering spectra were corrected for background and transmission and radially averaged using the NCNR's data reduction package. Fitting was performed using the institute's model package which was put together by Steve Kline (http://www.ncnr.nist.gov/resources/). Micelles were assumed to scatter as homogenous hydrocarbon droplets, with the contrast calculated as the difference between the scattering length densities of D_2O and dodecane.* Errors for each parameter in a multivariate fit are calculated individually by Igor, and were found to be less than 1%. Overall errors for combinations of parameters are not calculated.

2.5.3 Solution behaviour: small-angle X-ray scattering

While neutron scattering provides the best manner of observing dilute micellar solutions, the narrow wavelength distribution of small-angle X-ray scattering – in which contrast is provided by differences in electron density – make it a better method for characterizing highly ordered materials. Liquid crystalline phases are easily identified by the spacing of their diffraction peaks, with the q-value of these used to calculate lattice spacings [194].

The small-angle X-ray scattering data discussed in Chapter 6 were collected by Jeannette McAlpine at the ANSTO facility in Sydney. A 30 wt% solution of 4MDPC was allowed to equilibrate for two days and was then loaded into glass capillaries and sealed with capillary wax. Measurements were performed on a Bruker Nanostar with a rotating anode Cu K_α (1.541 Å) source, three pinhole collimation and a q range of $0.005 - 0.2\,\text{Å}^{-1}$.

2.5.4 Phase behaviour: polarizing optical microscopy

The easiest and most common method of investigating the aqueous phase behaviour of surfactants is to perform a flooding or penetration experiment. A small amount of surfactant is placed on a microscope slide and a coverslip is carefully pressed down over it. Water is introduced at the edge of the coverslip, and is drawn under it by capillary

*Modelling the micelles as core-shell particles was not found to improve the results.

forces. A concentration gradient then forms between the pure surfactant in the centre of the slide, and a dilute aqueous solution at the edge of the slide. Between these two extremes, the surfactant/water mixture must span every intermediate concentration, and as a result, the observer is usually able to detect every mesophase formed by the surfactant. Because evaporation from the edge of the coverslip is relatively fast and can produce undesirable mixing effects, the slide/coverslip arrangement is often replaced by a flat capillary, with surfactant and water introduced from opposite ends.

Detection and identification of these phases is made possible by placing the slide or capillary on a microscope fitted with two polarizing filters that are rotated at 90^o to each other. With nothing between these films, light filtered through the first has a polarization perpendicular to that of the second, and is therefore prevented from passing through to the observer. This allows isotropic and anisotropic surfactant phases to be distinguished. When an isotropic sample is placed between the polarizers, the symmetry of the sample does not alter the polarization of the light, and the image remains dark. However, when an anisotropic (birefringent) sample is placed between the polarizers, the light is partially scattered and depolarized, which allows a proportion of it to pass through the second filter and be detected.

Different anisotropic phases display characteristic optical textures when viewed between polarizers. These textures were originally identified empirically [195], and no model has yet appeared that describes accurately how they are produced. Nevertheless, they are readily reproducible. Isotropic phases (bicontinuous cubic, micellar cubic and micellar) cannot be so unambiguously recognized. However, their position in the concentration gradient relative to the birefringent phases generally allows them to be identified. In addition, the shape of an air bubble in a cubic phase is often indicative: the bubble may be deformed by the highly viscous, gel-like phase.

Polarizing optical microscopy was performed on surfactants using a Leica DMLB microscope equipped with crossed polarizers, quarter-wave plate and DC 300 digital camera. Where elevated temperatures were required, a Linkam heating plate (maximum temperature 62.5°C[†]) was placed underneath the sample on the microscope stage.

[†]The actual temperature of the sample was generally several degrees cooler than this, depending on the ambient temperature.

2.5.5 Adsorbed layer structure: atomic force microscopy

Atomic force microscopy (AFM) is now a commonly used technique in many areas of research. In surfactant science it is principally used for imaging and characterizing films and structures at the solid-liquid interface. An atomic force microscope consists of a fluid cell which contains the sample, and a nanoscopic tip that is used to scan the surface of interest. As the tip interacts with the surface, its movement is detected by the deflection of a laser beam onto a photosensitive diode. A variety of force-related information can be acquired from this interaction, including electrostatic repulsion, friction and spring constants. In the case of adsorbed surfactant layers, an important function of AFM is the ability to provide images of the adsorbed structures. Imaging is usually conducted in soft-contact mode, in which the tip is deflected by electric double-layer repulsion while being scanned over the surfactant layer.

In this work, atomic force microscopy by soft-contact imaging was carried out by Dr. Robert Chan and Regina Schwering using a Multimode Scaning Probe Microscope with a Nanoscope III controller (Veeco Instruments Inc). Silicon nitride cantilevers with nominal spring constants of $0.3\,\mathrm{nm}^{-1}$ were cleaned under ultraviolet light for thirty minutes prior to use. Mica was used as the substrate and was cleaved at least twice using adhesive tape. The surfactants were generally made up to concentrations of one or two times their critical micelle concentration. Samples were injected into the AFM cell and allowed to thermally equilibrate for at least two hours before imaging was performed. A scan rate of 12–15 Hz was used for scan sizes of 200–300 nm.

Chapter 3

Methacrylate surfactants

"The more he looked inside the more Piglet wasn't there."

A. A. Milne, The House At Pooh Corner

3.1 Introduction

A common polymerizable moiety appearing among surfmers is the methacryloyl group. In general, it is attached either as part of the surfactant's alkyl tail, or to its hydrophilic head. The latter structure is the basis for a family of methacrylate-based surfactants, which are synthesized by quaternization of dimethylaminoethylmethacrylate (DMAEMA) with alkyl bromides [196,197]. A common example is the C12-tailed *N*-(2-methacryloyloxyethyl)-*N*-dodecyl-*N*, *N*-dimethylammonium bromide (denoted MEDDAB; see Table 2.1 for naming conventions).

While the C16 variant (MEHDAB), was first described in 1984 as a catalyst for the surface hydrolysis of polyester fabric [198], more complete characterizations of the methacrylate/bromide by Nagai et al. [196, 199] and Hamid and Sherrington [197, 200] appeared shortly after. The first mention of MEDDAB in polymeric form had in fact appeared earlier. Panarin et al. described a cationic copolymer incorporating MEDDAB units; DMAEMA and vinylpyrrolidone had been copolymerized, and then reacted with alkyl halides to form the ammonium salts [201].

In more recent times, these surfmers have found application in a variety of areas, particularly in the polymerization of self-assembled surfactant systems. They have been used to investigate the in situ polymerization of micelles [73, 202–204], and in

attempts to preserve the structure of lyotropic mesophases such as the sponge [205], hexagonal [206] and lamellar phases [70]. These studies have met with varying degrees of success, due to the insoluble nature of the homopolymers [196].

A variety of copolymers have also been produced [65,205,207,208], both through the direct reaction of the surfmers with various conventional monomers, or by full or partial quaternization of polymerized tertiary amines, as described by Panarin et al. [201]. Both copolymers and homopolymers have been used in the encapsulation of silica particles [209], and as catalysts, coagulants, demulsifiers, dispersants, decolourants and antimicrobial hydrogels. The $MEDDA^+$ cation has also been paired with polymerizable counterions, such as 2-methacryloyloxyethylsulfonate; the ionomers which result from polymerizing these species are believed to display interesting rheological properties [210].

It has also been noted that these and related compounds undergo spontaneous polymerization; that is, without deliberate chemical or photolytic initiation. Yasuda et al. found that surfactants with longer alkyl chains displayed higher rates of spontaneous polymerization [211], suggesting that the self-assembly of the molecules was important. In more recent work on neutral and cationic methacrylates and methacrylamides, Kazantsev and Kuznetsova proposed a radical mechanism for this phenomenon [212, 213].

From a surfactant chemistry point of view, the solution and phase behaviours of the methacrylate surfactants have also been investigated. Some inconsistencies exist in the literature; the value of the critical micelle concentration (CMC) of MEDDAB represents a case in point. In their original characterization of MEDDAB and its homopolymer, Nagai et al. obtain a value of 6.0 mM using dye solubilization and conductivity [196]. Hamid and Sherrington find between 1.9 and 3.6 mM using dye absorption, surface tension and conductivity measurements [197], and McGrath and Drummond cite 7.3 mM using conductivity [70]. Recently, Gutierrez-Hijar et al. used a variety of techniques to obtain three separate values: 0.78 mM, 2.0 mM and 6.9 mM. The first two are attributed to premicellar aggregation and CMC respectively. In the case of the third, the authors use indirect observations to assign it as a sphere-to-rod transition [214].

It is well established that dodecyltrimethylammonium bromide (DTAB) has a CMC of 14–15 mM [215]. Whatever is believed to be the true CMC for MEDDAB, it is clear that it is lowered relative to DTAB. The addition of the ethyl methacrylate group must therefore increase the overall hydrophobicity of the molecule, despite the presence of the

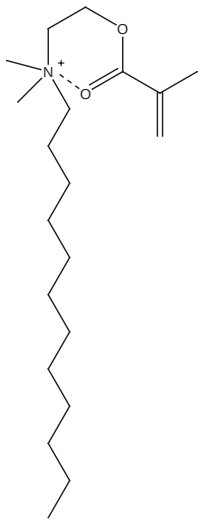

Figure 3.1: Intramolecular association of methacrylate surfmers, proposed by Hamid and Sherrington [197].

polar ester moiety. Hamid and Sherrington suggest [197] that this is due to the overall charge density of the molecule being reduced by an intramolecular association between the carbonyl oxygen and the ammonium centre (see Figure 3.1). Though no direct evidence exists for this structure, the explanation has proven popular [70, 206, 214, 216].

Work has also been performed on the concentrated phase behaviour of MEDDAB [70,206]. Pawlowski et al. examined the mesophases of MEDDAB both in its monomeric state and after exposure to varying doses of γ-ray irradiation. At low conversion, the surfactant forms essentially the same mesophases as the monomer, with the hexagonal phase shown to persist to higher temperatures. No indication is given in this work, however, that the MEDDAB monomer was checked for the presence of spontaneously polymerized species prior to phase determination [206].

To date, no work has been published on the effect of different counterions on these surfactants, nor has their surface adsorption behaviour been elucidated. Here we present a range of data on a selection of methacrylate surfmers. Seven have been studied, with chain lengths of between eight and sixteen carbons, paired with bromide, chloride and acetate counterions. In addition to CMC measurements, their room-temperature phase behaviour was investigated. Data on their micellar geometry were provided by small-angle neutron scattering, and their adsorption onto mica, graphite and silica surfaces was studied with atomic force microscopy (AFM). This chapter also details experimental attempts to control the free-radical polymerization of these surfmers for the purpose

of producing oligomeric species. Both conventional and chain transfer polymerizations were explored, but these were frustrated by problems related to analysis.

3.2 Monomer characterization

3.2.1 Critical micelle concentration

The critical micelle concentrations of the methacrylate surfactants were determined by conductivity, as described in Section 2.5.1. Table 3.1 shows these and the corresponding degrees of micelle ionization, along with literature values for analogous trimethylammonium surfactants for comparison. The CMCs follow the expected trends, decreasing as both the length of the carbon chain and the binding strength of the counterion increase.

Chain length (y)/	yTAx		MEyDAx	
counterion (x)	CMC (mM)	α	CMC (mM)	α
C12/acetate	30.5[a]	0.69[a]	13	0.75
C12/chloride	20[b]	0.37[b]	9.1	0.49
C12/bromide	14.5[a]	0.26[a]	6.5	0.34
C16/acetate	–	–	1.1	0.82
C16/chloride	1.4[c]	0.37[c]	0.55	0.61
C16/bromide	0.8[c]	0.22[c]	0.34	0.50

Table 3.1: Critical micelle concentrations and degree of micelle ionization (α) for methacrylate surfactants (MEyDAx), and comparison with literature values for analogous trimethylammonium surfactants (yTAx). [a] Ref. [7] [b] Ref. [217] [c] Ref. [218]

The degrees of micelle ionization were calculated using the ratio of slopes method [193]. This method tends to overestimate α, but is sufficient for the limits of accuracy of this study. Unexpectedly, the C16 methacrylates appear to have more highly charged micelles than their C12 analogues. This goes against the usual trend of increased counterion binding with increased tail length [219, 220], but has been observed before (though not commented upon) for MEDDAB and MEHDAB [214].

The difference in CMC between MEDDAB and its non-methacrylate analogue DTAB has already been mentioned. The same pattern is observed in all the methacrylate surfactants: each has a lower CMC than its trimethylammonium analogue, suggesting that

the methacrylate group has a hydrophobizing effect.

As regards the controversy over the CMC of MEDDAB, our value is in agreement with the range of values obtained by Nagai et al. [196] and McGrath and Drummond [70]. It is also similar to that ascribed by Gutierrez-Hijar et al. to a micellar sphere-to-rod transition [214].

3.2.2 Small-angle neutron scattering

Micellar geometry

The micellar geometry of the methacrylate surfactants was studied using small-angle neutron scattering (SANS), and Table 3.2 shows the fitting parameters used to model these data. Measurements were performed at 23°C on solutions of varying concentration in D_2O;* all concentrations are in weight percent, except for the extremely soluble short-chained surfactant MEODAB, which is in mole/L. Polydispersities of 0.12 or less are indistinguishable from smearing of the data due to the wavelength spread in the neutron beam.

Table 3.3 compares three models with data from a solution of 1 wt% MEDDAB. The three calculated curves are for populations of polydisperse and monodisperse charged spheres, and charged cylinders, and it is the first of these that gives the closest fit to the experimental data. The molar concentration of this solution is approximately 27 mM, well above the transition observed at 6–7 mM. Given this, it is difficult to agree with Gutierrez-Hijar et al. in their assessment of this as a shift from spheres to rods. However, at 10 wt% (equal to approximately 0.3 M) MEDDAB does appear to form short cylindrical micelles with an aspect ratio around 3.

Figures 3.2–3.5 compare the effects of chain length and counterion (spectra from the C16 surfactants are shown in Appendix A). Fitting parameters for all the curves shown here and in the appendix are listed in Table 3.2).

Figure 3.2 compares surfmers of different chain lengths, showing the bromide salts of the eight-, twelve- and sixteen-carbon chain surfmers. As expected, volume fractions increase with chain length, indicating that the solubility – and therefore the CMC – of the surfactant is decreasing. All three surfactants form spherical micelles. The dramatically different shape of the MEODAB scattering curve is due its very high solubility: the concentration of monomeric (non-self-assembled) surfactant is high enough to screen

*MEHDAA was not available at the time of measurement.

Surfactant	Conc. (wt%)	Model	Fitted vol. frac. (%)	Radii[a] (Å)	Poly-dispersity	Charge
MEODAB	0.2 M	Hard spheres	1.0	13.4	–	–
MEDDAA	1	Charged cylinders	0.51	13 × 51	–	7
	10	Charged polydisperse spheres	6.9	17.0	0.18	28
MEDDAC	0.3	Charged polydisperse spheres	0.05	16.8	0.19	5
	1	Charged polydisperse spheres	0.60	16.6	0.17	18
	10	Charged cylinders	8.2	16 × 40	–	50
MEDDAB	0.3	Charged polydisperse spheres	0.09	19.1	0.17	4
	1	Charged polydisperse spheres	0.68	19.4	0.13	20
	10	Charged cylinders	7.3	17 × 54	–	23
MEHDAC	0.1	Charged polydisperse spheres	0.09	22.3	0.10	13
	1	Charged polydisperse spheres	0.92	23.0	0.12	19
	10	Charged oblate ellipsoids	9.7	19 × 30	–	33
MEHDAB	0.1	Charged polydisperse spheres	0.1	23.1	0.15	10
	1	Charged polydisperse spheres	0.82	25.2	0.15	18
	10	Charged prolate ellipsoids	8.2	63 × 23	–	27

Table 3.2: SANS fitting parameters for methacrylate surfactants. Errors for each parameter in a multivariate fit are calculated individually by the Igor program and were less than 1%. [a] In the case of cylinders, radius × length.

the charge on the micelles. This produces a scattering curve that is representative of small spherical micelles with a hard-sphere interaction.

Figures 3.3–3.5 illustrate the effect of the counterion, comparing the acetate, chloride and bromide salts of the C12-tailed $MEDDA^+$ cation at different concentrations. Here the results are for the most part as might be expected. The counterions increase in

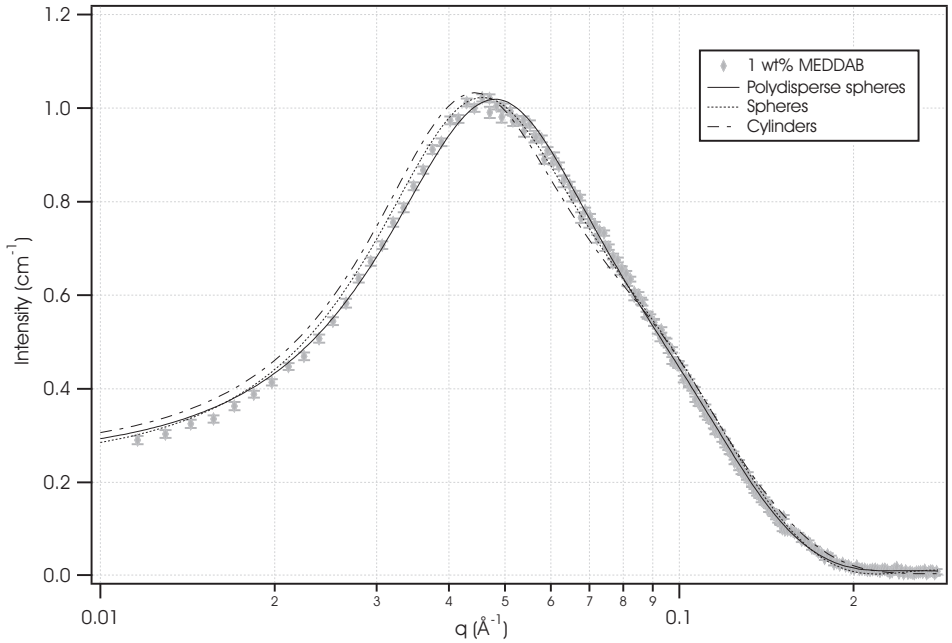

Model	Fitted vol. frac. (%)	Radius[a] (Å)	Poly-dispersity	Charge	χ^2
Polydisperse spheres	0.68	19.4	0.13	20	380
Spheres	0.68	20.5	–	16	1600
Cylinders	0.78	16 × 40	–	22	2300

Table 3.3: SANS fitting parameters and χ^2 (goodness of fit) for three different models applied to the scattering spectrum of 1 wt% MEDDAB. All models incorporate a screened Coulomb structure factor (i.e. the micelles are assumed to be charged). In the figure above, intensity is plotted on a linear scale to aid in differentiating the curves. [a] In the case of cylinders, radius × length.

binding strength in the series acetate < chloride < bromide. A more strongly binding counterion partially neutralizes the headgroup charge of an ionic surfactant, reducing its solubility and increasing its packing parameter. In keeping with this, the SANS data reveals MEDDAB to have higher scattering volume fractions and larger micelles (with correspondingly lower curvature) than MEDDAC and MEDDAA.

The data from MEDDAA shows the sample to contain significant contamination from polymeric material. While at 1 wt% and 10 wt% the maximum is, as expected, at lower intensity and higher q than that of MEDDAC, it shows a considerable upturn at low q. The 0.3 wt% sample (see Figure 3.4) is below the CMC of MEDDAB, and yet

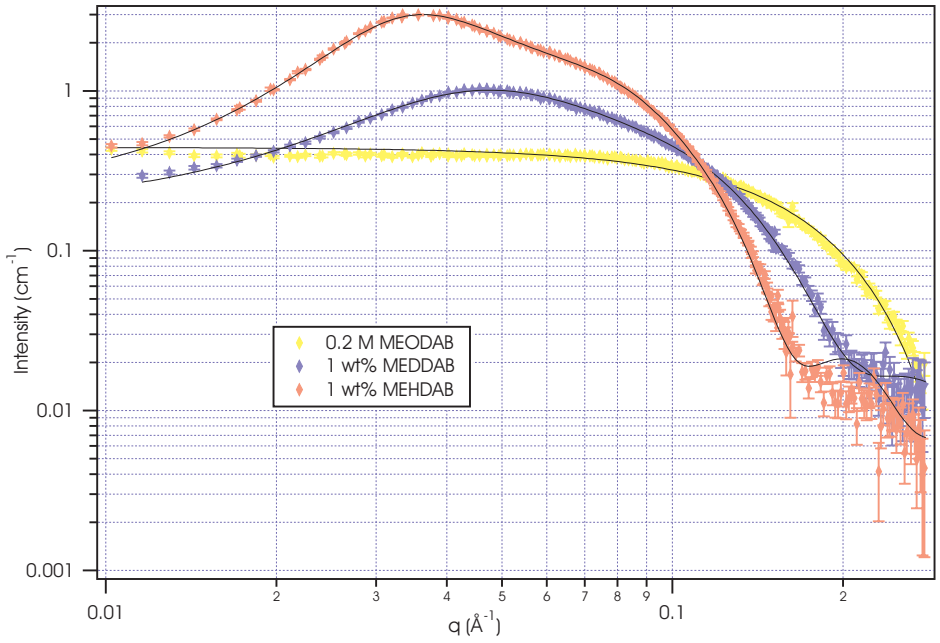

Figure 3.2: SANS data (coloured points) and fitted curves (black lines) for 1 wt% solutions of the bromide salts of octyl, dodecyl and hexadecyl methacrylate surfactants. Fitting parameters are shown in Table 3.2.

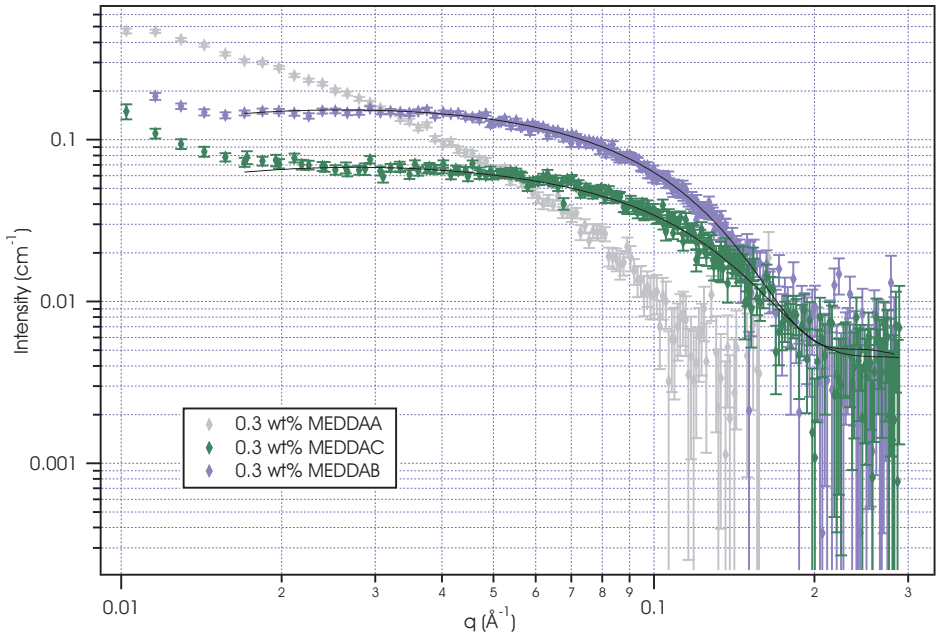

Figure 3.3: SANS data (coloured points) and fitted curves (black lines) for 0.3 wt% solutions of the acetate, chloride and bromide salts of the MEDDA$^+$ cation. Fitting parameters are shown in Table 3.2.

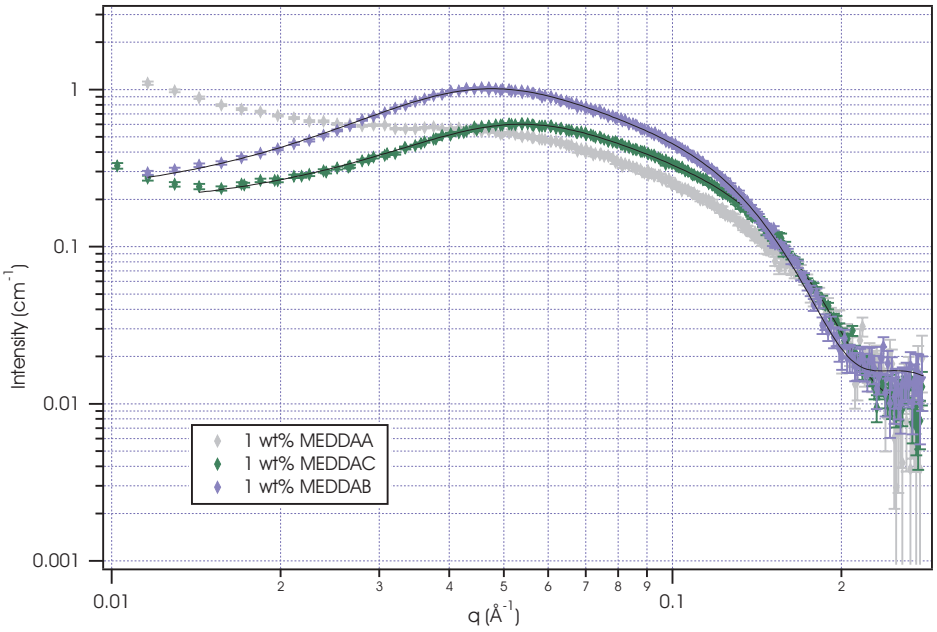

Figure 3.4: SANS data (coloured points) and fitted curves (black lines) for 1 wt% solutions of the acetate, chloride and bromide salts of the $MEDDA^+$ cation. Fitting parameters are shown in Table 3.2. The blue MEDDAB curve is the same data as in Figure 3.2.

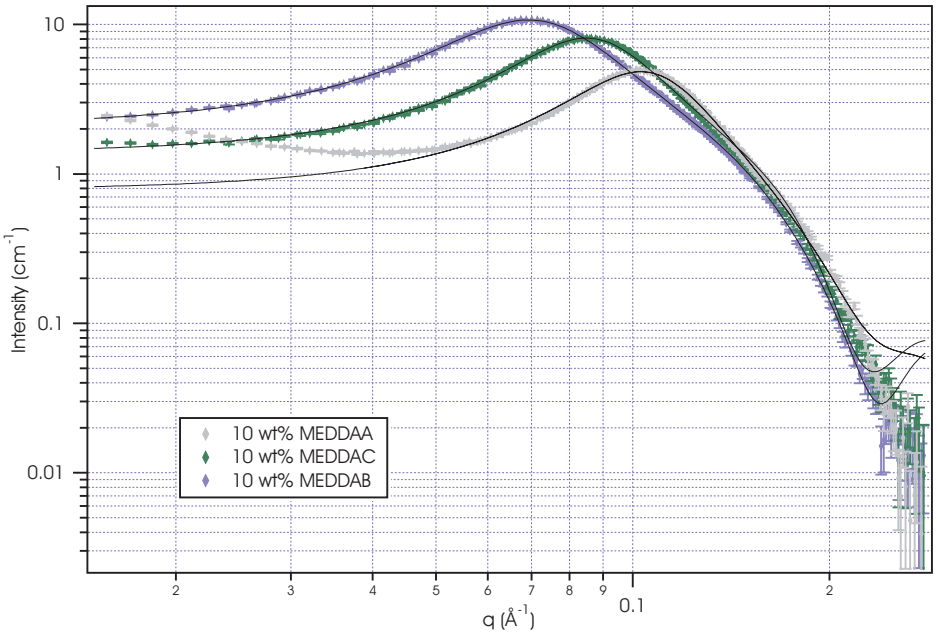

Figure 3.5: SANS data (coloured points) and fitted curves (black lines) for 10 wt% solutions of the acetate, chloride and bromide salts of the $MEDDA^+$ cation. Fitting parameters are shown in Table 3.2.

scattering is still observed. The data are therefore the result of scattering from both micelles and polymeric aggregates, and this affects the fitting of the curves. As shown in the table, the best fit obtained for the 1 wt% MEDDAA solution is a model of cylindrical micelles, which is inconsistent with the spherical morphology shown by MEDDAC and MEDDAB. At 10 wt% however, the micelle peak is strong and well differentiated from the the low-q upturn. If the latter is ignored, the data is fitted well by spheres (see Figure 3.5).

The C16 surfactants show similar behaviour. Again the trend is toward larger micelles for the more strongly binding counterion, yet as Table 3.2 shows, the volume fraction is larger for MEHDAC than for MEHDAB. This too may be due to the presence of a small amount of polymerized material in the MEDDAC sample – molecules not large enough to produce the low-q effect characteristic of large aggregates, but sufficient to influence the concentration of micelles. The continual difficulties experienced in analysing the methacrylate surfacants mean that no firm evidence exists to back this statement up. Nevertheless, the ease with which these surfactants were observed to spontaneously polymerize makes it the most likely explanation.

Effect of temperature

The CMCs of ionic surfactants generally increase with temperature, an effect which is largely due to decreased counterion binding and hence greater solubility. In SANS, this is observed as a decrease in the scattering intensity of the sample and a shift in the maximum, since the concentration and the size of the micelles are reduced. To investigate this effect, several of the methacrylate surfactants were heated in temperature steps and then cooled to room temperature again. This was performed in the beam line, and spectra were acquired at 23°C, 30°C, 40°C, 50°C, 65°C and 80°C. On cooling, spectra were acquired at 50°C and 23°C.

Data and fitted parameters from 1 wt% solutions of MEDDAC and MEDDAB, along with data for 1 wt% solutions MEDDAA are given in Appendix A. All show the expected reduction in intensity as temperature increases. The scattering volume fraction and the micelle size decrease monotonically to 80°C, and then return to their original values upon cooling.

In addition to this effect, the low-q upturn in the MEDDAA data that makes fitting problematic increases with temperature and does not decrease upon cooling. A similar change (though smaller in magnitude) is observed for the MEDDAB sample (see Fig-

ure 3.6). This is due to further spontaneous polymerization at elevated temperatures, and serves as evidence of the need to regard binary phase diagrams of these surfactants with caution.

MEDDAC also shows an upturn at low q, which becomes dramatically larger at high temperature. This change is not permanent, however, and disappears upon cooling. This, and the contrast with the behaviour of MEDDAB, suggests that it is an artefact. A likely explanation is the appearance of bubbles in the sample as the temperature rose, followed by their dissolution upon cooling.

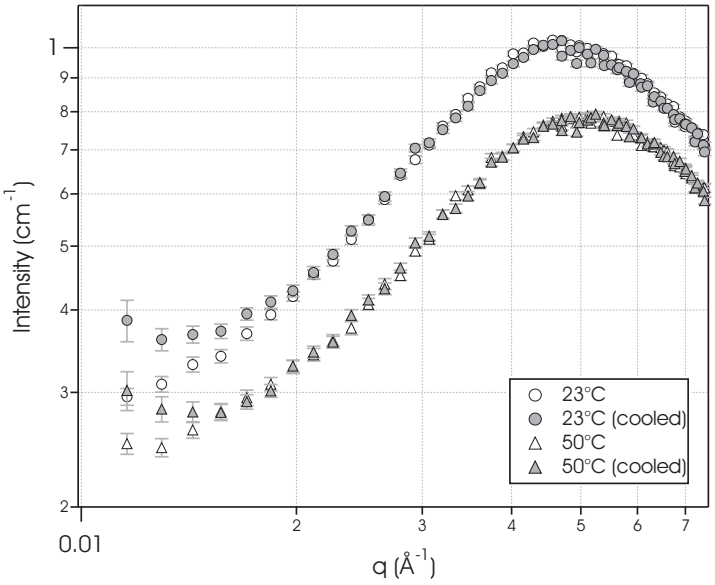

Figure 3.6: SANS spectra of 1 wt% MEDDAB. The solution was heated to 80°C and then cooled; the spectra here show the appearance of a low-q upturn after heating.

3.2.3 Phase behaviour

The phase behaviour of the methacrylate surfactants at ambient temperature (no higher than 30°C) was investigated using flooding experiments. Most of the surfactants show very similar phase sequences (see Table 3.4), although the concentrations at which they form obviously differ. In most cases, the lowest-concentration mesophase formed is the hexagonal phase. This is consistent with the SANS results, which show an increase in the eccentricity of the micellar shape as the surfactant concentration increases.

Since acetate is the most weakly binding counterion of the three investigated, and a high degree of intermicellar repulsion is necessary to form the discrete cubic phase, it

is no surprise that it is the two acetate salts that form this phase. This supports the interpretation of the SANS data that the best fit of a cylindrical model to the 1 wt% solution is an artefact due to the presence of polymer, and that the polydisperse spheres fit to the 10 wt% solution is genuine.

The only surfactant that differs significantly in its phase behaviour is MEODAB. This forms the lamellar mesophase only at high concentrations, a situation that is well-documented for short-tailed surfactants such as this [221].

Surfactant	I_1	H_1	V_1	L_α
MEODAB	–	–	–	✓
MEDDAA	25°C*	✓	✓	✓
MEDDAC	–	✓	✓	✓
MEDDAB	–	✓	✓	✓
MEHDAA	28°C*	✓	✓	✓
MEHDAC	–	✓	✓	✓
MEHDAB	–	✓	25°C*	✓

Table 3.4: Phase sequences for methacrylate surfactants at ambient temperature. * Upper temperature limit.

3.2.4 Adsorbed layer structure

The adsorbed layer structures on mica, graphite and silica of MEDDAA and MEDDAB were investigated with atomic force microscopy. Surfactant solutions were made up at concentrations of twice the CMC and the adsorbed layers on mica were imaged using soft-contact mode. Figure 3.7 shows a selection of images on mica.

In contrast to the spherical morphology adopted by the methacrylate surfmers in solution, the only structures seen at the solid-liquid interface for MEDDAA and MEDDAB were bilayers. Such behaviour is seen in other surfactants with short side-chains [222], and is likely to be the result of the geometrical constraints imposed by adsorption at a solid surface. That is, the binding of the charged nitrogen centre to the mica surface means that the methacrylate side chain is forced perpendicular to the surface, like a second tail. The preferred curvature of the surfactant is therefore decreased, and a bilayer forms.

In an attempt to increase the curvature of the structures, cesium chloride and sodium

bromide were added to MEDDAB. Cations from added salt bind to the mica surface, decreasing the surface charge density and thereby increasing the average curvature of the structures that adsorb to it [17]. Samples with added salt concentrations of up to 0.2 M were examined, and in all cases, the adsorbed layer appeared to be a bilayer. With no added salt, the force curve showed the bilayer thickness to be 3.2 nm. At concentrations of 50 mM and above, however, large (ca. 200 nm) irregular aggregates appeared on the surface, and the bilayer thickness varied by several nanometres; this is probably an indication of polymer in the sample. Higher salt concentrations would increase anion binding to the cationic polymer, decreasing its solubility and causing it to aggregate and separate from the surrounding monomeric surfactant bilayer. The relatively long times (approximately two hours) allowed for these samples to equilibrate before images were acquired would have been sufficient for partial polymerization to occur.

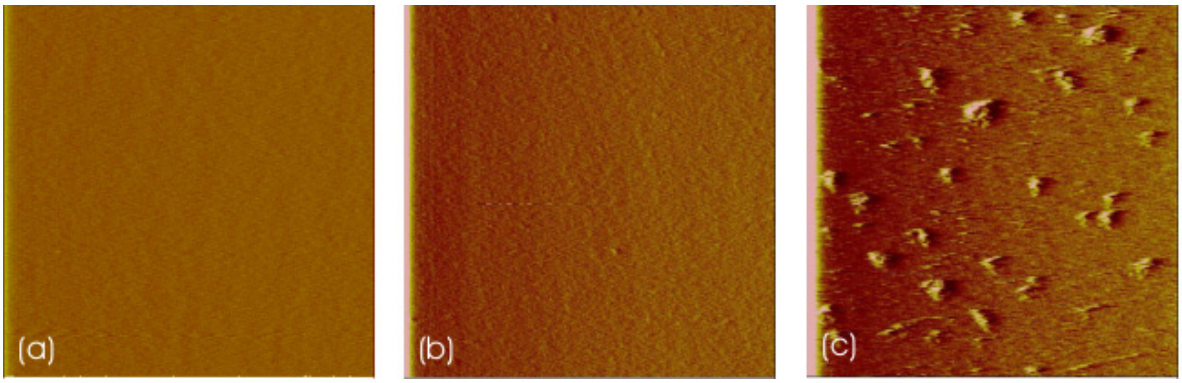

Figure 3.7: Atomic force micrographs of MEDDAB at a concentration of 2×CMC with (a) no added salt (300 nm scan size); (b) 0.025 M NaBr (3 μm scan size); (c) 0.05 M NaBr (3 μm scan size).

3.3 Polymerization

Three techniques were employed to control the polymerization of the methacrylate surfactants in order to produce oligomers. The first of these was the use of high concentrations of initiator, and the other two were based on chain transfer: reversible addition-fragmentation chain transfer (RAFT), and catalytic chain transfer (CCT). The experimental details of these techniques are described in Section 2.3.

3.3.1 High initiator concentration

The effort to produce surfactant oligomers began with a series of experiments using high initiator concentrations (10–80 mol% relative to the surfactant) and covering a range of reaction conditions. The rationalization was that the high levels of both initiation and termination would result in short oligomers. Apart from the initiator concentration, the variables were the initiator type (benzoyl peroxide/AIBN/V50), the solvent (chloroform/toluene/dimethyl-sulfoxide/water), and the time and temperature of reaction. In all cases, the product was insoluble in water.

In these experiments, conversion could be monitored in real time by near-infrared spectrometry (Section 2.4.3) or checked by NMR. Figure 3.8 shows conversion over time for a set of experiments in which the initiator concentration was varied. However, monitoring the rate of reaction gives no indication of the product's molecular weight, and despite a number of techniques being tried, no reliable analysis of the degree of polymerization could be obtained. No species other than the monomer could be observed in either electrospray or MALDI mass spectrometry, severe fronting occurred with SEC in a variety of solvents, and the species were apparently too long to be observed using HPLC. These problems appear to be a feature of the polymerized quaternary ammonium compound, since mass spectrometry and GPC were successfully used with the neutral polymers of methyl methacrylate and dimethylaminomethacrylate (see Section 3.3.3), and long-chain methacrylates being used by other researchers in the group at the time.

Some reactions were performed in aqueous solution using V50 (a water-soluble AIBN analogue). While molecular-weight information was equally difficult to obtain in these experiments, the appearance of the solutions after polymerization was interesting. The higher the concentration of initiator, the less water-soluble the product appeared to be. In addition, the mass spectra of these samples showed a significant peak at a lower weight than the unreacted monomer. Together, these observations suggest that the extremely high radical concentrations contributed to degradation into water-insoluble components. In essence, the harsh conditions of an environment with such high radical concentrations appear to negate the already dubious possibility of producing short oligomers by this method.

Similar polymerizations of MEDDAA and MEDDAB were monitored by small-angle neutron scattering. Spectra were acquired every fifteen minutes during the reaction

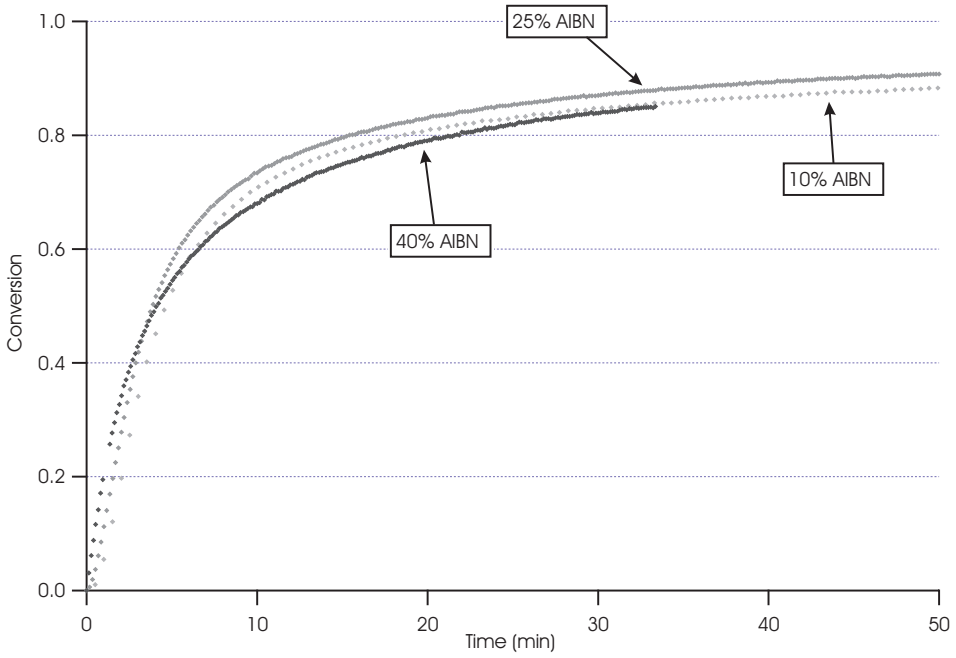

Figure 3.8: Kinetic data for polymerizations of MEDDAB with varying amounts of initiator; reactions were performed in DMSO at 80°C and monitored with near-infrared spectroscopy.

in an effort to observe structural changes. Due to the reactivity of the monomers and a delay between making up the solutions and being able to place them in the beam, substantial polymerization occurred before the first spectrum was acquired. All subsequent spectra were not greatly different to the first, and at the end of the reaction, both the MEDDAB and MEDDAA samples were opaque and insoluble.

Upon cooling to room temperature, the appearance and scattering behaviour of the MEDDAB sample remained the same. In contrast, the MEDDAA sample lost its opacity and became a clear, stiff gel. The SANS spectrum changed dramatically, with the peak broadening and shifting to lower q (see Figure 3.9), perhaps suggesting the swelling of polymer chains by water. Observation of the gel through crossed polarizers showed it to be isotropic, with shear-induced birefringence. As with the other methacrylate surfactants, however, no characterization of the molecular weight was possible.

3.3.2 Reversible addition-fragmentation chain transfer

Reversible addition-fragmentation chain transfer was deemed to be a suitable technique for producing oligomers because of its proven ability to control molecular weight and its

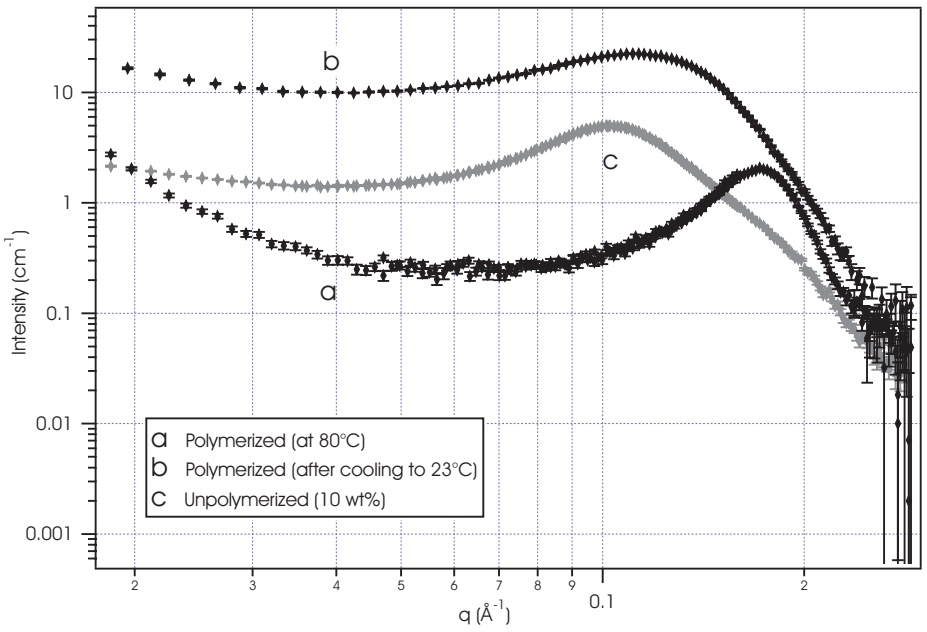

Figure 3.9: MEDDAA was thermally polymerized in the neutron beam, producing a thick opaque precipitate at high temperature that cooled to a stiff isotropic gel at room temperature. The spectrum of unpolymerized 10 wt% MEDDAA is shown for comparison.

flexibility in terms of reaction conditions. However, at the time of these experiments, the use of RAFT to produce species of very low molecular weight had not been extensively researched.

The RAFT agent used was cumyl dithiobenzoate (CDB; see Figure 1.11). Polymerizations were monitored in real time by near-infrared spectrometry, and several reactions were performed using methyl methacrylate as a model monomer. Because the aim was to produce extremely short oligomers, very high concentrations of CDB were required. The experiments showed the expected temperature dependence, the well-documented inhibition period at the start of the reaction, and a conversion that depended not only on temperature and initiator concentration, but also on RAFT-agent concentration.

The method was repeated using MEDDAB (examples are shown in Figure 3.10), and followed up with time series in which one reaction was monitored by NIR and used to determine the quenching time of parallel identical reactions. In this way, a set of samples with a range of conversions was obtained.

However, the same problems that frustrated the analysis of the high-initiator experiments were experienced here, and we were unable to measure molecular weights which

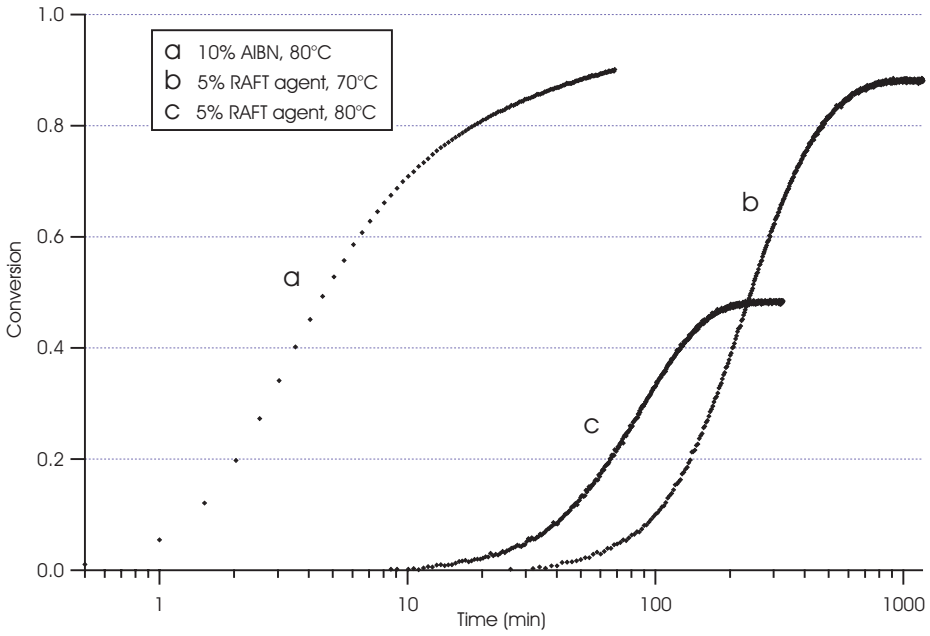

Figure 3.10: Kinetic data for polymerizations of MEDDAB with 5% cumyl dithiobenzoate and 1% AIBN. The x-axis is scaled logarithmically to allow the 10% AIBN reaction from Figure 3.8 to be shown for comparison. Reactions were performed in DMSO and monitored with near-infrared spectroscopy.

could be correlated with the observed progress of the reaction. This made it impossible to tune the reaction conditions in any systematic fashion. In addition, as with the high-initiator reactions, the product was in all cases substantially or completely insoluble in water.

3.3.3 Catalytic chain transfer

Catalytic chain transfer is routinely used for making low molecular-weight species such as oligomers and macromonomers. An advantage of the technique is that since most chains are initiated and terminated by transfer of a hydrogen atom from and to the catalyst, no additional chemical functionality remains on the final product molecules. Since the goal here is to produce surfactant oligomers, the presence of an extra functional group that might affect the physical properties of the compound could be problematic.

The catalyst used was bis[(difluoroboryl)diphenyl-glyoximato] cobalt(II) (COPhBF; see Figure 3.11). As with the RAFT method, initial reactions were performed on methyl methacrylate (MMA) and dimethylaminomethacrylate (DMAEMA). These sim-

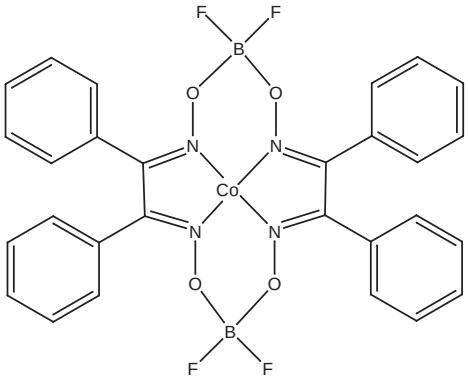

Figure 3.11: Bis[(difluoroboryl)diphenyl-glyoximato] cobalt(II).

ple, well-characterized monomers were used in order to test the method while avoiding the analysis problems experienced with MEDDAB. Relative success was obtained, with a broad distribution of short oligomers ($DP_n = 4$–12) produced and detected by MALDI mass spectrometry and SEC.

This 'proof of principle' result suggests that the method should be transferable to the methacrylate surfactants. However, when the same methods were applied to the methacrylate surfactants (MEODAB, MEDDAC and MEDDAB), the product was insoluble in water and could not be analysed.

3.4 Discussion

The work described in this chapter constitutes a partial characterization of the family of methacrylate surfactants. As described in the introduction, the literature contains work on MEDDAB and MEHDAB, but so far no studies of the counterion effect or the adsorbed layer structure exist.

The most obvious difficulties in working with these compounds is their tendency to spontaneously polymerize and the lack of a robust technique for purifying them. While the insolubility of long polymer chains in water allows them to be easily removed, this is not necessarily the case for shorter species. Recrystallization is also ineffective in this regard, and may even compound the problem. As a consequence, the determinations of critical micelle concentration and phase behaviour cannot be regarded as highly accurate.[†] The variation that exists in the literature regarding the CMC of MEDDAB

[†]This should be kept in mind particularly for MEDDAA, which was found to be especially prone to

is in part testament to this.

Despite these problems, the measured CMCs are within the expected concentration range relative to their alkyltrimethylammonium analogues, and in general follow the expected trends. This is not the case for the micelle ionization degrees of the C16 surfactants relative to the C12s. These are expected to be smaller, but are in fact uniformly larger. While this anomaly is likely to be due in some way to the methacrylate group, the exact reason remains unknown. The phenomenon has, however, been reported before for MEDDAB and MEHDAB [214].

Most of the surfactants investigated with small-angle neutron scattering are shown to form spherical micelles at and below 1 wt%. In the case of MEDDAB this concentration is equivalent to 27 mM, thus contradicting the claim by Gutierrez-Hijar et al. that the phase transition repeatedly reported at around 6–7 mM is a morphological sphere-to-cylinder transition.

These researchers, and Hamid and Sherrington, have used multiple techniques to observe a transition at approximately 2 mM, which they identify as the true CMC [197, 214]. SANS data from a 0.3 wt% solution of MEDDAB (equivalent to 8.2 mM) show the volume fraction of micelles at this concentration to be around 0.09%. Taking the density of the surfactant to be approximately 1 g cm^{-3}, one may calculate that if the CMC were 2 mM, then the volume fraction of micelles in this sample should be around 0.25%. If the CMC is 6.5 mM, then the expected volume fraction is 0.07%.

In addition to this, the CMC of *N*-dodecyl-*N*-hexyl-*N*, *N*-dimethylammonium bromide has been reported to be 3.06 mM [193, 222]. This surfactant has a C6 side chain that mimics the ethyl methacrylate group of MEDDAB in length, but is more hydrophobic. It would be illogical for such a compound to have a higher CMC than MEDDAB.

At first glance, MEDDAA representes an apparent exception to the morphological trend of spherical micelles, since at 1 wt% the scattering data is best fitted by a model of cylinders. This artefact is due to the presence of polymerized material, which appears to manifest in the scattering spectrum as an upturn at low q. The effect is even clearer at 0.3 wt%, where the monomeric surfactant is below its CMC. However, at 10 wt% the data corresponds to polydisperse spheres. At this concentration, the intense micellar scattering peak is sufficiently differentiated from the polymeric contribution that the

spontaneous polymerization. Because of the weakly basic nature of the acetate counterion, wet solid samples or solutions of this surfactant also undergo slow hydrolysis.

model fit more accurately reflects the true micellar shape. This is supported by the fact that the first concentrated mesophase formed by MEDDAA is a micellar cubic phase.

At 10 wt%, the MEDDAC and MEDDAB data are best fitted by cylindrical micelles, while MEHDAC and MEHDAB are seen to form distorted ellipsoids. This is consistent with the fact that all form hexagonal phases at higher concentration.

The fact that the methacrylate surfactants form spherical micelles in dilute solution suggests that under such conditions the methacrylate chain acts more as part of the headgroup than as an additional tail. This is not in conflict with Hamid's idea that it adopts an annular structure through attraction between the carbonyl oxygen and the charged nitrogen. On the other hand, it provides no strong evidence for it, since the same effect could be produced if the methacrylate group were simply to inhabit the palisade layer without forming any association with the nitrogen. It is worth noting that the clearly non-associating dodecylhexyldimethylammonium bromide (mentioned above) also forms spherical micelles at low concentrations [223].

When adsorbed to a mica surface, dodecylhexyldimethylammonium bromide is seen to form a bilayer [222]. The methacrylate surfacants behave in the same manner. It seems that the geometry of this arrangement – with the charged ammonium bound directly to the surface – dictates that the methacrylate (or hexyl) group must point away from the surface. This causes it to act like an additional tail and leads to structures of low curvature. In the experiments performed here, the addition of salt up to concentrations of 0.2 M produced no change in the bilayer structure.

The attempts to control the free-radical polymerization of the methacrylate surfactants were largely unsuccessful. In the first instance this was due to the inability to analyse the polymeric products, leading to a lack of insight into how to modify the polymerization reactions. However, there is no a priori reason why such methods should be unsuccessful, at least in the case of the chain-transfer techniques. CCT has been widely used to produce short oligomers of methyl methacrylate with narrow polydispersity [80], and similar results were obtained here in 'proof of principle' experiments with MMA and DMAEMA. In the case of RAFT, while some RAFT agents have been found to yield very broad molecular-weight distributions with methacrylates, this was found to be because of the re-initiating power of the R-group relative to the methacrylate radical. Careful selection or design of new RAFT agents has overcome this problem [82], and RAFT has recently been shown to work on compounds that resemble the methacrylate surfactants [111, 112, 224]. Therefore, while achieving control over these reactions is by

no means facile, if the analysis problem were to be overcome, either or both of RAFT and CCT should be useful for this purpose.

As a final comment, observations in the course of working with the methacrylate surfactants suggest that the counterion has an effect – whether direct or indirect – on the the monomers' tendency to spontaneously polymerize. As mentioned earlier, the acetate surfactants were particularly prone to this reaction. Spontaneous polymerization in aqueous solution has previously been noticed for simpler methacrylates and methacrylamides [225]. While the exact mechanism for the reaction remains unclear, a radical reaction was proposed, and the ability of the monomers to self-organize in aqueous solution implicated. It was suggested that a redox interaction between an anion and the monomer vinyl bond produces two radicals capable of initiating polymerization. An alternative explanation for the particular case of the acetate is suggested by our recent work on the vinylpyridinium monomers. A sufficiently nucleophilic anion such as hydroxide can initiate anionic polymerization in an electron-deficient double bond; the weakly basic nature of the acetate counterion may therefore be indirectly responsible for the 'spontaneous' polymerization of MEDDAA.

Chapter 4

Vinylpyridinium surfactants

"The slogan 'press on' has solved and always will solve the problems of the human race."

Calvin Coolidge

4.1 Introduction

The difficulties experienced in working with the methacrylate surfactants led to the decision to try a different surfmer as the starting point for producing oligomeric surfactants. Vinylpyridinium-based surfactants were chosen, since these compounds are structurally related to the well-known family of alkylpyridinium surfactants [170, 226–230]. The polymerizable moiety is based on the vinylpyridine monomer, the isomers of which have received much attention in the past (see Section 1.3).

The vinyldodecylpyridinium surfactants studied here (see Table 2.2 for naming conventions) are rarely mentioned in the literature [163, 231] and, as far as we are aware, the acetate salt in particular has not yet been studied. From the point of view of surfactant science, this is unsurprising, since their extreme reactivity means the purification and reproducible characterization of these compounds are problematic. Vinylalkylpyridinium polymers (pVAPs) have been studied to some extent, but are generally produced by the quaternization of pre-synthesized polyvinylpyridine (often commercially sourced), rather than by polymerization of the vinylalkylpyridinium monomer. As well as attempts to modify the properties of pVAPs by copolymerization [232] or varying the level of quaternization [132–134, 233], their potential application as photopattern-

ing agents in electroless plating [234], and their interaction with negatively-charged phospholipid vesicles [235] have been investigated.

In this chapter, the characterization of a selection of vinyldodecylpyridinium surfactants is presented. 2- and 4-vinyl-*N*-dodecylpyridinium trifluoromethanesulfonate were synthesized by the in-house Organic Synthesis Centre and were then ion-exchanged to give the bromide, chloride and acetate salts. The acetate salts were never obtained as pure solids, since it was found that attempting to concentrate the solution following ion exchange, whether by evaporation of organic solvent or freeze-drying of aqueous solution, inevitably caused a reaction that appeared to be polymerization. Yet despite this, the freeze-dried 2VDPA (though not the 4VDPA) remained water-soluble. HPLC showed the 2VDPA to be a mixture of short oligomers, and it was further analysed by small-angle neutron scattering along with pure samples of the chloride and bromide salts. In addition, spectra of 4VDPA were obtained from a 0.2 M aqueous solution of 4VDPA diluted with D_2O. The reaction that occurred during the freeze-drying process will not be discussed here, since it formed the basis for the work which constitutes Chapter 5.

4.2 Monomer characterization

4.2.1 Critical micelle concentration

Determining the critical micelle concentration of these compounds reproducibly was always going to be difficult, because of the ease with which they polymerize. Although repeated practice improved the facility with which these sensitive surfactants were handled, small amounts of water-insoluble material were often found in samples that had appeared pure by NMR. Further, the shorter oligomers were found to be water-soluble (see Chapter 5), so their presence may not always have been detected. Even when they were detected, it is next to impossible to remove the oligomeric material from the monomer.

Using the purest samples we were able to obtain, the CMC values shown in Table 4.1 were reproducible to ± 0.2 mM. The CMCs of the acetate salts were never satisfactorily determined, because of the extreme difficulty of obtaining the pure solid monomer.

Despite these problems, the measured CMCs follow a consistent trend and do not conflict with literature values of unsubstituted dodecylpyridinium analogues. The vinyl

Surfactant	CMC (mM)	α
DPC[a]	16.2	0.49
DPB[a]	11.1	0.36
2VDPC	10.1	0.55
2VDPB	7.5	0.38
4VDPC	9.5	0.54
4VDPB	7.1	0.30

Table 4.1: Critical micelle concentrations and micelle ionization degrees (α) for vinyldodecylpyridinium surfactants (n-VDPx) and the analogous dodecylpyridinium chloride and bromide (DPC and DPB). [a] Ref. [230]

substituent lowers the solubility of the surfmers relative to the unsubstituted surfactants. Among the surfmers, the slightly higher solubility of the 2-substituted compounds is in accordance with previous observations on long-chain alkylpyridinium compounds with ring substituents [236, 237].

4.2.2 Small-angle neutron scattering

Micellar geometry

The micellar geometry of the vinylpyridinium surfactants was studied using small-angle neutron scattering (SANS). Measurements were performed at 23°C on solutions of varying concentration in D_2O. Table 4.2 shows the fitting parameters used to model these data. Note that some spectra were collected over a narrower range of q than others due to time constraints. All concentrations are in weight percent. Polydispersities of 0.12 or less are indistinguishable from smearing of the data due to the wavelength spread in the neutron beam.

The data that follows covers all six vinylpyridinium surfactants over a range of concentrations, but there are several points to be noted. Firstly, several of the samples, 4VDPB in particular, were contaminated with oligomeric species. This does not appear to have significantly affected the micellar dimensions as determined from the scattering data, but it does contribute to scattering at low q. This complicates the fitting process, making it particularly difficult to determine the micellar charge. Secondly, because of the sensitivity of the acetate surfactants to freeze-drying, the 4VDPA sample was stored as an aqueous solution of approximately 0.2 M concentration. This was then diluted

Surfactant	Conc. (wt%)	Model	Fitted vol. frac.(%)	Radii (Å)	Poly-dispersity	Charge
2VDPA	0.3	Charged oblate ellipsoids	0.28	13(±0.16) × 38	–	14
	1	Charged oblate ellipsoids	0.74	15 × 35	–	52
	10	Charged oblate ellipsoids	6.7	16 × 41	–	44
2VDPC	0.3	No aggregates	–	–	–	–
	1	Charged polydisperse spheres	0.58	15.0	0.15	12
	10	Charged polydisperse spheres	7.8	17.2	0.13	14
2VDPB	0.3	Unknown[a]	–	–	–	–
	1	Charged polydisperse spheres	0.56	17.0	0.16	8
	10	Charged prolate ellipsoids	6.8	24 × 18	–	21
4VDPA	0.3	No aggregates	–	–	–	–
	1	Charged polydisperse spheres	0.48	13.4	0.13	15
4VDPC	0.3	No aggregates	–	–	–	–
	1	Charged polydisperse spheres	0.58	15.0	0.16	11
4VDPB	0.3	Unknown[a]	–	–	–	–
	1	Charged polydisperse spheres	0.48	18.0	0.13	10

Table 4.2: SANS fitting parameters for vinyldodecylpyridinium surfactants. Errors are as for Table 3.2. [a] These samples were contaminated with oligomer/polymer, and the micelle peak could not be fitted.

1:6 with D_2O for SANS. The higher concentration of hydrogen in the solvent means that the contrast between it and the micelles is reduced, and the scattered intensity is reduced slightly. Thirdly, wherever 2VDPA is mentioned, this refers to the oligomerized sample that reacted during freeze-drying, which is presented here for comparison and is discussed further in later chapters.

Figure 4.1 shows SANS spectra taken from 1 wt% solutions of the vinylpyridinium

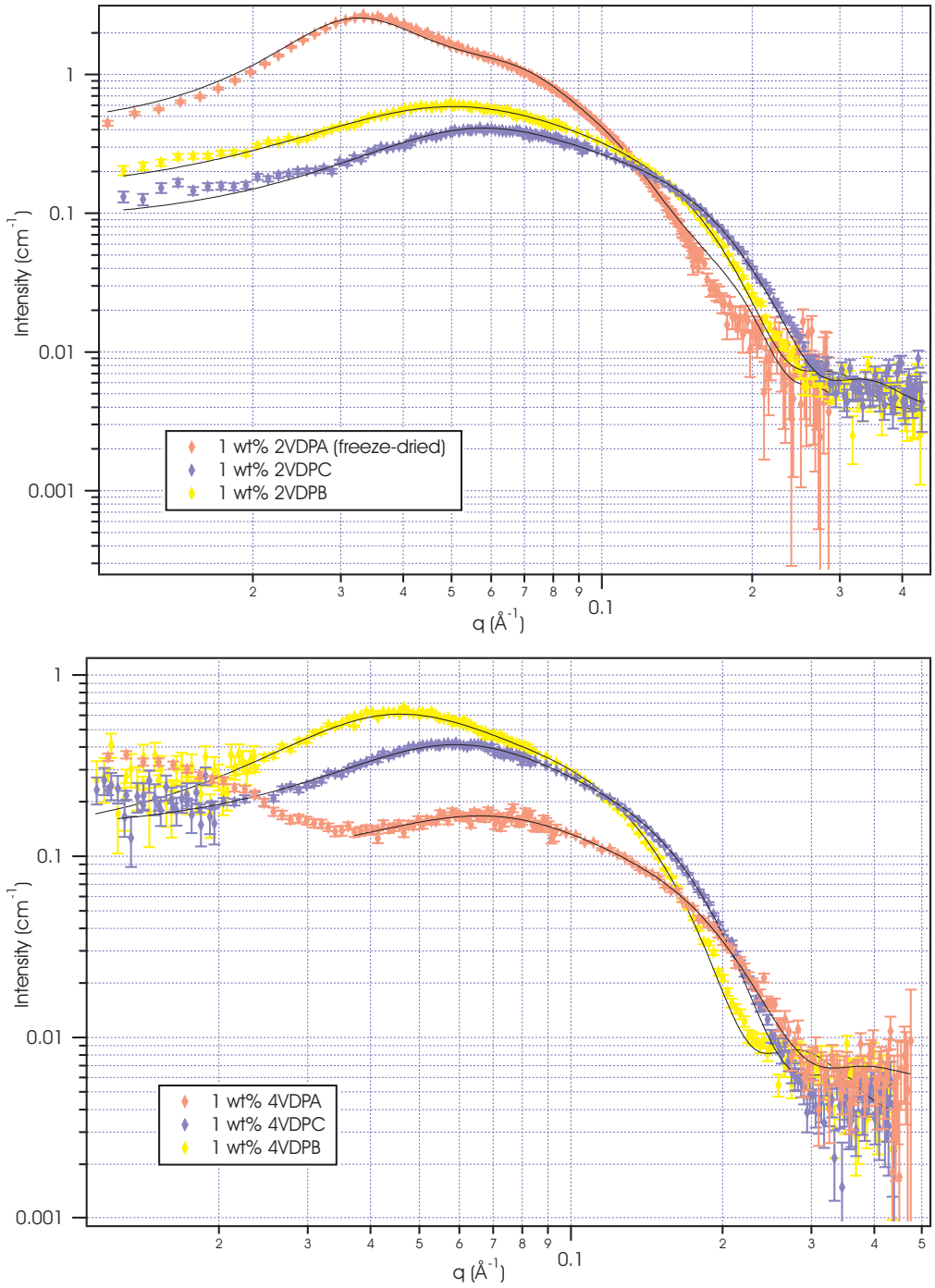

Figure 4.1: SANS spectra (coloured points) and fitted curves (black lines) for 1 wt% solutions of 2-substituted (top) and 4-substituted (bottom) vinylpyridinium surfmers in D_2O. The 4VDPA sample was in 1:6 H2O/D2O; this resulted in a lower contrast and the spectrum is therefore slightly less intense than it otherwise would be. Note that the 2VDPA sample was oligomerized by freeze-drying, and is shown for comparison. Fitting parameters are shown in Table 4.2.

surfactants, along with fitted curves. Further data are shown in Appendix B. The fitting parameters are listed in Table 4.2, and show the expected trends. With the exception of the oligomerized 2VDPA, micelles of the acetate and chloride salts are smaller and more highly charged than those of the bromides. In general, the 2- and 4-substituted isomers appear to form micelles of very similar morphology, with almost all the spectra well fitted by models of polydisperse spheres. The 0.3 wt% solutions of the two bromides were both contaminated with oligomer, making it impossible to determine whether micelles were present. For these surfactants, this concentration is equivalent to 8.5 mM, which is only just above the surfactants' CMCs: any micellar scattering would therefore have been of very low intensity.

The spectra of the freeze-dried 2VDPA stand in contrast to the chloride and bromide salts. Since acetate is a more weakly binding counterion than chloride, pure 2VDPA should be more soluble than the other two surfmers, and have smaller, more highly charged spherical micelles. Instead, the 2VDPA data are best fitted by a model of oblate (pancake-like) ellipsoids. In addition, the sample shows significantly more intense scattering than the chloride and bromide, indicating it is less soluble (or in other words, that the volume fraction of micelles is greater).

Effect of temperature

The effect of temperature on the three 2-substituted surfmers was investigated. While in the beam line, 1 wt% samples were heated in temperature steps and then cooled to room temperature again. Spectra were acquired at 23°C, 30°C, 40°C, 50°C, 65°C and 80°C. On cooling, spectra were acquired at 50°C and 23°C. A selection of unfitted spectra from these series are shown in Figure 4.2, with those from the original and final cooled samples emphasised in blue.*

In all cases, the intensity of the micelle peak decreases with heating as expected. However, because of the ability to spontaneously polymerize, the spectra are dominated by chemical rather than physical changes. As 2VDPB is heated, the scattered intensity at low q increases steadily. At the same time, the shoulder at around 0.07 Å^{-1} – the micellar peak – decreases in intensity. The cooled spectrum is nearly identical to the

*The 2VDPB spectra shown in Figure 4.2 used a sample that was found to contain a small amount of oligomer/polymer. While this was not sufficient to cause low-q scattering, it has changed the shape of the 2VDPB micelles from spheres to rods (compare the 23°C spectrum with the 2VDPB spectrum in Figure 4.1). This is unlikely to have changed the behaviour on heating to any great extent.

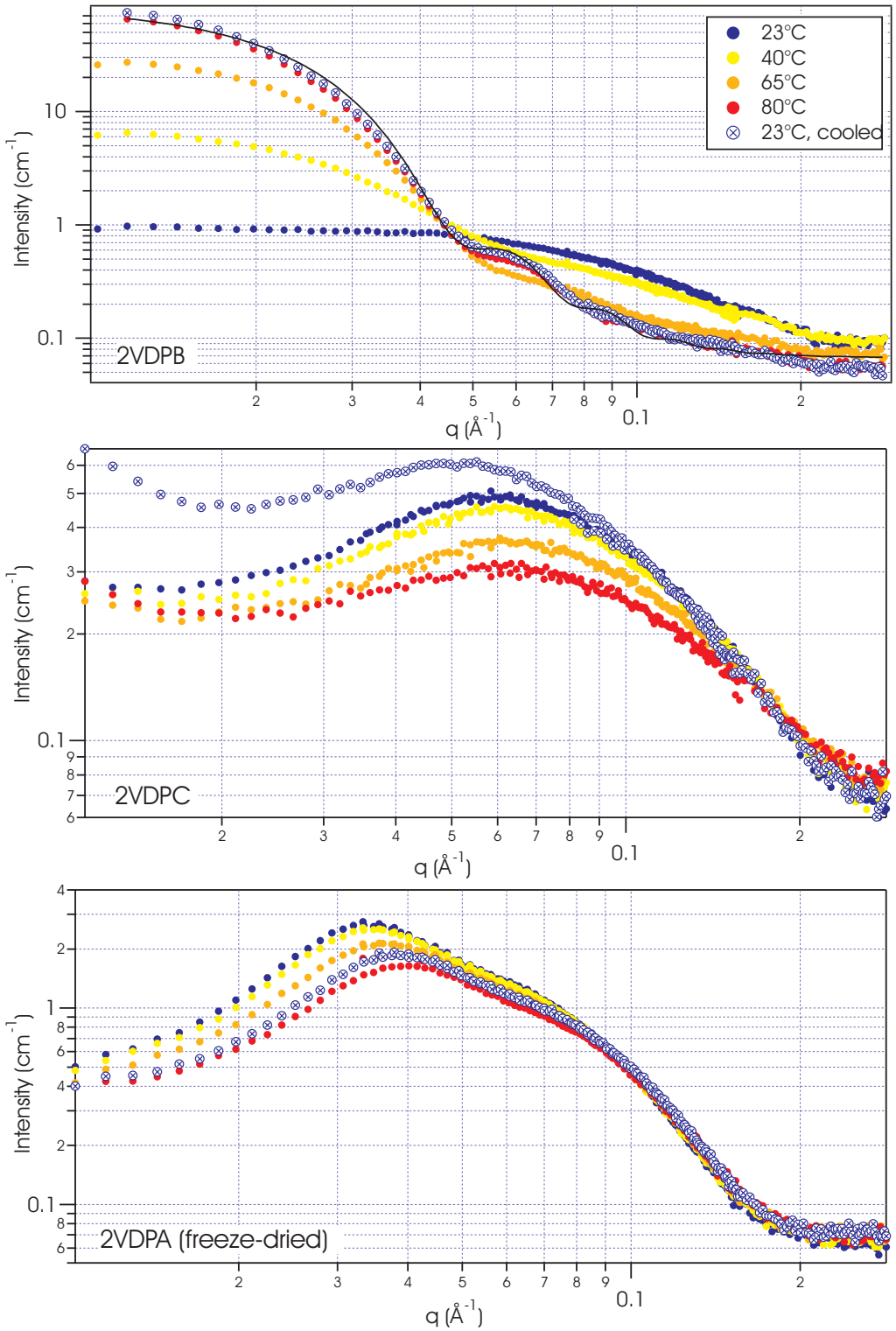

Figure 4.2: Uncorrected SANS spectra from serial heating of 2VDP-bromide, chloride and (freeze-dried) acetate. In the top graph, the cooled 23°C data is fitted to a model of hard polydisperse spheres with the following parameters: volume fraction 0.46%, radius 90 Å, polydispersity 0.14.

80°C spectrum, and the shape of these spectra is typical of a population of large, roughly spherical particles. In the top graph of Figure 4.2, the cooled spectrum is fitted by a model of large polydisperse spheres with a hard-sphere interaction, suggesting that this uncontrolled and spontaneous polymerization has nevertheless produced a fairly well-defined population of particles with an average radius of 90 Å.

A less drastic change is seen with 2VDPC. After heating and cooling, a small low-q upturn is observed, two orders of magnitude lower in intensity than in the 2VDPB spectrum. At the same time, the micellar interaction peak has shifted to slightly lower q and increased in intensity relative to the original solution.

There may be two reasons for this, though it is difficult to separate them without further evidence. The first is the degree of polymerization: the effect of the counterion on spontaneous polymerization in these compounds has not been studied, and it may be that the more highly dissociated chloride salts polymerize to a lesser extent. This would explain the retention of a peak due to structures of micellar dimensions. However, the chloride salts are also more soluble than the bromides, which would contribute to a lower scattered intensity from polymerized species.[†]

The behaviour of the 2VDPA solution on heating is quite different to the two monomers. No increase in large molecular-weight species is apparent, and while the micellar peak decreases as expected with heating, it then remains smaller when cooled. Fitting of this peak gives an almost identical volume fraction of micelles to the original solution, but structures that are less eccentric in profile. Clearly the species in this pre-polymerized sample are not able to polymerize further, and may even be partially degrading to produce micelles closer to those expected of the monomer. The reasons for this are discussed further in the next chapter.

4.2.3 Phase behaviour

Table 4.3 summarizes the phase behaviour of four vinylpyridinium surfactants as determined by flooding (penetration) experiments. In three of the four compounds – 2VDPB, 4VDPC and 4VDPB – the only mesophase formed is the hexagonal phase. In addition to a hexagonal phase, 2VDPC forms a lower-concentration stiff isotropic phase. Since this is an ionic surfactant, and since neutron scattering identifies the micellar geometry

[†]For instance, free-radical polymerized 2VDPC, while insoluble in water at room temperature, dissolves at 80°C. This is not the case for the bromide.

Surfactant	I_1	L_2	H_1	V_1	L_α
2VDPC	✓	55°C*	✓	–	–
2VDPB	–	–	✓	–	–
4VDPC	–	–	✓	–	–
4VDPB	–	–	✓	–	–

Table 4.3: Phase sequences for vinyldodecylpyridinium surfactants. *Fluid isotropic (L_2) phase forms above this temperature.

as spherical up to at least 10 wt%, this is likely to be a discrete cubic phase.

A similar comparison can be made for 2VDPB. The lowest-concentration (and only) mesophase formed by 2VDPB is hexagonal, consisting of hexagonal close-packed cylinders. This is consistent with the prolate geometry that SANS identifies for the micelles for this surfactant, and suggests that the micelles become cylindrical at higher concentrations than the 10 wt% measured. The absence of lamellar phases is consistent with the reported behaviour of dodecylpyridinium surfactants [227, 238].

It was additionally noticed that when the temperature of a 2VDPC flooding experiment was raised above 55°C, an additional fluid isotropic phase reproducibly appeared (see Figure 4.3), intermediate between the I_1 and H_1 phases. It cannot be ruled out that this is a feature caused by low levels of oligomer contamination. However, an effort was made to expose the surfmer to elevated temperatures for only a short period of time. In addition, Figure 4.2 (yellow and orange curves) shows that even after 2VDPC

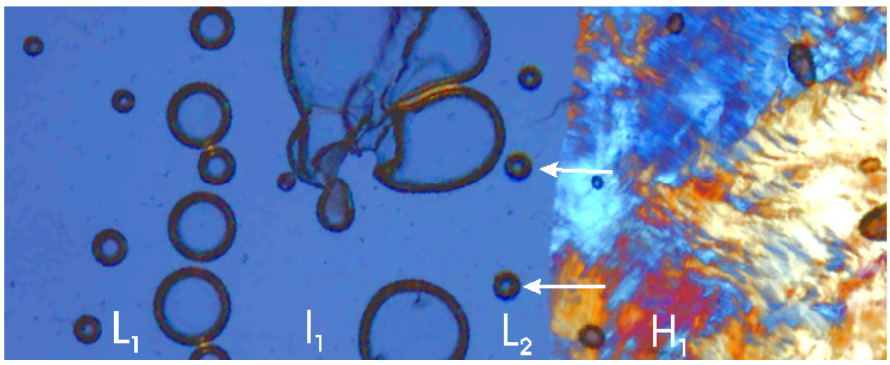

Figure 4.3: Flooding experiment of 2VDPC at 55°C. A low-viscosity fluid isotropic phase has formed between the discrete cubic and hexagonal phases. This is evident from the spherical (rather than deformed) shape of the bubbles (white arrows).

was held at similar temperatures for much longer (1–2 hours), only a relatively low level of polymer was present. It is therefore fairly safe to say that this is a true feature of the monomer rather than the result of contamination.[‡] Because of its position in the sequence of phases, it is likely to consist of disordered cylindrical micelles [221].

4.2.4 Adsorbed layer structure

Atomic force microscopy was used to investigate the adsorbed layer structure of 2VDPC at the mica-solution interface. A typical image, acquired by Dr. Robert Chan, is shown in Figure 4.4.

2VDPC affords a largely featureless image suggesting an adsorbed bilayer. This contrasts with the non-polymerizable dodecylpyridinium chloride, which has been observed to form globular aggregates on mica [239]. It seems unlikely that a substituent such as vinyl would cause such a drastic morphological shift from globular aggregates to a bilayer. A more likely explanation for this anomaly is that the time in which the sample was allowed to equilibrate before the image was acquired was sufficient to allow some degree of spontaneous polymerization to occur. The longer, more hydrophobic species would then preferentially adsorb, and could provide the template for a bilayer.

Finding an unambiguous solution to this anomaly requires a study of non-polymerizable structural analogues of these molecules, e.g. ethyldodecylpyridinium salts. This was not possible within the time constraints of this work.

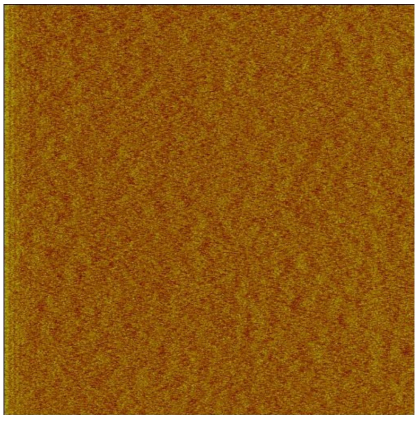

Figure 4.4: Atomic force micrograph of 2VDPC at 2×CMC (100 nm scan size).

[‡]Note, however, that determining the exact temperature at which this phase forms and its composition *without* contamination by oligomer is nontrivial.

4.3 Discussion

For similar reasons to the methacrylate surfactants, the unambiguous characterization of the vinyldodecylpyridinium surfactants has inherent problems. Obtaining pure samples and then maintaining their purity is difficult; in the case of the acetate it frustrated most attempts at characterization. In the end, it was determined that the safest way to store the acetate salts was at $-80°C$ in dilute methanol or aqueous solution with a small amount of added radical inhibitor.

Basic characterization of the bromide and chloride salts, however, afforded results that are consistent with literature information on the behaviour of analogous pyridinium surfactants. The CMCs of the surfmers are uniformly lower than those of dodecylpyridinium salts due to the mildly hydrophobic nature of the vinyl group. While the effect on solubility of the substituent position in alkylpyridiniums has not been widely studied, those observations that do exist correlate with our results: namely that a *para* subtituent has a greater hydrophobizing effect than an *ortho* one [236, 237]. This can be rationalized on the basis that the *ortho* vinyl group is within the sphere of influence of the charged nitrogen; the hydrogen bonding of surrounding water is therefore less peturbed by its presence than by that of a *para* group.

The micellar morphology of these surfmers was studied by SANS, and was shown to be generally spherical. Dimensions followed the expected trends regarding counterion binding strength, but little difference was seen between the 2- and 4-substituted isomers. Despite its more weakly-binding counterion, the already-polymerized 2VDPA showed lower solubility and oblate micelles. With no evidence of large polymeric aggregates, this suggests that the spontaneous reaction it underwent during freeze-drying produced short oligomeric surfactant species, rather than a polysoap. This is developed further in Chapter 5.

Heating the micellar solutions tended to produce the expected decrease in micellar size, but was more indicative of the great propensity of these surfactants to spontaneously polymerize. This was not the case for the already-polymerized 2VDPA, the micelles of which underwent a slight but permanent reduction in size.

The concentrated phase behaviour for these surfmers is quite uniform. As surfactant concentration increases, the micellar phase of 2VDPC becomes a discrete cubic phase, indicating that the spherical micelles observed by SANS remain spherical and highly charged up to the concentration of the mesophase. However the lowest-concentration

mesophase formed by 2VDPB and 4VDPC/B is the hexagonal phase, suggesting that the spherical micelles undergo a sphere-to-rod micelle transition at some point.

Unsubstituted alkylpyridinium surfactants show similar phase sequences. Dodecylpyridinium chloride forms discrete cubic and hexagonal phases [221], while the bromide analogue forms only the hexagonal phase [227, 238]. The absence of the discrete cubic phase in the latter case – and in the case of the VDPBs – indicates greater binding of the counterion. This has the effect of raising the packing parameter of the surfactant such that elongated (cylindrical) micelles form in preference to the discrete cubic phase. The absence in all cases of any low-curvature phases at high concentration (e.g. V_1 and L_α) suggests that the aromatic headgroup may tilt, causing a larger effective headgroup area. As with other surfactants with bulky headgroups (triethyl, tripropyl etc. [221]), the steric contribution to the headgroup area prevents the surfactant – in the absence of additives – from attaining a packing parameter that will favour bicontinuous or lamellar structures.

Our investigation of the adsorbed layer structures formed by the surfmers on mica was limited, and only bilayer-like structures were observed. This seems odd, given that dodecylpyridinium chloride forms globules. This may be another artefact due to spontaneous polymerization, and further work is needed to resolve it.

While not discussed here, a series of polymerization experiments were performed with the surfmers, using the excess initiator method. All of these produced insoluble products, although polymerized 2VDPC proved to be soluble at 80°C. While it was originally intended to apply the chain-transfer techniques to this new family of surfmers, the research took a different turn before these experiments were performed. This new direction is discussed in the following chapter.

Chapter 5

A new route to oligomerization

"The fascination of what's difficult..."

W. B. Yeats

5.1 Introduction

As discussed in Section 1.3, quaternized vinylpyridines (i.e. vinylpyridinium compounds) are particularly reactive as monomers, and will polymerize under a range of conditions and by several different mechanisms. The two most important of these are free-radical and anionic polymerization. While it was originally intended that the same free-radical techniques attempted with the methacrylate surfactants would be applied to these surfmers, it was a variant of the anionic mechanism that turned out to be more useful.

The generalized anionic polymerization of vinylpyridines and vinylpyridiniums is represented in Figure 1.16. The polymerization of this family of compounds has been investigated from a variety of angles, with one series of studies looking at the stereochemistry of addition during the polymerization of vinylpyridines [240–244]. In this work, Hogen-Esch et al. used carefully controlled conditions to produce dimers, trimers and tetramers of vinylpyridine. The initiating species was made by adding alkyllithium agents to ethylpyridine. This generated a carbanion by abstracting one of the α-protons on the ethylpyridine. Vinylpyridine was then slowly distilled *in vacuo* into a solution of the carbanion in THF at $-78°$C. Reaction proceeded by anionic polymerization as in Scheme 2 of Figure 1.16. The oligomer size was determined by the ratio of carbanion to

vinylpyridine, and termination was effected either by addition of a proton source (e.g. methanol) or reaction with methyl iodide, to produce the neutral final product.

A difference in the reaction rates and stereochemistry of the 2- and 4-vinylpyridine monomers was noted. This was attributed to intramolecular coordination by the 2-vinylpyridine product, occurring between the nitrogens on two adjacent units and a metal cation from the initiating carbanion [242, 244].

More recent work by Alunni et al. looks at the opposite reaction: elimination reactions performed on haloethylpyridines/pyridiniums and similar compounds to form vinylpyridines. This has relevance for biological enzymatic reactions [129, 130, 245, 246]. The rate of this elimination was found to be greatly increased by quaternization - whether by a proton [129], a methyl group [130], or by coordination with a metal cation (zinc or cadmium) [245]. The ratio of the reaction rates with and without quaternization was called the activating factor.

This work was based around determining whether the elimination occurs by an E2 or E1 mechanism. The E1 mechanism proceeds via a carbanion intermediate, which is stabilized by resonance with a pyridone methide or enamine structure. As discussed in Section 1.3, this stabilization is considerably enhanced by quaternization of the pyridine ring. Such a difference in stability between the quaternized and unquaternized compounds accounts for the significant activating factor seen in the elimination reaction, and it was therefore concluded that the mechanism was E1.

The novel oligomerization reaction described in this chapter comprises a combination of the reactions studied by the groups of Hogen-Esch and Alunni, and relies heavily on the superior stability of the quaternized carbanion. Inasmuch as it can be classed as a form of polymerization, the reaction resembles a step-growth rather than a chain-growth polymerization, and proceeds via an elimination/addition mechanism. It allows vinylpyridinium species to be oligomerized in a controlled fashion under very undemanding conditions, and in such a way as to allow changes in self-assembled structures to be observable by scattering in real time. It is also used here to produce a series of oligomer mixtures, the phase behaviour and surface adsorption of which are investigated in the following chapter. It is referred to here as linkage by elimination/addition, or LELA.

5.2 Anionic polymerization

Investigations into this area began as attempts to prevent the spontaneous polymerization of the vinylpyridinium surfmers. This process occurs both by free-radical and anionic mechanisms and under a variety of conditions, but three in particular were remarkable and are described below. While most of the schematics depict the 4-substituted surfmer or compounds derived from it, all these mechanisms are equally applicable to the 2-substituted compound (see Table 2.2 for naming conventions).

5.2.1 Reactions of the vinyldodecylpyridinium surfmers

Aqueous reaction with base

Addition of sodium hydroxide, sodium carbonate, ammonia, methylamine or other strong bases to an aqueous solution of any of the vinylpyridinium surfmers caused an immediate precipitation of brown polymerized surfactant. This could be dissolved in fresh or ethanol-stabilized chloroform; the 2-substituted surfmers gave a yellow-brown solution, while the 4-substituted surfmers gave a blue or green solution. If old, unstabilized chloroform were added to the latter, decolourization occurred. It was later shown that decolourization was a function of pH:* the addition of acid to a coloured solution of 4VDPX would remove the colour, but it could then be regenerated by the addition of sufficient base.

^{1}H NMR showed these samples to be completely polymerized, with broad peaks indicative of relatively long chains. No difference could be observed between the spectra of the coloured and uncoloured solutions.

This reaction occurred at room temperature in a solution that had not been deoxygenated, and in the presence of impurities. More importantly, it occurred in the most protic solvent available - water. This indicated that if the mechanism were anionic, as the initiation method suggested, the propagating carbanion was stable enough to survive potential termination by the usual routes [76].

*Without the addition of a stabilizer such as ethanol, chloroform is known to degrade over time to form phosgene and hydrochloric acid.

Freeze-drying

In producing the bromide, chloride and acetate salts of the surfmers by ion exchange, it was necessary to protect the surfactants at all times from light and heat. Following the exchange, the aqueous solutions were frozen in liquid nitrogen, covered in aluminium foil and placed on a freeze-dryer. In the case of the bromides and chlorides this was effective, and produced relatively pure solid surfactant.

However, freeze-drying the solutions of 2VDPA and 4VDPA caused the surfactants to react, with ^{1}H NMR showing complete disappearance of the vinylic protons. In the case of 2VDPA, the solid was dark brown, sticky, water-soluble and retained surface-active properties (e.g. foaming). The 4VDPA was dry, grainy and insoluble in water, although on contact with water, the initially pale brown grains instantly became pale blue. Over the course of several days, the substance became a dark turquoise colour, and after several months, once more became brown. Like the polymer that precipitated with the addition of hydroxide, it dissolved easily in fresh or ethanol-stabilized chloroform to form an intensely blue-green solution, but the addition of acid caused decolourization. In addition, and despite its insolubility in pure water, it could be dissolved in a tiny volume of alcohol and then diluted infinitely with water without precipitation.

In this case, as the aqueous solution underwent freeze-drying, the weakly basic nature of the acetate counterion caused the concentration of hydroxide ions to increase along with that of the surfmer. In a reaction similar to that described above, polymerization resulted. However, in the case of 2VDPA, the degree of polymerization was low enough that the chains retained water-solubility and surfactant properties.[†]

Spontaneous addition of alcohols

It was noticed that samples of the 4-substituted surfmer (regardless of the counterion), prepared for NMR by dissolution in deuterated methanol, turned pale blue over the course of a day or so. Monitoring such solutions by NMR and mass spectrometry for a week showed that the vinyl bond reacted spontaneously with methanol, deuterated methanol and ethanol to form 4-(2-methoxyethyl)- or 4-(2-ethoxyethyl)-*N*-dodecylpyridinium.

There were also changes in the ^{1}H spectrum that suggested that a small amount of polymerization was taking place. To eliminate the possibility that spontaneous

[†]Later analysis by HPLC showed this sample to consist primarily of trimer.

free-radical polymerization was occurring, the stable radical (and radical scavenger) TEMPO was added to these solutions [247]. This did not prevent the development of the colour, nor did mass spectrometry reveal any evidence to suggest that TEMPO had been incorporated into growing chains.

Instead, it was found that with the addition of a small amount of base (e.g. triethylamine), the reaction could be accelerated. This was accompanied by an increase in the intensity of the colour. Again, the colour could be (repeatedly) removed by acid, and regenerated with base.

5.2.2 Anionic polymerization as a synthesis method

Combining these observations, it was clear that these surfmers possessed several properties which could prove useful not only for controlling their polymerization, but also in adapting the reaction to in situ polymerizations of self-assembled surfacant systems. Firstly, the propagating species is stable under very undemanding conditions, including the use of water as a solvent. Secondly, the properties of the freeze-dried 2VDPA sample showed that with sufficiently short oligomers, surfactant properties are retained – a fact which was never satisfactorily proven for the methacrylate surfactants. Thirdly, the reaction of the NMR solutions showed that the same reaction could be performed in organic solvents, which meant that oligomers could also be produced in 'bulk' (i.e. in non-self-assembled solutions), also simplifying solvent removal after the reaction.

The reaction was therefore tested by adding 4VDPC in methanol to a methanolic solution of sodium hydroxide. The mixture was stirred for ten minutes, during which time it developed a deep green colour. A small amount of concentrated hydrochloric acid was added to terminate the polymerization (i.e. forcing the carbanion to protonate), which decolourized the solution. Finally, the methanol was removed by rotary evaporation. NMR on the product showed a mixture consisting principally of 4-methoxy-N-vinylpyridinium chloride (4MDPC; see Table 2.3 for naming conventions), with smaller amounts of oligomeric material. The mechanism of this base-initiated reaction is summarized in Figure 5.1. The same reaction can be performed with 2VDPX; in this case the solution becomes a pale lavender colour upon addition of the base, but this later turns orange-brown.

The challenge from here was to develop a method for reproducibly making short oligomers, and a method similar to that used by Hogen-Esch et al. was therefore devised.

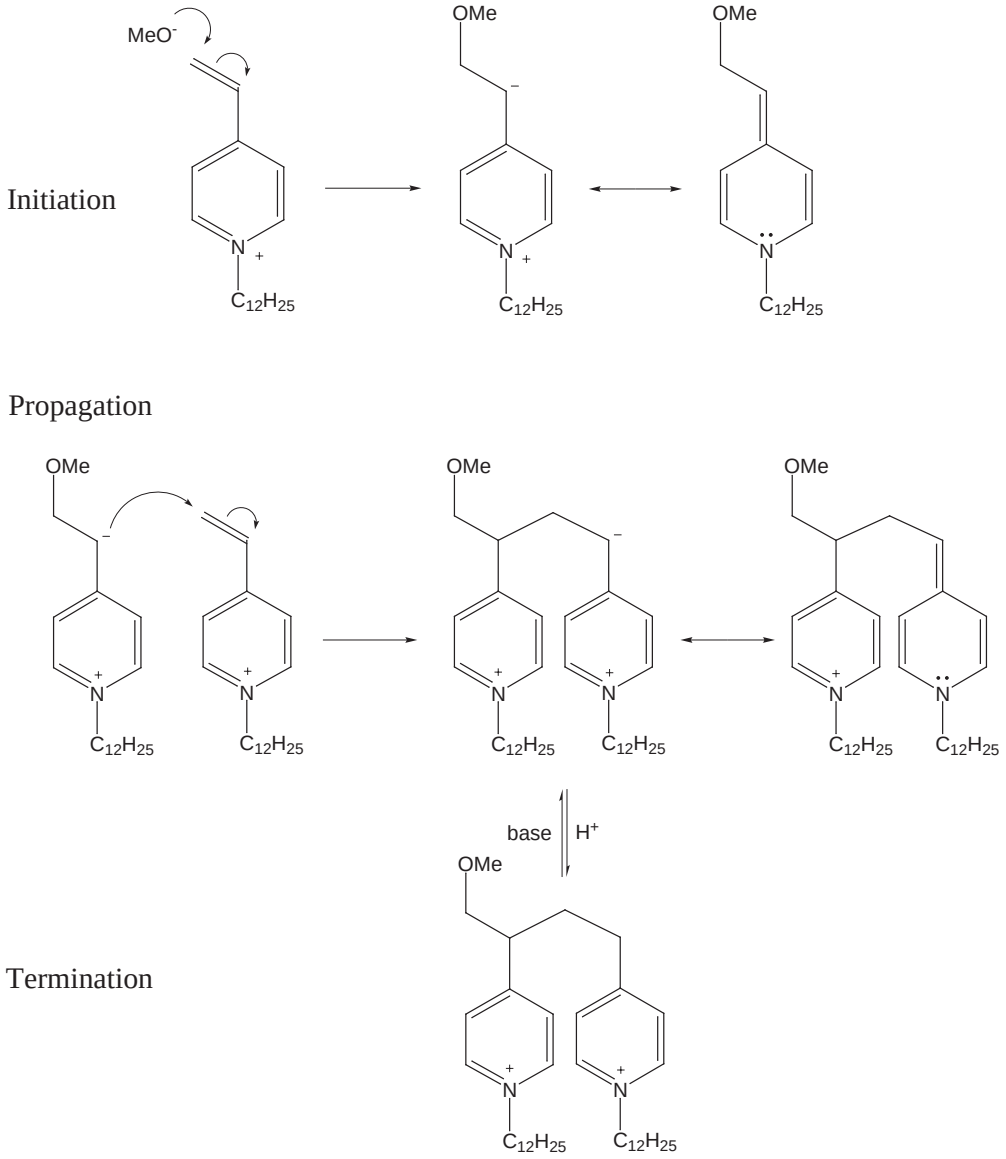

Figure 5.1: Base-initiated anionic polymerization of 4VDP.

In such a reaction, the initiating species would be generated by the addition of base to 4-vinyldodecylpyridinium chloride (for example), as in the initiation step in Figure 5.1.

Oligomers of defined length could then be made by reacting this initiating species with measured aliquots of surfmer. The reaction could be terminated at any point with acid. From here on, the 2- and 4-MDP cations will be referred to as 'unimers', in order to distinguish them from the vinyl monomer.

5.3 The LELA reaction: Linkage by ELimination/Addition

5.3.1 Production of 2- and 4MDPC

Developing the first step of this process – making pure unimer – required several variables to be optimized. The most important of these were the relative and absolute concentrations of the surfmer and base, the temperature and the rate of addition. The most effective method involved dilute solutions (5–10 mM), with quick addition of the surfmer to the base, vigorous stirring and quenching with acid within 60 seconds. Figure 5.2 shows the ^{1}H NMR spectra of the monomer and unimer.

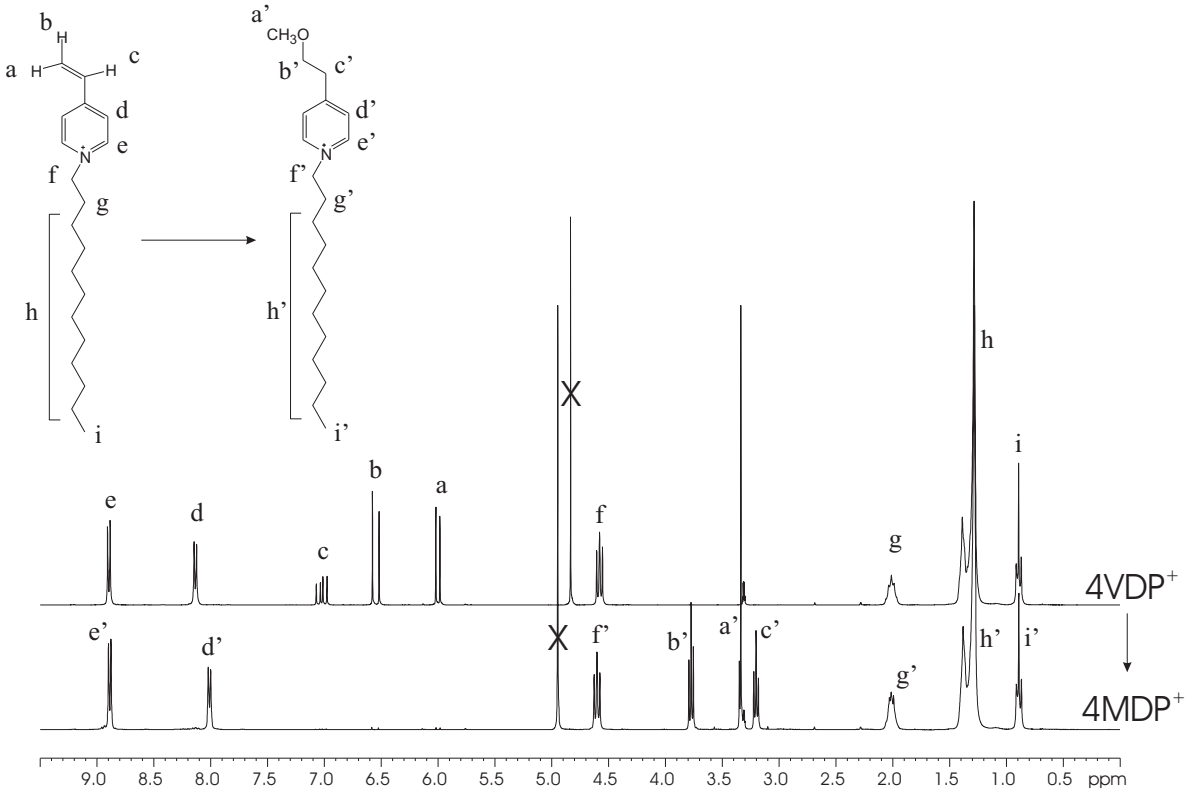

Figure 5.2: ^{1}H NMR spectra of the 4-vinyl-*N*-dodecylpyridinium chloride and 4-(2-methoxyethyl)-*N*-dodecylpyridinium chloride in deuterated methanol. The solvent residual peak (used as a reference) is visible as a short multiplet at 3.31ppm. The samples are hygroscopic and contained a small amount of water: these peaks are marked with an X. The 4MDPC sample was not recrystallized, and contains trace amounts of oligomer and the original monomer.

It should be noted that in the long run, it makes more sense to synthesize the unimers – without risk of polymerization – by quaternizing 2- or 4-methoxyethylpyridine with bromododecane. At this stage of the research, however, learning to control the reaction was as important as producing pure unimer.

Unexpectedly, an excess of base turned out to be unnecessary, with relative concentrations of 10 mol% and 50 mol% of hydroxide (generating methoxide in solution) being equally effective. (For reasons that will be discussed later, higher concentrations of base actually tended to produce more insoluble material.) This suggests that in the absence of added acid, the active species can abstract a proton from a molecule of solvent, thereby regenerating the methoxide anion (see Figure 5.3). In addition, at least at such low surfactant concentrations, this process is faster than propagation, meaning that nearly quantitative conversion to the addition product can be achieved.

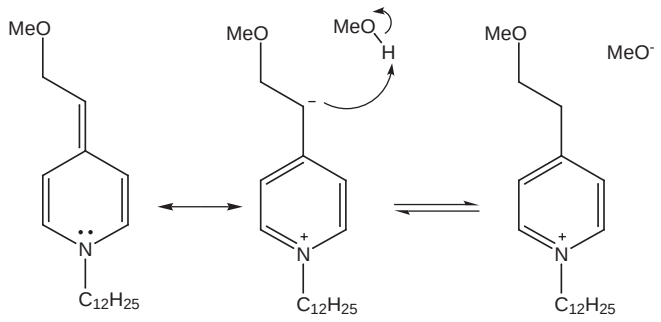

Figure 5.3: Regeneration of base.

After synthesis, the unimer can be purified using a modification of the chromatographic procedure described by Bluhm and Li [47]. This involves first passifying silica gel by the addition of sodium bromide, and has the side-effect of ion-exchanging the unimer to the bromide salt. This can be reversed later if necessary by ordinary ion exchange.

However, a successful conversion to the unimer does not constitute the end of this reaction. A reaction solution, shown by ^{1}H NMR to have been completely converted into unimer but left unquenched, undergoes further reaction to spontaneously produce oligomers. For this reason, the Hogen-Esch method of oligomerization was not attempted, and this apparently 'vinyl-less' oligomerization was investigated.

5.3.2 Detection and purification of oligomers

Before describing the oligomerization reaction, it is worth noting the methods used to identify and manipulate mixtures of oligomers. Identification is achieved by several methods. ^{1}H NMR reveals a slight downfield shift for the aromatic protons when oligomerization occurs. Mixtures of short oligomers can also be separated by HPLC, and are easily detected by the strong UV absorbance of the pyridinium ring. Using an electrospray mass spectrometer in line with an HPLC system, each chromatographic peak can be positively identified: this is effective for species up to tetramers. Figure 5.4 shows a typical HPLC trace for a mixture of oligomers derived from 4VDPC.

To some extent, oligomers can be fractionated according to their solubility properties. Mixtures of short oligomers stirred in acetone will separate into an acetone-soluble fraction, consisting of unimer and very small amounts of dimer and trimer, and an

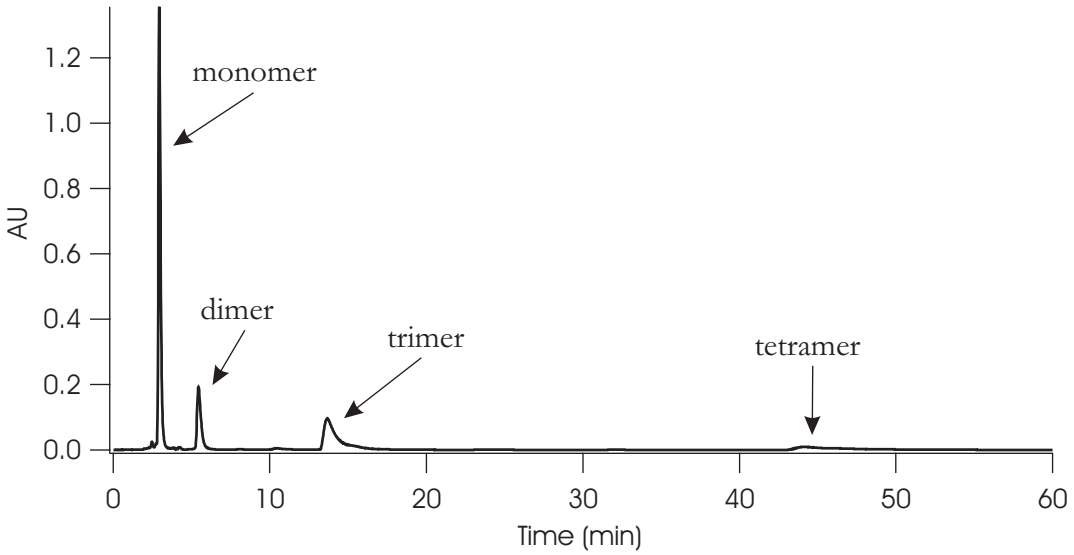

Figure 5.4: Reverse-phase HPLC trace showing the composition of a mixture of 4MDPC-based oligomers. The eluent was 10 vol% water and 10 vol% dichloromethane in methanol with 0.2 M NaCl. Detection was by UV absorbance at 257 nm.

acetone-swollen solid, comprising the remainder of the longer oligomers. Due to the limits of HPLC, we have been unable to identify species longer than the tetramer, but a critical length exists above which the oligomers/polymers are insoluble in water. All oligomers can be salted out of aqueous solution with the addition of excess chloride.

In addition, there is a likelihood that the chromatographic protocol based on that of Bluhm and Li and used to purify the unimer (see Section 2.3.5) could also be modified to

separate the oligomers. Thin-layer chromatography on oligomer mixtures, using silica gel treated with a methanolic solution of sodium bromide, showed good separation with chloroform/methanol eluents. Further work is needed to verify whether this is a practical method for producing pure oligomers.

5.3.3 The oligomerization reaction

The basis of LELA is that the unimer compounds described above spontaneously oligomerize in basic solution. Initial attempts at the reaction started by taking the vinylpyridinium surfmer, converting it into the methoxyethylpyridinium unimer as described above, and then leaving the reaction solution unquenched. However, the results are identical – and avoid unwanted long-chain polymer from conventional anionic polymerization – if one starts with a solution of unimer and raises the pH. The reaction is believed to proceed as follows.

The initial step involves the deprotonation of the unimer, converting it into the active zwitterion. This is an equilibrium, and is identical to the initiation step described for the Hogen-Esch process (see Figure 5.5). The reaction solution now contains both active and inactive unimers. As shown in Figure 5.6, and in a reaction very similar to that described by Alunni, the active unimer is able to undergo elimination to (re)form the vinyl compound. The rate of production of the vinyl monomer is slow, but it is followed by a fast addition reaction, in which the monomer is attacked by another active unimer to form a dimer.

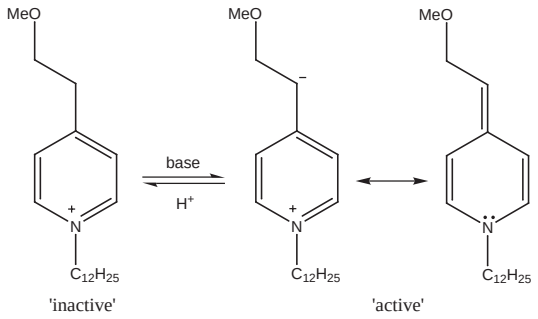

Figure 5.5: Deprotonation (initiation).

The ability for elimination to follow deprotonation means that it is also possible that the oligomers undergo a chain degradation reaction (illustrated in Figure 5.7).

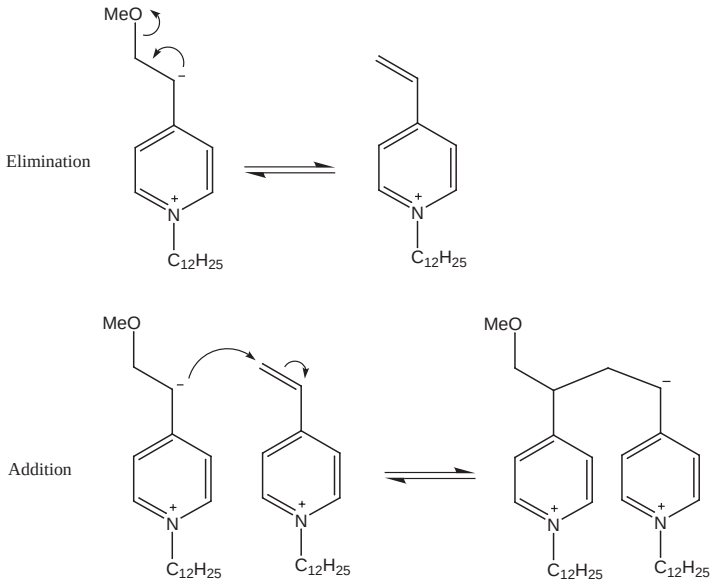

Figure 5.6: Propagation: formation of a dimer by the LELA reaction.

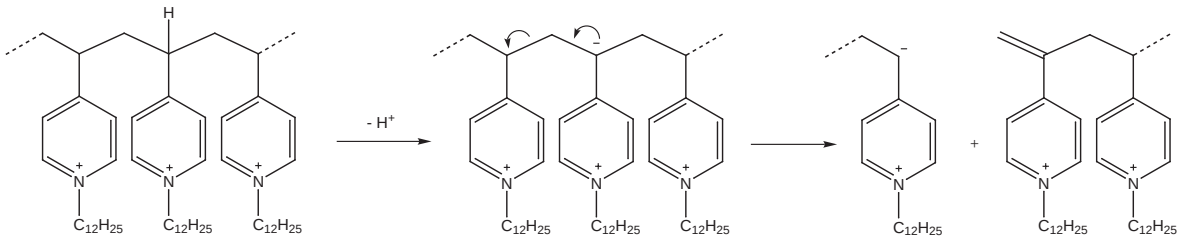

Figure 5.7: Degradation: mechanism for base-catalysed chain degradation of vinylpyridinium oligomer/polymer.

Some evidence has been obtained for this reaction: for instance, two weak ^{1}H peaks corresponding to the CH_2 end of the vinyl bond are often seen in oligomer mixtures at $6.0 - 6.5$ ppm. Further, as discussed in Section 4.2.2, heating of a micellar solution of the freeze-dried (oligomerized) 4VDPA produces behaviour indicative of a reduction in the average oligomer length. A similar effect is mentioned by Avent et al. in their study of small and polymeric pyridinium molecules [248].

While our kinetic experiments did not reach equilibrium (see Figure 5.9) they showed signs of moving in that direction. We expect that after a certain time, depending on factors such as temperature and the concentration of surfactant and base, an equilibrium is reached between propagation and degradation reactions and the distribution of

oligomers becomes stable. More kinetic work is required to confirm this.

There is also the possibility that the growth mechanism incorporates elements of step-growth polymerization. This is because elimination or degradation produces a vinyl bond on the 'left-hand' end of an oligomer (i.e. the end at which growth originally began). This allows linkage to occur at both ends, and even for two longer species to link together, e.g. an active dimer attacking a vinyl-trimer to produce a pentamer. In all however, the reaction bears a strong similarity to the reverse anionic polymerization reported for cyanoacrylate emulsions by Limouzin et al. in 2003 [249].

These processes continue as long as the solution remains basic, and in the case of the 4-substituted compounds, this is indicated by the green colour of the solution. In each propagation or degradation step, the basic anion used up in forming an active zwitterion is regenerated from the leaving group when elimination occurs. Hence, the base has a catalytic role, and both propagation and degradation are only stopped by the addition of acid, which protonates all the active species and decolourizes the solution. This protonation is easily reversed, giving the reaction the characteristics of a living polymerization. Permanent termination – where required – should be achievable by methylating the oligomers instead of protonating them [243]. This reaction has not yet been attempted with these compounds.

5.3.4 Chemical kinetics: NMR and HPLC

The experiments from which the following data were collected all took place in methanolic solutions of sodium hydroxide. Figure 5.8 shows NMR spectra of the 4MDPC oligomerization solution quenched after various time periods. The downfield extract shows the shift in the aromatic protons (d,e) upon oligomerization. The upfield extract (which is slightly offset for clarity) shows the disappearance of the methoxyethyl protons (a,b,c) and their replacement by the backbone protons (b',c').

Figure 5.9 shows the changing percentages of oligomer in three different reactions. The percentages were calculated by taking a chromatogram at each time step and integrating the absorbance peak of each species. Graphs A and B show reactions of 4MDPC with 50 mol% and 10 mol% sodium hydroxide respectively. The effect of the higher concentration of base is clear: the rate of propagation is higher and a greater proportion of longer oligomers is formed before equilibrium is attained. This reflects that fact that a higher pH will shift the deprotonation equilibria to the right, producing

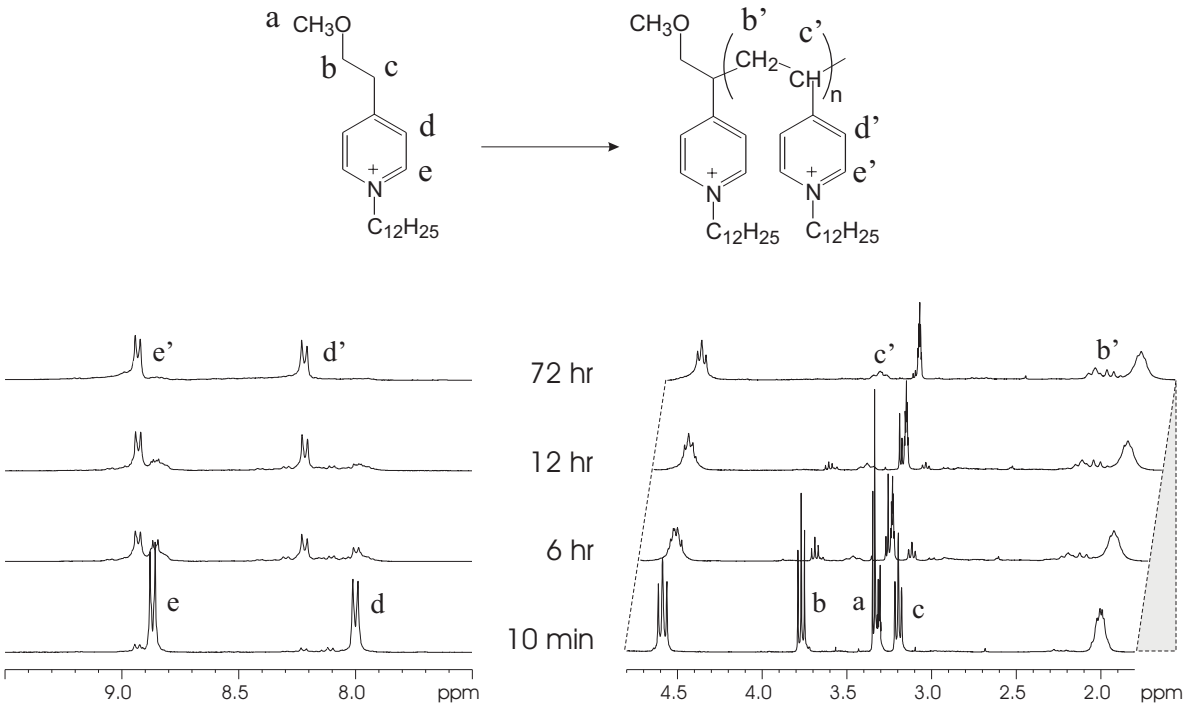

Figure 5.8: Extracts from ^{1}H NMR spectra from the oligomerization of 4MDPC. The solvent residual peak (used as a reference) is visible as a short multiplet at 3.31ppm. Note that the upfield spectra are offset for clarity.

a greater concentration of active species.

Graph C shows a reaction of 2MDPC, with the same concentration of base as in Graph A.[‡] The rate of consumption of the unimer is similar (not identical), but the relative proportions of oligomer are quite different. 4MDPC appears to have a tendency to form longer species more quickly. In particular, it seems that the 4-substituted dimer reacts to form longer species at approximately the same rate as it is produced. Given that its concentration is so much lower than that of the unimer, this suggests it is more reactive. However, given the step-growth nature of the reaction and the fact that this data doesn't allow us to distinguish between the nucleophile and the species being attacked, it is impossible to determine the exact nature of this difference. The effect may be due to the relative pK_as of longer and shorter species, or a counterion or intramolecular coordination effect that affects the reactivities of active molecules similar to that described by Hogen-Esch et al. [242, 244]. Alternatively it may be a

[‡]The 2MDPC tetramer had too long a retention time to be detected by HPLC in this case.

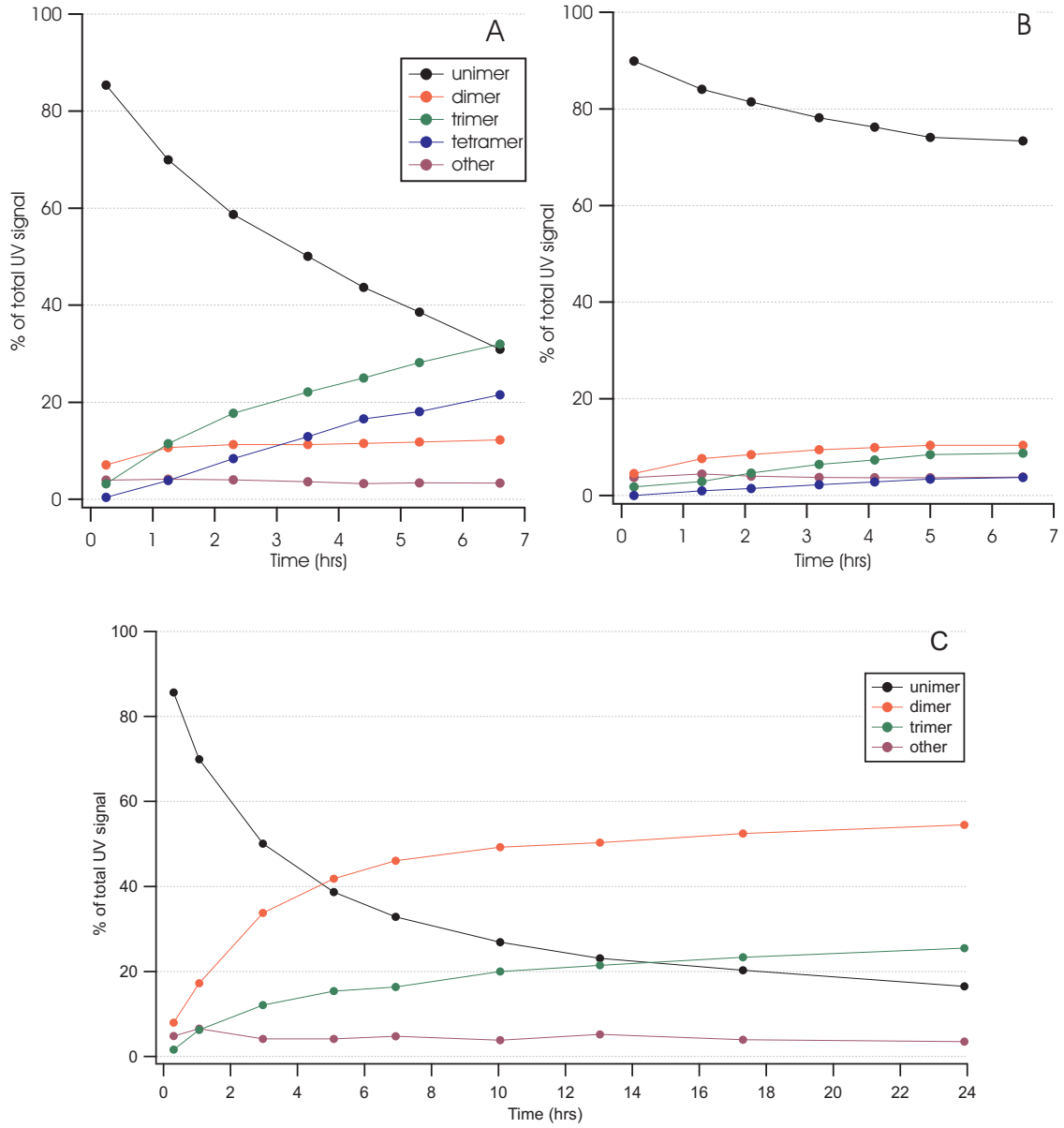

Figure 5.9: Progress of LELA reactions over time. (Top) 7.5 mM 4MDPC in methanol with (A) 50 mol%. NaOH and (B) 10 mol% NaOH. (Bottom) 7.5 mM 2MDPC in methanol with 50 mol% NaOH. Data was collected by quenching a sample of the reaction at each time period and analysing it by HPLC with UV absorbance detection. 'Other' indicates unassigned impurities in the chromatogram.

result of the interplay between propagation and degradation.

As the reaction proceeds, the number of molecules in solution decreases, and with it, the number of end units carrying a leaving group. The rate of propagation therefore decreases as well. Simultaneously, the concentration of backbone units increases, and

with it the rate of degradation. Given the current data, it seems that the reaction could be pushed to give longer average molecular weights by increasing any or all of the surfactant concentration, pH and temperature. However, there may be a non-trivial contribution from the degradation process under such conditions, and excessively high concentrations of base will cause irreversible degradation of the pyridinium rings [119]. As it is, it is very convenient to be able to restrict the reaction to low average molecular weights.

Unfortunately, time restrictions prevented the kinetics of the aqueous reaction from being studied. A direct comparison is thus impossible at the present time, but would make for interesting work in the future.

5.3.5 Physical kinetics: SANS

While the experiments described so far employed the same reactant and solvent, many variations could potentially be made to the solvent, base, and the leaving group on the pyridinium compound. For instance, work on elimination reactions of haloethylpyridinium compounds by Alunni et al. suggests that these would work equally well, with the rate adjustable by changing the halogen. Of more immediate interest to a surfactant chemist, however, is whether this reaction would work in water.

The reaction was therefore repeated using an aqueous solution of 7.5 mM 4MDPC and 50 mol% sodium hydroxide. Of primary concern in this experiment was that the oligomers should remain solvated and self-assembled. Over the course of 24 hours, no sign of precipitation was observed, and HPLC indicated that the reaction was progressing as expected.[§]

The significance of this successful transfer to the aqueous medium is that any morphological changes to self-assembled structures in the solution should be observable in situ. For this purpose, a series of small-angle neutron scattering experiments were performed.

A range of different concentrations and ratios of 4MDPC and sodium hydroxide were studied, but it was found that in the more concentrated solutions (e.g. 30 mM 4MDPC with 100 or 50 mol% OH) significant early morphological shifts were completed too

[§]Another variation of the reaction that was briefly investigated used the small pyridinium compound 2-(2-hydroxyethyl)-*N*-methylpyridinium iodide (2HEMPI). Here the LELA leaving group is hydroxide. A 2 wt% solution in D_2O was allowed to react with 1 mole equivalent of NaOD overnight. It was investigated with ^{1}H NMR, which showed extensive oligomerization.

quickly to be observed by SANS. At lower OH ratios or lower 4MDPC concentrations, however, a clear progression was found.

Figure 5.10 shows a series of spectra collected from a 30 mM solution of 4MDPC in D_2O with 25 mol% sodium hydroxide. The base was added to the surfactant solution immediately before being placed in the beam; the first spectrum collected is at $t_{reaction} =$ 30 s. In the interests of clarity, error bars are not shown and the background has not been subtracted. In the lower image, the full spectra of unreacted 30 mM 4MDPC and $t_{reaction} = 90$ min are shown. A polydisperse spheres model with hard-sphere interaction was used to fit the reaction spectrum with the following parameters: volume fraction 0.3%, average radius 93 Å, polydispersity 0.2. The origin of the discrepancy between data and model at low q is unknown, but may indicate the presence of larger particles outside the observed q-range. With slightly higher volume fraction and particle size, the model is able to fit this region perfectly, but at the expense of the interference fringes at mid-range q (e.g. at $q = 0.06\,\text{Å}^{-1}$).

There are three notable features to this set of spectra. Firstly, the micellar shoulder seen in the unreacted solution initially increases in intensity, and then decreases steadily to background levels over the course of the reaction. Secondly, scattering at low-q increases, indicating the growth of particles larger than micelles. The lower figure shows that this is not simply the Porod-limit scattering of precipitated polymer, for it levels off at around $q = 0.01\,\text{Å}^{-1}$. Thirdly, as the reaction proceeds a small but relatively sharp peak appears at $q \sim 0.17 - 0.19\,\text{Å}^{-1}$.

Intuitively, it might be expected that as a 30 mM solution of surfactant changed from unimers to oligomers, there would be a shift from spherical or short rod-like micelles to long cylindrical or worm-like micelles. Instead, we see the micelle population depleted and the formation of moderately large but not overly polydisperse particles. In addition, a short peak appears at high q, which is consistent with the spacing in an ordered mesophase. This peak appears all but the most dilute reactions, and as the average size of the low-q particles increased, it becomes sharper and more intense, and shifts to slightly higher q.

Overall, this data gives the impression that as the reaction proceeds, nanoparticles of an ordered mesophase form and grow as the average oligomer length increases. (While a more comprehensive SAXS study is needed to confirm this interpretation, supporting results are discussed in the following chapter.) The low fitted volume fraction (0.3% in a $\sim$ 1 wt% solution) may be indicative of two things. First, if the particles are

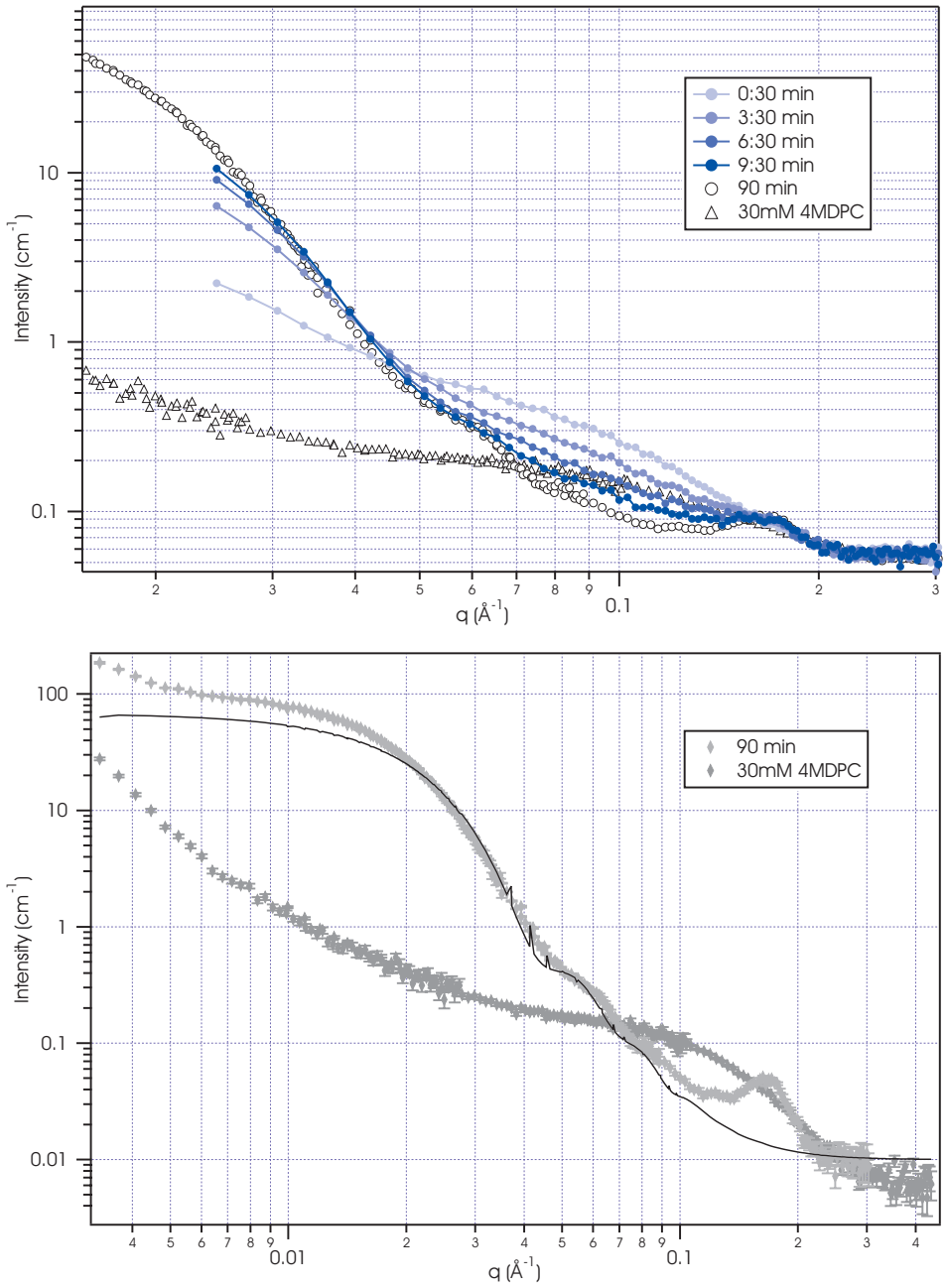

Figure 5.10: SANS spectra of aqueous LELA reactions over time. (Top) 30 mM 4MDPC in D_2O with 25 mol%. NaOH. (Bottom) Before and after: unreacted 4MDPC and 90 min after mixing.

fragments of an ordered mesophase, they contain a percentage of D_2O which would lower the overall contrast and thereby decrease the apparent volume fraction. Second, the slight upturn at the low-q edge of the spectrum and the discrepancy between the

fitted spectrum suggests that there may be a second, larger population of particles in solution: in other words, there may be a bimodal distribution of particles.

As noted above, the aqueous environment is likely to alter the kinetics of the reaction compared to the methanolic reactions discussed in the previous section. HPLC and NMR facilities were not available when the SANS measurements were made, so a direct comparison of the compositions of the methanol and aqueous reactions has not yet been made.

5.4 Discussion

The work in this chapter relates to LELA, a new polymerization-based method for producing oligomeric surfactants from pyridinium compounds. It is something of a Frankenstein reaction, combining the charged propagating species from the anionic polymerization of vinylpyridiniums with an elimination/addition mechanism, and possibly having some step-growth polymerization character. It can also be activated and deactivated by changing the pH, classifying it as a living polymerization.

Both anionic polymerization and elimination/addition in vinylpyridinium compounds are well known, and the reversible anionic polymerization of cyanoacrylates has also been investigated. However, this particular linkage reaction has apparently never been reported. This is unsurprising given its slow rate and the rather specialized areas in which it can be applied. There is a neat confluence, however, between the characteristics of this reaction and the desire to observe physical changes in a surfactant system that is shifting from unimeric to oligomeric species.

The chemical kinetics of the reaction can be observed with NMR, mass spectrometry and HPLC. Because it can be performed in water, however, it is also possible to use scattering techniques to observe the physical kinetics of the self-assembled structures formed by the changing surfactants.

The high beam-flux and contrast of small-angle neutron scattering means this technique was well suited for observing this process. Using 4-substituted unimer and sufficiently low concentrations of base, it was possible to follow the initial disappearance of a micellar peak and the simultaneous growth of a population of larger particles. As the larger particles grow, a small peak at high q appears and becomes sharper, suggesting that the particles are internally ordered and may in fact be fragments of a concentrated surfactant mesophase. Further evidence in support of this interpretation is discussed

in Chapter 6.

Because of time limitations, a number of possible variations and improvements on the LELA reaction have not yet been explored. Further work could therefore include:

- adjusting the reaction conditions to more closely resemble the method used by Hogen-Esch [241], i.e. by the addition of controlled aliquots of unimer to some initiating species. This should give a more controlled reaction with a narrower distribution of lengths, thereby allowing oligomers to be synthesized in larger quantities and greater purity.

- improving the chromatographic purification protocol in order to separate mixtures of oligomers. This would be useful for a comparison with the behaviour of mixtures, and therefore a more thorough characterization of the effect of oligomer length on surfactant properties.

- undertaking a more careful study of the kinetics and mechanism of the reaction.

- experimenting with different leaving groups on the unimer and/or functionalization on the initiating species. The former could be used to influence the reaction rate (the haloethylpyridiniums studied by Alunni [130] would be particularly suitable in this regard); the latter the surfactant properties of the oligomers.

- experimenting with transferring the reaction to non-aqueous solvents that induce reverse micelles (hydrocarbons, toluene etc.).

In terms of surfactant chemistry, the main disadvantage of LELA is that it is currently confined to alkylpyridinium compounds. This is because several key features of the reaction (particularly the rate and the ability to perform it in water) rely on the stability afforded to the propagating carbanion by the pyridinium ring.

In principle however, there exist other compounds which might be manipulated to undergo variations of the reaction. Figure 5.11 shows alternative compounds that could potentially undergo the LELA reaction. While not all of these seem immediately suited as potential surfactants, it may be possible to locate the reactive moiety in the surfactant tail. This could open up another suite of oligomeric surfactants and self-assembled structures.

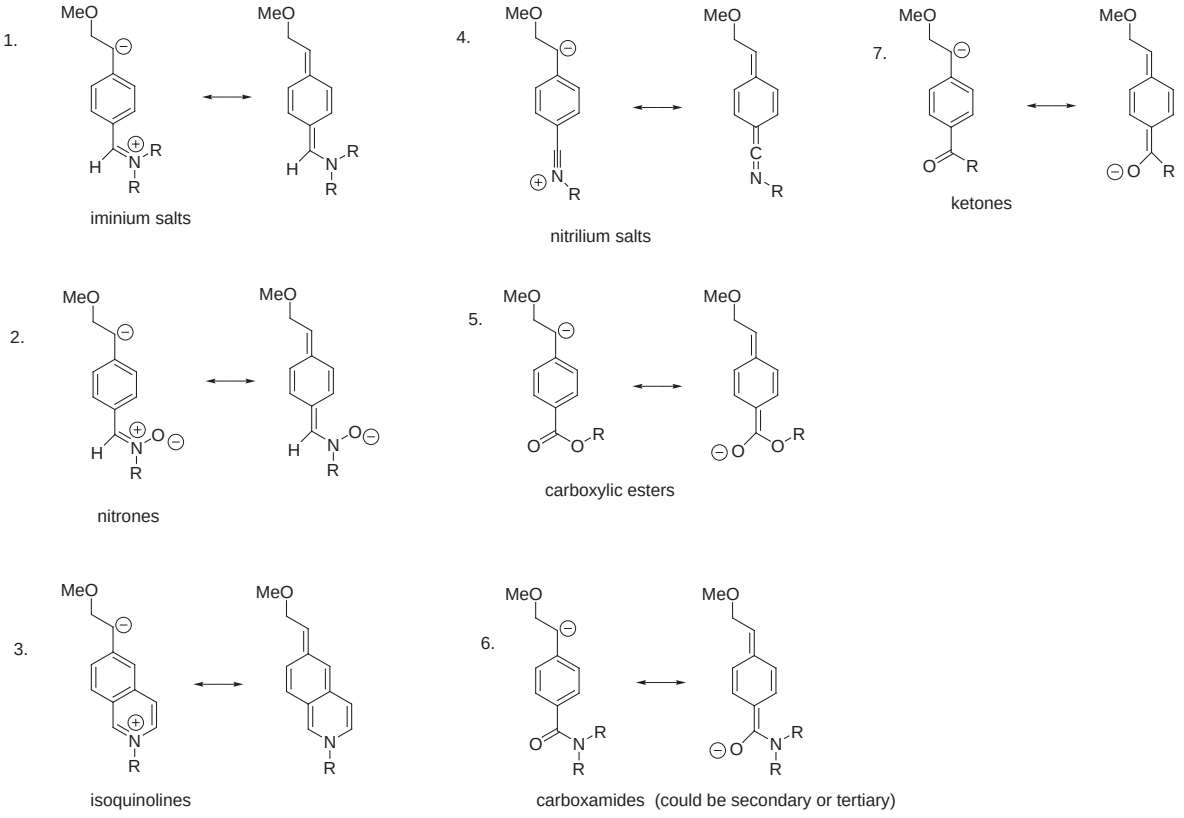

Figure 5.11: Possible chemical groups that could undergo the LELA reaction.

Chapter 6

Alkylpyridinium surfactants: unimers and oligomers

"In a knot of eight crossings, which is about the average-size knot, there are 256 different 'over-and-under' arrangements possible.... Make only one change in this 'over-and-under' sequence and either an entirely different knot is made or no knot at all may result."

THE ASHLEY BOOK OF KNOTS

6.1 Introduction

The LELA reaction, described in the previous chapter, was used to make mixtures of alkylpyridinium oligomers. In some cases, the vinylpyridinium surfmers were used as the starting point; in others we began with the alkylpyridinium unimers. Both methods produced similar results, although starting with unimer reduced the likelihood that long insoluble polymer will form.

The results that follow focus on the mesophase behaviour of both the unimers and the oligomer mixtures. While in the future it will be valuable to characterize the self-assembly of the purified oligomers, the purification protocol used for the unimers has not yet been optimized for longer species.

6.2 Phase behaviour

6.2.1 Unimers: 4MDPC and 4MDPB

4MDPC was produced by reaction of 4-vinyl-*N*-dodecylpyridinium chloride with methanolic sodium hydroxide, as previously described (see Tables 2.2 and 2.3 for naming conventions. A portion of the product was purified by column chromatography on a silica column passified with sodium bromide; this gave pure 4MDPB, which at room temperature takes the form of a waxy solid with a very slightly pinkish colour. The remaining portion of 4MDPC (a viscous yellowish liquid) was not purified further; it contained $3-5\%$ dimer, and any other impurities were not detectable by NMR.

Figure 6.1 shows a flooding experiment performed on the unpurified 4MDPC. The top picture shows surfactant concentration increasing from left to right. The isotropic surfactant is on the right, and the texture of a hexagonal phase is visible in the middle. To the left in the dilute region, an unusual stripy texture has formed. The smaller images show magnifications of this texture.

The stripy texture has been assigned as a two-phase region, since the stripes appear to adhere to the glass surface but can be detached with shearing, after which they float around and appear stable in the dilute isotropic phase. Note in the bottom left image of Figure 6.1 that the arrangement of the stripes appears to mirror the domains of the hexagonal phase from which they have developed.

It is particularly rare to see a two-phase region in a flooding experiment. In theory every surfactant concentration from 0 to 100% is spanned in such an experiment. However, at concentrations where two phases coexist (that is, where no one phase is stable), a discontinuity forms. The alternative would be for one phase to be dispersed in the other.* In this case, at the interfacial boundary on every dispersed particle, water and/or surfactant would exchange between the two phases until equilibrium was reached. In regions of higher concentration, the higher-concentration phase would eventually completely predominate. Similarly at lower concentrations, the lower-concentration phase would predominate. Equilibrium would be established when the interfacial area was minimized. This is the point at which there is a single boundary – a concentration discontinuity – and it is this situation that naturally forms as the surfactant and water mix in a flooding experiment. For a two-phase region to form therefore implies that the fragments of the dispersed phase (in this case the higher-

*The most common instance of this behaviour is the formation of vesicles (cell-like spherical or ellipsoidal bilayer structures) in dilute solutions of certain surfactants.

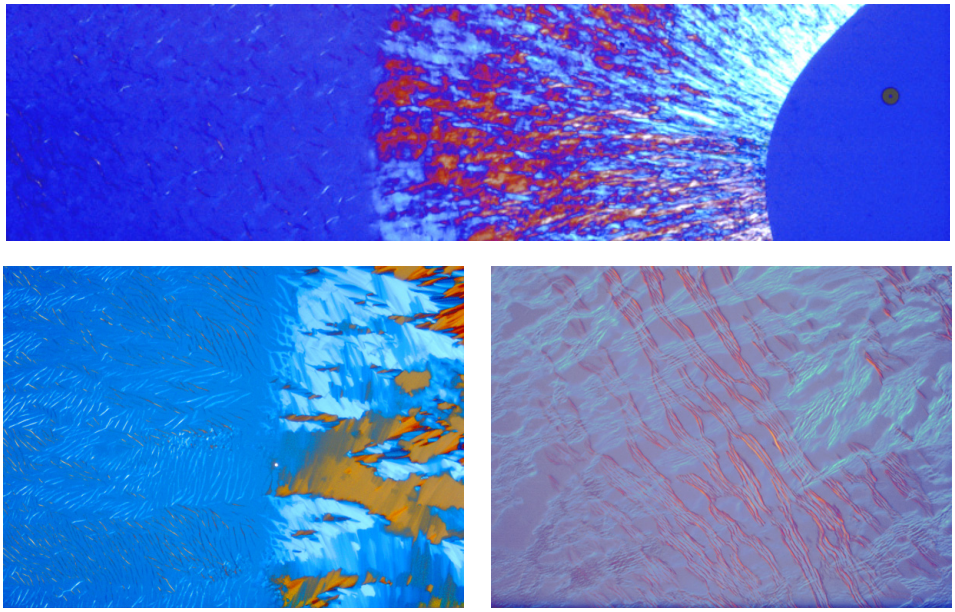

Figure 6.1: 4MDPC mixture of ∼ 95% unimer, 5% dimer; (top) full flooding experiment, showing from left to right, two-phase region, hexagonal phase and concentrated isotropic surfactant; (bottom left) enlarged section showing hexagonal texture and two-phase region; (bottom right) two-phase region at 400× magnification.

concentration hexagonal phase) are particularly stable and that interfacial transport is minimal, thereby allowing the fragments to persist.

It might be argued that this behaviour is due to the presence of small amounts of dimer. However, comparable behaviour is observed for the purified bromide salt, 4MDPB (see Figure 6.2). Immediately adjacent to the waxy surfactant crystals, a concentrated fluid isotropic phase forms, followed by a hexagonal phase. A stripy texture does not immediately form on the dilute side of this phase; rather, the hexagonal phase breaks up into amorphous fragments that, with time, anneal into homogenous patches with a recognizable hexagonal texture.

Taken together, these observations suggest that the concentrated isotropic and hexagonal phases formed by both unimers are inverse phases (L_2 and H_2), in which the tails of the surfactant form an apolar continuum and the cores of the cylindrical micelles are formed from hydrated surfactant headgroups.

The two-phase region formed by both surfactants was investigated further using bulk samples. The birefringent fragments were stable for at least several days[†] down to

[†]A 20 wt% sample of 4MDPC was observed again after three months, at which point the fragments

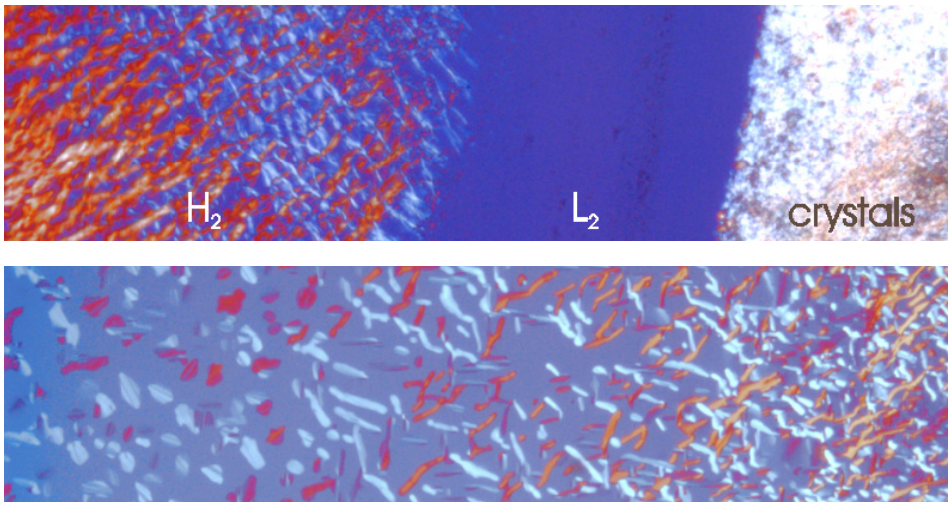

Figure 6.2: Flooding experiments of 4MDPB unimer; (top) from right to left, surfactant crystals, fluid isotropic (L_2) phase and hexagonal phase (not shown here is the dilute side of the hexagonal phase, which takes the form of small fragments floating in the dilute isotropic phase); (bottom) after sitting overnight, the fragmented side of the hexagonal phase has annealed into patches of hexagonal texture.

concentrations of around 10 wt% for the 4MDPC mixture, and 1 wt% for 4MDPB. This supports the idea that the observed hexagonal texture has an inverted structure, since normal hexagonal phases tend to be diluted and then dissolve into micelles at moderate to low surfactant concentrations.

Figure 6.3 shows three micrographs of a 20 wt% solution of 4MDPC. Image (a) shows the solution approximately an hour after it was made up, and immediately after placement on the microscope slide. The small fragments are partially birefringent, but are not recognizable as any particular phase. After equilibrating overnight (image (b)), the fragments have consolidated into tiny single-phase regions with an obvious hexagonal texture. Image (c) is an unpolarized image of the same fragments, and shows the phase boundaries and homogenous nature of the particles.

These observations were confirmed by performing small-angle X-ray scattering on a two-phase sample of 4MDPC (30 wt%). Figure 6.4 clearly shows a two-phase system consisting of a micellar solution (the broad peak centred at 0.17 $Å^{-1}$) and an ordered phase (producing the sharp peak at 0.19 $Å^{-1}$). If the ordered phase is taken to be

had aggregated into a single hexagonal domain.

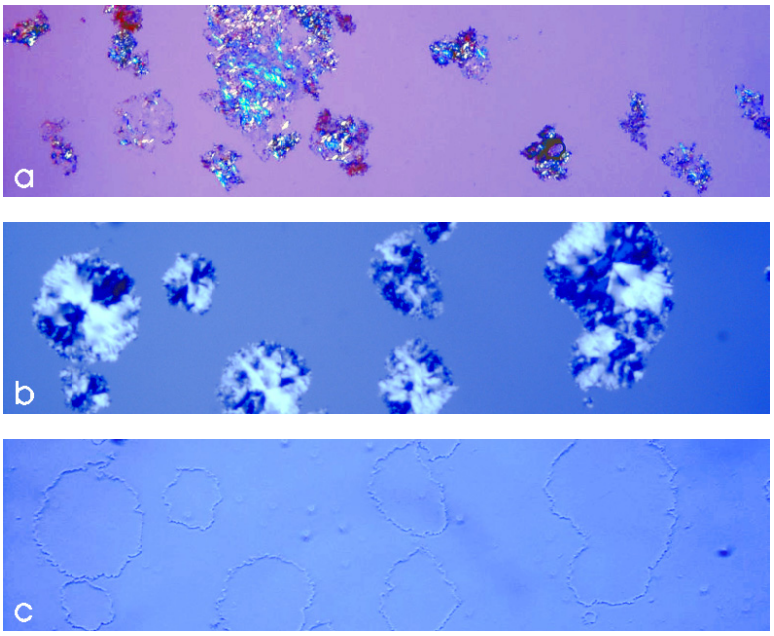

Figure 6.3: 20 wt% 4MDPC in water (200× mag.); (a) immediately after placement on microscope slide; (b) after sitting overnight; (c) identical to middle photo without polarization.

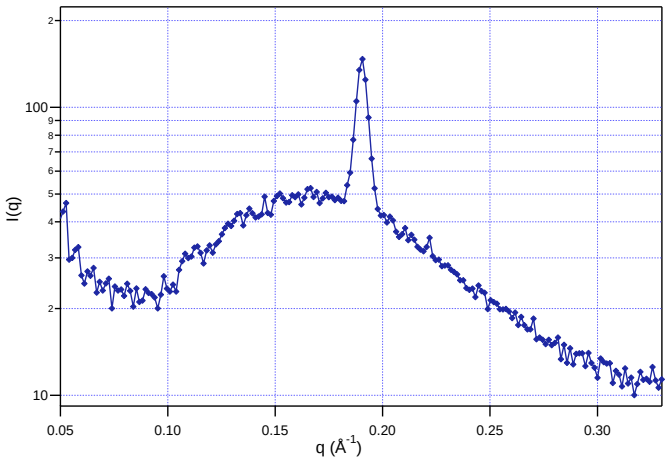

Figure 6.4: Small-angle X-ray scattering spectrum of 30 wt% 4MDPC. The sharp peak confirms that the fragments in this two-phase sample have internal order.

hexagonal and the sharp peak is the primary diffraction peak (Q^*),[‡] then the nearest-neighbour spacing (d) is calculated to be 38 Å, which is consistent with the size of the surfactant and the concentrated nature of the reverse phase.

[‡]Note that the next peak would lie at 0.33 $Å^{-1}$ ($\sqrt{3}Q^*$), outside the range of this spectrum.

This result immediately suggests a line of further investigation: namely, whether this surfactant could be used to produce stable submicron particles of the H_2 phase, known as hexosomes [13]. Given that pyridinium compounds – both surfactants and simpler compounds – have already been investigated for antibiotic and other biological properties, this could have a number of useful applications.

6.2.2 4MDPC-based oligomers

Once the oligomerization reaction was better understood, a series of oligomer mixtures were made, and their bulk phase behaviour and surface adsorption investigated. Table 6.1 shows the composition of five 4MDPC-based samples as determined by HPLC. The four columns for each sample represent the proportion of unimer, dimer, trimer and tetramer respectively.

Figure 6.5 shows flooding experiments of these samples. The surfactant concentration increases from left to right, and four of the micrographs have had a local equalization transformation applied to part of the image in order to make phase boundaries clearer. The images have not been manipulated in any other way.

Sample #1 is very similar to that described in the previous section, consisting of unimer with a very small amount of dimer and a trace of trimer. The hexagonal texture and two-phase region are both present, and to the far right is the isotropic surfactant.

Sample #2 has slightly larger proportions of dimer and trimer and a trace of

Sample	%				
	monomer	dimer	trimer	tetramer	other
#1	91	5	1	0	3
#2	77	12	7	1	3
#3	73	14	9	1	3
#4	67	17	12	1	3
#5	54	14	23	6	3

Table 6.1: Compositions of the five mixtures of 4MDPC-based oligomers, determined by HPLC with UV detection. Each value is the percentage of total UV signal due to that oligomer, and is assumed to be linearly related to weight percent. 'Other' indicates unassigned impurities in the chromatogram.

tetramer. The two-phase region is no longer visible, and the hexagonal texture ap-

pears to change slightly at higher dilutions. The inset and the spherical shape of the bubble show that only a fluid isotropic phase exists to the left of the hexagonal texture.

Sample #3 has slightly higher proportions of oligomer again. The concentrated birefringent phase now has an unusually fibrous texture, but in the absence of any evidence to the contrary, this will continue to be referred to as the hexagonal phase.

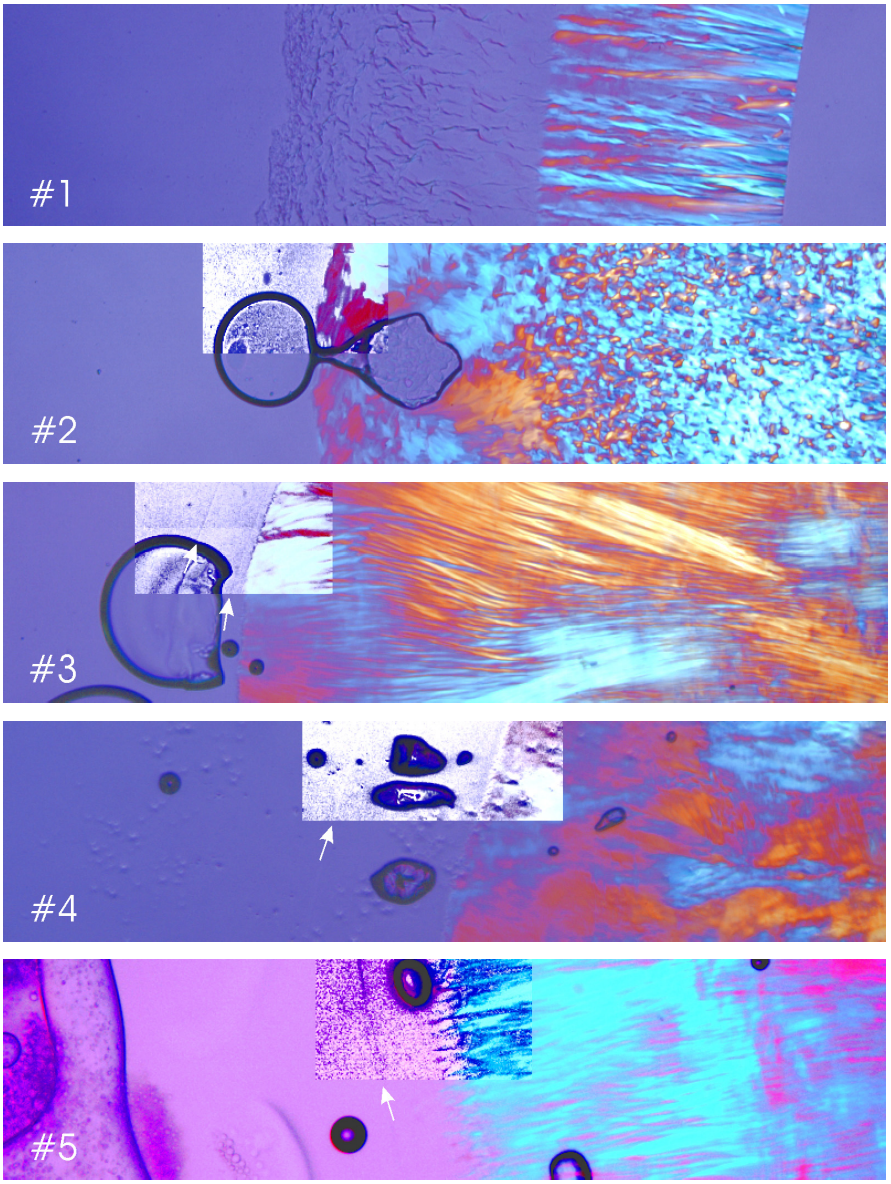

Figure 6.5: Flooding experiments of five mixtures of 4MDPC oligomers. Phase boundaries have been highlighted using local equalization on a section of the original image, and are marked with arrows.

On the dilute side, two new isotropic phases have formed. The phase boundaries,

made clearer in the inset, are marked with arrows. Unusually, the more concentrated (narrower) phase is fluid, as evidenced by the small spherical bubble just below the right-hand arrow, while the more dilute (wider) band to the left is of high viscosity. To the far left is the usual dilute fluid isotropic phase.

Sample #4 contains 17% and 12% of dimer and trimer respectively, with still only a trace (approximately 1%) of tetramer. It does not form the concentrated fluid isotropic phase seen in Sample #3; instead, the stiff isotropic phase and the hexagonal phase share a common interface.

Sample #5 has slightly over 50% unimer, more trimer than dimer, and about 6% tetramer. This unusual distribution is the result of a longer reaction time and the previously noted tendency of the 4-substituted compounds to form longer oligomers in preference to dimer. This sample forms a significant new phase. Along with the hexagonal and stiff isotropic phases, a fluid isotropic phase forms which is immiscible with the dilute micellar phase. A coarse emulsion of these two phases is visible at the left of the image. Heating of this sample showed that the phases began to mix at temperatures above 50°C, but at the limit of our heating stage (around 57°C depending on the ambient temperature), they were still not fully miscible. Upon cooling, they demixed immediately to form an emulsion.

This behaviour appears similar to that of an asymmetric zwitterionic gemini synthesized in the group of Fredric Menger. They identify the more concentrated fluid phase as a coacervate – a dilute fluid phase that that is incompatible with own solvent [55] – and observed a sponge-like structure with cryo-HRSEM. Coacervates are usually formed by the addition of salt to colloidal systems [250], and Menger's gemini system was the first instance of a binary system forming such a phase. In the case of this oligomer mixture, it is possible that the coacervate is enriched with longer oligomers, while the dilute micellar phase has most of the unimer.

6.3 Small-angle neutron scattering

6.3.1 4MDPC-based oligomers

The dilute solution behaviour of Samples #1–#4 was studied by small-angle neutron scattering. Solutions were prepared at concentrations of 1 wt% and, for Samples #1 and #4, 10 wt%. Figure 6.6 shows the offset spectra of the four mixtures compared

with the same concentration of unpurified 4MDPC unimer. All samples show a micellar peak, but the fitting of this is complicated by low-q scattering. It is interesting to note that in none of these samples is Porod-limit (q^{-4}) scattering observed. Rather, as the proportion of oligomer increases, the slope of the low-q scattering decreases slightly from $q^{-2.5}$ to q^{-2} in case of Sample #4. This is suggestive of large particles with a

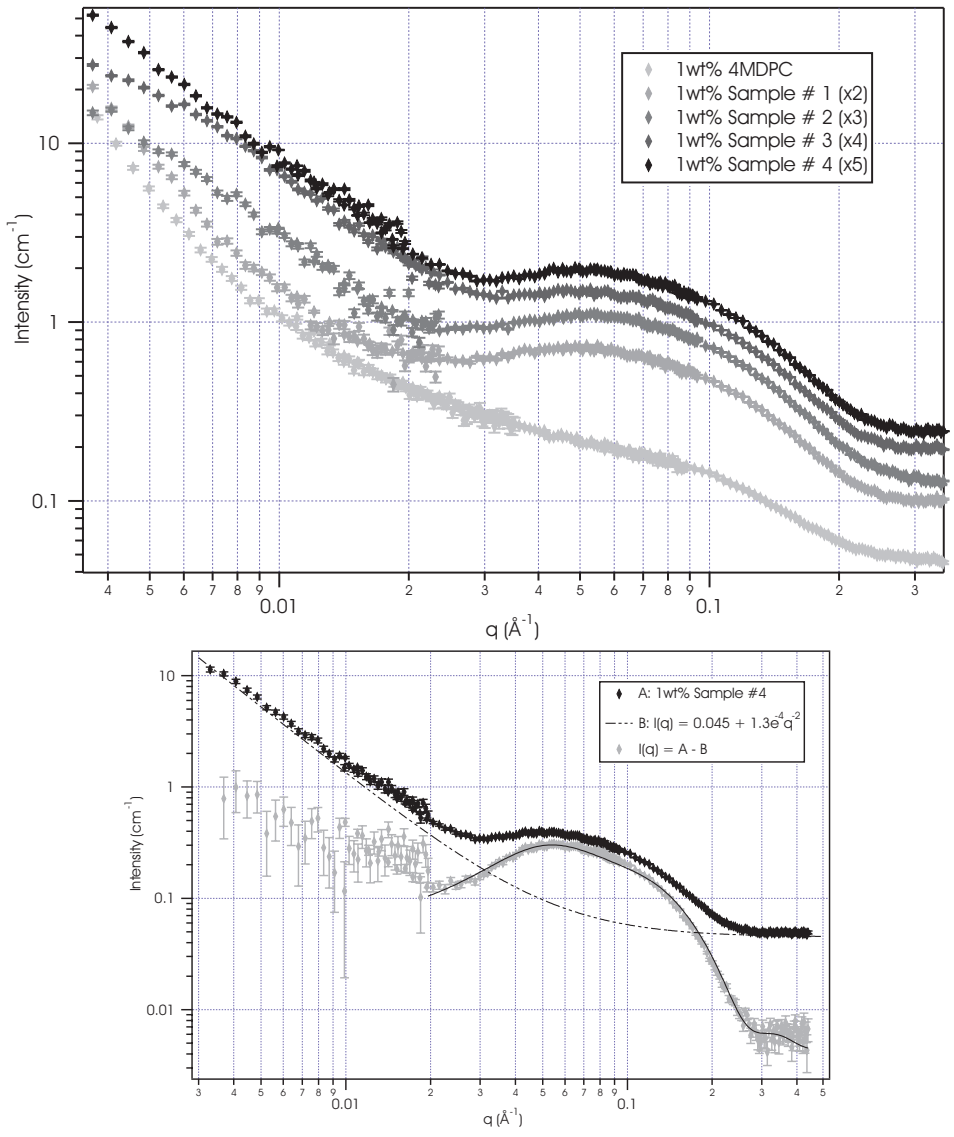

Figure 6.6: (top) Offset SANS spectra of 1 wt% solutions of 4MDPC oligomer mixtures; (bottom) a q^{-2} power law is subtracted from the Sample #4 spectrum and the result is fitted with a polydisperse charged spheres model (fitting parameters are in Table 6.2).

lamellar structure [194].

If this power-law scattering is subtracted from the Sample #4 spectrum, the resulting curve can be fitted by a model of polydisperse charged spheres with a radius of 15 Å. While it would be premature to assign this geometry to all the samples, the strong similarity of the micellar regions in the spectra (with the possible exception of 4MDPC) suggests that it is a good approximation. It seems, therefore, that these solutions consist of a small population of micelles accompanied by larger particles, possibly with a lamellar structure.

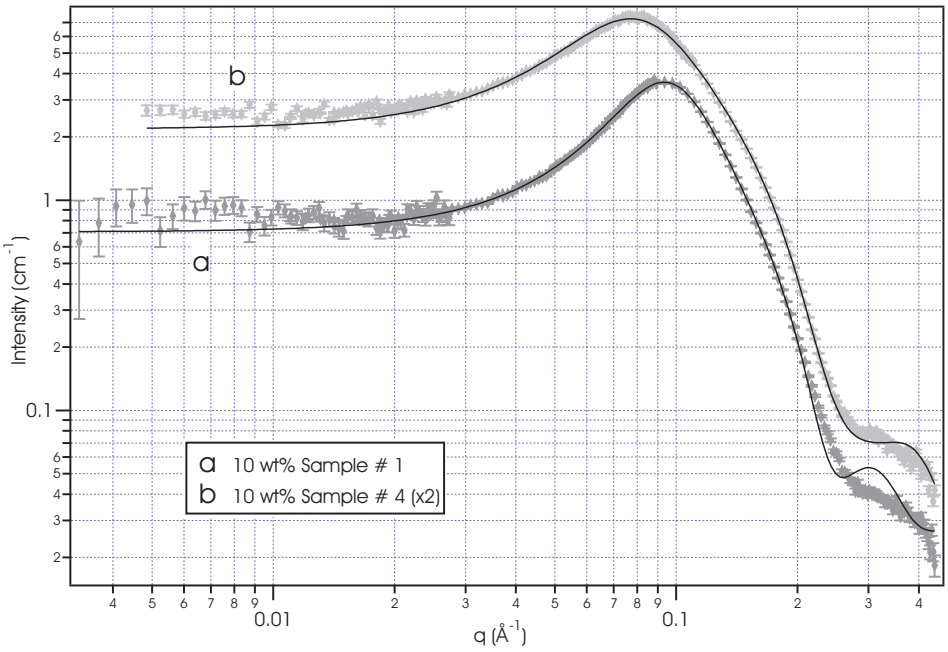

Figure 6.7: SANS data (coloured points) and fitted curves (black lines) of 10 wt% solutions of Samples #1 and #4 (offset).

Given this and the fact that the 4MDPC unimer appears to be even less soluble on its own, it was surprising to find that spectra from 10 wt% solutions of Samples #1 and #4 show no low-q scattering, but are instead indicative of conventional micellar solutions. Figure 6.7 shows these two spectra and the fitted curves; the fitting parameters are listed in Table 6.2.

Sample #1 is best fitted by polydisperse spheres, while Sample #4 – which has a greater proportion of oligomer – appears to form cylindrical micelles. This is consistent with oligomers tending to form structures of lower curvature. If the ubiquitous hexagonal phase is a reverse phase in all the samples, this observation suggests that the stiff isotropic phase formed by Samples #3 and #4 may be a bicontinuous cubic (V_1 or V_2)

Surfactant	Conc. (wt%)	Model	Fitted vol. frac. (%)	Radii (Å)	Poly-dispersity	Charge
Sample #4 (adjusted)	1	Charged polydisperse spheres	0.3	15.0	0.17	12
Sample #1	10	Charged polydisperse spheres	5.1	17.0	0.15	18
Sample #4	10	Charged cylinders	4.7	15×38	–	14

Table 6.2: SANS fitting parameters for oligomer mixtures.

phase, which would have a curvature between that of normal cylindrical micelles and a reverse hexagonal phase.

6.3.2 LELA reactions

Section 5.3.5 in the previous chapter discussed the use of SANS to observe the physical kinetics of LELA reactions. While this was not possible in all the LELA reactions, spectra from the reacted samples followed a clear trend. Figure 6.8 shows a set of fitted spectra (and fitting parameters) from three LELA reactions, acquired two days after the reactions were started. Chemical analysis of these samples was not possible at the SANS facility, but that after such a reaction period, much of the surfactant may be oligomerized. Each spectrum can be fitted with a polydisperse hard-spheres model, and the particle size increases with the concentrations of both surfactant and base.

For greater surfactant concentrations, this is likely to be due primarily to the larger amount of material available to form these particles. A higher pH increases the rate of the LELA reaction, so after identical reaction times, the reaction with 100 mol% OH has proceeded further than that with 50 mol%. If it is assumed that the size of these particles is related to the average oligomer length, then the faster reaction will also have produced larger particles.[§]

As noted in the previous chapter, a small peak is observed in the more concentrated reaction solutions at $q \approx 0.17 - 0.19\,\text{Å}^{-1}$. This increases in sharpness and intensity, and shifts to slightly higher q in samples with larger particles. Comparing its position with that of the sharp peak in the SAXS spectrum of 30 wt% 4MDPC unimer (Figure 6.4)

[§]After 5 days, the intensely blue-green 100 mol% reaction solution was passed through a 0.2 μm filter. The filtrate was completely clear and colourless and showed minimal scattering.

suggests that they may have a similar origin. As the flooding experiments of the oligomer mixtures show, the hexagonal phase features prominently in this family of surfactants, and – in analogy with the unimers – there is a strong likelihood that the particles formed by the LELA reaction are nanometre-sized fragments of reverse hexagonal phase; or in other words, hexosomes.

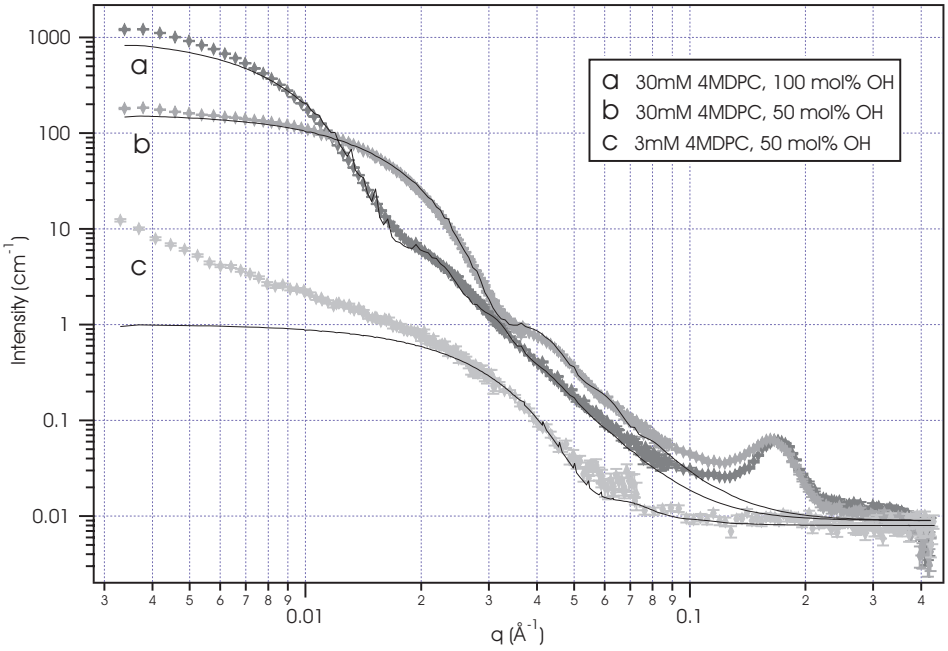

Figure 6.8: SANS spectra of four aqueous LELA reactions at $t_{reaction}$ = 2 days. Fitting parameters: (A) volume fraction 0.3%, avg. radius 240 Å; (B) volume fraction 0.3%, avg. radius 120 Å; (C) volume fraction 0.01%, avg. radius 70 Å.

This cannot be definitively asserted without further evidence: in particular a SAXS analysis of the LELA reaction solution and transmission electron micrographs of the particles are needed. Since the SANS experiments above were performed only one week before submission of this thesis, the opportunity to collect these data has not yet arisen, and will be the subject of further research.¶

In the meantime, it is interesting to observe the structures formed by a solid sample of purified 4MDPB which, for reasons unknown, oligomerized spontaneously. Figure 6.9

¶During the period between initial and final submission of this thesis, cryo-transmission electron micrographs were collected which provide preliminary confirmation that the particles are faceted and of hexagonal symmetry. These and further data relating to this point will be published in a forthcoming paper.

shows three optical micrographs of this sample, smeared onto a microscope slide and flooded with water. Roughly cylindrical structures have formed, which upon shearing disintegrate into finer and finer bundles of birefringent fibres.

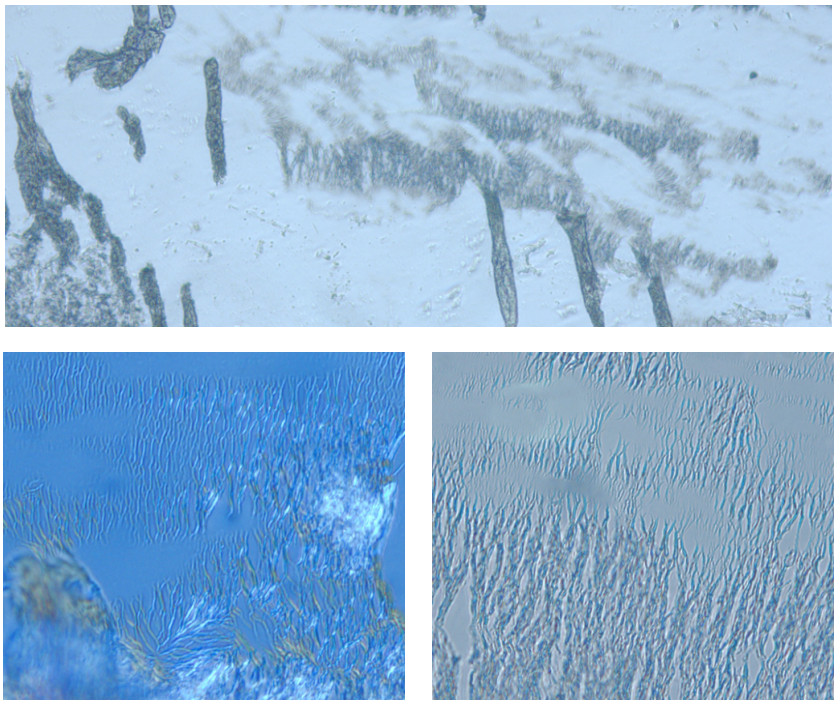

Figure 6.9: Fibrillar structures in a sample of purified 4MDPB that spontaneously oligomerized. The two lower images show the structures with (left) and without (right) crossed polarization and are at 400× magnification.

6.4 Self-assembly in non-aqueous solvents

As mentioned in Section 5.3.2, while the vinylpyridinium unimers dissolve readily in acetone, the oligomers have limited solubility. Sample #5 was therefore stirred in acetone overnight, and the resulting lump of undissolved surfactant extracted and dried. The soluble and 'insoluble' fractions[‖] were analysed by HPLC, and their compositions are shown in Figure 6.10. The 'insoluble' fraction consists primarily of trimer and tetramer: it will therefore be referred to as the oligomer-only fraction. Flooding experiments with water, formamide, dimethylformamide and acetone were then performed on the oligomer-only fraction and on the original Sample #5. Table 6.3 summarizes

[‖]As shown later, it is not strictly true to say that this fraction is insoluble in acetone.

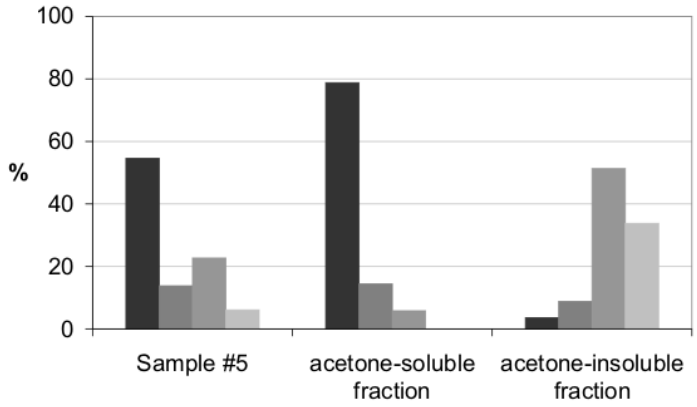

Figure 6.10: Sample #5 separated into fractions according to solubility in acetone; the graph shows the proportion of (from left to right) unimer, dimer, trimer and tetramer in each sample.

		Increasing surfactant concentration ⟶		
Surfactant	Solvent	Coacervate	Stiff isotropic	Hexagonal
#5 (complete)	water	✓	✓	✓
#5 (complete)	formamide	✓	–	✓
#5 (complete)	dimethylformamide	–	–	✓
#5 (complete)	acetone	–	–	✓
#5 (oligomers)	water	emulsion	–	✓
#5 (oligomers)	formamide	✓	✓	✓
#5 (oligomers)	dimethylformamide	✓	–	✓
#5 (oligomers)	acetone	lamellar	✓	✓

Table 6.3: Phase sequences in different solvents for the complete Sample #5 mixture, and the oligomer-only mixture extracted from Sample #5.

the phases formed in these experiments, and Figure 6.11 shows micrographs of several examples.

Taking Sample #5 (complete) first, the behaviour in formamide was similar to that in water, except that the stiff isotropic phase does not form. In dimethylformamide, neither the coacervate nor the stiff isotropic phase form, and only the hexagonal texture is present.

With almost all the unimer removed, the mixture's behaviour in water is hard to characterize. The hexagonal texture is still seen, but a turbid emulsion forms at lower

concentrations – it is possible that this is another coacervate. In the organic solvents, similar phase sequences to those formed by the complete mixture are seen, but shifted to less polar solvents. For example, the same phase sequence formed in water by the complete mixture occurs in formamide for the oligomer-only mixture (see Figure 6.11). In the less polar dimethylformamide, the oligomer-only mixture no longer forms the stiff isotropic phase – just as in the switch between water and formamide for the complete mixture.

The most intriguing behaviour shown by the oligomer-only mixture occurs in acetone. Although these oligomers were separated from the unimer precisely because they did not dissolve in acetone, the mixture actually forms a rich set of concentrated mesophases in the solvent. As in the other solvents, the phase formed at high surfactant concentrations is hexagonal. Next to it is an isotropic phase, the viscosity of which appears to be moderately high, but not gel-like. At low concentrations, a very fluid lamellar phase forms, which sometimes has a standard dense lamellar texture and sometimes appears with large isotropic regions like the example in Figure 6.11.

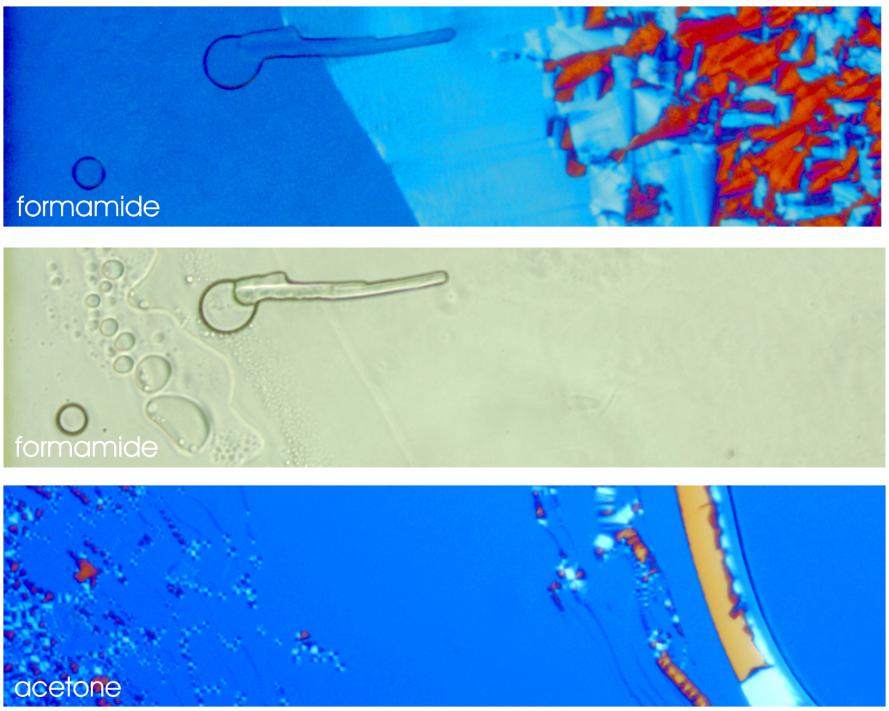

Figure 6.11: Oligomer-only fraction of 4MDPC oligomer mixture in (from top) formamide, formamide (without crossed polarizers) and acetone.

6.5 Surface adsorption

Figure 6.12 shows atomic force micrographs of Samples #1–#4 on mica. No long-range order is seen, but the films formed by the mixtures become rougher as the oligomer content increases.

In studies of mixed surfactant systems, the more hydrophobic compound tends to adsorb preferentially to the solid-liquid interfaces [229]. The roughness of the adsorbed layers in the samples studied here increases with the proportion of longer, more hydrophobic oligomers, and may be indicative of multiple patchy layers.

Relatively little work exists in the literature on the surface-adsorbed structures of

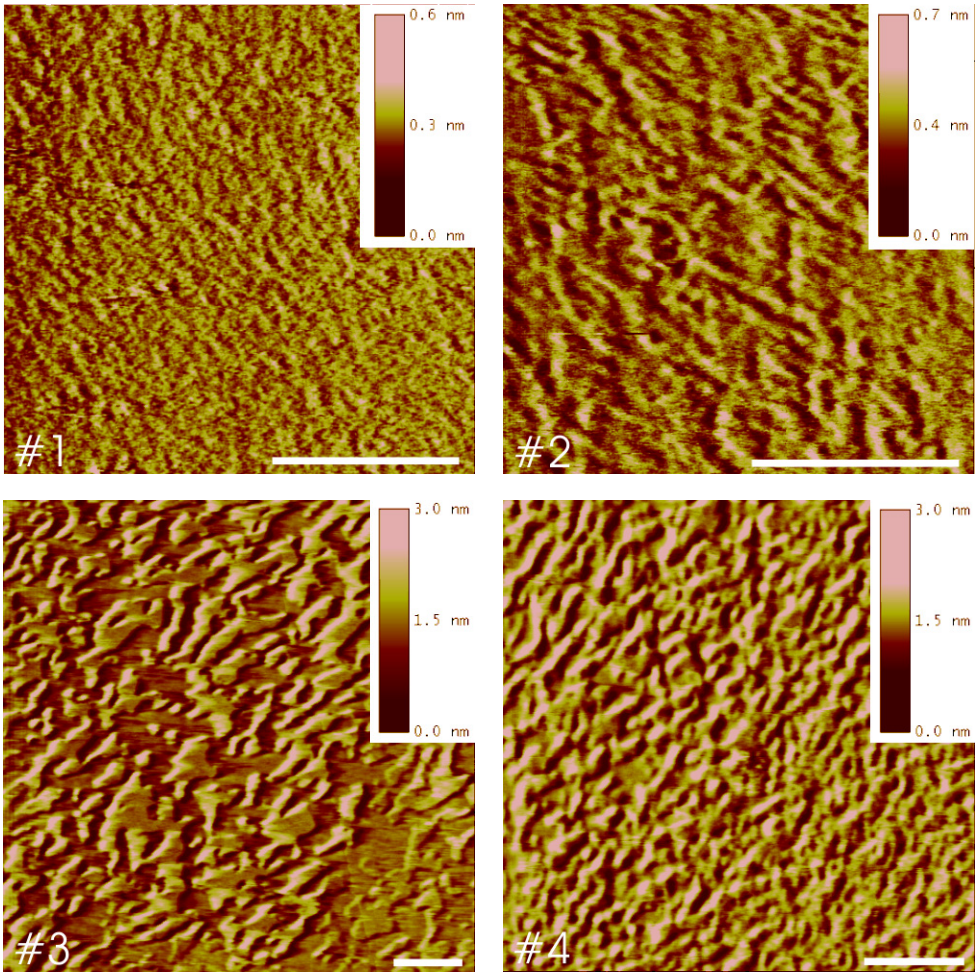

Figure 6.12: Atomic force microscopy of the 4MDPC oligomer mixtures (see Table 6.1 for compositions). Imaging is conducted in soft-contact mode, surfactant solutions are 10 mM, bars are 1 μm.

gemini and oligomeric surfactants [19]. The quaternary ammonium geminis 12-2-12 and 12-4-12 have been observed to form bilayers and rods respectively on mica [222, 251]. Images have also been made in our laboratory of the trimeric surfactant 12-3-12-3-12 on mica. At temperatures lower than 28°C, it forms stable flat patches similar to those seen in Sample #3 [252].

The mixtures studied here are all based on the 4-substituted unimer, and the position of the spacer groups is likely to disrupt the binding of the headgroups to the mica. In a unimer, the headgroup may tilt to bring the nitrogen proximal to the mica, and in a dimer it might be possible for both headgroups to lie flat. However, for longer oligomers, the spacer group probably prevents all the headgroups in a given molecule from simultaneous tight binding. This could lead to an irregular monolayer and thus to an overall roughness of the final adsorbed layer.

However, without further and more systematic studies, no definite conclusions can be drawn about the adsorption behaviour of these mixtures. A comparison of 2- and 4-subsituted oligomers would be useful, along with reference studies of pure unimer and/or analogues such as 2- and 4-ethyl-*N*-dodecylpyridinium chloride.

6.6 Discussion

The LELA reaction, described in the previous chapter, was used to produce mixtures of oligomeric pyridinium surfactants. The self-assembly of these compounds was studied under a variety of conditions using several different techniques.

The 4MDPC and 4MDPB unimers constitute something of a curiosity, since despite being single-chained, they seem to prefer to form inverse structures. An L_2 phase forms at very high surfactant concentrations; this is followed by a hexagonal phase, which remains stable in a two-phase system with the dilute micellar phase down to very low concentrations. Such behaviour suggests a reverse hexagonal phase, and it is therefore likely that with sonication the fragments could be dispersed as hexosomes [13, 14].

This is particularly unusual for single-chained surfactants, and is likely to be due to the hydrophobic nature of the methoxyethyl group and its position on the pyridinium ring. In normal micelles, this short chain is forced to reside in the aqueous continuum, making micellization a less favourable process overall. In contrast, an L_2 or H_2 phase would allow the charged nitrogen centre to be hydrated to some extent while minimizing the entropic cost of exposing an essentially hydrophobic micellar surface to bulk water.

While the work in this chapter focussed on the 4-substituted surfactants, it would be instructive to compare the behaviour of the 2-substituted analogues.

As the loading of oligomer in the surfactant mixture increases, more complex phase behaviour evolves. Isotropic phases of varying viscosities form in some mixtures, and with nearly equal weights of oligomer and unimer, a intermediate-concentration fluid isotropic phase forms that is immiscible with the dilute micellar phase. Such a phase is very unusual in salt-free systems, being more common in colloids that phase-separate with added electrolyte [250]. The location of these phases between the micellar and reverse hexagonal phases, as well as the fact that they form only with a certain percentage of oligomer present, suggests that they may be bicontinuous sponge and cubic phases. SANS data indirectly support this interpretation, and additionally suggest that the particles formed in LELA reactions (where the unimer content becomes negligible) may be hexosomes.

To sidestep briefly, recall the freeze-dried 2VDPA mentioned in Chapter 4. HPLC showed this sample to consist primarily of trimer (with a relatively high degree of impurities). Its high solubility and the apparent absence of any reverse hexagonal phase suggests that positioning the spacer group in the *ortho* position may lead to quite different behaviour. Further work on this family would therefore provide an interesting counterpoint to the results presented here.

Mixtures with a high percentage of oligomer also self-assemble in organic solvents, including formamide and dimethylformamide. In acetone, a mixture containing almost no unimer forms a lamellar texture at moderate to low surfactant concentrations: this was the only situation in which this phase was seen.

It is important to note that none of these 'non-aqueous' flooding experiments took place under completely dry conditions. Due to time restrictions they were of an exploratory nature only, and as a consequence no effort was made to dry the organic solvents or ensure the hygroscopic surfactant remained free from water. Nevertheless, different phase behaviour is observed in different solvents and there is an apparent tendency for a given phase sequence to occur in less polar solvents for longer oligomers. While no conclusive statements can yet be made regarding the origin of this behaviour, it suggests that solvophobic forces with origins other than hydrogen-bonding play a part. Further studies of the longer oligomers in water-free systems could therefore provide interesting data.

The surface adsorption behaviour of the oligomer mixtures displays no long-range

order, and is similar to that observed for a pure trimeric quaternary ammonium surfactant. This may have either a kinetic origin – due to the multiple adsorption points of an oligomeric surfactant – or may result from the orientational restrictions placed on the oligomer by the spacer group. This could be resolved by studying the purified oligomers, and comparing them with both their 2-substituted analogues and existing quaternary ammonium oligomeric surfactants.

The behaviour of the unimers and oligomers described in this chapter was quite unexpected, and much of the data presented here was collected in the months immediately prior to the submission of this thesis. To fully appreciate the physical behaviour of these surfactants, further characterization is clearly required. Nevertheless, the data collected so far are generally consistent and suggest that these surfactants will repay further study.

Chapter 7

Chromophoric properties of alkylpyridinium compounds

"Singularity is almost invariably a clue."

Arthur Conan Doyle, The Adventures of Sherlock Holmes

7.1 Introduction

The chromophoric nature of the compounds derived from the 4-vinyl-*N*-dodecylpyridinium monomers was a valuable clue in determining the oligomerization mechanism of both the 4-substituted and 2-substituted unimers. Initially it was a source of curiosity, apparently unrelated to the issue at hand. However, attempts to explain the source of the colour led to ideas about the mechanism of anionic polymerization and eventually the LELA reaction.

Chromophorism in simple pyridinium compounds has been intermittently reported in the literature. Coleman et al. found that performing the quaternization of 4-methylpyridine with bromobutane in nitrobenzene produced a green-coloured solution [140]. This could be prevented by careful purification of the nitrobenzene prior to the reaction.

In the early 1980s, a group working on the quaternization of polyvinylpyridine observed that the bromide salts of some small pyridinium compounds and of quaternized poly-4-vinylpyridine were coloured when prepared by certain synthetic routes [136,138]. These included preparation at high temperatures (333K) or in solvents of low permittivity. It was found that the compounds were never coloured when synthesized in

ethanol, but that coloured solids retained their colour when dissolved in ethanol. A *para*-substitutent was apparently necessary for the colour to appear. In contrast, the iodide salts of the same compounds were colourless solids, and formed pale yellow solutions. This was attributed to the charge-transfer complex formed between pyridinium salts and iodide anion that has been well documented by Kosower [115, 165, 166]. The colours of the bromide salts were also attributed to charge-transfer complexes of unknown origin.

Several years later, the same group reported further observations [248]:

> "The n.m.r. spectra do not indicate the existence of any species which can be regarded as impurities. The spectra are entirely as expected from the presence of a single pyridinium salt in the coloured and colourless forms. What has also been observed is that these otherwise stable solutions are sensitive to the presence of added base. The main observations are summarized, since they concern hydrogen-deuterium exchange and do not throw any new light on the source of the colour where it exists. The addition of one drop of 10% $NaOD/D_2O$ solution instantly turned the quaternized products of 4-methyl and 4-ethyl pyridine dark green. Within a few minutes the methyl and methylene protons had been replaced by deuterium ... Quaternized polymer also turned dark green when base was added ... The dark green colour could be removed by addition of DCl, with no change in the ^1H spectrum, i.e. the initial colouration, when it is present, does not seem to be related to the reactions induced by added hydroxide."

In addition, they withdrew their earlier explanation of the colour as being due to a charge-transfer complex, noting only that in spectra of 4-methyl-*N*-n-propylpyridinium bromide, Beer's Law was obeyed for peaks at 401 nm and 485 nm [248].

Charge-transfer complexes that include pyridinium compounds are known, and examples of these were described in Section 1.3.3 of the introduction. In the work mentioned above, a major difficulty lay in the apparent absence of an electron donor. Yet, as has already been discussed in previous chapters, under the right conditions pyridinium compounds readily form zwitterions which undergo resonance with a pyridone methide structure. Pyridone methides are very similar to quinones, and charge-transfer complexes between quinones and pyridiniums have been documented [114].

In light of this, this chapter presents evidence to suggest that the colour shown by

4-substituted surfmer-derived compounds is due to a charge-transfer complex, which may occur inter- or intramolecularly.

7.2 4MDP oligomers

7.2.1 Qualitative observations

In the course of investigating the LELA reaction, a number of observations were made regarding the chromophoric properties of the 4-substituted pyridinium compounds. They relate to the mechanistic observations in Section 5.2.1 and are summarized here.

In almost all cases, the development of a blue or green colour was the result of the addition of base to a solution of either 4VDPX or 4MDPX. In some cases, however, the colour appeared without any base having been added. Brown polymeric 4VDPX was produced both by precipitatation out of basic aqueous solution, and in the case of the acetate salt, by freeze-drying. If this (water-insoluble) solid was dissolved in methanol or chloroform, it immediately became blue/green. NMR samples of 4VDPX in deuterated methanol also developed a pale blue colour over approximately 24 hours, which then deepened with time if the solution were kept. Chloroform solutions of 4VDPA monomer that were concentrated by evaporation polymerized and turned blue-green. In all cases, the intensity of the colour appeared to be related to the extent of polymerization.

Any coloured solution could be decolourized by the addition of acid, and the colour regenerated by the addition of base. When 4MDPC is synthesized from the vinylpyridinium monomer, a solution of the monomer is quickly added to a methanolic solution of sodium hydroxide. The solution immediately turns yellow, which becomes grass-green within sixty seconds. With incremental additions of acid, the colour becomes steadily bluer, passing through bright sky-blue, before finally becoming colourless or yellowish with an excess of acid. The bright blue colour is not always seen - if an excess of strong acid is added all at once, the colour passes directly from green to colourless, suggesting that the blue colour is due to a species or interaction that occurs at intermediate pH.

The brown polymer produced by freeze-drying a solution of 4VDPA exhibited additional strange behaviour. While completely insoluble in water, when grains of the substance came into contact with water, they turned pale blue/green within seconds. Freeze-dried once more and then kept in a sample vial, the polymer became a dark

turquoise colour which persisted for several months. Eventually the substance became brown again; when dissolved in methanol, it formed a solution which was initially red, but which became green overnight.

7.2.2 UV-visible absorption study

The development of the colour over time was investigated in an early study of the LELA reaction. Using HPLC data from a UV absorbance detector, Figure 7.1 shows the change in composition with time of a solution originally comprising 7.5 mM 4VDPA in methanol with 55 mol% sodium hydroxide.

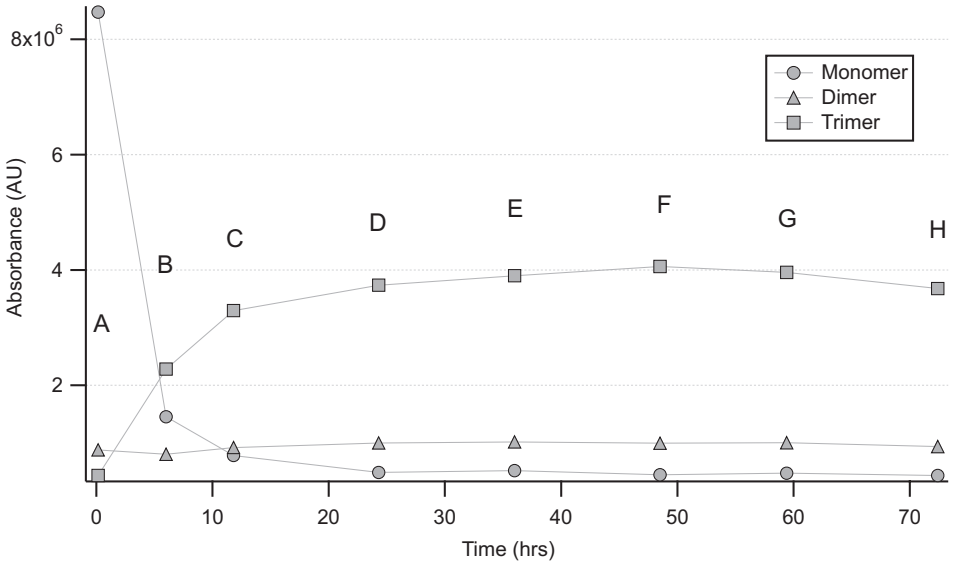

Figure 7.1: Progress of LELA reaction on 4MDPC (7.5 mM in methanol, 55 mol% NaOH). Letters A–H identify samples referred to in later diagrams.

The chromatograms used to collect this data were taken before the HPLC protocol for this procedure had been optimized, meaning the trimer was the longest species observed. Assuming that each pyridinium unit within an oligomer absorbs to the same extent as an unreacted unimer, it is evident from summing the total absorbance over each chromatogram (i.e. at each time point) that almost 50% of absorbing species become undetectable in the first 24 hours. NMR of these solutions does not indicate any substantial degradation, suggesting that this is due to the production of oligomers too long to be resolved by HPLC.

The data in Figure 7.1 was collected at each time interval by removing a portion of

the reaction solution, quenching it with acid and analysing it. In addition to HPLC and NMR analysis, the progress of the reaction – and the development of the characteristic green colour – was followed with UV-visible spectroscopy.

Figure 7.2 shows the seven of the eight reaction samples, along with the visible part of their absorbance spectra. Samples were diluted 1:5 in methanol, and spectra were collected before and after quenching. The first graph shows the development of the visible absorbance of the unquenched reaction. Note particularly the peak at 640 nm: a long-wavelength absorption such as this is unusual in an organic compound that does not contain a highly conjugated system. It is also worth noting that this peak begins to diminish at the same point as the trimer curve in Figure 7.1, suggesting degradation is occurring.

The second graph reproduces the traces of the first in green, and the spectra of the quenched samples A–H are superimposed in red. While there are a number of features of the original spectra that are affected by the addition of acid, the most notable are the disappearance of the 640 nm peak, and a peak at 400 nm. To the naked eye, this manifests as a change in colour from green to yellow. The features of the spectrum that appear with time but are not affected by the addition of acid are presumed to arise from degradation products.*

Figure 7.3 shows the ultraviolet region of the oligomers' absorbance spectrum. Here the reaction solution was diluted 1:50 with methanol, since the UV peaks are much more intense. For clarity, only a subset of samples is shown. Sample A is significantly different to all the other samples, and very little difference is seen between the unquenched and quenched solutions. With more oligomer and much less unimer, Samples B–H show a red shift, and quenching produces a slight decrease in intensity, particularly at the longest reaction times (Sample H).

The pH responsiveness of the 4MDP chromophorism, the relationship between the intensity of the colour and the oligomer or polymer length, and the long wavelength of absorption despite the lack of a large conjugated system all suggest that the source of the colour is related to an interaction occurring between adjacent pyridinium units. A possible explanation for such an interaction can be drawn from the base-sensitive tautomerism of vinyl- and alkylpyridinium compounds, which was discussed in Chapters 1 and 5.

*A similar yellow hue is seen in unpurified unimer. This colour is due to impurities and can be removed by column chromatography to leave the pinkish unimer.

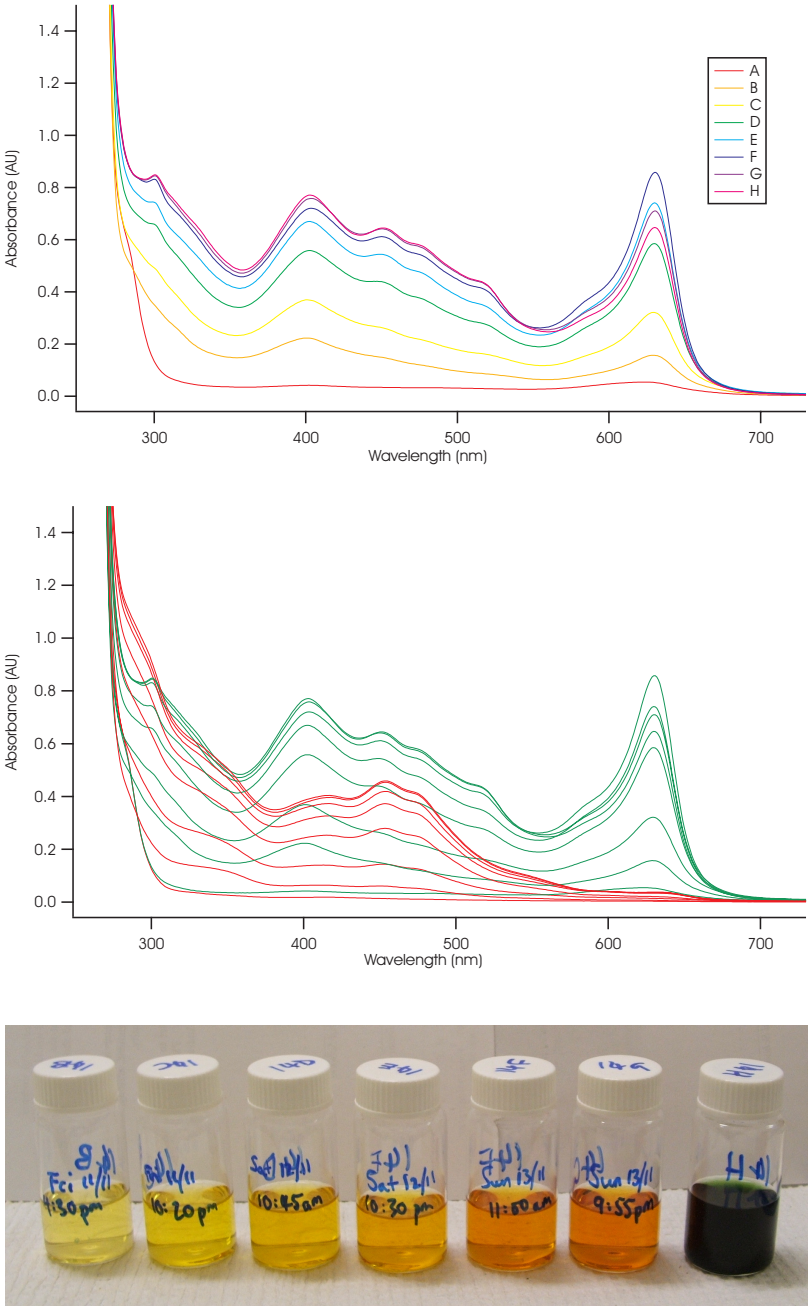

Figure 7.2: (top) development of visible absorbance in a LELA reaction over the course of four days (letters refer to samples in Figure 7.1, and the concentration of unimer-equivalent units in each sample is 1.5 mM); (middle) spectra from above are reproduced in green, and red traces represent the same set of samples after quenching with hydrochloric acid; (bottom) Samples B–G after quenching, and Sample H before quenching.

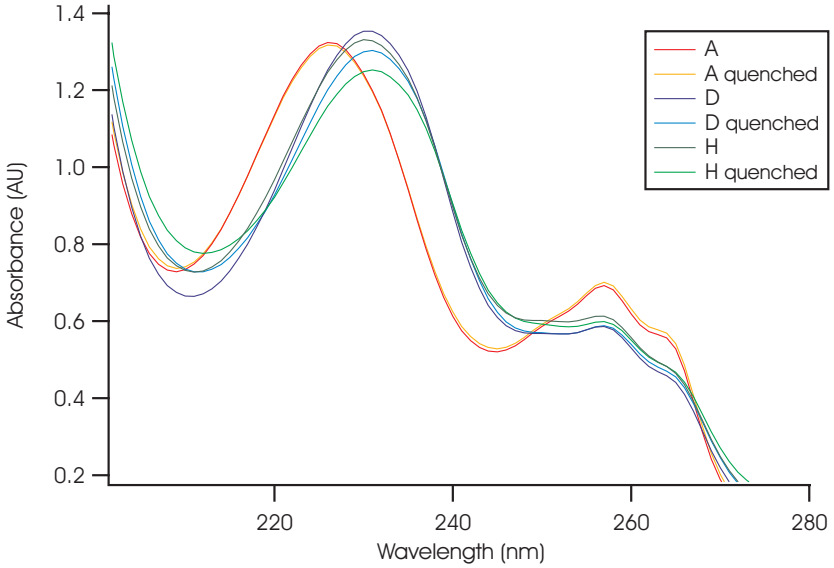

Figure 7.3: Ultraviolet absorbance of dilute samples from the 4MDPC series. Quenched samples have had hydrochloric acid added to them.

The loss of a proton from the backbone of an oligomer or polymer would produce a negatively charged unit within the molecule, which could then resonate between the zwitterionic form and the pyridone methide form (the latter only is shown in Figure 7.4). Intramolecular charge-transfer complexes have already been shown to form in copolymers and similar molecules containing electron acceptors and donors. It is therefore possible that units with the zwitterion/pyridone methide structure can act as electron donors to neighbouring cationic pyridinium rings.

It should also be possible for this interaction to occur intermolecularly between 'active' and 'inactive' unimers (i.e. zwitterionic and protonated respectively). In the case of 4MDPC, however, it is impossible to completely separate the base-catalysed oligomerization/degradation from any base-induced intermolecular complexation. To test this hypothesis, therefore, a series of experiments were performed on small analogous alkylpyridinium salts that cannot undergo the LELA reaction.

7.3 Analogous alkylpyridinium salts

If the hypothesis advanced in the previous section is correct, there exists a simple alkylpyridinium moiety such that any compound having it should, in a basic environment, be able to form a coloured charge-transfer complex. The features of this

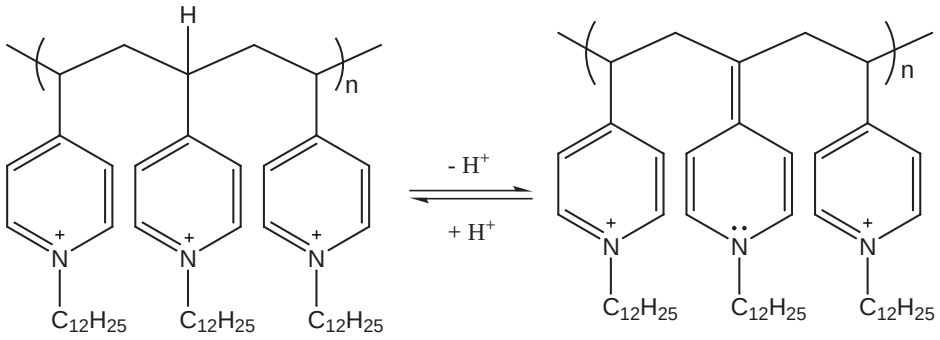

Figure 7.4: Tautomerism in a vinyldodecylpyridinium oligomer/polymer. The formation of an intramolecular charge-transfer complex between neighbouring electron-rich zwitterion/pyridone methide units and pyridinium units is a possible explanation for the chromophorism of the compounds.

moiety are simple: the pyridine ring should be permanently quaternized (as opposed to simply protonated) and it should have a *para* substituent with α-protons.[†] The effect of these features is to allow easy deprotonation of the pyridinium, producing the resonance-stabilized zwitterion/pyridone methide. This in turn enables the possibility of interaction between protonated and deprotonated molecules.

Three simple alkylpyridinium salts were therefore synthesized (see Section 2.2). As shown in Figure 7.5, 4-methyl-*N*-methylpyridinium iodide (4MMPI) and 4-ethyl-*N*-methylpyridinium iodide (4EMPI) both have potentially labile protons, while 4-tertbutyl-*N*-methylpyridinium iodide (4tBMPI) does not. None of these can undergo elimination, and should therefore not oligomerize.

The three compounds were dissolved in deuterated methanol, and the colourless solutions characterized by ^{1}H NMR (see Section 2.2.4). Several drops of neat triethylamine (TEA) were then added, the NMR tube was shaken thoroughly and a new spectrum was acquired. The spectra of 4MMPI and 4EMPI (see Figure 7.6) showed that, as expected, the α-protons in both compounds exchanged with deuterons from the solvent. Equally predictably, the spectrum of 4tBMPI showed no change other than the appearance of two peaks due to the TEA.

None of the three solutions showed any immediate change in colour. However, four to five hours later, the 4MMPI and 4EMPI solutions had developed pale but distinct

[†]Observations in the laboratory suggest that *ortho* substitutents produce similar behaviour, but the effect is less striking and was not investigated here.

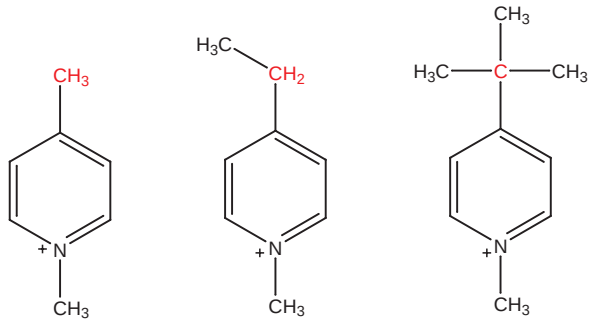

Figure 7.5: (left to right) 4-methyl-*N*-methylpyridinium, 4-ethyl-*N*-methylpyridinium and 4-tertbutyl-*N*-methylpyridinium cations. The α-carbons and protons are marked in red.

turquoise and yellow-green colours respectively, which disappeared upon the addition of acid. The 4tBMPI solution remained colourless. ^{1}H NMR spectra taken several days later showed no sign of oligomerization or any other reaction.

4MMPI and 4EMPI were subsequently characterized with UV-visible spectroscopy. Pure methanol solutions of the compounds show absorbances only in the UV (see Table 7.1). To investigate the appearance of colour in alkylpyridinium solutions, the absorbance spectrum of 4MMPI in a basic environment was observed over time. Samples of 4MMPI in methanol (3 mL) were made up at concentrations of 0.01 M, 0.02 M and 0.04 M, and 5 μL of neat triethylamine (TEA) was added to each. This equated to molar ratios of amine to pyridinium of 1.2, 0.6 and 0.3 respectively. The development of colour was then monitored by UV-visible spectroscopy.

	ε (L/mole.cm)		
Compound	222 nm	251 nm	263 nm
4MMPI	19000	3600	3000
4EMPI	19600	3900	3100

Table 7.1: Extinction coefficients for the UV absorbances of alkylpyridinium compounds.

Figure 7.7 shows visible spectra collected hourly from 0.01 M 4MMPI. Two peaks appear in the visible region at similar wavelengths to the major peaks seen for the oligomer solutions in Figure 7.2. To make the kinetics clearer, Figure 7.8 plots the maximum absorbance (i.e. peak height, not area) of both peaks over time for all three concentrations of 4MMPI.

The sources of the two visible absorbance peaks have not been identified. It is

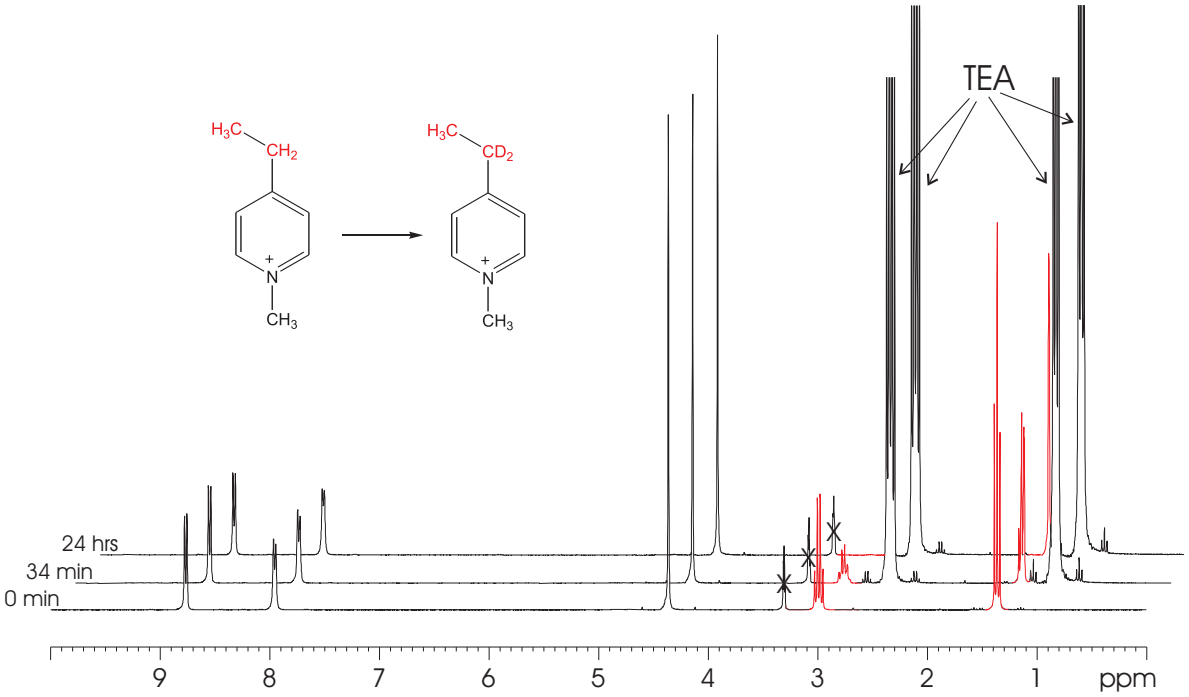

Figure 7.6: ^{1}H NMR spectra showing the exchange over time of α-protons in 4EMPI with the addition of triethylamine, and no sign of oligomerization. Peaks due to the protons on the ethyl group are marked in red. TEA peaks are due to added triethylamine; peaks marked with X are the solvent residual peaks, used as a reference.

therefore impossible to calculate extinction coefficients, and in the absence of further evidence, it would be premature to put a quantitative interpretation on these preliminary data. Nevertheless, a number of points are worth noting.

While neither peak fits simple kinetic models (indicating the presence of multiple chemical species and/or competing equilibria), the initial growth rates of the 464 nm peak are first order with the concentration of 4MMPI. However, the maximum absorbances reached are not: while the 0.02 M maximum is twice that of the 0.01 M, the 0.04 M maximum is not quite twice that of the 0.02 M solution. This may indicate that the base (having dropped to a molar ratio of 0.3) has become a limiting reagent, but that it is not directly involved in the formation of the absorbing species.

The shape of the growth curve of the 648 nm peak is sigmoidal, and the inflection point of the curve occurs at approximately the same time as the maximum absorbance of the shorter-wavelength peak is reached. This could imply that the species or complex responsible for this absorbance contains or relies on the 464 nm species.

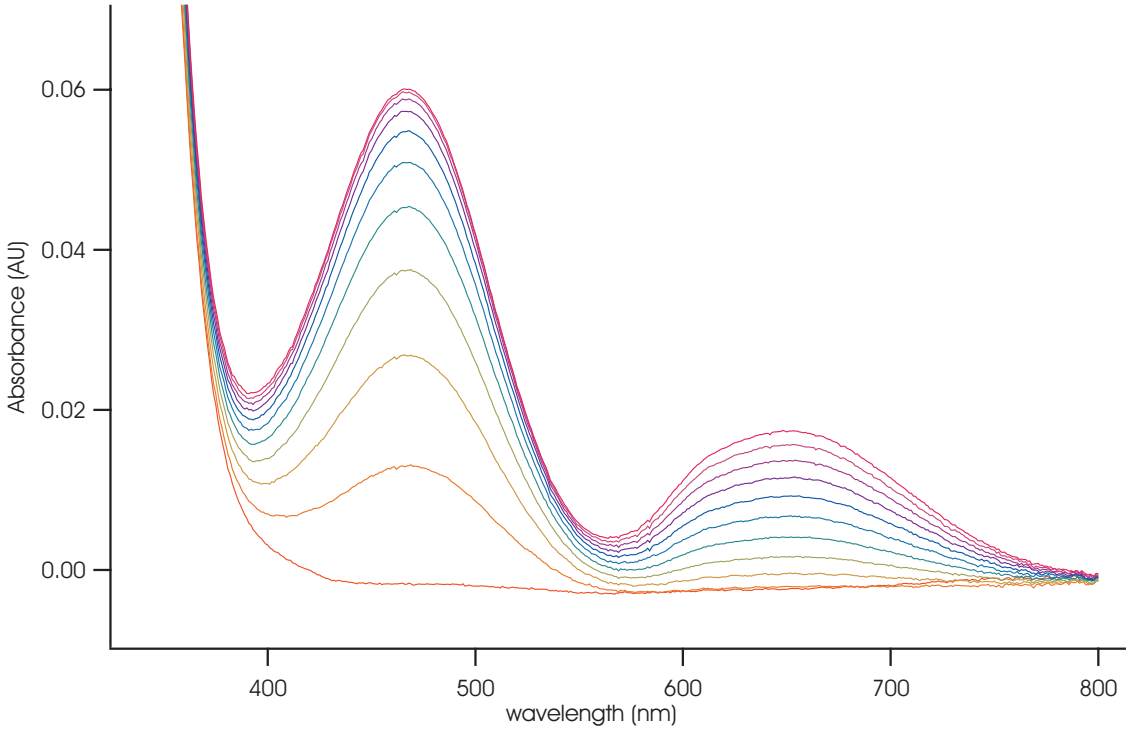

Figure 7.7: The changing visible absorption spectrum of 0.01 M 4-methyl-*N*-methylpyridinium iodide in methanol, after the addition of 5 μL triethylamine. The red spectrum is $t = 0$; spectra are one hour apart.

However, the 648 nm curve for the 0.04 M solution is non-trivial. The initial impression is again that the base has become a limiting reagent. However, the shorter-wavelength peak still reaches a higher overall absorbance than in the 0.02 M solution, so that if the growth of the 648 nm peak is dependent on this species, it ought also to have a higher absorbance. In addition, the shape of this kinetic curve is subtly different to the others, and it is possible that it is an artefact of some kind. Unfortunately a lack of time prevented this being repeated.

The relative heights of the 4MMPI visible peaks differ from those of the oligomer solution, which show a more intense absorbance at the longer wavelength. In addition, despite the oligomer samples having one-tenth the concentration of unimer-equivalent units[‡] of the 0.01 M 4MMPI solution, their visible absorbance is an order of magnitude greater. Both of these observations indicate that the physical proximity of pyridinium units imposed by oligomerization favours the long-wavelength absorption.

[‡]Dimers and trimers have, for instance, two and three unimer-equivalent units respectively.

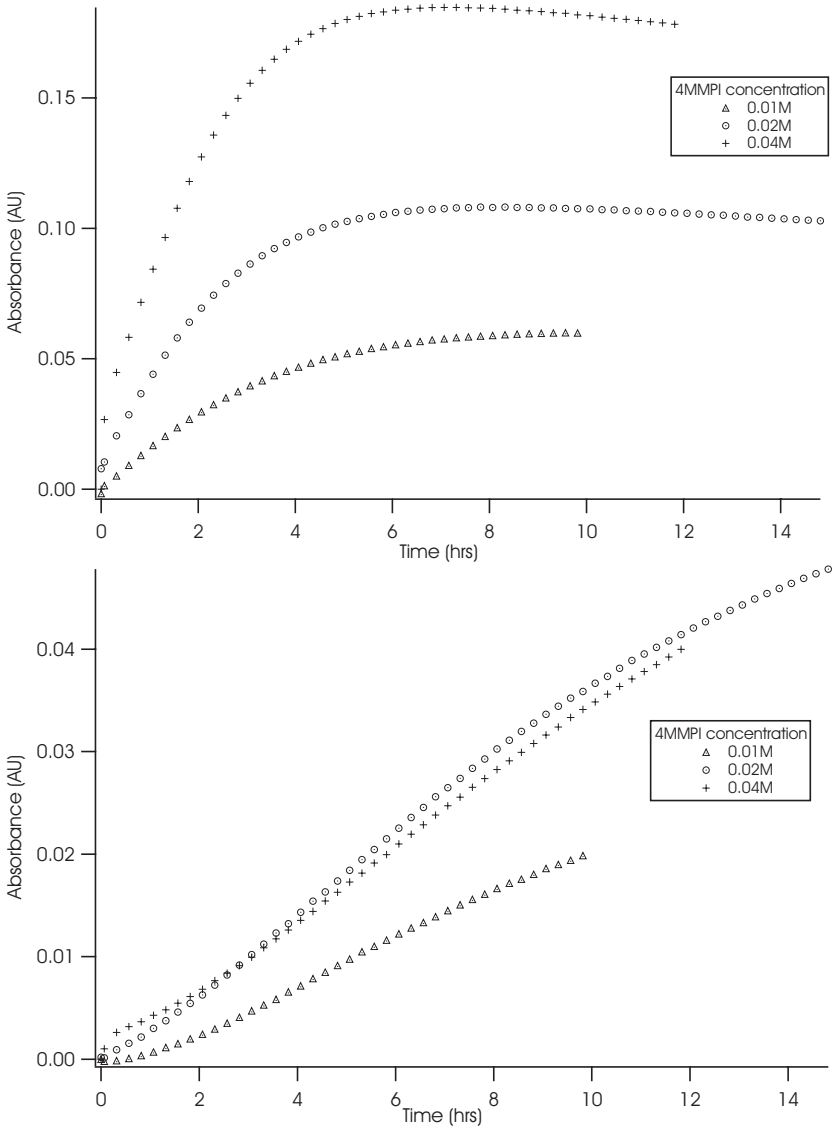

Figure 7.8: Growth over time of peaks at 464 nm (top) and 648 nm (bottom) in methanol solutions of 4-methyl-*N*-methylpyridinium iodide with triethylamine. The concentration of 4MMPI is shown in the legend; 5 μL TEA was added to each 3 mL sample.

7.4 Theoretical calculations

In order to gain some insight into the source of the observed visible absorbances, theoretical calculations were performed on model compounds by Dr. Jeff Reimers. All calculations were done using B3LYP optimization using the 6-31G* basis set with a methanol dielectric. The results of the calculations are shown in Table 7.2.

To eliminate the possibility that the colour is due simply to the presence of the

pyridone methide structure, excitation energies were calculated for the 4-methyl-*N*-methylpyridinium cation in both its protonated and deprotonated forms. Bond lengths in the latter are consistent with a substantial resonance contribution by the pyridone methide structure (see Figure 7.9), and the lowest-energy transition was found to be 333 nm. This indicates that it alone is insufficient to account for the long-wavelength absorbance observed in experiments.

Calculations were then performed on a deprotonated model dimer, also in a methanol dielectric continuum. The optimized geometries of the two lowest-energy configurations (structures 1 and 2) are shown in Figure 7.10. In both cases, the calculated bond lengths of the cationic and zwitterionic halves of the dimer are very similar to those found for the monomers, and are consistent with the resonance contribution of the pyridone methide structure. Calculated excitation energies for these two configurations are shown in Table 7.2 along with those of the unimers, and it is clear that the forced proximity of

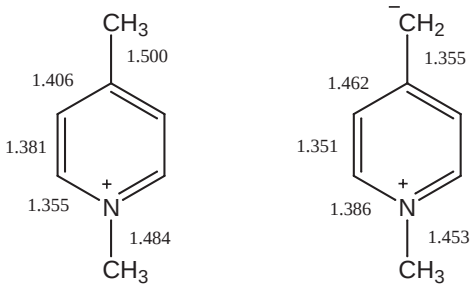

Figure 7.9: Calculated bond lengths (Å) for protonated (left) and deprotonated (right) 4-methyl-*N*-methylpyridinium. Values for the latter indicate a resonance contribution from the pyridone methide structure.

Excited states	4MMP monomer (protonated)		(deprotonated)		deprotonated dimer (Structure 1)[a]		(Structure 2)[b]	
	eV	nm	eV	nm	eV	nm	eV	nm
1	5.421	228.7	3.720	333.3	1.640	756.0	1.450	855.3
2	5.854	211.8	4.840	256.2	2.540	488.2	2.337	530.6
3	6.981	177.6	6.096	203.4	3.597	344.7	3.560	348.3
4	6.984	177.5	6.722	184.5	4.529	273.7	4.316	287.3

Table 7.2: Calculated excitation energies for monomer and dimer molecules. [a]Relative energy = 0 kcal mol^{-1}. [b]Relative energy = 8 kcal mol^{-1}.

two pyridinium units is sufficient to cause excited states at much lower energies.

Further work is needed to probe the possible contribution of the counterion and individual solvent molecules, and to elucidate the nature of each of the excitations, since it is still not clear exactly what is responsible for the low-energy transitions. However, the evidence collected so far is not in conflict with experimental observations suggesting that the colouration is due to a combination of deprotonation and association between adjacent pyridinium units.

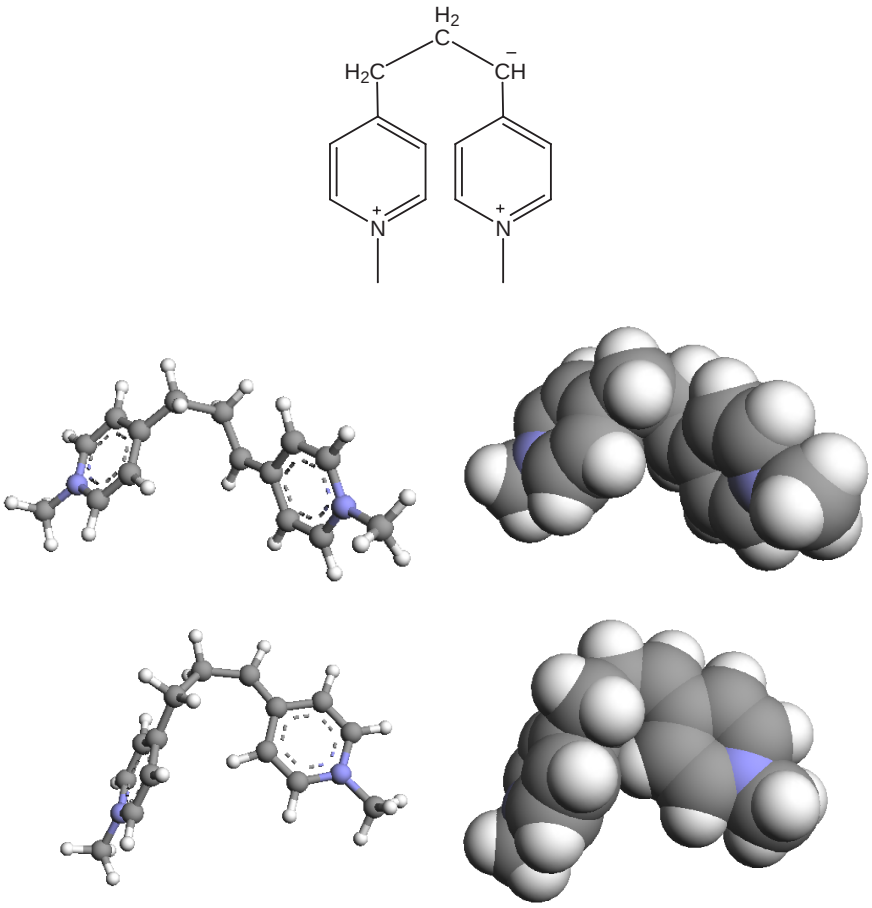

Figure 7.10: (top) the deprotonated model dimer used in calculations; (middle) Structure 1 (relative energy = 0 kcal mol^{-1}); (bottom) Structure 2 (relative energy = 8 kcal mol^{-1}).

7.5 Discussion

Because of the peripheral nature of this work to the main aim of the project, it necessarily received a lower priority than the synthesis and study of the surfactant oligomers. As

a consequence, this chapter represents not a completed project but rather the preliminary exploration of an area of interest. Nevertheless, enough data was collected relating to the chromophorism of the 4-substituted compounds to make it worth presenting.

Experimental observations made in the course of this work indicate that pH-sensitive chromophorism should be exhibited by all quaternized pyridinium compounds with *para* – and possibly *ortho* – ring substitutents having α-protons.

The colours that appear at high pH tend to manifest more slowly than the rate of exchange of the α-protons, particularly in unimeric compounds. This is taken to be evidence that the colour is not due simply to the pyridone methide-like deprotonated structure. In addition, oligomers become coloured with the addition of base at a much faster rate than unimers, suggesting that the proximity of pyridinium units within an oligomer favours the development of colour.

Intramolecular charge-transfer complexes have been observed in macromolecules and copolymers containing electron-accepting and -donating moieties [179–182, 184]. The formation of such complexes between neighbouring protonated (pyridinium) and deprotonated (zwitterion/pyridone methide) units is a possible explanation for this behaviour. If a charge-transfer complex is responsible for the colour in the system studied here, it would be the first instance of such behaviour in a homopolymer.

Calculations support the experimental observations, showing that the observed long-wavelength absorptions cannot be due simply to an excited state of a deprotonated unimer or oilgomer unit; i.e. they are due to something more complex. They also show that intramolecular interactions – as yet unidentified – result in low-energy excited states for the dimer, which would produce visible colouration of the compound.

A major experimental difficulty in studying the chromophorism of the MDP-based oligomers is that the alkaline environment needed to produce the colour also causes them to react further. It is therefore impossible to separate the effects of this reaction from any purely physical interactions that might be responsible for the colour.

It was for this reason that the model compounds, 4MMPI and 4EMPI, were examined. Due to time constraints, the development of the long-wavelength peak in basic solutions of 4MMPI was not followed to completion. Performing such an experiment over a wider range of concentrations would provide information on the chemical or physical equilibria underlying this process. These are likely to include contributions from α-proton exchange and the physical association between pairs of molecules.

It would also be instructive if the model dimer (Figure 7.10) were to be synthesized

and examined. This would provide a direct correlation between experiment and theory, and – because such a compound cannot undergo the LELA reaction – would make the determination of extinction coefficients easier.

Chapter 8

Conclusion

"...tho' with great difficulty I am got hither, yet now I do not repent me of all the trouble I have been at to arrive where I am."

John Bunyan, The Pilgrim's Progress

The work described in this thesis was performed with the aim of developing an easy synthesis for oligomeric surfactants that relies on polymerization rather than conventional organic synthetic methods. Having found such a method only after many false starts, there remained limited opportunities to investigate the rich phase behaviour of the resulting family of surfactants. Nevertheless, enough data has been collected – relating to both the original surfmers and the unimers and oligomers produced by the LELA reaction – to give a general picture of the interesting properties of these compounds, as well as to form the basis for a variety of further work.

Surfmer characterization

Basic characterization was performed on a number of methacrylate- and vinylpyridinium-based surfmers. Apart from MEDDAB and MEHDAB (the bromide salts of the methacrylate surfmers), these compounds are not well represented in the literature.

The tendency of all of these surfmers to spontaneously polymerize constitutes a significant difficulty in their characterization. Quantitative measures such as the critical micelle concentration are subject to error, the exact determination of which is itself fraught with problems. Despite this, the CMCs measured here are within the expected ranges, and follow the expected trends.

The CMCs decrease with increasing chain length and counterion binding strength: these effects have long been documented in the literature. For the vinylpyridiniums the position of the ring substituent has a small effect, with 4VDPs having lower CMCs than 2VDPs. The methacrylate moiety is seen to have a moderately hydrophobizing effect, with the methacrylate surfmers having CMCs intermediate between their alkyltrimethylammonium and alkylhexyldimethylammonium analogues.

Small-angle neutron scattering shows that almost all the surfactants form spherical or near-spherical micelles at concentrations of 1 wt%. An apparent exception to this was MEDDAA, but this sample was shown to contain a significant percentage of polymerized material that skewed the fitting of the scattering data.

At higher concentrations, SANS indicates that MEDDAA and 2VDPC micelles are spherical, a result which is supported by the observation that both these surfactants form discrete cubic phases. Excluding MEHDAA (which was not examined with SANS), all the other surfmers form increasingly eccentric ellipsoidal or cylindrical micelles, consistent with the lowest-concentration mesophase being the hexagonal phase. Like MEDDAA, MEHDAA forms a discrete cubic phase at room temperature, suggesting that it too probably forms spherical micelles.

The nature and position of the polymerizable moiety in the methacrylate surfactants has been the subject of some discussion in the literature. The fact that these surfmers form spherical micelles suggests that – at least in dilute solution – the methacrylate chain acts more as part of the headgroup than as an additional tail. However, when adsorbed to mica, these surfactants form only bilayers. This is consistent with the behaviour of other surfactants with short side-chains, and indicates that binding of the charged nitrogen to the mica constrains the methacrylate, along with the hydrocarbon tail, to stand perpendicular to the surface.

A limited study was made of the adsorbed layer structure of the vinylpyridinium surfmers, and only bilayers were observed. This is inconsistent with previous studies of pyridinium surfactants, and is not easily rationalized in terms of the additional vinyl group. It is possible that the equilibration time allowed before images were acquired was sufficient for some polymerization to occur, which would affect the adsorbed structure. Atomic force microscopy is also subject to fluctuations and artefacts, which could have affected the result. Further work is required to resolve this inconsistency.

Free-radical polymerization

Unsuccessful attempts were made to produce oligomers by controlling the free-radical polymerization of the methacrylate surfactants. This was largely due to the unsolved problem of how to analyse the polymerized products: an almost complete lack of feedback severely hampered efforts to improve the experimental method.

However, the literature contains examples of both catalytic chain transfer and RAFT being used to produce short oligomers from a variety of monomers. Indeed, RAFT polymerization is being used in our laboratory to produce small amphiphilic diblock copolymers. The problems encountered with the methacrylate surfmers should therefore not be taken as excluding the possibility of future success. Should the unusual analysis problems be overcome, it is likely that oligomers could be produced from these surfactants.

In addition, only time constraints prevented chain-transfer methods being tried on the vinylpyridinium surfactants. Given that – unlike the methacrylates – vinylpyridinium oligomers are easily identified by a combination of mass spectrometry, NMR and HPLC, optimization of such methods would be much easier.

It should be noted that such methods, were they to become viable, would have the synthetic advantage of making possible the bulk production of oligomers. This is in contrast to the LELA reaction, which requires low concentrations and large volumes of solvent, and is therefore relatively inefficient.

The LELA reaction

It was found that certain alkylpyridinium compounds, when exposed to a basic environment, undergo an elimination/addition reaction that links the molecules together to form oligomers. For a compound to participate in this reaction, it requires an *ortho*- or *para*-substituted alkyl group of (at least) two carbons, with the β-carbon having a substituent that can act as a leaving group during elimination. Additionally, the ring nitrogen must be quaternized, since the resulting positive charge stabilizes the reactive carbanion during the reaction.

Because of the late stage at which this reaction was discovered, its kinetics, stereochemistry and the exact details of its mechanism have not been comprehensively studied, and further work is required before it is fully understood. Nevertheless, it has been used here to produce mixtures of oligomers for characterization, and to study changes

in self-assembled morphology with increasing oligomer length.

With regard to the original aim of this thesis, there are two disadvantages to this reaction. One is that it is currently confined to alkylpyridinium compounds, and the other is that it appears to work best at low concentrations. Both of these problems mean that it does not immediately constitute a solution to the limited availability of oligomeric surfactants. However, as a tool for studying a particular family of oligomeric surfactants it has a great deal of potential, and these two disadvantages are not necessarily insurmountable.

Unimer/oligomer characterization

Initial investigations were made into the physical properties of the oligomers produced in the LELA reaction. In particular, brief studies were made of the dilute and concentrated phase behaviour, self-assembly in the course of the LELA reaction, and the adsorbed layer structures formed by the oligomer mixtures on mica.

All mixtures were found to form a hexagonal phase. Pure and close to pure unimer additionally show a broad two-phase region, with the hexagonal phase persisting down to concentrations as low as 1 wt% depending on the counterion. This suggests that it is an inverse (H_2) phase. As the average oligomer length in the surfactant mixture increases, more complex phase behaviour is observed, with stiff and fluid isotropic phases being observed, along with – in one case – a coacervate. The latter type of phase is particularly unusual in a salt-free system. This variety in phase behaviour is an example of the potential tunability of mixtures of oligomeric surfactants.

SANS was used to observe changes in self-assembled structures as aqueous LELA reactions progressed. A shift was seen from micelle-sized structures to nanometre-sized, roughly spherical particles with apparent internal order. It is suggested that these are particles of reverse hexagonal phase, or hexosomes.

Mixtures with a high percentage of oligomer also showed self-assembly in organic solvents such as formamide, dimethylformamide and acetone, although it should be noted that these systems were not thoroughly dry.

When adsorbed on mica, the oligomer mixtures form films that display no long-range order, and which increase in roughness with the average oligomer length. In one case, flat randomly-shaped patches are seen to form, resembling behaviour seen previously in a trimeric quaternary ammonium surfactant.

Chromophoric properties

The chromophoric properties of the pyridinium surfactants were useful in deducing the mechanism and methods of control of the LELA reaction, and their source was naturally a topic of interest. Data presented here indicate that a large variety of pyridinium compounds should exhibit pH-sensitive chromophorism, including common polymers such as polyvinylpyridine quaternized with alkyl groups.

It is tentatively suggested that this behaviour is due to the formation of a charge-transfer complex between protonated and deprotonated molecules (i.e. an intermolecular complex) or oligomer/polymer units (i.e. an intramolecular complex). In such a complex, the protonated unit would act as the electron acceptor, while with zero net charge, the deprotonated zwitterion/pyridone methide structure would be the donor.

The data collected during this work do not contradict this interpretation, but neither do they constitute proof of it. Calculations performed by Dr. Reimers support the idea that interaction between protonated and deprotonated units could cause low-energy excited states that lead to absorption in the visible region. It was also verified that such absorbances cannot be due to a deprotonated unimer or oligomer unit alone.

Further work, both theoretical and experimental, is required before the source of the colour is unambiguously identified. If a charge-transfer complex is responsible, however, it would be the first instance of such behaviour in a homopolymer. Its applications may be limited, however, by the fact that the basic environment necessary to produce the colour is also a catalyst for degradation of the polymer backbone.

Future work

It is hoped that the results presented in this thesis can provide the starting point for a variety of further research.

For the sake of completeness, a more complete and careful characterization of the polymerizable surfactants could be undertaken. However, there would need to be a significant need for the data given the amount of work involved in purification.

There is still plenty of potential in the idea of producing oligomeric surfactants using free-radical polymerization, particularly with the RAFT technique being applied to an increasingly wide range of monomers. The expertise needed for this means, however, that it would be best performed by a polymer chemist rather than a surfactant chemist.

There are a number of lines of work that could come from the LELA reaction and

the oligomers produced by it. These include more detailed studies of the relationship between oligomer length and micelle morphology, the properties of both pure oligomers and mixtures, the potential for producing hexosomes, and work on the optimization, kinetics and even stereochemical nature of the reaction itself.

Finally, the chromophoric properties of the alkylpyridinium family have not heretofore been described, and it is hoped that they are of sufficient interest to be pursued further. Given that charge-transfer complexes, particularly in polymers, are the focus of a considerable number of research efforts, it may be that this system will find a useful niche.

Bibliography

[1] Pliny the Elder, *Naturalis Historia*. Book 28, **Ch. 51**.

[2] G. A. Baker and S. Pandey, 'Amphiphilic self organization in ionic liquids'. *ACS Symp. Ser.* **2005**, *901*, 234–243.

[3] D. W. R. Gruen, 'The packing of amphiphile chains in a small spherical micelle'. *J. Colloid Interface Sci.* **1981**, *84*, 281–283.

[4] D. W. R. Gruen, 'A model for the chains in amphiphilic aggregates. 1. Comparison with a molecular dynamics simulation of a bilayer'. *J. Phys. Chem.* **1985**, *89*, 146–153.

[5] K. D. Collins and M. W. Washabaugh, 'The Hofmeister effect and the behavior of water at interfaces'. *Q. Rev. Biophys.* **1985**, *18*, 323–422.

[6] B. W. Ninham and V. Yaminsky, 'Ion binding and ion specificity: The Hofmeister Effect and Onsager and Lifshitz Theories'. *Langmuir* **1997**, *13*, 2097–2108.

[7] J. E. Brady, D. F. Evans, G. G. Warr, F. Grieser and B. W. Ninham, 'Counterion specificity as the determinant of surfactant aggregation'. *J. Phys. Chem.* **1986**, *90*, 1853–1859.

[8] D. Cochin, R. Zana and F. Candau, 'Photopolymerization of micelle-forming monomers. 2. Kinetic study and mechanism'. *Macromolecules* **1993**, *26*, 5765–5771.

[9] D. J. Mitchell, G. J. T. Tiddy, L. Waring, T. Bostock and M. P. McDonald, 'Phase behaviour of polyoxyethylene surfactants with water. Mesophase structures and partial miscibility (cloud points)'. *J. Chem. Soc., Faraday Trans. 1* **1983**, *79*, 975–1000.

[10] C. Tanford, 'Theory of micelle formation in aqueous solutions'. *J. Phys. Chem.* **1974**, *78*, 2469–2479.

[11] J. N. Israelachvili, D. J. Mitchell and B. W. Ninham, 'Theory of self-assembly of hydrocarbon amphiphiles into micelles and bilayers'. *J. Chem. Soc., Faraday Trans. 2* **1976**, *72*, 1525–1568.

[12] J. Gustafsson, H. Ljusberg-Wahren, M. Almgren and K. Larsson, 'Cubic lipid-water phase dispersed into submicron particles'. *Langmuir* **1996**, *12*, 4611–4613.

[13] J. Gustafsson, H. Ljusberg-Wahren, M. Almgren and K. Larsson, 'Submicron particles of reversed lipid phases in water stabilized by a nonionic amphiphilic polymer'. *Langmuir* **1997**, *13*, 6964–6971.

[14] C. Fong, I. Krodkiewska, D. Wells, B. J. Boyd, J. Booth, S. Bhargava, A. McDowall and P. G. Hartley, 'Submicron dispersions of hexosomes based on novel glycerate surfactants'. *Aust. J. Chem.* **2005**, *58*, 683–687.

[15] S. Manne and H. E. Gaub, 'Molecular-organization of surfactants at solid-liquid interfaces'. *Science* **1995**, *270*, 1480–1482.

[16] S. Manne, J. P. Cleveland, H. E. Gaub, G. D. Stucky and P. K. Hansma, 'Direct visualization of surfactant hemimicelles by force microscopy of the electrical double-layer'. *Langmuir* **1994**, *10*, 4409–4413.

[17] W. A. Ducker and E. J. Wanless, 'Adsorption of hexadecyltrimethylammonium bromide to mica: Nanometer-scale study of binding-site competition effects'. *Langmuir* **1999**, *15*, 160–168.

[18] G. G. Warr, 'Surfactant adsorbed layer structure at solid/solution interfaces: impact and implications of AFM imaging studies'. *Curr. Opin. Colloid Interface Sci.* **2000**, *5*, 88–94.

[19] R. Zana and J. Xia (eds.), *Gemini Surfactants*, *Surfactant Science Series*, vol. 117. New York: Marcel Dekker, Inc. **2004**, ISBN 0-8247-4705-4.

[20] F. M. Menger and C. A. J. Littau, 'Gemini-surfactants: synthesis and properties'. *J. Am. Chem. Soc.* **1991**, *113*, 1451–1452.

[21] M. J. Rosen, T. Gao, Y. Nakatsuji and A. Masuyama, 'Synergism in binary mixtures of surfactants: mixtures containing surfactants with two hydrophilic and two or three hydrophobic groups'. *Colloids Surf. A* **1994**, *88*, 1–11.

[22] F. M. Menger and J. S. Keiper, 'Gemini surfactants'. *Angew. Chem. Int. Edn.* **2000**, *39*, 1906–1920.

[23] R. Zana, 'Dimeric and oligomeric surfactants. Behavior at interfaces and in aqueous solution: a review'. *Adv. Colloid Interface Sci.* **2002**, *97*, 205–253.

[24] M. J. L. Castro, J. Kovensky and A. F. Cirelli, 'Gemini surfactants from alkyl glucosides'. *Tetrahedron Lett.* **1997**, *38*, 3995–3998.

[25] C. Gao, A. Millqvist-Fureby, M. J. Whitcombe and E. N. Vulfson, 'Regioselective synthesis of dimeric (gemini) and trimeric sugar-based surfactants'. *J. Surf. Detergents* **1999**, *2*, 292–302.

[26] M. J. L. Castro, J. Kovensky and A. F. Cirelli, 'New family of nonionic gemini surfactants. Determination and analysis of interfacial properties'. *Langmuir* **2002**, *18*, 2477–2482.

[27] L. Pérez, J. L. Torres, A. Manresa, C. Solans and M. R. Infante, 'New family of nonionic gemini surfactants. Determination and analysis of interfacial properties'. *Langmuir* **1996**, *12*, 5296–5301.

[28] E. Piera, M. R. Infante and P. Clapés, 'Chemo-enzymatic synthesis of arginine-based gemini surfactants'. *Biotechnol. Bioeng.* **2000**, *70*, 323–331.

[29] R. Oda, I. Huc, D. Danino and Y. Talmon, 'Aggregation properties and mixing behavior of hydrocarbon, fluorocarbon, and hybrid hydrocarbon-fluorocarbon cationic dimeric surfactants'. *Langmuir* **2000**, *16*, 9759–9769.

[30] R. Oda, I. Huc and S. Candau, 'Gemini surfactants, the effect of hydrophobic chain length and dissymmetry'. *Chem. Commun.* **1997**, *21*, 2105–2106.

[31] R. Oda, I. Huc, J.-C. Homo, B. Heinrich, M. Schmutz and S. Candau, 'Elongated aggregates formed by cationic gemini surfactants'. *Langmuir* **1999**, *15*, 2384–2390.

[32] P. Renouf, C. Mioskowski and L. Lebeau, 'Dimeric surfactants: first synthesis of an asymmetrical gemini compound'. *Tetrahedron Lett.* **1998**, *39*, 1357–1360.

[33] A. V. Peresypkin and F. M. Menger, 'Zwitterionic geminis. Coacervate formation from a single organic compound'. *Org. Lett.* **1999**, *1*, 1347–1350.

[34] V. Seredyuk, E. Alami, M. Nyden, K. Holmberg, A. V. Peresypkin and F. M. Menger, 'Adsorption of zwitterionic gemini surfactants at the air-water and solid-water interfaces'. *Colloids Surf. A* **2002**, *203*, 245–258.

[35] N. Hattori, A. Yoshino, H. Okabayashi and C. J. O'Connor, 'Conformational analysis of (phenylenedimethylene)bis(n-octylammonium)dibromides in aqueous solution. Conformational change upon micellization'. *J. Phys. Chem. B* **1998**, *102*, 8965–8973.

[36] F. M. Menger, J. S. Keiper and V. Azov, 'Gemini surfactants with acetylenic spacers'. *Langmuir* **2000**, *16*, 2062–2067.

[37] L. D. Song and M. J. Rosen, 'Surface properties, micellization, and premicellar aggregation of gemini surfactants with rigid and flexible spacers'. *Langmuir* **1996**, *12*, 1149–1153.

[38] M. Dreja, S. Gramberg and B. Tieke, 'Cationic amphitropic gemini surfactants with hydrophilic oligo(oxyethylene) spacer chains'. *Chem. Commun.* **1998**, *13*, 1371–1372.

[39] R. Zana, M. Benrraou and R. Rueff, 'Alkanediyl-α,ω-bis(dimethylalkylammonium bromide) surfactants. 1. Effect of the spacer chain length on the critical micelle concentration and micelle ionization degree'. *Langmuir* **1991**, *7*, 1072–1075.

[40] R. Zana, H. Levy, D. Papoutsi and G. Beinert, 'Micellization of two triquaternary ammonium surfactants in aqueous solution'. *Langmuir* **1995**, *11*, 3694–3698.

[41] M. In, V. Bec and O. Augerre-Chariol, 'Quaternary ammonium bromide surfactant oligomers in aqueous solution. Self-association and microstructure'. *Langmuir* **2000**, *16*, 141–148.

[42] R. Valivety, I. S. Gill and E. N. Vulfson, 'Application of enzymes to the synthesis of amino acid-based bola and gemini surfactants'. *J. Surf. Detergents* **1998**, *1*, 177–185.

[43] C. A. Bunton, L. Robinson, J. Schaak and M. F. Stam, 'Catalysis of nucleophilic substitutions by micelles of dicationic detergents'. *J. Org. Chem.* **1971**, *36*, 2346–2350.

[44] F. Devinsky, L. Masarova and I. Lacko, 'Surface activity and micelle formation of some new bisquaternary ammonium salts'. *J. Colloid Interface Sci.* **1985**, *105*, 235–239.

[45] F. M. Menger and V. A. Migulin, 'Synthesis and properties of multiarmed geminis'. *J. Org. Chem.* **1999**, *64*, 8916–8921.

[46] T. S. Kim, T. Kida, Y. Nakatsuji and I. Ikeda, 'Preparation and properties of multiple ammonium salts quaternized by epichlorohydrin'. *Langmuir* **1996**, *12*, 6304–6308.

[47] L. H. Bluhm and T. Li, 'Chromatographic purification of quaternary ammonium and pyridinium compounds on normal phase silica gel'. *Tetrahedron Lett.* **1998**, *39*, 3623–3626.

[48] W. Ulbricht and R. Zana, 'Alkanediyl-α,ω-bis(dimethylalkylammonium bromide) surfactants. Part 8. Pressure-jump study of the kinetics of micellar equilibria in aqueous solutions of alkanediyl-α,ω-bis(dimethyldodecylammonium bromide) surfactants'. *Colloids Surf. A* **2001**, *487*, 183–185.

[49] R. Zana, 'Alkanediyl-α,ω-bis(dimethylalkylammonium bromide) surfactants'. *J. Colloid Interface Sci.* **2002**, *246*, 182–190.

[50] F. Kern, F. Lequeux, R. Zana and S. J. Candau, 'Dynamic properties of salt-free viscoelastic micellar solutions'. *Langmuir* **1994**, *10*, 1714–1723.

[51] A. Espert, R. von Klitzing, A. Colin, R. Zana and D. Langevin, 'Behavior of soap films stabilized by a cationic dimeric surfactant'. *Langmuir* **1998**, *14*, 4251–4260.

[52] A. Bernheim-Groswasser, R. Zana and Y. Talmon, 'Sphere-to-cylinder transition in aqueous micellar solution of a dimeric (gemini) surfactant'. *J. Phys. Chem. B* **2000**, *105*, 4005–4009.

[53] R. Oda, I. Huc and S. J. Candau, 'Gemini surfactants as new, low molecular weight gelators of organic solvents and water'. *Angew. Chem. Int. Edn.* **1998**, *37*, 2689–2691.

[54] R. Oda, I. Huc, M. Schmutz, S. J. Candau and F. C. MacKintosh, 'Tuning bilayer twist using chiral counterions'. *Nature* **1999**, *399*, 566–569.

[55] F. M. Menger, A. V. Peresypkin, K. L. Caran and R. P. Apkarian, 'A sponge morphology in an elementary coacervate'. *Langmuir* **2000**, *16*, 9113–9116.

[56] M. J. Rosen and D. J. Tracy, 'Gemini surfactants'. *J. Surf. Detergents* **1998**, *1*, 547–554.

[57] M. J. Rosen, 'Geminis: a new generation of surfactants'. *CHEMTECH* **1993**, *23*, 30–33.

[58] M. Summers and J. Eastoe, 'Applications of polymerizable surfactants'. *Adv. Colloid Interface Sci.* **2003**, *100–102*, 137–152.

[59] A. Guyot, 'Advances in reactive surfactants'. *Adv. Colloid Interface Sci.* **2004**, *108–109*, 3–22.

[60] A. Guyot and F. Vidal, 'Inifer surfactants in emulsion polymerization'. *Polym. Bull.* **1995**, *34*, 569–576.

[61] J. M. Asua and H. A. S. Schoonbrood, 'Reactive surfactants in heterophase polymerization'. *Acta Polym.* **1998**, *49*, 671–686.

[62] O. Soula and A. Guyot, 'Styrenic surfmer in emulsion copolymerization of acrylic monomers. I. Synthesis and characterization of polymerizable surfactants'. *Langmuir* **1999**, *15*, 7956–7962.

[63] C. L. Ong, L. M. Gan, C. K. Ong, H. S. O. Chan and G. Xu, 'Unusual ionic behavior in microemulsion-polymerized membranes'. *J. Phys. Chem. B* **1999**, *103*, 7573–7576.

[64] W. Xu, K. S. Siow, Z. Q. Gao, S. Y. Lee, P. Y. Chow and L. M. Gan, 'Microporous polymeric composite electrolytes from microemulsion polymerization'. *Langmuir* **1999**, *15*, 4812–4819.

[65] M. Dreja, W. Pyckhout-Hintzen and B. Tieke, 'Copolymerization behavior and structure of styrene and polymerizable surfactants in three-component cationic microemulsion'. *Macromolecules* **1998**, *31*, 272–280.

[66] M. Pyrasch and B. Tieke, 'Copolymerization of styrene and reactive surfactants in a microemulsion: control of copolymer composition by addition of nonreactive surfactant'. *Colloid Polym. Sci.* **2000**, *278*, 375–379.

[67] E. D. Sprague, D. C. Duecker and C. E. Larrabee, 'Association of spin-labeled substrate molecules with poly(sodium 10-undecanoate) and the sodium 10-undecanoate micelle'. *J. Am. Chem. Soc.* **1981**, *103*, 6797–6800.

[68] B. Durairaj and F. D. Blum, 'Synthesis and dynamics of oligomeric micelles'. *Langmuir* **1989**, *5*, 370–372.

[69] S. Liu, Y. I. González, D. Danino and E. W. Kaler, 'Polymerization of wormlike micelles induced by hydrotropic salt'. *Macromolecules* **2005**, *38*, 2482–2491.

[70] K. M. McGrath and C. J. Drummond, 'Polymerization of liquid crystalline phases in binary surfactant/water systems. Part 4. Dodecyldimethylammonium-ethyl methacrylate bromide'. *Colloid Polym. Sci.* **1996**, *274*, 612–621.

[71] R. N. A. H. Lewis, D. A. Mannock, R. N. McElhaney, D. C. Turner and S. M. Gruner, 'Effect of fatty acyl chain length and structure on the lamellar-gel to liquid-crystalline and lamellar to reversed hexagonal phase transitions of aqueous phosphatidylethanolamine dispersions'. *Biochem.* **1989**, *28*, 541–548.

[72] Y.-S. Lee, J.-Z. Yang, T. M. Sisson, D. A. Frankel, J. T. Gleeson, E. Aksay, S. L. Keller, S. M. Gruner and D. F. O'Brien, 'Polymerization of nonlamellar lipid assemblies'. *J. Am. Chem. Soc.* **1995**, *117*, 5573–5578.

[73] P. Dais, C. M. Paleos, G. Nika and A. Malliaris, 'Positional effects of the methacrylate group on polymerization and microstructure of micelle-forming quaternary ammonium salts studied by NMR spectroscopy'. *Makromol. Chem.* **1993**, *194*, 445–450.

[74] K. Tajima and T. Aida, 'Controlled polymerizations with constrained geometries'. *Chem. Commun.* **2000**, *24*, 2399–2412.

[75] D. Cochin, F. Candau and R. Zana, 'Photopolymerization of micelle-forming monomers. 1. Characterization of the systems before and after polymerization'. *Macromolecules* **1993**, *26*, 5755–5764.

[76] G. Odian, *Principles of Polymerization*. New York: Wiley-Interscience, 3rd ed. **1991**.

[77] G. Moad and D. H. Solomon, *The Chemistry of Free Radical Polymerization*. Oxford: Pergamon **1995**, ISBN 0 08 042078 8.

[78] K. Matyjaszewski and T. P. Davis (eds.), *Handbook of Radical Polymerization*. Hoboken: John Wiley and Sons, Inc. **2002**.

[79] J. Chiefari, Y. K. Chong, F. Ercole, J. Krstina, J. Jeffery, T. P. T. Le, R. T. A. Mayadunne, G. F. Meijs, C. L. Moad, G. Moad, E. Rizzardo and S. H. Thang, 'Living free-radical polymerization by reversible addition-fragmentation chain transfer: the RAFT process'. *Macromolecules* **1998**, *31*, 5559–5562.

[80] A. A. Gridnev and S. D. Ittel, 'Catalytic chain transfer in free-radical polymerizations'. *Chem. Rev.* **2001**, *101*, 3611–3659.

[81] M. Farina, 'Chemistry and kinetics of the chain transfer reaction'. *Macromol. Symp.* **1987**, *10*, 255–272.

[82] G. Moad, Y. Chong, A. Postma, E. Rizzardo and S. H. Thang, 'Advances in RAFT polymerization: the synthesis of polymers with defined end-groups'. *Polymer* **2005**, *46*, 8458–8468.

[83] N. S. Enikolopyan, B. R. Smirnov, G. V. Ponomarev and I. M. Belgovskii, 'Catalyzed chain transfer to monomer in free radical polymerization'. *J. Polym. Sci., Polym. Chem. Edn.* **1981**, *19*, 879–889.

[84] L. V. Karmilova, G. V. Ponomarev, B. R. Smirnov and I. M. Belgovskii, 'Metalloporphyrins as chain transfer catalysts in radical polymerization and stereoselective oxidation'. *Russ. Chem. Rev.* **1984**, *53*, 132.

[85] J. P. A. Heuts, L. M. Muratore and T. P. Davis, 'Preparation and characterization of oligomeric terpolymers of styrene, methyl methacrylate and 2-hydroxyethyl

methacrylate: A comparison of conventional and catalytic chain transfer'. *Macromol. Chem. Phys.* **2000**, *201*, 2780–2788.

[86] D. J. Forster, J. P. A. Heuts and T. P. Davis, 'Conventional and catalytic chain transfer in the free-radical polymerization of 2-phenoxyethyl methacrylate'. *Polymer* **2000**, *41*, 1385–1390.

[87] D. M. Haddleton, E. Depaquis, E. J. Kelly, D. Kukulj, S. R. Morsley, S. A. F. Bon, M. D. Eason and A. G. Steward, 'Cobalt-mediated catalytic chain-transfer polymerization (CCTP) in water and water/alcohol solution'. *J. Polym. Sci., Part A: Polym. Chem.* **2001**, *39*, 2378–2384.

[88] F. R. Mayo, 'Chain transfer in the polymerization of styrene: the reaction of solvents with free radicals'. *J. Am. Chem. Soc.* **1943**, *65*, 2324–2329.

[89] A. A. Gridnev, I. M. Belgovskii and N. S. Enykolopyan, 'Kinetics and molecular weight distribution during intensive catalysis of chain transfer to monomer'. *Vysokomol. Soedin. B* **1986**, *28*, 85–89.

[90] J. P. A. Heuts, G. E. Roberts and J. D. Biasutti, 'Catalytic chain transfer polymerization: an overview'. *Aust. J. Chem.* **2002**, *55*, 381–398.

[91] R. Mülhaupt, 'Catalytic polymerization and post-polymerization catalysis fifty years after the discovery of Ziegler's catalysts'. *Macromol. Chem. Phys.* **2003**, *204*, 289–327.

[92] A. A. Gridnev, 'Kinetics of alpha-methylstyrene oligomerization by catalytic chain transfer'. *J. Polym. Sci., Part A: Polym. Chem.* **2002**, *40*, 1366–1376.

[93] P. Delduc, C. Tailhan and S. Z. Zard, 'A convenient source of alkyl and acyl radicals'. *Chem. Commun.* **1988**, *4*, 308–310.

[94] R. T. A. Mayadunne, E. Rizzardo, J. Chiefari, Y. K. Chong, G. Moad and S. H. Thang, 'Living radical polymerization with reversible addition-fragmentation chain transfer (RAFT polymerization) using dithiocarbamates as chain transfer agents'. *Macromolecules* **1999**, *32*, 6977–6980.

[95] R. T. A. Mayadunne, E. Rizzardo, J. Chiefari, J. Krstina, G. Moad, A. Postma and S. H. Thang, 'Living polymers by the use of trithiocarbonates as reversible

addition-fragmentation chain transfer (RAFT) agents. ABA triblock copolymers by radical polymerization in two steps'. *Macromolecules* **2000**, *33*, 243–245.

[96] C. Barner-Kowollik, T. P. Davis, J. P. A. Heuts, M. H. Stenzel, P. Vana and M. Whittaker, 'RAFTing down under: tales of missing radicals, fancy architectures, and mysterious holes'. *J. Polym. Sci., Part A: Polym. Chem.* **2003**, *41*, 365–375.

[97] G. Moad, E. Rizzardo and S. H. Thang, 'Living radical polymerization by the RAFT process'. *Aust. J. Chem.* **2005**, *58*, 379–410.

[98] S. Perrier and P. Takolpuckdee, 'Macromolecular design via reversible addition-fragmentation chain transfer (RAFT)/xanthates (MADIX) polymerization'. *J. Polym. Sci., Part A: Polym. Chem.* **2005**, *43*, 5347–5393.

[99] B. Y. K. Chong, J. Krstina, T. P. T. Le, G. Moad, A. Postma, E. Rizzardo and S. H. Thang, 'Thiocarbonylthio compounds [S:C(Ph)S-R] in free radical polymerization with reversible addition-fragmentation chain transfer (RAFT polymerization). Role of the free-radical leaving group (R)'. *Macromolecules* **2003**, *36*, 2256–2272.

[100] G. Moad, J. Chiefari, Y. K. Chong, J. Krstina, R. T. A. Mayadunne, A. Postma, E. Rizzardo and S. H. Thang, 'Living free radical polymerization with reversible addition-fragmentation chain transfer (the life of RAFT)'. *Polym. Int.* **2000**, *49*, 993–1001.

[101] S. W. Prescott, M. J. Ballard, E. Rizzardo and R. G. Gilbert, 'RAFT in emulsion polymerization: what makes it different?' *Aust. J. Chem.* **2002**, *55*, 415–424.

[102] P. Vana, J. F. Quinn, T. P. Davis and C. Barner-Kowollik, 'Recent advances in the kinetics of reversible addition fragmentation chain-transfer polymerization'. *Aust. J. Chem.* **2002**, *55*, 425–431.

[103] A. A. Toy, P. Vana, T. P. Davis and C. Barner-Kowollik, 'Reversible addition fragmentation chain transfer (RAFT) polymerization of methyl acrylate: Detailed structural investigation via coupled size exclusion chromatography-electrospray ionization mass spectrometry (SEC-ESI-MS)'. *Macromolecules* **2004**, *37*, 744–751.

[104] J. Krstina, G. Moad, E. Rizzardo and C. L. Winzor, 'Narrow polydispersity block copolymers by free-radical polymerization in the presence of macromonomers'. *Macromolecules* **1995**, *28*, 5381–5385.

[105] S. G. Gaynor, J.-S. Wang and K. Matyjaszewski, 'Controlled radical polymerization by degenerative transfer: Effect of the structure of the transfer agent'. *Macromolecules* **1995**, *28*, 8051–8056.

[106] J. F. Quinn, E. Rizzardo and T. P. Davis, 'Ambient temperature reversible addition-fragmentation chain transfer polymerization'. *Chem. Commun.* **2001**, *11*, 1044–1045.

[107] Y. Mitsukami, M. S. Donovan, A. B. Lowe and C. L. McCormick, 'Water-soluble polymers. 81. Direct synthesis of hydrophilic styrenic-based homopolymers and block copolymers in aqueous solution via RAFT'. *Macromolecules* **2001**, *34*, 2248–2256.

[108] M. S. Donovan, A. B. Lowe, T. A. Sanford and C. L. McCormick, 'Sulfobetaine-containing diblock and triblock copolymers via reversible addition-fragmentation chain transfer polymerization in aqueous media'. *J. Polym. Sci., Part A: Polym. Chem.* **2003**, *41*, 1262–1281.

[109] S. Yusa, Y. Shimada, Y. Mitsukami, T. Yamamoto and Y. Morishima, 'pH-responsive micellization of amphiphilic diblock copolymers synthesized via reversible addition-fragmentation chain transfer polymerization'. *Macromolecules* **2003**, *36*, 4208–4215.

[110] C. L. McCormick and A. B. Lowe, 'Aqueous RAFT polymerization: Recent developments in synthesis of functional water-soluble (co)polymers with controlled structures'. *Acc. Chem. Res.* **2004**, *37*, 312–325.

[111] Y. A. Vasilieva, D. B. Thomas, C. W. Scales and C. L. McCormick, 'Direct controlled polymerization of a cationic methacrylamido monomer in aqueous media via the RAFT process'. *Macromolecules* **2004**, *37*, 2728–2737.

[112] M. Mertoglu, A. Laschewsky, K. Skrabania and C. Wieland, 'New water-soluble agents for reversible addition-fragmentation chain transfer polymerization and their application in aqueous solutions'. *Macromolecules* **2005**, *38*, 3601–3614.

[113] A. J. Convertine, B. S. Lokitz, A. B. Lowe, C. W. Scales, L. J. Myrick and C. L. McCormick, 'Aqueous RAFT polymerization of acrylamide and N,N-dimethylacrylamide at room temperature'. *Macromol. Rapid Commun.* **2005**, *26*, 791–795.

[114] R. Foster, *Organic Charge-Transfer Complexes*, *Organic Chemistry: A Series of Monographs*, vol. 15. London: Academic Press **1969**, ISBN 12-262650-8.

[115] E. M. Kosower, 'Additions to pyridinium rings. III. Chemical and biochemical implications of charge-transfer complex intermediates'. *J. Am. Chem. Soc.* **1956**, *78*, 3497–3501.

[116] M. Holler, H. S. Sin, A. James, A. Burger, D. Tritsch and J.-F. Biellmann, '(*E*)-1-alkyl-4-[2-(alkylsulfonyl)-1-ethenyl]pyridinium salts: Reaction with thiol groups giving rise to chromophoric (*e*)-1-alkyl-4-[2-(alkylsulfanyl)-1-ethenyl]pyridinium salts'. *Chem. Eur. J.* **2000**, *6*, 2053–2062.

[117] A. E. Chichibabin, 'Tautomerism in the pyridine series'. *Ber.* **1927**, *60*, 1607–1617.

[118] A. E. Chichibabin and S. W. Benewolenskaya, 'Tautomerism in the pyridine series: diphenylpyridylmethanes and some of their derivatives'. *Ber.* **1928**, *61*, 547–555.

[119] K. Schofield, *Hetero-aromatic nitrogen compounds: pyrroles and pyridines*. London: Butterworths **1967**.

[120] W. E. Doering and R. A. N. Weil, 'Electrophilic reactions of 2- and 4-vinylpyridines'. *J. Am. Chem. Soc.* **1947**, *69*, 2461–2466.

[121] L. C. Anderson and N. V. Seeger, 'The absorption spectra of some methylpyridine derivatives'. *J. Am. Chem. Soc.* **1949**, *71*, 343–345.

[122] J. A. Berson, J. E. M. Evleth and Z. Hamlet, 'Nitrogen analogs of sesquifulvalene. I. Synthesis and properties'. *J. Am. Chem. Soc.* **1965**, *87*, 2887–2900.

[123] G. V. Boyd and A. D. Ezekiel, 'Stable pyridine anhydro-bases'. *J. Chem. Soc. (C)* **1967**, 1866–1868.

[124] C. Hansch and W. Carpenter, 'Catalytic synthesis of heterocycles. IX. Dehydrocyclization of 2-methyl-5-ethyl-4-pyridinethiol to 6-methyl-5-azathianaphthene'. *J. Org. Chem.* **1957**, *22*, 936–939.

[125] L. Bauer and J. L. A. Gardella, 'Addition of thiourea to 2- and 4-vinylpyridines'. *J. Org. Chem.* **1961**, *26*, 82–85.

[126] A. P. Phillips, 'The addition of amines to 4-vinylpyridine'. *J. Am. Chem. Soc.* **1956**, *78*, 4441–4443.

[127] C. K. M. Heo and J. W. Bunting, 'Nucleophilicity towards a vinylic carbon atom: Rate constants for the addition of amines to the 1-methyl-4-vinylpyridinium cation in aqueous solution'. *J. Chem. Soc., Perkin Trans. 2* **1994**, 2279–2290.

[128] H. Suzuki and Y. Tanaka, 'An unusually acidic methyl group directly bound to acridinium cation'. *J. Org. Chem.* **2001**, *66*, 2227–2231.

[129] S. Alunni and A. Busti, 'Mechanism and proton activating factors in base-induced β-elimination reactions of 2-(2-chloroethyl)pyridine'. *J. Chem. Soc., Perkin Trans. 2* **2001**, 778–781.

[130] S. Alunni, V. Laureti, L. Ottavi and R. Ruzziconi, 'Catalysis of the β-elimination of HF from isomeric 2-fluoroethylpyridines and 1-methyl-2-fluoroethylpyridinium salts. Proton-activating factors and methyl-activating factors as a mechanistic test to distinguish between concerted E2 and E1cb irreversible mechanisms'. *J. Org. Chem.* **2003**, *68*, 718–725.

[131] U. P. Strauss, N. L. Gershfeld and H. Spiera, 'Charge reversal of cationic poly-4-vinylpyridine derivatives in KBr solutions'. *J. Am. Chem. Soc.* **1954**, *76*, 5909–5911.

[132] U. P. Strauss and N. L. Gershfeld, 'The transition from typical polyelectrolyte to polysoap. I. Viscosity and solubilization studies on copolymers of 4-vinyl-*N*-ethylpyridinium bromide and 4-vinyl-*N*-*n*-dodecylpyridinium bromide'. *J. Phys. Chem.* **1954**, *58*, 747–753.

[133] U. P. Strauss, N. L. Gershfeld and E. H. Crook, 'The transition from typical polyelectrolyte to polysoap. II. Viscosity studies of poly-4-vinylpyridine derivatives in aqueous KBr solutions'. *J. Phys. Chem.* **1956**, *60*, 577–584.

[134] U. P. Strauss and B. L. Williams, 'The transition from typical polyelectrolyte to polysoap. III. Light scattering and viscosity studies of poly-4-vinylpyridine derivatives'. *J. Phys. Chem.* **1961**, *65*, 1390–1395.

[135] K. Matsuzaki, T. Matsubara and T. Kanai, 'Stereoregularity of poly(2-vinylpyridine) and poly-(4-vinylpyridine)'. *J. Polym. Sci., Polym. Chem. Edn.* **1977**, *15*, 1573–1583.

[136] E. A. Boucher, E. Khosravi-Babadi and C. C. Mollett, 'Kinetics of quaternization of 4-methyl and 4-ethyl pyridine with *n*-propyl and *n*-butyl bromide in sulpholane'. *J. Chem. Soc., Faraday Trans. 1* **1978**, *74*, 427–431.

[137] E. A. Boucher, E. Khosravi-Babadi and C. C. Mollett, 'Quaternization of poly(4-vinyl pyridine). Kinetic and viscometric measurements'. *J. Chem. Soc., Faraday Trans. 1* **1979**, *75*, 1728–1735.

[138] E. A. Boucher and C. C. Mollett, 'Coloured and colourless charge-transfer complexes of small and polymeric quaternary pyridinium bromides'. *J. Chem. Soc., Faraday Trans. 1* **1982**, *78*, 1401–1404.

[139] P. L. Kronick and R. M. Fuoss, 'Quaternization kinetics. II. Pyridine and 4-picoline in propylene carbonate'. *J. Am. Chem. Soc.* **1955**, *77*, 6114.

[140] B. D. Coleman and R. M. Fuoss, 'Quaternization kinetics. I. Some pyridine derivatives in tetramethylene sulfone'. *J. Am. Chem. Soc.* **1955**, *77*, 5472–5476.

[141] E. A. Boucher, 'Reaction kinetics of polymer substitutents. Neighboring-subsituent effects in single-substitutent reactions'. *J. Chem. Soc., Faraday Trans. 1* **1972**, *68*, 2295–2304.

[142] E. A. Boucher and C. C. Mollett, 'Kinetics and mechanism of the quaternization of poly(4-vinyl pyridine) with 1-bromopropane'. *J. Polym. Sci., Polym. Phys.* **1977**, *15*, 283–289.

[143] E. A. Boucher, J. A. Groves, C. C. Mollett and P. W. Fletcher, 'Kinetics and mechanism of the quaternization of poly(4-vinyl pyridine) with ethyl, *n*-propyl, *n*-butyl, *n*-hexyl and benzyl bromide in sulfolane'. *J. Chem. Soc., Faraday Trans. 1* **1977**, *73*, 1629–1635.

[144] K. Yamaguchi and Y. Minoura, 'Polymerization of vinyl monomers with salts of Brønsted acids'. *J. Polym. Sci., Part A-1* **1970**, *8*, 1571–1586.

[145] V. A. Kabanov, K. V. Aliev and V. A. Kargin, 'Specific polymerization of 4-vinylpyridine salts'. *Vysokomol. Soedin. A* **1968**, *10*, 1618–1632.

[146] S. Iwatsuki, T. Kokubo, K. Motomatsu, M. Tsuji and Y. Yamashita, 'Studies on the charge-transfer complex and polymerization. Part XVIII. Spontaneous polymerization of 2-vinylpyridine accompanying quaternization by methyl iodide'. *Makromol. Chem.* **1968**, *120*, 154–160.

[147] V. A. Kabanov, K. V. Aliev, O. V. Kargina, T. Patrikeeva and V. A. Kargin, 'Specific polymerization of vinylpyridinium salts. Polymerization on macromolecular matrixes'. *J. Polym. Sci., Polym. Symp.* **1967**, *16*, 1079–1094.

[148] V. A. Kabanov, T. Patrikeeva, O. V. Kargina and V. A. Kargin, 'Organized polymerization of vinylpyridinium salts'. *J. Polym. Sci., Polym. Symp.* **1968**, *23*, 357–363.

[149] V. A. Kabanov and V. A. Petrovskaya, 'Formation of stereoregular poly(4-vinylpyridine) in polymerization of 4-vinylpyridine in aqueous solutions'. *Vysokomol. Soedin. B* **1968**, *10*, 797–798.

[150] J. C. Salamone, B. Snider and W. L. Fitch, 'Polymerization of 4-vinylpyridinium salts. I. The counterion initiation mechanism'. *J. Polym. Sci., Part B: Polym. Lett.* **1971**, *9*, 13–17.

[151] J. C. Salamone, B. Snider and W. L. Fitch, 'Polymerization of vinylpyridinium salts. II. Hydrogen-transfer polymerization'. *Macromolecules* **1970**, *3*, 707–709.

[152] J. C. Salamone, B. Snider and W. L. Fitch, 'Polymerization of 4-vinylpyridinium salts. III. A clarification of the mechanism of spontaneous polymerization'. *J. Polym. Sci., Part A-1* **1971**, *9*, 1493–1504.

[153] J. C. Salamone, E. J. Ellis and S. C. Israel, 'Polymerization of vinylpyridinium salts. V. Syntheses and spontaneous polymerization studies of 2-vinyl-*N*-alkylpyridinium salts'. *J. Polym. Sci., Part B: Polym. Lett.* **1972**, *10*, 605–613.

[154] J. C. Salamone, E. J. Ellis, C. R. Wilson and D. F. Bardoliwalla, 'Polymerization of vinylpyridinium salts. VI. Spontaneous polymerization by concentrated sulfuric acid'. *Macromolecules* **1973**, *6*, 475–476.

[155] J. C. Salamone, A. C. Watterson, T. D. Hsu, C.-C. Tsai and M. U. Mahmud, 'Polymerization of vinylpyridinium salts. IX. Preparation of monomeric salt pairs'. *J. Polym. Sci., Polym. Lett. Edn.* **1977**, *15*, 487–491.

[156] J. C. Salamone, M. U. Mahmud, A. C. Watterson and A. P. Olson, 'Polymerization of vinylpyridinium salts. XII. Occurrence of radical polymerization in spontaneous reactions'. *J. Polym. Sci., Polym. Chem. Edn.* **1982**, *20*, 1153–1167.

[157] J. C. Salamone, M. K. Raheja, Q. Anwaruddin and A. C. Watterson, 'Polymerization of vinylpyridinium salts. XIII. Preparation of 4-vinyl-*N*-methylpyridinium *p*-styrenesulfonate charge transfer ion-pair comonomer'. *J. Polym. Sci., Polym. Lett. Edn.* **1985**, *23*, 656–659.

[158] I. Mielke and H. Ringsdorf, 'Untersuchung von Vinylpyridiniumverbindungen. II. Polyadditionsreaktion von 4-Vinylpyridiniumsalzen'. *J. Polym. Sci., Part B: Polym. Lett.* **1971**, *9*, 1–12.

[159] I. Mielke and H. Ringsdorf, 'Untersuchung von Vinylpyridiniumverbindungen. III. Über den Mechanismus der 'spontanen Polymerisation' von 4-Vinylpyridiniumsalzen in Wasser'. *Makromol. Chem.* **1971**, *142*, 319–324.

[160] H. Ringsdorf and G. Walter, 'Untersuchung von Vinylpyridiniumvorbindungen IV. Polyreaktionen von 2-Vinylpyridiniumsalzen'. *Makromol. Chem.* **1971**, *149*, 295–301.

[161] I. Mielke and H. Ringsdorf, 'Polyreaktionen in orientierten Systemen. II Polymerisation von 4-Vinylpyridiniumsalzen in micellar geordneten Lösungen'. *Makromol. Chem.* **1972**, *153*, 307–322.

[162] V. Martin, H. Ringsdorf, H. Ritter and W. Sutter, 'Polyreaktionen in orientierten Systemen. VI. Mizellare Assoziationen in 4-Vinylpyridiniumsalzlösungen'. *Makromol. Chem.* **1975**, *176*, 2029–2039.

[163] P. Ranganathan, W. K. Fife and M. Zeldin, 'Thermal properties of *N*-substituted 4-vinylpyridinium ions and their polymers'. *J. Polym. Sci., Part A: Polym. Chem.* **1990**, *28*, 2711–2717.

[164] J. H. K. Hall and A. B. Padias, ' 'Charge transfer' polymerization and the absence thereof!' *J. Polym. Sci., Part A: Polym. Chem.* **2001**, *39*, 2069–2077.

[165] E. M. Kosower and P. E. Klinedinst, 'Additions to pyridinium rings. II. Charge-transfer complexes as intermediates'. *J. Am. Chem. Soc.* **1956**, *78*, 3493–3497.

[166] E. M. Kosower, 'The effect of solvent on spectra. I. A new empirical measure of solvent polarity: Z-values'. *J. Am. Chem. Soc.* **1958**, *80*, 3253–3260.

[167] R. A. Mackay, J. R. Landolph and E. J. Poziomek, 'Experimental evidence concerning the nature of the two charge-transfer bands in pyridinium iodides'. *J. Am. Chem. Soc.* **1971**, *93*, 5026–5030.

[168] R. A. Mackay and E. J. Poziomek, 'Pyridinium iodide salts. Correlation of experimental parameters with self-consistent extended Hückel (SCEH) calculations'. *J. Am. Chem. Soc.* **1972**, *94*, 4167–4170.

[169] T. R. Griffiths and D. C. Pugh, 'Correlations among solvent polarity scales, dielectric constant and dipole moment, and a means to reliable predictions of polarity scale values from current data'. *Coord. Chem. Rev.* **1979**, *29*, 129–211.

[170] P. Mukerjee and A. Ray, 'Charge-transfer interactions and the polarity at the surface of micelles of long-chain pyridinium iodides'. *J. Phys. Chem.* **1966**, *70*, 2144–2149.

[171] P. Mukerjee and A. Ray, 'The specificity of counterion adsorption to micelles of dodecylpyridinium iodide and their critical concentrations'. *J. Phys. Chem.* **1966**, *70*, 2150–2157.

[172] A. Ray and P. Mukerjee, 'Some aspects of interionic charge-transfer interactions of alkylpyridinium ions in ion pairs and on micelles'. *J. Phys. Chem.* **1966**, *70*, 2138–2143.

[173] W. Slough and A. R. Ubbelohde, 'Electron-donor and -acceptor complexes with aromatic systems. Part III. Absorption spectra of some benzoquinolines and of their complexes with bromine in solution'. *J. Chem. Soc.* **1957**, 911–917.

[174] W. Slough and A. R. Ubbelohde, 'Electron-donor and -acceptor complexes with aromatic systems. Part V. Polarisation bonding in solid complexes formed by some heterocyclic aromatic molecules'. *J. Chem. Soc.* **1957**, 982–989.

[175] W. Slough, 'Charge-transfer bonding in molecules combined in polymeric structures. Part 1. Spectroscopic investigation of halogen and halide ion interactions'. *Trans. Faraday Soc.* **1959**, *55*, 1030–1035.

[176] T. Sulzberg and R. J. Cotter, 'Charge-transfer complexing in polymer mixtures. IV. Acceptor polymers from nitrophthalic acids and their mixtures with donor polymers from aryliminodiethanols'. *J. Polym. Sci., Part A-1* **1970**, *8*, 2747–2758.

[177] S. Shifrin, 'Charge transfer and excitation-energy transfer in a model for enzyme-coenzyme interactions'. *Biochim. Biophys. Acta* **1964**, *81*, 205–213.

[178] S. Shifrin, 'A systematic examination of charge transfer interactions of a coenzyme model'. *Biochim. Biophys. Acta* **1965**, *96*, 173–178.

[179] A. J. Zych and B. L. Iverson, 'Synthesis and conformational characterization of tethered, self-complexing 1,5-dialkoxynaphthalene/1,4,5,8-naphthalenetetracarboxylic diimide systems'. *J. Am. Chem. Soc.* **2000**, *122*, 8898–8909.

[180] S. Ghosh and S. Ramakrishnan, 'Aromatic donor-acceptor charge-transfer and metal-ion-complexation-assisted folding of a synthetic polymer'. *Angew. Chem. Int. Edn.* **2004**, *43*, 3264–3268.

[181] A. D. Shukla, D. Strawser, A. C. B. Lucassen, D. Freeman, H. Cohen, D. A. Jose, A. Das, G. Evmenenko, P. Dutta and E. M. van der Boom, 'Covalent assembly of stilbene-based monolayers: Factors controlling molecular interactions'. *J. Phys. Chem. B* **2004**, *108*, 17 505–17 511.

[182] A. C. B. Lucassen, M. Vartanian, G. Leitus and M. E. van der Boom, '4'-bromo-2',3',5',6'-tetrafluorostilbazole: Donor and acceptor site for halogen bonding and π-stacking in one rigid-rod-type molecule'. *Cryst. Growth Des.* **2005**, *5*, 1671–1673.

[183] L. P. Ellinger, 'The polymerization of vinylcarbazole by electron acceptors I'. *Polymer* **1964**, *5*, 559–578.

[184] N. C. Yang and Y. Gaoni, 'Charge-transfer interaction in organic polymers'. *J. Am. Chem. Soc.* **1964**, *86*, 5022–5023.

[185] L. Roitman and H. J. Harwood, 'Spontaneous copolymerization of *N*-methyl-4-vinylpyridinium salts with sodium 4-vinylbenzenesulfonate'. *Polym. Prepr.* **1984**, *25*, 152–153.

[186] K. M. McGrath, *Polymerisation of surfactant lyotropic liquid crystalline phases.* Ph.D. thesis, Australian National University **1994**.

[187] J. Eastoe, S. Nave, A. Downer, A. Paul, A. Rankin and K. Tribe, 'Adsorption of ionic surfactants at the air-solution interface'. *Langmuir* **2000**, *16*, 4511–4518.

[188] M. M. Knock and C. D. Bain, 'Effect of counterion on monolayers of hexadecyltrimethylammonium halides at the air-water interface'. *Langmuir* **2000**, *16*, 2857–2865.

[189] L. Luciani, R. Denoyel and J. Rouqerol, 'Poly(ethoxy) anionic surfactants: micellization and adsorption at the solid/liquid interface'. *Colloids Surf. A* **2001**, *178*, 297–312.

[190] G. J. C. Paul, I. Marcotte, J. Anastassopoulou, T. Theophanides, M. Arkas, C. M. Paleos and M. J. Bertrand, 'Investigation of the clustering processes occurring in liquid secondary ion mass spectrometry for alkyl quaternary ammonium bromides'. *J. Mass Spec.* **1996**, *31*, 95–100.

[191] S. Rodríguez-Morales, R. L. Compadre, R. Castillo, P. J. Breen and C. M. Compadre, '3D-QSAR, synthesis, and antimicrobial activity of 1-alkylpyridinium compounds as potential agents to improve food safety'. *Eur. J. Med. Chem.* **2005**, *40*, 840–849.

[192] D. S. Robins and I. L. J. Thomas, 'The effect of counterions on micellar properties of 2-dodecylaminoethanol salts: I. Surface tension and electrical conductance studies'. *J. Colloid Interface Sci.* **1968**, *26*, 407–414.

[193] R. Zana, 'Ionization of cationic micelles: Effect of the detergent structure'. *J. Colloid Interface Sci.* **1980**, *78*, 330–337.

[194] P. Lindner and T. Zemb (eds.), *Neutron, X-Ray and Light Scattering: Introduction to an Investigative Tool for Colloidal and Polymeric Systems*. The Netherlands: North-Holland, Elsevier Science Publishers B. V. **1991**, ISBN 0-444-88946-9.

[195] F. B. Rosevear, 'The microscopy of the liquid crystalline neat and middle phases of soaps and synthetic detergents'. *J. Am. Oil Chem. Soc.* **1954**, *31*, 628–639.

[196] K. Nagai, Y. Ohishi, H. Inaba and S. Kudo, 'Polymerization of surface-active monomers. I. Micellization and polymerization of higher alkyl salts of dimethylaminoethyl methacrylate'. *J. Polym. Sci., Polym. Chem. Edn.* **1985**, *23*, 1221–1230.

[197] S. M. Hamid and D. C. Sherrington, 'Novel quaternary ammonium amphiphilic (meth)acrylates: 1. Synthesis, melting and interfacial behavior'. *Polymer* **1987**, *28*, 325–331.

[198] S. M. Gawish, M. Bourgeois and G. Ambroise, 'New quaternary surfactants for alkaline hydrolysis of polyesters'. *American Dyestuff Reporter* **1984**, *73*, 37–42.

[199] K. Nagai and Y. Ohishi, 'Polymerization of surface-active monomers. II. Polymerization of quaternary alkyl salts of dimethylaminoethyl methacrylate with a different alkyl chain length'. *J. Polym. Sci., Part A: Polym. Chem.* **1987**, *25*, 1–14.

[200] S. M. Hamid and D. C. Sherrington, 'Novel quaternary ammonium amphiphilic (meth)acrylates: 2. Thermally and photochemically initiated polymerizations'. *Polymer* **1987**, *28*, 332–339.

[201] E. F. Panarin and I. I. Gavrilova, 'Copolymers of vinylpyrrolidone with dimethyl- and diethylaminoethyl methacrylate and polyelectrolytes based on them'. *Vysokomol. Soedin. B* **1977**, *19*, 251–254.

[202] S. Hamid and D. Sherrington, 'Polymerized micelles: fact or fancy?' *Chem. Commun.* **1986**, *12*, 936–938.

[203] J. Michas, C. Paleos and P. Dais, 'Polymerization of head and tail methacrylate micelle-forming surfactants and thermotropic liquid-crystalline character of these monomers and their polymers'. *Liq. Cryst.* **1989**, *5*, 1737–1745.

[204] G. Nika, C. M. Paleos, P. Dais, A. Xenakis and A. Malliaris, 'Aggregational behavior of polymeric micelles of methacrylate functionalized quaternary ammonium salts'. *Prog. Colloid Polym. Sci.* **1992**, *89*, 122–124.

[205] D. Pawlowski and B. Tieke, 'Copolymerization of styrene with a cationic surfactant monomer in three-component lyotropic mesophases'. *Langmuir* **2003**, *19*, 6498–6504.

[206] D. Pawlowski and B. Tieke, 'Change of structure and phase behaviour during homo- and copolymerisation of (2-methacryloyloxyethyl)-dodecyldimethylammonium bromide in a hexagonal lyotropic mesophase'. *Prog. Colloid Polym. Sci.* **2001**, *117*, 182–188.

[207] K. Nagai, I. Fujii and N. Kuramoto, 'Polymerization of surface-active monomers. 4. Copolymerization of long-chain alkyl salts of 2-dimethylaminoethyl methacrylate with methyl methacrylate or styrene'. *Polymer* **1992**, *33*, 3060–3065.

[208] D. Cochin, A. Laschewsky and F. Nallet, 'Emulsion polymerization of styrene using conventional, polymerizable, and polymeric surfactants: a comparative study'. *Langmuir* **1997**, *30*, 2278–2287.

[209] K. Nagai, Y. Ohishi, K. Ishiyama and N. Kuramoto, 'Polymerization of surface-active monomers. III. Polymer encapsulation of silica gel particles by aqueous polymerization of quaternary salt of dimethylaminoethyl methacrylate with lauryl bromide'. *J. Appl. Polym. Sci.* **1989**, *38*, 2183–2189.

[210] J. C. Salamone, A. M. Thompson, C. H. Su and A. C. Watterson, 'Associated polymers in solution'. *Polym. Mater. Sci. Eng.* **2004**, *61*, 518–521.

[211] Y. Yasuda, K. Rindo, R. Tsushima and S. Aoki, 'Spontaneous polymerization of amphiphilic vinyl monomers. 4. Spontaneous polymerization of methacrylic derivatives of quaternary ammonium bromides with a long alkyl chain'. *Makromol. Chem.* **1993**, *194*, 1893–1899.

[212] N. A. Kuznetsova, O. A. Kazantsev, K. V. Shirshin, T. A. Khokhlova and A. P. Malyshev, 'Hydrolysis of N,N-dimethylaminoethyl methacrylate and its salts in concentrated aqueous solutions'. *Russ. J. Appl. Chem., translation of Zh. Prikl. Khim.* **2003**, *76*, 1117–1120.

[213] O. A. Kazantsev, K. V. Shirshin, A. P. Sivokhin, N. A. Kuznetsova and A. P. Malyshev, 'Spontaneous polymerization of *N*-(3-dimethylaminopropyl)methacrylamide salts in concentrated aqueous solutions'. *Russ. J. Appl. Chem., translation of Zh. Prikl. Khim.* **2004**, *77*, 303–306.

[214] D. P. Gutierrez-Hijar, F. Becerra, J. E. Puig, J. F. A. Soltero-Martinez, M. B. Sierra and P. C. Schulz, 'Properties of two polymerizable surfactants aqueous solutions: Dodecylethylmethacrylatedimethylammonium bromide and hexadecylethylmethacrylatedimethylammonium bromide. I. Critical micelle concentration'. *Colloid Polym. Sci.* **2004**, *283*, 74–83.

[215] P. Mukerjee and K. J. Mysels, *Critical Micelle Concentrations of Aqueous Surfactant Systems*. Washington, DC: U.S. Department of Commerce **1971**, ISBN NSRDS-NBS 36.

[216] C. Novakov, N. Vladimirov, R. Stamenova and C. Tsvetanov, 'Anionic polymerization of monomers bearing quaternary ammonium groups 1. Polymerization of methacrylate derivatives'. *Macromol. Symp.* **2000**, *161*, 169–181.

[217] B. L. Bales and R. Zana, 'Characterization of micelles of quaternary ammonium surfactants as reaction media I: Dodecyltrimethylammonium bromide and chloride'. *J. Phys. Chem. B* **2002**, *106*, 1926–1939.

[218] L. Sepulveda and J. Cortes, 'Ionization degrees and critical micelle concentrations of hexadecyltrimethylammonium and tetradecyltrimethylammonium micelles with different counterions'. *J. Phys. Chem.* **1985**, *89*, 5322–5324.

[219] J. M. del Rio, C. Pombo, G. Prieto, V. Mosquera and F. Sarmiento, 'Effect of temperature and alkyl chain length on the micellar properties of *n*-alkyltrimethylammonium bromides in a low pH medium'. *J. Colloid Interface Sci.* **1995**, *172*, 137–141.

[220] K. Hiramatsu, K. Kameyama, R. Ishiguro, M. Mori and H. Hayase, 'Properties of dilute aqueous solutions of double-chain surfactants, alkyldodecyldimethylammonium bromides with a change in the length of the alkyl chains'. *Bull. Chem. Soc. Japan* **2003**, *76*, 1903–1910.

[221] E. S. Blackmore and G. J. T. Tiddy, 'Phase behaviour and lyotropic liquid crystals in cationic surfactant-water systems'. *J. Chem. Soc., Faraday Trans. 2* **1988**, *84*, 1115–1127.

[222] F. P. Duval, R. Zana and G. G. Warr, 'Adsorbed layer structure of cationic gemini and corresponding monomeric surfactants on mica'. *Langmuir* **2006**, *22*, 1143–1149.

[223] D. Danino, Y. Talmon and R. Zana, 'Alkanediyl-α,ω-bis(dimethylalkylammonium bromide) surfactants (dimeric surfactants). 5. Aggregation and microstructure in aqueous solutions'. *Langmuir* **1995**, *11*, 1448–1456.

[224] Y. A. Vasilieva, C. W. Scales, D. B. Thomas, R. G. Ezell, A. B. Lowe, N. Ayres and C. L. McCormick, 'Controlled/living polymerization of methacrylamide in aqueous media via the RAFT process'. *J. Polym. Sci., Part A: Polym. Chem.* **2005**, *43*, 3141–3152.

[225] O. A. Kazantsev and K. V. Shirshin, 'Spontaneous polymerization of (meth)-acrylamides in concentrated aqueous solutions'. *Polymer* **2004**, *45*, 5021–5029.

[226] M. J. Rosen, M. Dahanayake and A. W. Cohen, 'Relationship of structure to properties in surfactants. 11. Surface and thermodynamic properties of *N*-dodecylpyridinium bromide and chloride'. *Colloids Surf.* **1982**, *5*, 159–172.

[227] H. Edlund, M. Bydén, B. Lindström and A. Khan, 'Phase diagram of the 1-dodecylpyridinium bromide-dodecane-water surfactant system'. *Prog. Colloid Polym. Sci.* **1996**, *100*, 6–8.

[228] T. Perche, X. Auvray, C. Petipas, R. Anthore, E. Perez, I. Rico-Lattes and A. Lattes, 'Micellization of *N*-alkylpyridinium halides in formamide: Tensiometric and small angle neutron scattering study'. *Langmuir* **1996**, *12*, 863–871.

[229] T. W. Davey, G. G. Warr, M. Almgren and T. Asakawa, 'Self-assembly of hydrocarbon and fluorocarbon surfactants and their mixtures at the mica-solution interface'. *Langmuir* **2001**, *17*, 5283–5287.

[230] A. Gonzalez-Perez, L. M. Varela, M. Garcia and J. R. Rodriguez, 'Sphere to rod transitions in homologous alkylpyridinium salts: A Stauff-Klevens-type equation

for the second critical micelle concentration'. *J. Colloid Interface Sci.* **2006**, *293*, 213–221.

[231] W. K. Fife, P. Ranganathan and M. Zeldin, 'A general synthesis of 1-alkyl-4-vinylpyridinium ions. alkylation of 4-vinylpyridine with primary alkyl triflates'. *J. Org. Chem.* **1990**, *55*, 5610–5613.

[232] Y. Xin, Y. Hu, M. Zeldin and W. K. Fife, 'Copolymerization of hydrophilic and hydrophobic 1-alkyl-4-vinylpyridinium monomers'. *Macromolecules* **1993**, *26*, 4670–4674.

[233] K. Esumi, 'Interactions between surfactants and particles: dispersion, surface modification and adsolubilization'. *J. Colloid Interface Sci.* **2001**, *241*, 1–17.

[234] M. Nakagawa, N. Nawa and T. Iyoda, 'Selective Ni-P electroless plating on photopatterned cationic adsorption films influenced by alkyl chain lengths of polyelectrolyte adsorbates and additive surfactants'. *Langmuir* **2004**, *20*, 9844–9851.

[235] A. A. Yaroslavov, E. G. Yaroslavova, A. A. Rakhnyanskaya, F. M. Menger and V. A. Kabanov, 'Modulation of interaction of polycations with negative unilamellar lipid vesicles'. *Colloids Surf. B* **1999**, *16*, 29–43.

[236] G. H. Harris, R. S. Shelton, M. G. van Campen, E. R. Andrews and E. L. Schuma, 'Quaternary ammonium salts as germicides. IV. Quaternary ammonium salts derived from substituted pyridines'. *J. Am. Chem. Soc.* **1951**, *73*, 3959–3963.

[237] A. E. Westwell, M. O. Gunsch, P. T. Jacobs and E. W. Anacker, 'Ring substituent effects on decylpyridinium bromide micellization'. *J. Colloid Interface Sci.* **1990**, *137*, 92–101.

[238] H. Edlund, A. Lindholm, I. Carlsson, B. Lindström, E. Hedenström and A. Khan, 'Phase equilibria in dodecylpyridinium bromide-water surfactant systems'. *Prog. Colloid Polym. Sci.* **1994**, *97*, 134–140.

[239] T. W. Davey, G. G. Warr and T. Asakawa, 'Composition of mixed hydrocarbon and fluorocarbon surfactant adsorbed layers at mica-solution interfaces'. *Langmuir* **2003**, *19*, 5266–5272.

[240] C. J. Chang, R. F. Kiesel and T. E. Hogen-Esch, 'Anionic polymerization of polar monomers. I. Ultraviolet-visible spectroscopic and conductometric studies of ion pairs of alkali salts of vinyl 2-, 3-, and 4-pyridine-type carbanions and their crown ether complexes in aprotic media'. *J. Am. Chem. Soc.* **1975**, *97*, 2805–2810.

[241] W. L. Jenkins, C. F. Tien and T. E. Hogen-Esch, 'Oligomerization stereochemistry of vinyl carbon stereochemistry in anionic monomers. IV. Ion-pair structure and oligomerization of 2-vinylpyridine'. *J. Polym. Sci., Polym. Lett. Edn.* **1978**, *16*, 501–506.

[242] T. E. Hogen-Esch and C.-F. Tien, 'Oligomerization stereochemistry of vinyl monomers. 7. Diastereomeric ion pairs as intermediates in the stereoregular anionic oligomerization of 2-vinylpyridines. A proposed mechanism'. *Macromolecules* **1980**, *13*, 207–216.

[243] C. C. Meverden and T. E. Hogen-Esch, 'Oligomerization of vinyl monomers. 14. Thermodynamics of intramolecular cation coordination in the anionic oligomerization of 2-vinylpyridine'. *Makromol. Chem., Rapid Commun.* **1983**, *4*, 563–568.

[244] I. M. Khan and T. E. Hogen-Esch, '^{1}H and ^{13}C NMR studies of carbanion intermediates in the polymerization of 2-vinylpyridines in the THF-dimeric and trimeric models'. *Makromol. Chem., Rapid Commun.* **1983**, *4*, 569–574.

[245] S. Alunni, T. del Giacco, P. de Maria, G. Fifi, A. Fontana, L. Ottavi and I. Tesei, 'Metal ion catalysis in the β-elimination reactions of *N*-[2-(4-pyridyl)ethyl]quinuclidinium and *N*-[2-(2-pyridyl)ethyl]quinuclidinium in aqueous solution'. *J. Org. Chem.* **2004**, *69*, 3276–3281.

[246] S. Alunni, F. de Angelis, L. Ottavi, M. Papavasileiou and F. Tarantelli, 'Evidence of a borderline region between E1cb and E2 elimination reaction mechanisms: A combined experimental and theoretical study of systems activated by the pyridine ring'. *J. Am. Chem. Soc.* **2005**, *127*, 15 151–15 160.

[247] P. J. Wright and A. M. English, 'Scavenging with TEMPO to identify peptide- and protein-based radicals by mass spectrometry: Advantages of spin scavenging over spin trapping'. *J. Am. Chem. Soc.* **2003**, *125*, 8655–8665.

[248] A. G. Avent, E. A. Boucher, C. C. Mollett, S. C. Wallwork, J. P. Hemfrey, P. J. Rizkallah and M. J. Smallridge, 'Reaction kinetics and the spectroscopic and crystallographic nature of certain products from the quaternization of poly(4-vinyl pyridine) and of small pyridine molecules with alkyl bromides and iodides'. *J. Chem. Soc., Faraday Trans. 1* **1986**, *82*, 1589–1595.

[249] C. Limouzin, A. Caviggia, F. Ganachaud and P. Hemery, 'Anionic polymerization of *n*-butyl cyanoacrylate in emulsion and miniemulsion'. *Macromolecules* **2003**, *36*, 667–674.

[250] F. M. Menger and B. M. Sykes, 'Anatomy of a coacervate'. *Langmuir* **1998**, *14*, 4131–4137.

[251] S. Manne, T. E. Schäffer, Q. Huo, P. K. Hansma, D. E. Morse, G. D. Stucky and I. A. Aksay, 'Gemini surfactants at solid-liquid interfaces: Control of interfacial aggregate geometry'. *Langmuir* **1997**, *13*, 6382–6387.

[252] A. Blom and G. G. Warr **2006**, *Aust. J. Chem.* (submitted).

Appendix A

Methacrylate surfactants: supplementary SANS data

This appendix contains small-angle neutron scattering data relating to the methacrylate family of surfmers, and is a supplement to Chapter 3.

Figures A.1–A.3 are spectra from the C16 methacrylate surfactants at various concentrations.

Figures A.4–A.6 show spectra acquired while heating the C12 methacrylate surfactants, and are accompanied by tables showing fitting parameters for each curve.

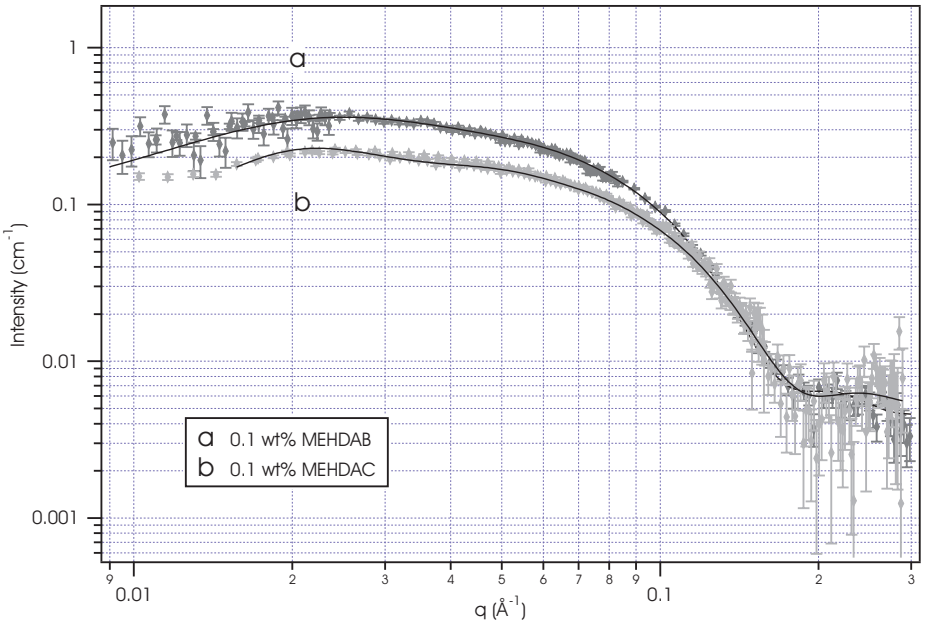

Figure A.1: SANS data (coloured points) and fitted curves (black lines) for 0.1 wt% solutions of the chloride and bromide salts of the $MEHDA^+$ cation. Fitting parameters are shown in Table 3.2.

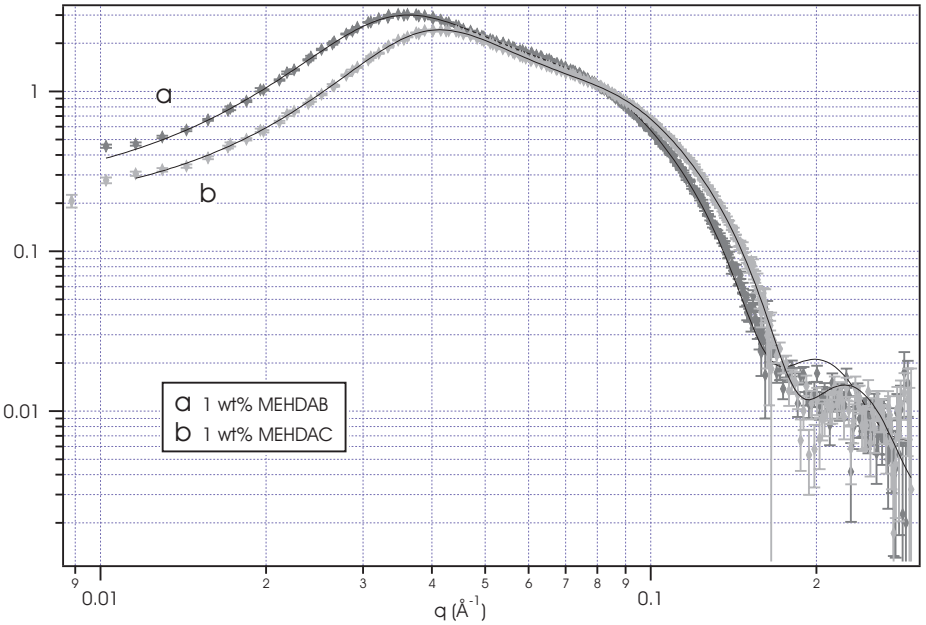

Figure A.2: SANS data (coloured points) and fitted curves (black lines) for 1 wt% solutions of the chloride and bromide salts of the $MEHDA^+$ cation. Fitting parameters are shown in Table 3.2.

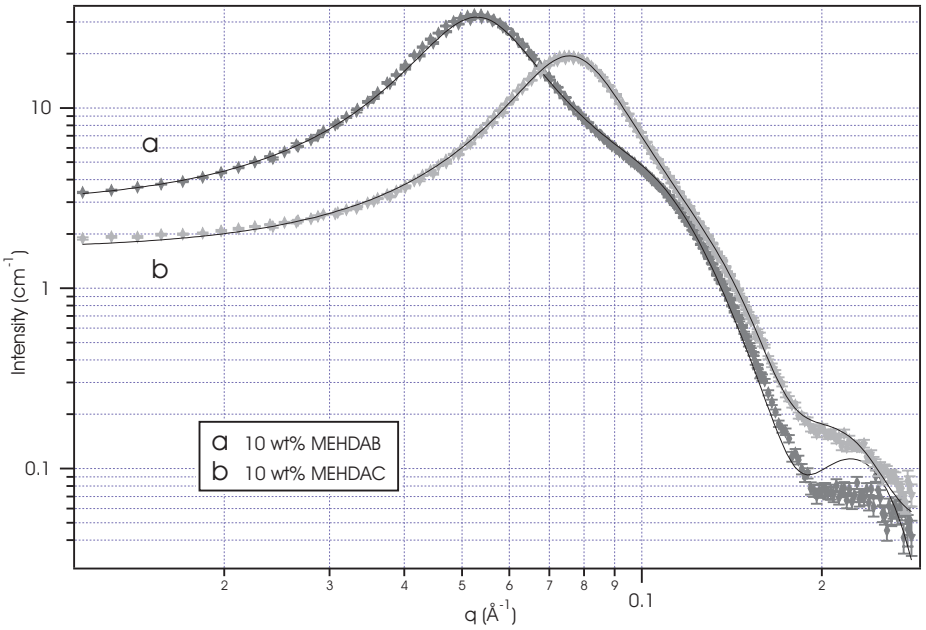

Figure A.3: SANS data (coloured points) and fitted curves (black lines) for 10 wt% solutions of the chloride and bromide salts of the MEHDA$^+$ cation. Fitting parameters are shown in Table 3.2.

* * *

The following data were collected using 1 wt% solutions of methacrylate surfactants, which were heated through a series of temperature steps and then cooled again to room temperature. In several cases, significant low-q upturns (due either to spontaneous polymerization or some other artefact) made fitting the data problematic. In these cases, some low-q data was excluded from the fitting function. The fitted parameters are shown in tables. For MEDDAA, the upturn was too significant to enable sensible values to be obtained.

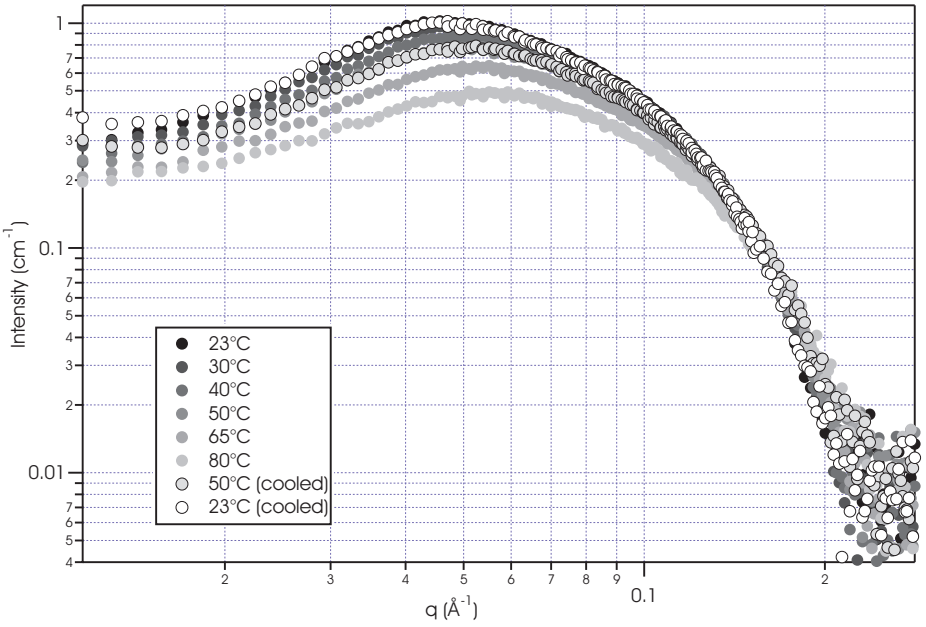

Figure A.4: SANS spectra of 1 wt% MEDDAB in D_2O.

MEDDAB, 1 wt%, fitted by polydisperse charged spheres				
Temperature	Fitted vol. frac. (%)	Radius (Å)	Polydispersity	Charge
23°C	0.69	19.0	0.16	11
30°C	0.69	18.7	0.16	11
40°C	0.68	18.1	0.16	11
50°C	0.66	17.5	0.17	10
65°C	0.62	16.5	0.20	8
80°C	0.57	15.7	0.19	8
50°C (cooled)	0.66	17.4	0.18	10
23°C (cooled)	0.68	18.9	0.16	10

Table A.1: SANS fitting parameters for 1 wt% solutions of MEDDAB in D_2O.

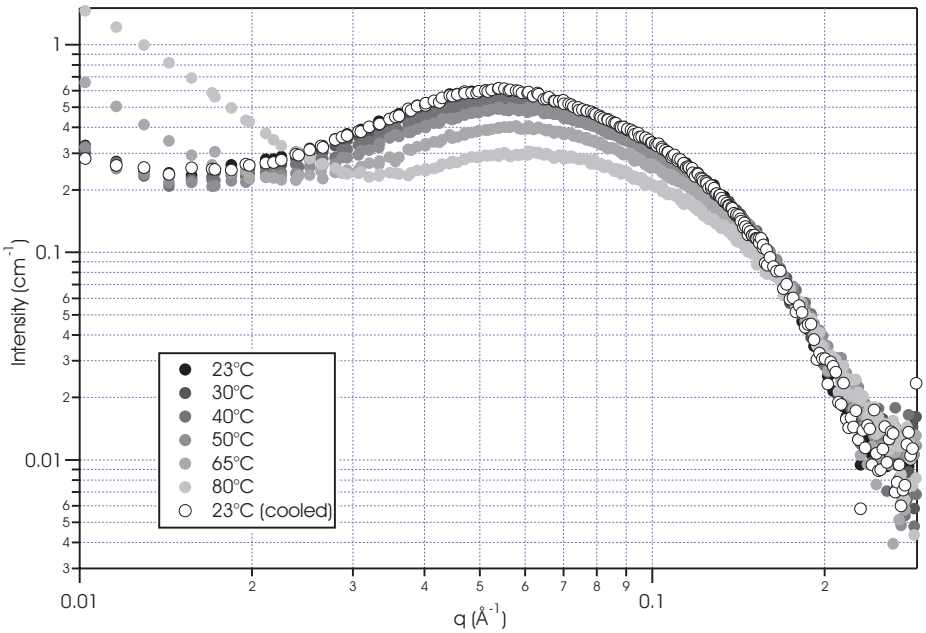

Figure A.5: SANS spectra of 1 wt% MEDDAC in D_2O.

MEDDAC, 1 wt%, fitted by polydisperse charged spheres				
Temperature	Fitted vol. frac. (%)	Radius (Å)	Polydispersity	Charge
23°C	0.60	16.5	0.18	13
30°C	0.60	16.2	0.18	13
40°C	0.59	15.7	0.20	13
50°C	0.57	15.3	0.20	12
65°C	0.53	14.6	0.21	11
80°C	0.45	13.8	0.22	15
23°C (cooled)	0.60	16.3	0.20	13

Table A.2: Fitting parameters for 1 wt% solutions of MEDDAC in D_2O.

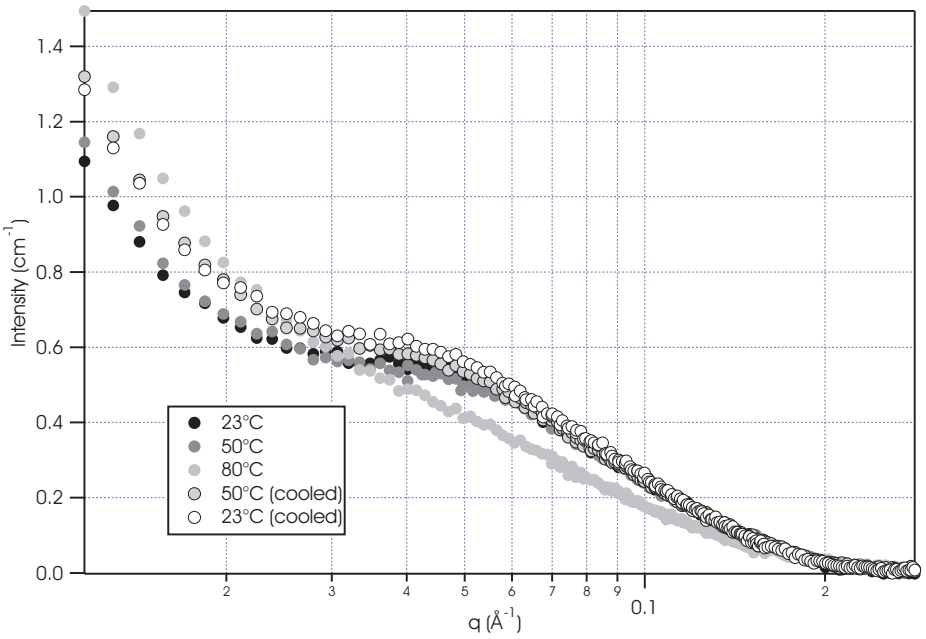

Figure A.6: SANS spectra of 1 wt% MEDDAA in D_2O. Note that spectra from intermediate temperatures are not shown, and the y-axis is on a linear scale. This was done to make it easier to distinguish the temperature-dependent shift in the spectra.

Appendix B

Vinylpyridinium surfactants: supplementary SANS data

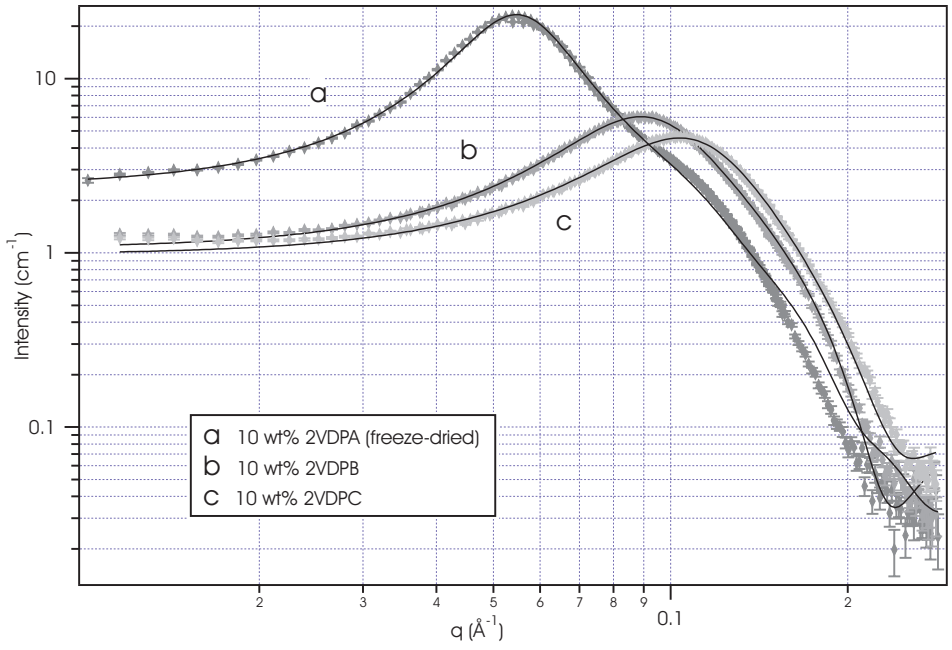

Figure B.1: SANS data (coloured points) and fitted curves (black lines) for 10 wt% solutions of the chloride and bromide salts of the 2VDP$^+$ cation, along with the freeze-dried 2VDPA sample. Fitting parameters are shown in Table 4.2.